PHYTOCHEMICAL, CHEMOPREVENTIVE AND ANTIMALARIAL ACTIVITY EVALUATION OF FIVE SELECTED MEDICINAL PLANTS FROM THE CAMEROONIAN FLORA

STEPHANIE LA BLANCHE GUETCHUENG TAMDEM

A thesis submitted in partial fulfilment of the requirements of Liverpool John Moores University for the degree of Doctor of Philosophy

November 2018

Dedicated

To

Brienne and Ethan

"If you want to shine like a sun, first burn like a sun"

A.P.J. Abdul Kalam

Acknowledgements

All the glory belongs to God, my savior and creator who has filled me with his graces, health and strength, during my stay in Liverpool.

This work will not have been possible had not been the financial support of the Commonwealth Scholarship through the Commonwealth Scholarship for PhD study in the UK (Ref CMCS-2015-107), funded by the UK Department for International Development.

I would like to express my sincere gratitude to my supervisory team, Prof Satyajit Sarker, Dr Kenneth Ritchie and Dr Lutfun Nahar for their invaluable contribution to the successful realization of this work. Their guidance, expert advice, encouragement and strong support throughout the course of the project are highly appreciated. Thank you for giving me the opportunity to work with you. I will be forever grateful.

I am grateful to the National Mass Facility Centre (Swansea, UK) and to Dr Nicola Dempster for recording the mass spectra.

Special thanks to Prof Roland Wolf (University of Dundee, UK), and Dr Andrews Evans for providing cell lines.

I would also like to address my sincere gratitude to the staff of the School of Pharmacy and Biomolecular Sciences for their assistance and help in diverse ways. Specially, Dr Fyaz Ismail for his encouragements, assistance with the NMR and MS analysis and for proofreading my thesis. I would also like to thank Dr Daniel Graham, Dr Jerry Bird, Dr Nicola Dempster, Mr Geoffrey Henshaw and Mr Robert Allen for providing assistance and training during my work in the chemistry, LSB, MS and NMR laboratories, and Ms Angela Lewis for her help and support since my arrival at LJMU. Dr Omer Hamdi is thanked for proofreading and for his valuable advices.

I also feel indebted to all my colleagues of the natural product research group for their advices, assistance and companionship.

Finally, let me thank my family for their love, prayers and support throughout the project. Specially my mum who has been immeasurably supportive and has been a mother for my children during my absence, and my husband for his encouragement, timeless support and patience. This thesis represents the result of all your efforts and sacrifices.

Abstract

Screening of ethnomedicinal plants for antimalarial and chemopreventive activities among plants used in Cameroonian folklore medicine to treat fevers, malaria and tumour was conducted on *Croton oligandrus* (Euphorbiaceae), *Justicia hypocrateriformis* (Acanthanceae), *Pseudospondias microcarpa* (Anacardiaceae), *Zanthoxylum lepreurii* and *Zanthoxylum zanthoxyloides* (Rutaceae). The selection of plants was based on ethnomedicinal use and literature review. Bioassay-guided isolation of active components from the active plants was performed with the aim to scientifically validate their folklore usage. The plant materials were dried, ground, and Soxhlet-extracted, successively, with *n*-hexane, dichloromethane (DCM) and methanol (MeOH). The antimalarial and chemopreventive potential of the plants were evaluated using haem polymerisation and the luciferase assays, respectively. The *n*-hexane and the DCM extracts of *C. oligandrus*, and the DCM and MeOH extracts of *Z. zanthoxyloides* were the most active in the luciferase assay causing 18, 21, 34 and 36-fold induction of the level of luciferase in AREc32 cells, respectively. *Pseudospondias microcarpa* was the most active antimalarial plant with IC_{50} values of 73.9 ± 25.8, 2.5 ± 1.5 and 4.0 ± 1.7 µM for the stem bark *n*-hexane, DCM and MeOH extracts, respectively, and 13.0 ± 9.0 µM for the leaves MeOH extract. Fifty-one compounds including eleven novel ones were isolated from active fractions using column chromatography, thin layer chromatography and reversed-phase high-pressure liquid chromatography. Structural elucidation was carried out by spectroscopic means including 1D and 2D NMR and mass spectrometry. Crotonolins A-D, skimmianine, hesperidin and myrtopsine were identified as potent chemopreventive compounds with fold induction greater than 2. None of the isolated compounds demonstrated any inhibition of haem polymerisation. This study generated the first phytochemical report on *P. microcarpa*, the second of *C. oligandrus* and the third of *J.*

hypocrateriformis. The biogenesis and chemotaxonomy of isolated compounds have also been discussed.

Table of contents

List of abbreviations

δ	Chemical shift (ppm)
^{1}H-NMR	Proton nuclear magnetic resonance
^{13}C-NMR	Carbon nuclear magnetic resonance
1D, 2D	One dimensional, two dimensional
Acetone-d_6	Deuterated acetone
ACT	Artemisinin combined therapy
ADP:	Adenosine di-phosphate
AMU	Atomic mass units
ATP	Adenosine triphosphate
ARE	Antioxidant response element
B.C.	Before christ
Ca.	Around
CC	Open column chromatography
CD_3OD	Methanol deuterated
$CDCl_3$	Deuterated chloroform
cm	Centimeter
CNH	Cameroon national herbarium
COB	*Croton oligandrus* bark
conc	Concentration
COSY	Correlation spectroscopy
Cpd (s)	Compound (s)
CPP	Copalyl diphosphate
CR-UK	Cancer research United Kingdom
d	Doublet
DBE	Double bond equivalence
DCM	Dichloromethane
DMEM:	Dulbecco's modified eagle medium
DEPT	Distortionless Enhancement by Polarisation Transfer
DMSO	Dimethyl sulfoxide
DMSO-d_6	Deuterated dimethyl sulfoxide
DNA	Deoxyribonucleic acid
Doxy	Doxorubicin
ESI	Electrospray ionisation

EtOAc	Ethyl acetate
FBS:	Fetal bovine serum
Fig.	Figure
FT-IR:	Fourier transform infra-red
g	Gram
GBP	Great British pound
GGPP	Geranyl geranyl diphosphate
h	Hour
HMBC	Heteronuclear multiple bond coherence
HPLC	High performance liquid chromatography
HR	High resolution
HSQC	Heteronuclear single quantum coherence
Hz	Hertz
IC_{50}	Concentration needed to produce 50% of haem polymerisation inhibition
Inj. Vol.	Injection volume
J	Coupling constant
JHL	*Justicia hypocrateriformis* leaves
Keapl	Kelch-like ECH-associated protein 1
L	Liter
LC_{10}	Concentration needed to produce 10% of cells death
LC_{50} (LD_{50})	Concentration (or dosage) needed to produce 50% of cells death
LC/MS	Liquid chromatography–mass spectrometry
LCT	Liquid Chromatography Time of Flight
m	Multiplet (for NMR spectrum)
M	Molar (concentration)
m/z	Mass to charge ratio
MeOH	Methanol
mg	Milligram
MHz	Mega hertz
min	Minute
mL	Millilitre
mm	Millimetre
MS	Mass spectroscopy

MTT	3-(4,5-Dimethyithiazo-2-yl)-2,5-diphenyltetrazolium
nm	Nanometer
NMR	Nuclear magnetic resonance
NOESY	Nuclear Overhauser Enhancement spectroscopy
NQOI	Quinone reductase
Nrf2	Nuclear factor erythroid 2-related factor
OD	Optical density
ov	overlapping
PBS	Phosphate buffer saline
PMB	*Pseudospondias microcarpa* bark
PML	*Pseudospondias microcarpa* leaves
ppm	Parts per million
Pyr-d5	Deuterated pyridine
RBC	Red blood cell
RP	Reversed phase
s	Singlet
SDS	Sodium dodecyl sulfate
SEM	Standard error of mean
SPE	Solid phase extraction
t	Triplet
*t*BHQ	Tert-Butylhydroquinone
t_R , R_f	Retention time, Retention factor
TFA	Trifluoro acetic acid
TLC	Thin layer chromatography
TOCSY	Total Correlation spectroscopy
TOF	Time of Flight
µg	Microgram
µL	Microliter
µm	Micromole
UV-DAD	Ultraviolet-Diode array detector
VLC	Vacuum liquid chromatography
WHO	World health organisation
ZLF	*Zanthoxylum leprieurii* fruits
ZZF	*Zanthoxylum zanthoxyloides* fruits

List of figures

List of tables

Chapter 1 Introduction

1.1 Cancer

1.1.1 General overview

Cancer is one of the leading causes of mortality and morbidity worldwide, ranking second after heart disease (Ferlay *et al*., 2013). The term cancer relates to 200 or more separate diseases characterized by uncontrolled growth and spread of abnormal cells in the body (Trichopoulos *et al*., 1996). In 2015, approximately 8.8 million deaths worldwide were caused by cancer (WHO, 2018a), and in the UK, an estimated 359,960 new cases were registered in 2015, and about 163,444 deaths were due to cancer (CR-UK, 2018). Globally, one in six deaths are due to cancer and this number is projected to almost double by the year 2030, if no measures are taken to cure or prevent the disease (WHO, 2018a). Factors such as smoking, obesity, inadequate diet, lack of physical activity and pollution, increase the risk of getting cancer (Grundy *et al*., 2017). Traditional cancer therapies include radiation, chemotherapy and surgery. However, these treatments have limited efficacy, huge side effects and the vital prognostic is unquestionable when the cancer has reached the stage of metastasis. As most cancer results from lifestyles and environmental factors, cancer prevention could be a better way to reduce the incidence of the disease. Besides, always 'prevention is better that cure'.

1.1.2 Mechanism of cancer development

Cancer is a multiple step process and involves genetic and epigenetic changes. Such changes in just one cell can lead to the development of cancer (Fink, 1979). Carcinogenesis consists of three main stages: initiation, promotion and progression (Figure 1.1) (Murakami *et al*., 1996). Initiation can be induced by exposure to a carcinogen giving rise to spontaneous changes such as DNA damage in one or more stable

cells, leading to mutations in the genetic code (Counts and Goodman, 1994). If the mutation occurs in a gene, which controls cell growth, that cell may become a pre-cancerous cell (Cohen and Ellwein, 1995). If cell division occurs before repair of the damaged cell takes place, then the lesion will be present on the DNA of the daughter cell and will perpetuate into all the further progeny of that daughter cell. Further proliferations of the damaged cells due to exposure to promoting stimuli will give rise to a population of transformed cells and eventually will develop into a tumour (Cairns, 1981). Further stimulations of initiated cells in addition to mutations and chromosomal aberrations cause a fast increase in the tumour size and lead to increasing heterogeneity of the cell population (Devi, 2004). A tumour can be benign or malignant. Benign tumours are not usually life threatening and do not invade nearby cells or spread to others part of the body the way malignant tumours can. If untreated or unresponsive to treatment, malignant tumours can invade and destroy the surrounding tissues. As the tumour progresses under the effect of accumulation of multiple genetic alterations, some cells can be detached from the site of the primary growth, enter the circulating blood and lymph, and be transported to other organs/tissues. They can penetrate the vessels of the organ or tissues, continue to multiply in their new location and eventually develop into another clinically detectable tumour known as metastases (Yokota, 2000).

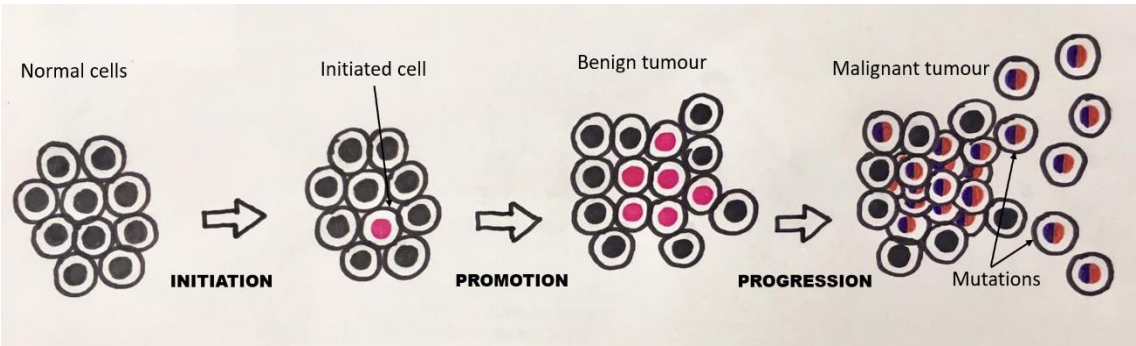

Figure 1.1 Different stages of cancer development

1.1.3 Cancer occurrence and mortality rates

In 2017, the most common causes of cancer death in the world were, lung (1.69 million deaths), liver (788,000 deaths), colorectal (774,000 deaths), stomach (754,000 deaths) and breast (571,000 deaths) (WHO, 2018a). It has been predicted that 42% of males and 39% of females will suffer from cancer at some point in their life. Most common fatal cancers in females affect breast, colon, lung and cervix, while in males they affect lung, prostate, colon and stomach (WHO, 2014). Acute lymphoblastic leukaemia and brain tumours are the most common cancers causing death in children, except in Africa where non-Hodgkin lymphoma occurs more often (WHO, 2014). In the UK, breast, lung, colon and prostate are the most common cancer sites and accounted for more than half of all cancer deaths in 2014 (CR-UK, 2018). A total of 14 million cancer cases were registered in 2012, and this number is expected to rise by about 70% over the next two decades with almost half of all new cases being registered in developing countries (Ferlay *et al*., 2013). Currently, 70% of cancer deaths worldwide occur in low- and middle-income countries (WHO, 2018a). The chance of survival highly depends on the type of cancer and extent of disease at the beginning of treatment. The 5-year survival rates of many cancer patients are still low, 4% only for cancer affecting pancreas (Pezzuto *et al.*, 2005). Making lifestyle changes such as stopping smoking, adopting a healthy diet and undertaking physical activity can reduce cancer incidence by 40% (Amin *et al*., 2009).

1.1.4 Cancer chemotherapy

Cancer chemotherapy is the use of cytotoxic drugs to destroy cancer cells. It can be used alone or in combination with surgery and/or radiotherapy. The toxic drugs interfere with DNA and cell division to preferentially kill cancer cells (Cheung-Ong *et al*., 2013). The

four main categories of cytotoxic drugs include alkylating agents, antimetabolites, hormonal agents and mitotic inhibitors. Alkylating agents derived from mustard gas, their anticancer properties are because of their ability to bind covalently with DNA via their alkyl groups (Lind, 2011). Therefore, DNA molecules are bound tightly together and cannot split during mitosis, thus preventing the proliferation of the cancer cell. Examples of these types of drugs include cisplatin and cyclophosphamide. Antimetabolites have similar structures with the metabolites with whom they interfere with in the organism. They act by blocking DNA dereplication thus preventing cell division. Some examples of antimetabolites are capecitabine and fludarabine. Hormonal agents are used to stimulate or inhibit the production and activity of some hormones involved in the development of certain cancers. Examples of such are leuprorelin and tamoxifen used in the treatment of prostate and breast cancers, respectively. Mitotic inhibitors are derived from plant natural products. They act by blocking cell division by preventing microtubule function (Rowinsky and Donehower, 1991). Examples of these drugs include etoposide and taxol (Figure 1.2).

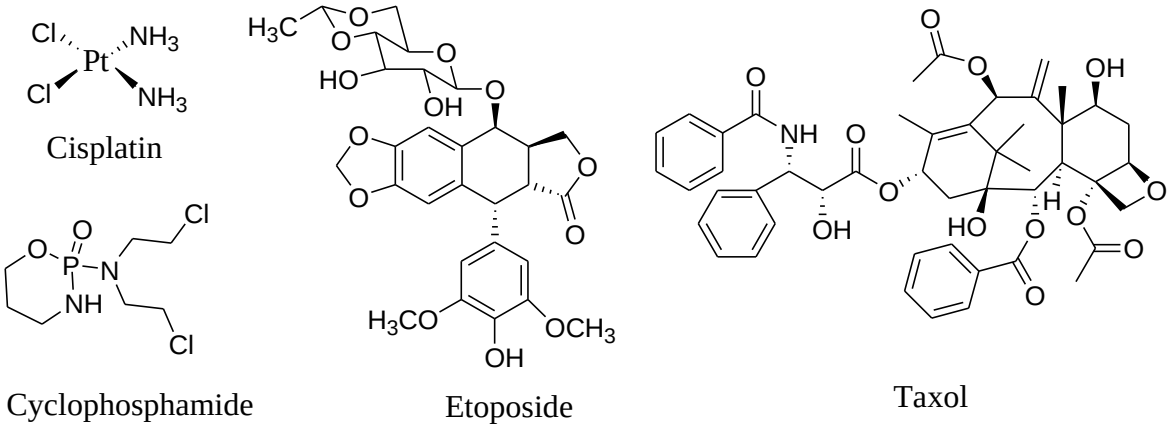

Figure 1.2 Some anticancer dugs

1.1.5 Treatment of cancer by traditional medicine

Traditional medicine is commonly used as both adjuvant and alternative to the use of synthetically manufactured chemotherapeutic drugs. Many surveys have identified plants used in different ethnic groups across the world for the treatment of cancer. An example of such survey could be the one carried out by Hartwell (1971), who combined data of 3000 plants used traditionally for the treatment of cancer. Phytochemical studies of these plants led to the isolation of almost 1000 compounds with potent anticancer properties and the discovery of lead compounds for the development of new cancer drugs (Cragg and Newman, 2016). Table 1.1 lists some examples of isolated anticancer agents from plants.

1.1.6 Cancer chemoprevention

Cancer chemoprevention is defined as the use of vaccines or pharmaceutical agents to inhibit, retard, or reverse the carcinogenesis process (Mettlin, 1997). Since carcinogenesis is a multiple stage process and takes many years or decades to develop, there are several chances to intervene in this process (Tamimi *et al*., 2002). Moreover, exogenous causative factors including smoking, diet, physical exercise, environmental pollution, exposition to potential carcinogens and radiations, can be controllable and preventable (Grundy *et al*., 2017). Inhibition of carcinogens, treatment of precancerous lesions, protection of persons at genetic risk and reduction of the incidence of cancer due to dietary epidemiology represent the four main lines address by cancer chemoprevention strategies (Surh, 1999). The ultimate goals of cancer chemoprevention research include identification of the most effective agents and/or to develop efficient approaches for clinical trial and ultimately, application to human population. Plant derived natural products offer a diverse source of

potential chemopreventive agents (Manna *et al*., 2000). Indeed, several compounds isolated from plants i.e. avicins (*Acacia victoriae*), ursolic acid (Basil), resveratrol (red grapes), curcumin (*Curcuma longa*), all from dietary vegetables and fruits, have shown the ability to inhibit human cancer cells growth and therefore, may serve as chemopreventive agents (Shishodia *et al*., 2003; Aggarwal *et al*., 2004; Howes, 2015).

Table 1.1 Examples of cytotoxic compounds isolated from plants

Plant sources	Isolated compounds	Activity	References
Acronychia bauer L.	Acronycine	Antitumour	(Duke, 1992)
Brucea species Miller	Bruceantin	Antitumour/ Antileukaemia	(Shah *et al*., 2014)
Bryophyllum pinnatum Salisb.	Bryophyllin-A	Antitumour	(Duke, 1992)
Camptotheca acuminata Decne	Camptothecin	Antileukaemia	(Pezzuto, 1997)
Cassia obtusifolia L.	Emodin	Against breast cancer	(Huang, *et al*., 2008)
Catharanthus roseus (L.) G. Don	Vincristine and vinblastine	Antileukaemia	(Pezzuto, 1997)
Cephalotaxus harringtonii (Forbes) K. Koch	Homoharringtonine	Antileukaemia	(Shah *et al*, 2014)
Rabdosia rubescens L.	Rubescensine B	Antihepatoma	(Chang, 1998)
Podophyllum peltatum L.	Etoposide and teniposide	Antitumour	(Pezzuto, 1997)
Stephania tetrandra Lour	Tetrandrine	Against lung cancer	(Duke, 1992)
Zanthoxylum nitidum L.	Nitidine chloride	Against lung cancer	(Chang, 1998)

Chemopreventive agents (Figure 1.3) can be natural or synthetic substances. Examples include the synthetic drugs raloxifene and tamoxifen used to prevent breast cancer in women (Chlebowski, 2015) and phenethyl isothiocyanate, a naturally occurring compound in some cruciferous vegetables with potential chemopreventive effects on prostate cancer (Wang, 2010). Chemopreventive agents are classified into two groups, blocking agents and suppressing agents (Wattenberg, 1985). Suppressing agents act in either the promotion or the progression stages during carcinogenesis by inhibiting the proliferation of initiated cells. Blocking agents act on the initiation stage of the carcinogenesis either by blocking the formation of the carcinogen, or by inhibiting interaction of the ultimate carcinogen with crucial cellular macromolecules such as DNA, RNA and protein (Figure 1.4) (Surh, 1999; Kuo et al., 2012).

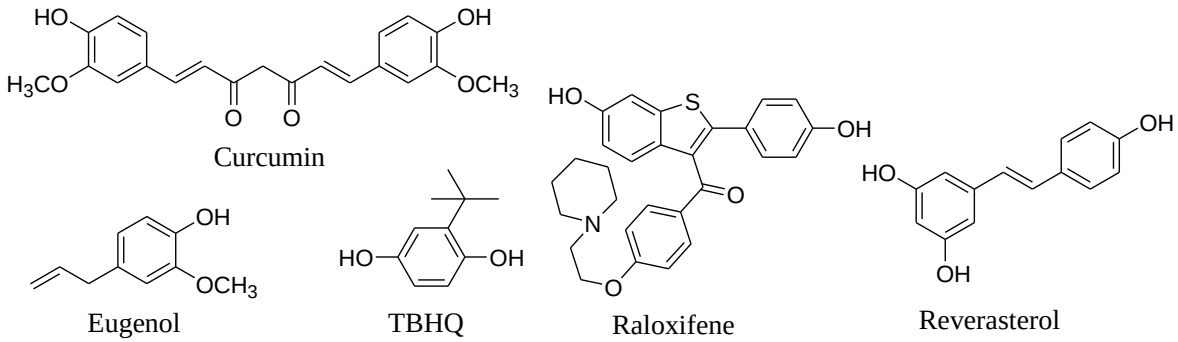

Figure 1.3 Some chemopreventive agents

1.1.7 Chemoprevention by dietary phytochemicals

Dietary phytochemicals are natural products commonly found in edible plants. They became an attraction for cancer chemoprevention research when researchers noticed that people adopting the Mediterranean diet (mean a diet of fish, vegetables, legumes, whole grains, potatoes, fruit and extra virgin olive oil) have the lower risk of developing cancer (Gotsis, 2015). Evidences later confirmed their anticancer and chemopreventive potential

(Shishodia *et al*., 2003; Aggarwal *et al*., 2004). Dietary phytochemicals mainly act as blocking agents by intervening in a range of cellular processes resulting in the inhibition of the early stages of the carcinogenesis (Sapienza and Issa, 2016). They prevent carcinogens from reaching targeted sites, support detoxification of highly reactive oxygen species, enhance innate immune surveillance and improve the elimination of initiated cells (Kotecha *et al*., 2016). The above-mentioned properties of dietary phytochemicals involve the activation of the nuclear factor erythroid-2 (NF-E2)-related factor 2 (Nrf2)-Kelch-like ECH associated protein 1 (Keap1).This complex activation consequently results in the induction of cellular defence mechanisms, including phase II detoxifying enzymes, phase III transporters, antioxidative stress proteins, and other stress-defence molecules that protect normal cells from reactive oxygen species (ROS) and/or reactive nitrogen species (RNS) and reactive metabolites of carcinogenic species known to be the causative agents of more than 600-types of cancer (Lee *et al.*, 2013; Landis-Piwowar *et al*., 2014).

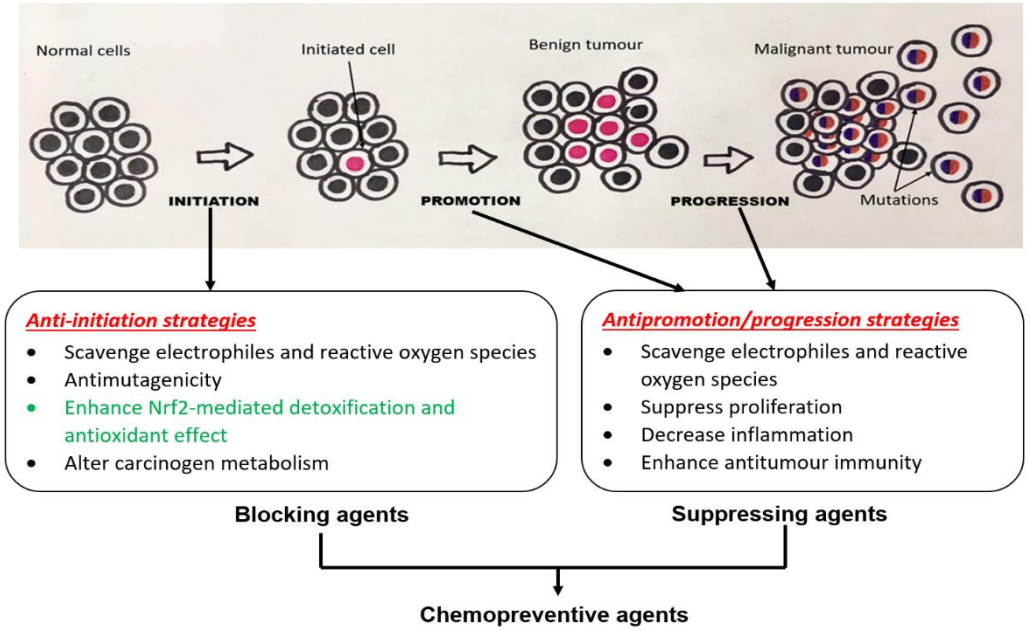

Figure 1.4 Multistage carcinogenesis and strategies for cancer chemoprevention (Adapted from Kuo *et al.*, 2012)

1.1.8 Phase II detoxification enzymes

One significant mechanism by which dietary phytochemicals protect cells from cancer is by the induction of the activity of drug metabolizing enzymes particularly of phase II detoxifying enzymes. Phase II detoxification enzymes provide the defence against foreign chemicals, to which humans are constantly exposed. Many xenobiotics are toxic and if they accumulate in the body, they may cause cell damages which will eventually kill the cell or develop into a cancer. Therefore, many enzymes with various specificities are required to reduce the toxicity of reactive intermediates, protect cells against oxidative or electrophilic challenges, and maintain chemical homeostasis in cells (Kwak *et al.*, 2001). Examples of reactions and Phase II enzymes involved in detoxification include: reduction reaction catalysed by NAD(P)H dehydrogenase, quinone 1 (NQO1); conjugation reactions catalysed by UDP-glucuronosyltransferase (UGT) and glutathione transferase (GST); oxygenation reaction catalysed by heme oxygenase-1 (HO-1) (Zimniak, 2008). The genes encoding the detoxifying enzymes are typically regulated through a consensus cis-enhancer sequences known as the antioxidant responsive element (ARE) or electrophile response element (EpRE), which are in their promoter region. ARE-mediated gene expression plays a central role in the cellular defence against oxidants and electrophiles (Chen and Kong, 2004). It is activated through the binding of the transcription factor, Nrf2, in response to cellular attack by ROS or any other compound with the capacity to either undergo redox cycling or be metabolically transformed to a reactive or electrophilic species (Nguyen *et al*., 2009). NQO1, for example, is a key enzyme that protects against quinone-derived reactive intermediates and maintains cellular pool of antioxidants such as tocopherol (Nioi and Hayes, 2004). Generally, an increase in the activity of NQO1 enhances the ability of an organism to detoxify numerous potentially harmful xenobiotics (Dinkova-Kostova and Kostov, 2012; Landis-Piwowar *et al*., 2014). Therefore, substances that increases the activity of NQO1 can be potential

chemopreventive agents with the ability to inhibit chemically induced cancer formation (Perez *et al.*, 2010).

1.1.9 Nrf2 as a target for cancer chemoprevention

Nrf2 is a protein that regulates the expression of many phase II detoxifying/antioxidant enzymes. Under normal condition, Nrf2 is sequestered in the cytoplasm by an actin-binding protein, Kelch-like ECH associating protein 1 (Keap-1) and maintains at very low levels regulated by proteasomal degradation (Jaramillo and Zhang, 2013). Upon exposure of cells to inducers such as chemopreventive agents, the sensor cysteines of the Keap-1 that control the Keap-1-dependent Nrf2 degradation is inactivated by the inducers and this therefore, allows *de novo* synthesized Nrf2 to accumulate, to dissociate from the Keap-1 and to translocate to the nucleus where it binds to ARE (Carvalho *et al.*, 2010), and transactivates phase 2 detoxifying and antioxidant genes and transporters, that defend cells from subsequent carcinogenic insults by reducing reactive compounds such as electrophiles and free radicals to less toxic intermediates whilst increasing the ability of the cell to repair any damage ensued (Jeong *et al.*, 2006; Lau *et al.*, 2008; Bryan *et al.*, 2013). Several studies have demonstrated that the major mechanism of protection against carcinogenesis is through Nrf2-mediated induction of drug metabolizing enzyme, particularly phase II detoxification and antioxidant enzymes (Lau *et al.*, 2008). Various compounds, such as naphthoflavone and *tert*-butyl hydroquinone (*t*BHQ), are potent chemopreventive agents because of their ability to induce phase II enzymes in mammalian cells (Jeong *et al*., 2008). As blocking agents, dietary phytochemicals protect DNA from mutation by activating the Nuclear factor (erythroid-derived 2)-like 2 (Nrf2) mediation detoxification and antioxidant effect thus making the Nrf2 to be a good drug

target for cancer prevention by phytochemicals (Jaramillo and Zhang, 2013; Reuland *et al*., 2013; Landis-Piwowar *et al*., 2014).

1.2 Malaria

1.2.1 General overview

Malaria is a disease endemic to tropical and subtropical regions of the world (Bloland, 2001). The disease is caused by protozoan parasites *Plasmodium*, transmitted to humans through the bites of infected female *Anopheles* mosquitoes. The most life-threatening and drug-resistant cases are due to infection by the species *P. falciparum* (Daily, 2006). The development of resistance to drugs poses one of the greatest threats to malaria control and has been linked to recent increases in malaria morbidity and mortality. The World Health Organization's 2016 'World Malaria Report' estimates that in 2016, 216 million cases of malaria were reported causing 445,000 deaths compared to 212 million cases reported in 2015 causing 446,000 deaths (WHO, 2017). Resistance to antimalarial drugs has threatened global malaria control since the emergence of resistance to chloroquine in the 1970s. WHO advocates Artemisinin Combination Therapy (ACT) as first line treatment for acute uncomplicated malaria, where the potentially life threatening parasite *P. falciparum* is the predominant infecting species with the aim to improve efficacy and to retard the development of resistance (Reyburn, 2010). However, this treatment is also vulnerable and resistance to artemisinin has already been registered in Western Cambodia (Noedl *et al*., 2008). Because of the potential consequences if resistance to artemisinin were to become widespread, one of the great scientific and medical concerns today is to develop new drugs or vaccines to fight against malaria.

1.2.2 Malaria occurrence and mortality rate

Malaria is one of the oldest diseases that affects human. The evidence of the occurrence of this disease, 5,000 years ago, was found in Chinese manuscript (Cox, 2010). The word malaria derived from the Italian word 'mal aria', which signifies bad air. The disease was first believed to have been caused by vapours given off by swamps by inhalation and was also called swamp fever. It was not until 1880 that the parasite responsible for the disease, known today as *Plasmodium*, was described by Alphonse Laveran (Cox, 2010). The vector responsible for the transmission of the disease, the mosquito *Anopheles*, was later identified by Ronald Ross in 1899 (Cox, 2010). Malaria is widespread in tropical and subtropical regions in sub-Saharan Africa, Central and South America, the Caribbean island of Hispaniola, the Middle East, the Indian subcontinent, South-East Asia, and Oceania (Figure 1.5). Despite its discovery several decades ago, and all the research implemented to prevent and eradicate the disease, malaria is still one of the leading causes of human mortality. Malaria is prevalent in 91 countries and occurs mainly in sub-Saharan Africa.

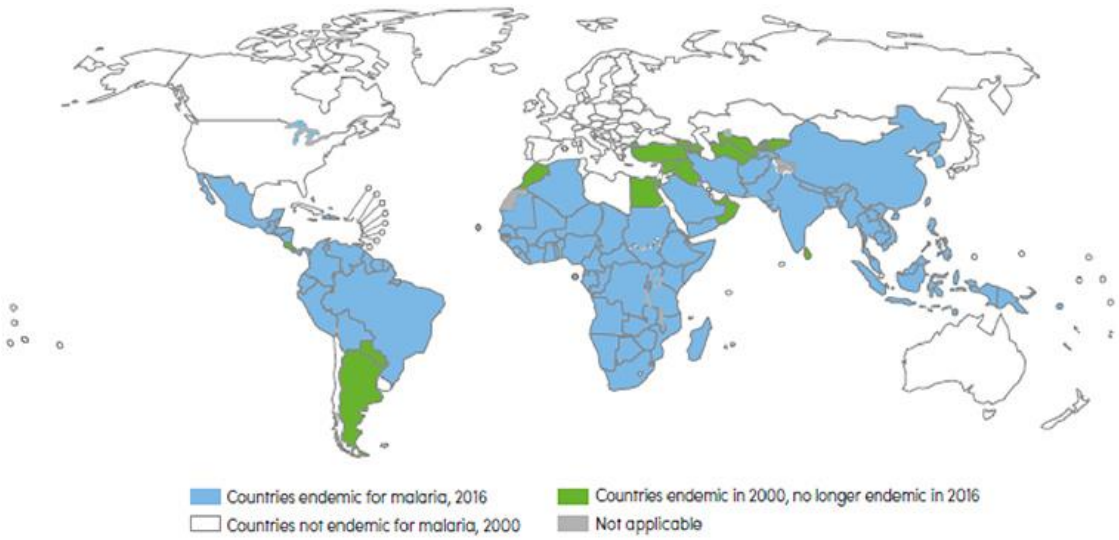

Figure 1.5 Geographic distribution of malaria (Source: WHO. World Malaria Report. Geneva, 2016. Licence: CC BY-NC-SA 3.0 IGO.)

According to the WHO malaria report 2017, an estimated of 216 million cases of malaria were reported in 2016, an increase of 4 million cases compared to 2015. The disease made 445,000 casualties in 2016, a similar number of deaths were observed the previous year (446,000). Sub-Saharan Africa is the most affected area with 90% of malaria cases and 91% of malaria deaths. South-East Asia is the second affected region with 7% and 6% of reported malaria cases and deaths, respectively. Children under 5 years old are the most affected by the disease and 70% of all malaria deaths occur in this age group. Malaria transmission and infection highly depend on the climate conditions and geographical position (Bloland and Organization, 2001). Warm temperatures promote the breeding of the mosquito vector, and highland (altitude >2,000 m) and arid areas (<1000 mm rainfall/year) are less prone to the disease in areas where malaria does occur (Ermert *et al*., 2011).

1.2.3 Life cycle of malaria *Plasmodium*

The *Plasmodium* is a genus of parasites comprising about 200 species (Chavatte *et al*., 2007). Five species including *P. falciparum*, *P. vivax*, *P. malariae*, *P. ovale* and *P. knowlesi* are responsible for malaria in humans. Malaria cases associated with the species *P. malariae* and *P. ovale* are less common. *P. knowlesi* mostly affects primates and do not seem to be a major threat to humans (Singh *et al*., 2004). Infections due to *P. falciparum* and *P. vivax* are the most life threatening. *P. vivax* can persist for years in the dormant stage in the liver and can cause clinical relapses at regular intervals (Carvalho *et al*., 2010). Almost 99% of malaria cases in sub-Saharan Africa are due to *P. falciparum*, which is the most prevalent in that region. *P. vivax* is predominant in the others area affected by the disease outside Africa and were responsible for 4% of malaria deaths globally in 2016 (WHO, 2017). All the *Plasmodium* species causing malaria in humans

are transmitted by mosquito species of the genus *Anopheles* (Igweh and Okwa, 2012). The life cycle of the malaria parasite, discovered by Ronald Ross in 1899, is complex and takes place in both human and mosquito tissues (Cox, 2010). A simplified schematic representation of the malaria cycle is depicted in Figure 1.6. The cycle starts with the injection of sporozoites by the vector, the mosquito *Anopheles*, into the subcutaneous tissue or directly into blood vessels (Miller *et al*., 2002). The sporozoites are then transported to the liver via the bloodstream where they infect the liver cells (hepatocytes) (Kappe *et al*., 2010). Within the liver, sporozoites can invade any cells and then, undergo asexual replication to develop into schizonts which are formed by thousands of merozoites, which are later released into the bloodstream upon rupture of the schizont membrane and infect the red blood cells (RBC) (Cowman and Crabb, 2006; Kappe *et al*., 2010). The liver stage normally lasts about 9-16 days. For infections due to *P. vivax* and *P. ovale*, sporozoites do not develop into schizonts immediately. They remain dormant in the liver as hypnozoite and that makes it difficult to diagnose and treat (Igweh and Okwa, 2012).

Within the RBC, a fraction of the merozoites initiate the intra-erythrocytic cycle that lasts about 36-48 h. They first develop into a ring-shaped form, then to a trophozoite form and later into schizont. Upon destruction of the RBC, the schizont released new merozoites into the bloodstream, which can infect new RBC and reinitiate the cycle. After several repeated cycles, when 10% of the bloodstream RBC are infected, clinical features associated with the disease can be observed in the patient (Wirth, 2002). The remaining merozoites differentiate into male and female gametocytes. The Mosquito *Anopheles* ingests those gametocytes during its blood meal. Within the mosquito, the gametocytes emerge from the red blood cells as gametes. The fusion of male and female gametes forms a zygote, which elongates into ookinete. The ookinete then later develops into an oocyst whose membrane's rupture will release thousands of sporozoites that will travel to the

insect salivary glands. After this stage, the cycle is complete and the mosquito is ready to initiate a new infection on a healthy individual during another blood meal.

Malaria symptoms appear approximately one week after infection. Common symptoms include periodic fever, shivering, cough, respiratory distress, pain in the joints, headache, watery diarrhoea, vomiting and convulsions (Miller *et al*., 2002). If malaria remains untreated, erythrocytes filled with mature stages of the parasite can adhere to the walls of capillary veins, causing vascular occlusion, severe anaemia, impaired consciousness, renal failure and cerebral death (cerebral malaria) (Miller *et al*., 2002; Tuteja, 2007).

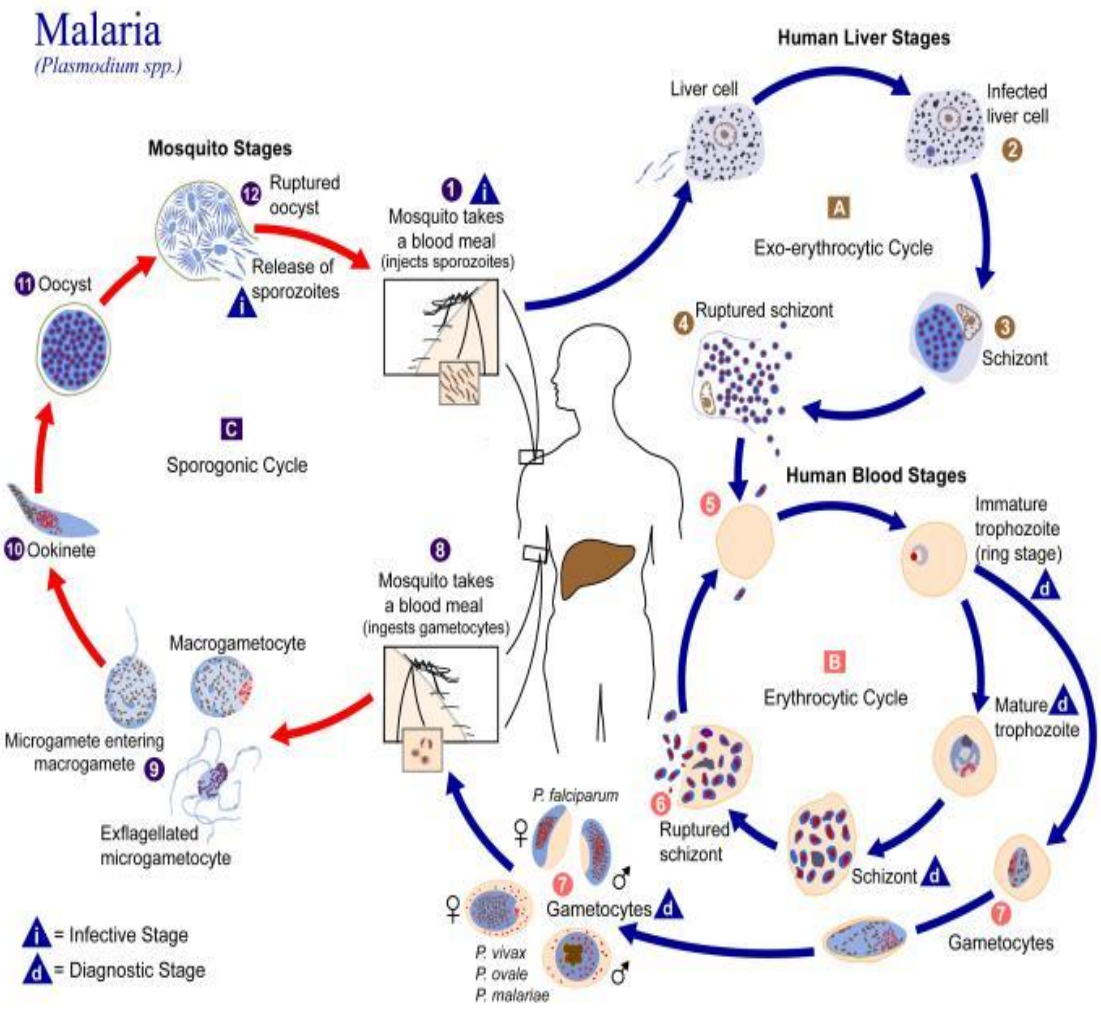

Figure 1.6 Life cycle of malaria cycle infection
(https://hu.wikipedia.org/wiki/Fájl:Plasmodium_lifecycle_PHIL_3405_lores.jpg)

1.2.4 Current antimalarial drugs and prevention

Malaria is a preventable and treatable disease. Several drugs have been developed to prevent and treat the disease, and several vaccines are currently under development or in clinical trials. The WHO recommends the use of the artemisinin based combined therapy as first line treatment for uncomplicated malaria due to infection by *P. falcifarum* (Prasad *et al*., 2015). Quinine along with its derivative has been used for the treatment of severe cases of malaria. These therapies have considerably lowered the mortality and morbidity rates due to malaria during the last three decades (Bloland and Organization, 2001).

1.2.4.1 Quinine and its derivatives

Quinine was the first drug to be used to treat malaria. It was serendipitously discovered in the 1600s, when a native from south America suffering from high fever was miraculously cured after drinking from a pool of water contaminated with the *Cinchona* tree (Cragg and Newman, 2005a). Extract of the bark of *Cinchona* with wine or water was used to treat fever associated to malaria until the isolation of quinine as its crystalline sulphate in 1820 by Pierre J. Pelletier and Joseph Caventou. The molecular formula of quinine was proposed by Paul Rabe in 1907, and later confirmed following its total synthesis by Robert B. Woodward and William Doering in 1944 (Achan *et al*., 2011). Quinine was the main antimalarial drug until the 1920s after which analogues notably chloroquine became more commonly used, due to them being more effective and having less side effects (Plowe, 2010). Quinine is still used today and remains the drug of last resort for the treatment of multidrug-resistant malaria (WHO, 2015). Other quinine derivatives in use today include chloroquine, primaquine, mefloquine and amodiaquine (Figure 1.7) (Bloland and Organization, 2001).

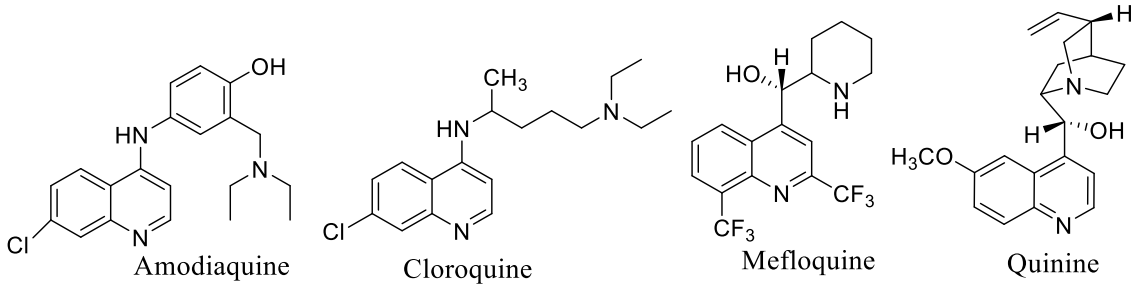

Figure 1.7 Some quinoline antimalarials

1.2.4.2 Antifolates

Folate compounds are derived from folic acid, which is formed from a pteridine ring, *p*-aminobenzoic acid and glutamate. They act on the folate biosynthetic pathway of the *Plasmodium*, a pathway essential to malaria parasite survival, either as inhibitors of dihydropteroate synthase (antifolates class I) or as inhibitors of dihydrofolate reductase (antifolates class II), hence the name antifolates (Nzila, 2006). Class I antifolates in use include proguanil, chlorproguanil, pyrimethamine and trimethoprim. Class II antifolates also called sulpha-drugs in useuse include dapsone, sulfamethoxazole and sulfadoxine (Figure 1.8) (Bloland, 2001). Each class when used alone are effective antimalarials, however, parasitological resistance can develop rapidly in that situation (Bloland and Organization, 2001). When used in combination, they produce a synergistic effect on the parasite and can be effective even in the presence of resistance to the individual components (Nzila, 2006). Antifolates are mainly used in sub-Saharan Africa regions where chloroquine resistant *P. falcifarum* is widespread. They have less or no action of *P. vivax* and *P. ovale* (Gregson, 2005).

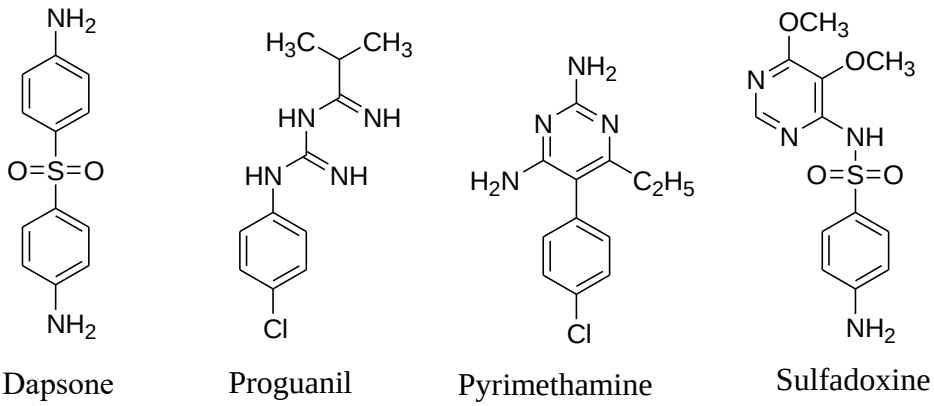

Dapsone Proguanil Pyrimethamine Sulfadoxine

Figure 1.8 Some antifolates used in malaria therapy

1.2.4.3 Artemisinin and related drugs

Artemisinin is a sesquiterpene lactone with antimalarial properties that was first isolated from the leaves of *Artemisia annua* (Tu, 2011). *A. annua* has been used for more than 2000 years in Chinese traditional medicine for the treatment of fever and chills (Tu, 2011). Artemisinin was discovered by Youyou Tu in 1972 as part of an antimalarial research project by the Chinese government. This discovery led her receive the Nobel Prize in Physiology or Medicine in 2015 (Xie, 2016). Artemisinin has later been used as a lead compound for the discovery of related antimalarials including artemether, dihydroartemisinin, artesunate and arteether (Figure 1.9) (Tu, 2017). WHO recommends the use of Artemisinin Combined Therapy (ACT) as first line treatment of uncomplicated malaria due to *P. falciparum* infection (WHO, 2018b). ACT is a combination of artemisinin or an artemisinin-derivative and a second drug with a different mechanism of action to enhance efficacy (Reyburn, 2010). Artemisinin and its derivatives must not be used as oral monotherapy, as this promotes the development of artemisinin resistance (WHO, 2018b).

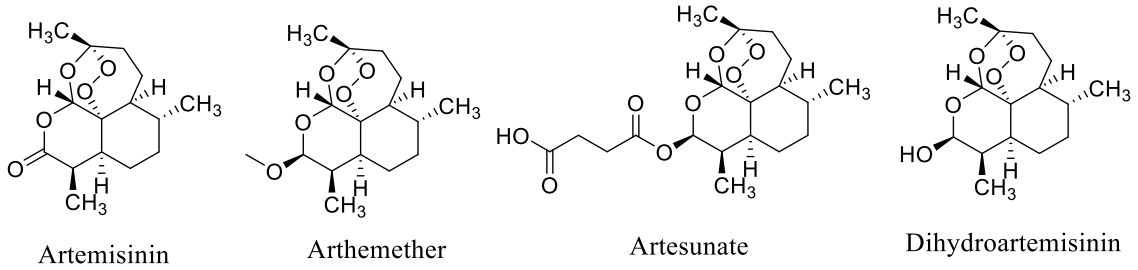

Figure 1.9 Artemisinin and derivatives

1.2.4.4 Other used antimalarial drugs

Other antimalarials currently in use include antibiotics, such as tetracycline, and its derivatives, clindamycin and thiostrepton. They are used either as a treatment or for prophylaxis in combination with quinine (Bloland and Organization, 2001). Lumefantrine, atovaquone and halofantrine are also antimalarials (Figure 1.10). They are used in area with *P. falciparum* multidrug resistance.

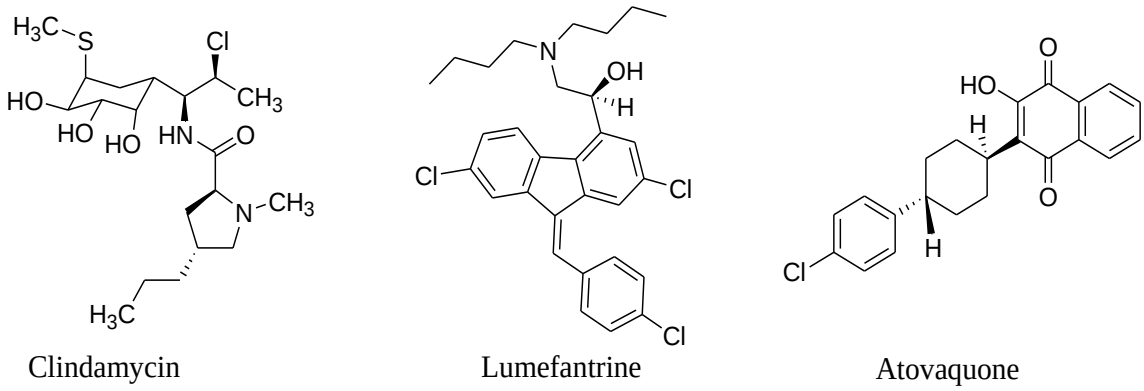

Figure 1.10 Other antimalarials: clindamycin, lumefantrine and atovaquone

1.2.5 Malaria prevention

The WHO has developed several policies to protect persons at risk of getting malaria in endemic regions and those travelling from non-malaria regions to malaria regions. These

include the control of the vector and chemoprophylaxis. In endemic regions, persons are protected from the mosquito *Anopheles* by the usage of long-lasting insecticidal nets (LLIN) and indoor residual spraying insecticides. LLIN are provided free of charge and all people at risk of malaria mainly children under 5 years old and pregnant women are encouraged to sleep under a well maintained LLIN every night. Preventive treatment with sulfadoxine-pyrimethamine are administrated on a trimestral basis to pregnant women and in addition to sulfadoxine-pyrimethamine, amodiaquine is administrated to children under 5 years old monthly. Similarly, for travellers from non-malaria to malaria regions, chemoprophylaxis using drugs that act on the blood stage of the *Plasmodium* and mosquito repellent lotions are used to prevent malaria. The WHO with partner organisations have also developed some vaccines against malaria (WHO, 2018b). The first of such, RTS,S/AS01 (RTS,S) developed with the partnership of GlaxoSmithKline will be available for use in 2018. RTS,S will be used to prevent children under 3 years old from getting malaria due to infection by *P. falciparum*. Another vaccine currently under development is Sanaria® PfSPZ Vaccine (*Plasmodium falciparum* sporozoite Vaccine), a clinical trial of which is currently being conducted in Equatorial Guinea (Olotu *et al*., 2018).

1.2.6 Malaria drug resistance

Even though the number of global malaria deaths has fallen by 48% since 2000, malaria is still a life threatening disease due to the development of resistance to existing drugs in most endemic areas affected and the difficulty to control the most effective malaria vector *Anopheles gambiae* (Prasad *et al*., 2015). The WHO defines antimalarial drug resistance as the ability of a parasite strain to survive and/or multiply despite the administration and absorption of a drug given in doses equal to or higher than the recommended but within

tolerance of the subject. The parasite must be sensitive to the used antimalarial and this later must be able to gain access to the parasite or the infected RBCs for the duration of the time necessary for its normal action (Bruce-Chwatt, 1986). Despite the long list of available antimalarials, parasites have developed resistance over time to almost all antimalarial drugs. Resistance to quinine was first reported in 1910 after its introduction in pure form in the 1840s, while resistance to artemisinin, introduced in malaria therapy in the 2000s, was recently registered in Cambodia and has since been spread in other areas of the world including south Asia, Serra Leone, Nigeria and Madagascar (Hien *et al*., 2012). Antimalarial drug resistance has been the main problem in the management of the disease.

1.2.6.1 Resistance to quinoline antimalarials

Resistance of *Plasmodium* to quinine was first reported in 1910 and later confirmed in 1938 (Clyde *et al*., 1972). Quinine resistant *Plasmodium* strains are rare in Africa but widespread in Southeast Asia and South America (Legrand *et al*., 2007). Resistance to quinine is usually low grade, with the drug retaining some activity but having its action delayed or diminished (Achan *et al*., 2011). Chloroquine became the cornerstone of malaria treatment in 1950s. However, just ten years after its introduction, high levels of resistance were recorded in Thailand and South America and have since been found in other countries including Malaysia, Vietnam, Cambodia and Burma and more recently in Sub-Saharan Africa.

1.2.6.2 Resistance to artemisinin and its derivatives

Artemisinin was first used in the 1980s in China. Interest to artemisinin began to grow with the advent of resistance of *Plasmodium* to existing antimalarials. In the 1990s, artemisinin was introduced in malaria therapy in Thailand and Cambodia, and then in other malaria regions (Meshnick, 2002). The first resistance of *P. falciparum* parasites to artemisinins was detected in Thailand-Cambodia border in the early 2000 (Denis *et al*., 2006). The resistance was confirmed in 2009 and has since been detected in Southeast Asia (Cambodia, Vietnam, Myanmar and Thailand) and in Africa (Nigeria, Madagascar and Sierra Leone) (Hien *et al*., 2012). Artemisinin and its derivatives are still effective; however, measures have been taken to reduce the chances of developing resistance in other malaria regions and to prevent the spread of resistance (Reyburn, 2010); the WHO bans monotherapy and recommends the use of artemisinin combined therapies (ACT) for the treatment of uncomplicated malaria. There are five available ACTs including artemether/lumefantrine, artesunate/amodiaquine, artesunate/mefloquine, dihydroartemisinin/piperaquine and artesunate/sulfadoxine-pyrimethamine (Prasad *et al*., 2015).

1.2.6.3 Resistance to antifolates

Resistance to pyrimethamine and proguanil, the firsts DHFR inhibitors introduce in the malaria therapy, developed shortly after their introduction in the late 1940s and early 1950s respectively in Southeast Asia (Gregson, 2005). Sulpha-drugs such as sulfadoxine and dapsone were introduced in the malaria therapy in the 1960s due to their long half-life and least toxicity (Triglia and Cowman, 1999). However, their usage was almost immediately limited due to the parasite to develop rapid resistance. Antifolates were

reintroduced in form of a combination formulation of DHFR and sulfa-drug (e.g., sulfadoxine-pyrimethamine), when subsequent studies revealed their strong synergistic action and ability to block the plasmodium DNA replication (Abdul-Ghani *et al*., 2013), however resistance to sulfadoxine-pyrimethamine developed and spread rapidly in South East Asia from the mid-1960s (Nzila, 2006). Because of the affordability of this combination, the WHO still recommends it for the treatment of chloroquine-resistant *P. falciparum* in Africa where the resistance to the combination is still limited to Tanzania (White, 2004; Nzila, 2006).

1.2.7 Mechanism of action of chloroquine: hemozoin as target for new antimalarials development

Among existing antimalarial drugs, resistance to quinine has been shown to develop slowly compared to others antimalarials. Quinine, 200 years after its discovery remains one of the most used effective antimalarials. Quinine in combination with an antibiotic e.g., doxycycline, tetracycline or clindamycin is recommended as second line treatment for uncomplicated malaria (when the first-line drug fails or is not available) and remains the first line treatment in combination with clindamycin of malaria in the first trimester of pregnancy (WHO, 2015). Several studies have been carried out to investigate the mechanism of action of quinine and other quinoline antimalarials. Quinoline antimalarials such as quinine and chloroquine, act by interfering with the digestion of haemoglobin in the blood stage of the malaria life cycle (Foley and Tilley, 1997). During the intra-erythrocytic stage, haemoglobin is digested by the parasite *Plasmodium* in its acidic vacuole. Toxic haem, which is dangerous for the parasite, is released and spontaneously converted to a less reactive dimer, hemozoin (Figure 1.11) (Slater, 1993; Egan *et al*., 1994). Quinoline, inhibits the haem's polymerisation to hemozoin and the consequence

is that the haem released during haemoglobin digestion is accumulated in the parisite's vacuole killing the parasite with its own toxic waste (Slater and Cerami, 1992; Egan *et al*.,1994; Sullivan, 2002). Resistance to quinoline antimalarials is manifested by the capacity of the parasite to expel chloroquine at a rate that does not allow chloroquine to reach levels required for inhibition of haem polymerization (Egan *et al*., 2001). Hemozoin synthesis is an indispensable pathway for the survival of the parasite and therefore, a good target for the development of new antimalarial drugs. Several screening techniques based on the quinolines antimalarials drugs mechanism have been developed during the recent years to assess the formation of hemozoin *in vitro* and screen compounds as inhibitors of the formation of hemozoin (Tripathi *et al*, 2001; Ncokazi and Egan, 2005).

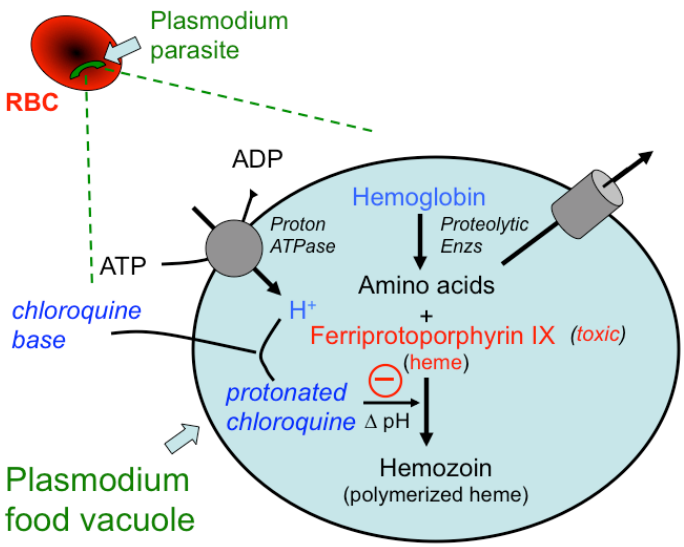

Figure 1.11 Quinoline antimalarials mode of action (from Ivers and Ryan, 2012)

1.2.8 Malaria and natural products

The two essential drugs used for the treatment of malaria, quinine and artesunate, are derived from the medicinal plants *Cinchona sp.* and *Artemisia annua* respectively. Plants

have been the source of medicines for humans and animals for centuries. Over a thousand-plant species are traditionally used for the treatment and prevention of malaria symptoms. Phytochemical studies of those plants led to the isolation of a range of compounds with potent antimalarial properties. Beaufay *et al*. (2018), Bero *et al*. (2010), and Kaur *et al*. (2009) have published comprehensive reviews (covering up to 2016) on natural occurring compounds from plants with promising antimalarial activities. More recently, the new tirucallane triterpene, *seco*-tiaminic acid B isolated from *Entandrophragma congoënse*, and the macrolide bastimolide B (Figure 1.12) isolated from the tropical marine cyanobacterium *Okeania hirsute* were found to possess antiplasmodial activity with IC_{50} values of 2.3 µg/mL and 5.7 µM, respectively (Happi *et al*., 2018; Shao *et al*., 2018).

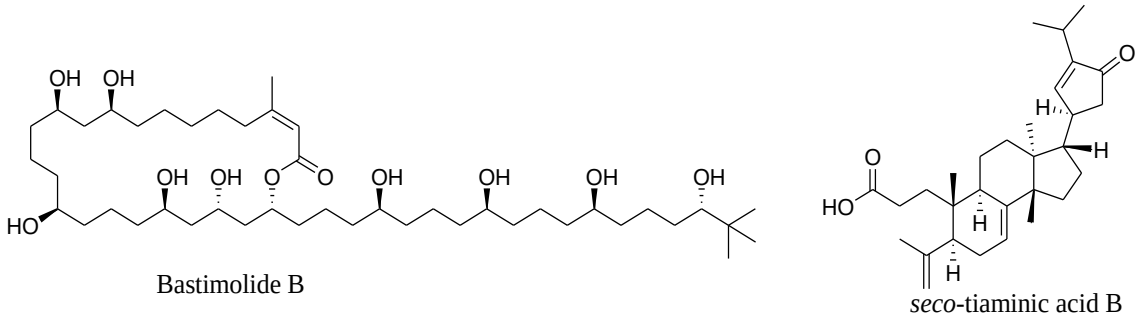

Figure 1.12 Recent antiplasmodial compounds from natural source

1.3 Natural products drug discovery

The use of medicinal plants in the treatment of human ailments can be traced for millennia (Solecki, 1975). Plants were used about 2600 B.C. in various forms including infusion, pills, ointments and oils gargles for the treatment of diverse ailments and cosmetics (Cragg and Newman, 2005b). Even today, plants are the almost exclusive source of healthcare for 80% of the world's population and particularly in developing countries (Ekor, 2014). On the international market, global trade of medicinal plants and related

products is estimated at about 40 billion GBP annually (Te, 2013). The knowledge associated with traditional medicine has promoted further investigations of medicinal plants as potential medicines (Dias *et al*., 2012). Phytochemical screenings show that antibacterial substances like alkaloids, flavonoids, glycosides, saponins and terpenoids are distributed in plant materials (Edeoga *et al*., 2005). Plant-derived compounds (phytochemicals) represent an interesting source of new bioactive agents (Ghosh *et al*., 2007). Almost 21% of drugs in use today are derived from natural products and 51% of the 1562 new chemical entities introduced between 1981 and 2014 can be traced to a natural product origin (Newman and Cragg, 2016). The ethnopharmacological properties of plants have been used as a primary foundation for early drug discovery (McRae *et al*., 2007). This has led to the discovery of the cancer drug Taxol isolated from the bark of *Taxus brevifolia* and the antimalarial drug quinine isolated from the bark of the *Cinchona* tree (Wani *et al*., 1971; Kremsner *et al*., 1994). Different approaches have so far been developed for drug discovery from natural products (the following will discuss the case of plants only) including random and non-random screenings such as taxonomic, chemotaxonomic, ethnobiological, metabolomic and information managed screening (Cordell *et al*., 1993; Schwikkard and Mulholland, 2014).

1.3.1 Random screening

Random screening is the arbitrary collection of a huge number of taxa for a large-scale screening (Balunas and Kinghorn, 2005). The plant kingdom comprises about 250,000 plant species on which only around 10% have been screened for their potential bioactivity (Iqbal *et al*., 2017). This approach is the method of choice in the absence of known taxa with the activity of interest. The collection process involves no intellectualization. All taxa are collected and screened irrespective of their usage. Bioassay-guided isolation is

used to identify the compounds of interest using various chromatographic and analytical techniques. Paclitaxel, sold under the brand name Taxol and used for the treatment of various types of cancer, was first isolated from the bark of *Taxus brevifolia* tree, collected in Washington State as part of a random screening approach carried out by the USA National Cancer Institute in their search for new anticancer drug (Wani *et al*., 1971; Cragg *et al*., 1993). Discovery of lead compounds by this approach is completely serendipitous and its success depends on the specificity of the bioassay and the volume of extracts available. In addition, random screening is time consuming, cost effective and only 1-5% of the collected samples screened usually show preliminary bioactive activity (DiMasi *et al*., 1991). However, with the advent of robotic and high throughput screening techniques the efficiency of random screening has increased, and it is now possible to carry out rapid and sensitive screening of high numbers of samples at low cost (Pereira and Williams, 2007).

1.3.2 Ethnobotanical screening

The ethnobotanical or ethnopharmacological screening is essentially based on the empirical usage of plants for therapeutic purposes. The decision to investigate a plant species is determined by the fact that the plant is already being used as medicine or as an insect repellent or for some cultural purpose (Gullo, 1994). The screening of the plant extracts and any isolated compounds is usually guided by what the plant is traditionally used for and any positive results would serve to validate the use of the plant traditionally as well as provide useful leads for further drug development. Several manuscripts describing the usage of plants for medicinal purposes, their dosage and mode of administration in various countries, notably in China, India, Mediterranean and South American countries are available. Ethnobotanical screening has been useful for the

discovery of lead compounds of valuable interest that have undergone chemical modifications to enhance their activity or reduce their toxicity. Fabricant and Farnsworth (2001) have demonstrated that 80% of the 94 medicinal plants from which 122 compounds have been isolated and used as drugs, have had an ethnomedical use identical or related to the current use of the active principle of the plant. In 1785, Withering, an English scientist, published a book on the use of the foxglove, *Digitalis purpurea*, for the treatment of heart disorders; the study of foxglove later led to the isolation of the cardiotonic agent, digitoxin (Fabricant and Farnsworth, 2001). There are many other significant drugs developed from traditional medicinal plants, e.g., quinine and artemisisin.

The main advantage of the ethnobotanical screening is that the active compounds isolated from a plant are likely to show the activity of interest than those derived from plant species with no history of human use. This approach is also valuable for the discovery of complex skeletons unconceivable during synthesis that can then been used as lead compounds for drug discovery. The main inconvenient with this approach is the inadequate design of ethnobotanical data collection, and the misinterpretation of the role medicinal plants play in the medical systems of local and indigenous communities (Etkin, 1993; De Albuquerque and Hanazaki, 2009). In addition, the plant identified may not contain any pharmacologically active compounds with the therapeutic effect observed being due the results of different factors (Moerman, 2007) including interactions with other components of the formulation as it is common for a secondary species of plant or additives such as wine to be added to complete the traditional formulation. Another limitation is the occurrence in the plant of compounds of interest at low concentration or as mixture of analogues making their separation difficult (Gullo, 1994).

1.3.3 Taxonomic and chemotaxonomic screening

Chemotaxonomic screening resides on the ability of plants from the same genus to biologically synthesize the same class of metabolites (Gullo, 1994). This approach then involves the study of species within a plant family or genera which are known to produce biologically active compounds such as alkaloids or flavonoids (Cordell *et al*., 1993). An example of drug, discovered using such approach, is digitoxin isolated from *Digitalis lanata*, a species from the same genus as *Digitalis purpurea* known to produce the cardiac glycoside digoxin (Farnsworth *et al*., 1985). This approach is useful for taxonomic study to characterize and classify plants in a family by generating a profile of their secondary metabolites. Compounds obtained are similar in structure and can be used for structure activity relationship studies (Gullo, 1994). The limitation of this approach is the variation of plant metabolites within the period of the year, site of collection and the absence of metabolites of interest due to mutations or genetic factors affecting the gene clusters responsible for their accumulation in the plant (Makins *et al*., 1983).

1.3.4 Virtual screening

Virtual Screening, which is also known as the 'information-managed approach' uses all available biological information and chemical data available in journals and databases to direct the search for new drugs (Cordell *et al*, 1993; Sarker and Nahar, 2018). This approach is useful in identifying structures that are more likely to bind to the target of interest (Rollinger *et al*., 2008). In addition to the panoply of articles published daily, there are several databases containing extensive libraries of compound properties as well as software programs available to simulate or predict the binding capability of a compound to the receptor or target of interest. NAPRALERT (Natural Product ALERT)

is the first of such databases, created and developed by Farnsworth and coworkers (Loub *et al*., 1985) which contains over 140,000 compounds isolated from natural sources. Other examples are the Combined Dictionary of Natural Products, Chemlab, ChEMBL and the Collaborative Drug Discovery (CDD) database. Such virtual screening approach is useful to identify active pharmacophores which may be optimised by chemical modification. The main benefit of this approach is to prevent the re-study of known compounds that have already been investigated. By dereplication strategies, databases are linked to hyphenated chromatographic methods e.g. CE-MS, GC-MS, HPLC-DAD-ESI-MS/MS, which allows the rapid identification of new chemical entities from complex matrices such as plant extracts. (Dinan, 2006; Sarker and Nahar, 2012). This virtual screening approach is very productive as evidenced by its use in the pharmaceutical industry (Cheng *et al*., 2012). However, it is expensive, time consuming and such databases must be highly collaborative and updated on a regular basis.

1.4 Cameroonian medicinal plants and their potential

Cameroon's population rely on medicinal plants for their primary healthcare. Indeed, due to the high cost of modern drugs, only 3 out of 20 patients can afford prescription drugs (Nkongmeneck *et al*., 2007; Kuete and Efferth, 2010). Cameroonian medicinal plants have exhibited a range of valuable activities including antimicrobial, antimalarial, antiproliferative, anti-inflammatory, antidiabetic, analgesic and antituberculotic (Kuete and Efferth, 2010). They have also shown to be rich in distinctive bioactive compounds (Kuete and Efferth, 2010; Ntie-Kang *et al*., 2013) such as michellamine B, an alkaloid isolated from the leaves of a Cameroonian native plant *Ancistrocladus korupensis* that has been found to be capable of the complete inhibition of cytopathic effects of HIV-1 and HIV-2 on human lymphoblastoid target cell *in vitro* (Boyd *et al*., 1994). Cameroonian

flora is rich with an estimated 7,850 known species of which only 37% have been studied (Onana, 2015). Additionally, current studies of Cameroonian medicinal plants continue to show that they are a potential rich source of biologically active compounds for the development of new medicines (Noté *et al*., 2016; Fankam *et al*., 2017; Happi *et al*., 2018).

1.5 Selected Cameroonian medicinal plants for this study

Plant materials were selected for this study based on ethnopharmacological information and an extensive literature survey. Plants used traditionally as remedies by local communities in Cameroon in their primary healthcare system for the treatment of malaria or anaemia related diseases were identified. Plants with minimal or no scientific data to validate their use were then selected and collected for further investigation. The following five plants belonging to four families were harvested: *Croton oligandrus* Pierre ex Hutch, *Pseudospondias microcarpa* (A. Rich.) Engl., *Ruspolia hypocrateriformis* (Vahl) Milne-Redh, *Zanthoxylum lepreurii* Guill. and Perr. and *Zanthoxylum zanthoxyloides* (Lam.) Zepern. and Timler.

1.5.1 *Croton oligandrus* Pierre ex Hutch

Scientific name	*Croton oligandrus* Pierre ex Hutch
Synonyms	*Croton oligandrum*
Family	Euphorbiaceae
Subfamily	Crotonoideae
English name	Croton **Tribe** Crotoneae
Vernacular name	Ebin (Cameroon)

Botanical description

Croton oligandrus Pierre ex Hutch (Figure 1.13) belongs to the Euphorbiaceae family. The Euphorbiaceae, also known as the spurge family, is the largest family of flowering plants of about 322 genera and 8910 (Webster, 1993). *Croton* is a genus with nearly 1300 species distributed in tropical and subtropical regions of the World (Berry *et al*., 2005). *C. oligandrus,* formally known as *Croton oligandrum*, is a tree of about 9-15 m high commonly found in western and central African secondary forests, especially in Cameroon and Gabon. Its leaves are sub-silvered underneath, oblong-elliptic or elliptic-lanceolate, sub-caudate and rounded at the base. The seeds are oblong, convex on the back, 12 mm long, 7 mm broad, slightly shining and a little wrinkled. The wood is white, and the bark has an ash-grey colour with a remarkable aromatic odour.


(a)


(b)

Figure 1.13 a) Ptericarp (scientific tropical archive, http://actd.iict.pt), and b) seeds of *C. oligandrus*

Ethnobotanical uses

Croton oligandrus is usually harvested in the wild for use as traditional medicine or as timber. In Cameroon, the bark decoction is taken orally to treat pneumonia and splenomegaly as well as for ritual practice (Jiofack *et al*., 2009; Mpondo *et al*., 2017). The same bark decoction is used in Gabon for the treatment of anaemia and colic (Betti,

2013). The powder is sniffed to treat nasal tumours and it is externally applied to treat scabies (Schmelzer, 2008).

Previous phytochemical investigations

Linalool **(1)** has been identified as the main constituent of *Croton* oil (Agnaniet *et al*., 2005). Abega *et al.* (2014) isolated the diterpenes 7-acetoxytrachiloban-18-oic acid **(2)**, crotonadiol **(3)**, crotonoligaketone **(4)**, crotonzambefuran **(5)** and imbricatadiol **(6)**, and the triterpenes 3-*O*-acetylaleuritolic acid **(7)**, lupeol **(8)**, β-sitosterol **(9)**, and stigmasterol **(10)** from the stem bark of *C. oligandrus* (Figure 1.14).

Previous pharmacological investigations

There is only one report which investigated the pharmacology of *C. oligandrus*. The stem bark's essential oil was screened for its antiradical and antioxidant activities, with no activity being found in both cases (Agnaniet *et al*., 2005).

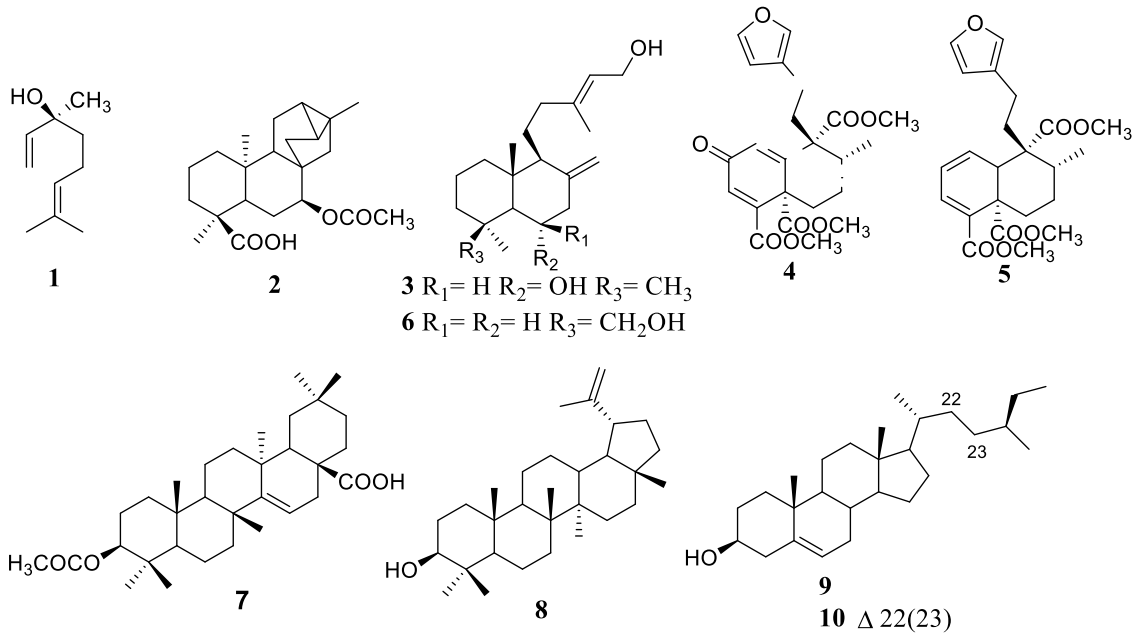

Figure 1.14 Isolated compounds from the bark of *C. oligandrus*

1.5.2 *Ruspolia hypocrateriformis* (Vahl) Milne-Redh

Scientific name	*Ruspolia hypocrateriformis* (Vahl) Milne-Redh
Synonyms	*Eranthemum affine* Spreng. *Eranthemum hypocrateriforme* (Vahl) R.Br. ex Roem.and Schult. *Justicia hypocrateriformis* Vahl *Pseuderanthemum hypocrateriforme* (Vahl) Radlk. *Siphoneranthemum hypocrateriforme* (Vahl) Kuntze
Family	Acanthaceae
Subfamily	Acanthoideae **Tribe** Justicieae
English name	Ruddy Rose, Pricklybush, Cameroun tea, blood tonic plant
Vernacular name	kifu ke menseh (Cameroon)

Botanical description

The Acanthaceae, acanthus family, is made up of 221 genera and 4000 species (Scotland and Vollesen, 2000). The family, distributed in tropical and subtropical regions of the World with a few species found in temperate regions, includes herbs, shrubs or rarely trees (Burch and Demmy, 1986). The *Ruspolia* comprises five species native to Africa with one species endemic to Madagascar (Milne-Redhead, 1936). *Ruspolia hypocrateriformis* (Vahl) Milne-Redh (synonym: *Justicia hypocrateriformis* Vahl) (Figure 1.15), is a shrub with scattered growth measuring above 1 m in height. The leaves are ovate or elliptic and glabrous when mature. The flowers are borne in showy terminal inflorescences with coral-red tubular flowers 3.75 cm long. (Burch and Demmy, 1986). Its natural habitat includes savanna, and secondary and deciduous forest areas from Senegal to west Cameroon, and it is dispersed to Uganda, Kenya and southern Africa (Milne-Redhead, 1936). In Cameroon, it is seen growing around homes and gardens.

Figure 1.15 Young flourishing plant of *R. hypocrateriformis* (Orji *et al.*, 2016)

Ethnobotanical uses

Ruspolia hypocrateriformis is a shrub used as ornamental and medicinal plant in Cameroon. The leaves are soaked or boiled in water, and the obtained juice is drunk to treat diarrhoea and anaemia (Adjanohoun *et al*., 1996; Noumi, 2015).

Previous phytochemical investigations

Phytochemical screening has revealed the presence of alkaloids, anthraquinones, flavonoids and saponins from the leaves of the species harvested in Cameroon (Agbor *et al*., 2014). Alkaloids and anthraquinones were absent from the Nigerian species (Orji *et al*., 2017). Pyrrolidine alkaloids including hypercratine **(11)**, norruspoline **(12)**, norruspolinone **(13)** and ruspolinone **(14)** have been isolated from the roots (Figure 1.16) (Roessler *et al*., 1978; Neukomm *et al*., 1983).

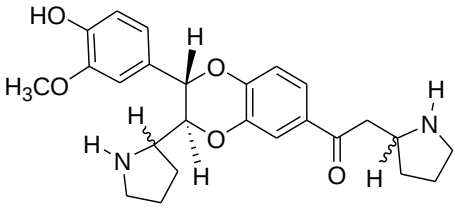

11

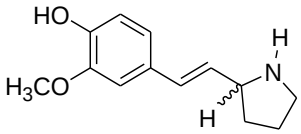

12

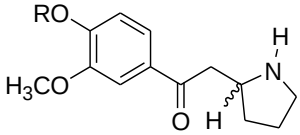

13 R= CH_3
14 R= H

Figure 1.16 Isolated compounds from the roots of *R. hypocrateriformis*

Previous pharmacological investigations

Previous pharmacological investigations revealed that *R. hypocrateriformis* aqueous extract possesses antidiarrhoeal activity supported by its antioxidant potential (Agbor *et al*., 2014) while a supplement of the hydro-ethanol extract daily may help in the management of lead poisoning (Orji *et al*., 2016).

1.5.3 *Pseudospondias microcarpa* (A. Rich.) Engl.

Scientific name	*Pseudospondias microcarpa* (A. Rich.) Engl.
Synonyms	*Sorindeia obliquifoliolata* Engl. *Spondias angolensis* O. Hoffm. *Spondias microcarpa* A. Rich.
Family	Anarcadiaceae
Subfamily	Spondiadoideae **Tribe** Spondiadeae
English name	African grape
Vernacular name	Gueme, Atom koe mpom (Cameroon)

Botanical description

The genus *Pseudospondias* belongs to the family Anacardiaceae. There are only two recognised species including *P. microcarpa* Engl. and *P. longifolia* Engl. distributed throughout sub-Sahara tropical Africa (Aubreville, 1950). *P. microcarpa* (A. Rich.) Engl. basionym *Spondias microcarpa* A. Rich. (Figure 1.17), is a spreading tree of up to 20 m high. The trunk is often irregular, twisted, the branches growing near the base and often covered with other plants. The leaves are oblong-ovate to elliptic, odd pinnate on stalks to 30 cm, with 2-8 pairs leaflets plus 1, each leaflet stalked, rather stiff, oval 5-20 cm, base very unequal, tip long pointed, darker above than below, the basal ones smaller. The

fruit are soft drupes measuring about 2.5 cm, red or blue-black when ripe are resinous, the stone inside is 4-sided and contains the seeds (Burkill, 1985).

Figure 1.17 Fruits and ptericarps of *P. microcarpa* (img. By J. Stevens, http://www.zambiaflora.com/speciesdata)

Ethnobotanical uses

Pseudospondias microcarpa produces edible fruits. The wood is soft and used as firewood, to produce charcoal and canoes (Ruffo *et al*., 2002). Many medicinal properties have been attributed to *P. microcarpa* across Africa. In Congo, the bark powder is used to treat scabies (Nglobua *et al*., 2013). The plant is also used for the treatment of malaria, dyspepsia, diarrhoea and opportunistic infections (Mbatchi *et al*., 2006; Bruno, 2013). The leaves decoction is drunk in Tanzania to relieve chronic cough and malaria (Kisangau *et al*., 2007). The wood is used as chewing stick in Benin while the bark decoction alleviates teeth problems (Adjanohoun *et al*., 1996; Akpona *et al*., 2009). In Sierra Leone, the bark and young leaves decoction is drunk to stimulate appetite (Macfoy, 2013). The plant is used in Ghana as a sedative and for treatment of diseases affecting the central nervous system (Burkill, 1985). The reddish resin contained in the bark is used in Liberia to treat jaundice and other diseases affecting the eyes (Burkill, 1985). The stem bark macerate is mixed with *Coster afer* and palm wine in Cameroon for the treatment of

helminthiasis and constipation (Noumi and Yomi, 2001). Other medicinal uses of the bark and leaves include the treatment of malaria, diabetes, anaemia, rheumatism, gonococci and elephantiasis (Burkill, 1985).

Previous phytochemical investigations

The presence of alkaloids, anthraquinones, cardiac glycosides, coumarins, flavonoids, polyphenols, quinones, saponins, tannins, and triterpenes were reported from the stem bark aqueous and MeOH-DCM extracts (Yondo *et al*., 2009). Alkaloids, tannins, terpenoids, steroids and heteroside cardiotonics have been reported from the leaves (Akpona *et al*., 2009).

Previous pharmacological investigations

The ethanolic extracts of the roots and stem bark of the plant harvested in Tanzania exhibited good antiplasmodial activity, with IC_{50} of 1.13 µg/mL and 4.33 µg/mL, respectively (Malebo *et al*., 2010). From the species harvested in Cameroon, the leaves and stem bark hydro-ethanolic extracts and the roots ethyl acetate extract showed moderate antimicrobial and antioxidant properties (Yondo *et al*., 2009). A moderate antiplasmodial activity against *Plasmodium* K1 strain and cytotoxic activity against HepG2 cell lines were also observed (Sidjui *et al*., 2016). *P. microcarpa* hydro-ethanolic extract possesses antidepressant-like effect, analgesic and anticonvulsant activities (Adongo *et al*., 2015). The extract has also showed anxiolytic-like activity similar to that of diazepam (Adongo *et al*., 2016).

1.5.4 *Zanthoxylum lepreurii* Guill. and Perr.

Scientific name	*Zanthoxylum lepreurii* Guill. and Perr.
Synonyms	*Fagara angolensis* Engl., *Fagara attiensis* Hutch. and Dalziel *Fagara beniensis* Engl., *Fagara membranifolia* Mildbr. *Fagara kibomboensis* De Wild., *Fagara nitens* (Hiern) Engl. *Fagara leprieurii* (Guill. and Perr.) Engl., *Fagara olung* Engl. *Fagara polyacantha* Engl., *Fagara stuhlmannii* (Engl.) Engl. *Zanthoxylum crenatum* A. Cheval., *Zanthoxylum nitens* Hiern *Zanthoxylum stuhlmannii* Engl., *Fagara kelekete* De Wild.
Family	Rutaceae
Subfamily	Toddalioideae **Tribe** Zanthoxyleae
English name	Satinwood, sand knobwood
Vernacular name	Melan, bongo (Cameroon)

Figure 1.18 Dried Fruits of *Z. leprieurii*

Botanical description

The genus *Zanthoxylum* L. belongs to the Rutaceae family and comprises about 200 species of pantropical trees. In Africa, the genus is represented by 35 species of economic importance for their usage as spice, edible fruit, medicinal plants and wood for

construction (Matu, 2011). The major characteristic of *Zanthoxylum* trees is that their trunks, branches, branchlets, leaf stalks and inflorescence axes are covered by prickles or spines (Adesina, 2005). *Zanthoxylum leprieurii* Guill. and Perr. is a medium tree of up to 15-25 m high found in rain forests and savanna woodland with brown branches armed with straight or sometimes curved spines (Tabuti, 2016). The leaves are alternate and impair-pinnate with 8-16 leaflets; leaflets are opposite or almost opposite, elliptical to oblong-elliptical, apex acuminate or caudate with oblique base. The flowers are unisexual, small and nearly sessile. Fruits (Figure 1.18) and seeds are almost globose measuring 4-5 mm and 3-3.5 mm in diameter, respectively. While the fruit are reddish and glandular pitted, the seeds are black and shiny. *Z. leprieurii* has a wide distribution and occurs from Senegal east to Ethiopia and south to Mozambique and eastern South Africa (Tabuti, 2016).

Ethnobotanical uses

The wood of *Z. leprieurii* is used in house and boat-building, carpentry, decorative and musical instrument construction and in the paper and pulp industry (Adesina, 2005). Different parts of the plant are traditionally used in Africa for medicinal purposes. The leaves are used for the treatment of stomatitis, gingivitis and bilharzia, while the roots are used as anti-ulcerative, antiseptic, urinary antiseptic, antisickling and antibacterial (Ngane *et al*., 2000). The stem bark is used as antimicrobial, digestive aid, antidiarrhoeic, anticancerous, anti-odontalgic and parasiticide (Ngoumfo *et al*., 2010). In Ghana, a decoction of the stem bark and root bark is used as a diuretic. The stem bark and leaves are used topically to treat wounds, syphilitic sores and leprous ulcers. The bark, when boiled in hot water produces vapour, which is inhaled to treat toothache and rheumatic pain. Decoction and poultice of stem bark is used for the treatment of skin and urinary tract infections, dysentery and intestinal worm infestation (Adesanya and Sofowora,

1983; Agyare *et al*., 2009). In Senegal, the powdered bark together with the latex of *Baissea axillaris* (Benth.) Hua is applied to tumours (Tabuti, 2016). In Cameroon, fruit are sold on local markets for their usage as spice (Ngoumfo *et al*., 2010). The leaves, stems and roots are used in the treatment of gonococci, urinary infections, dysentery, kidney pain and sterility (Noumi and Yomi, 2001). The fruit infusion is used for the treatment of sickle cell anaemia (Tabuti, 2016).

Previous phytochemical investigations

The phytochemistry of the *Zanthoxylum* genus has been thoroughly investigated in relation to its use for the treatment of sickle cell anaemia. Preliminary phytochemical screening of the stem bark aqueous-methanol extract of *Z. leprieurii* revealed the presence of alkaloids, flavonoids, carbohydrates and saponins (Tatsadjieu *et al*., 2003). Alkaloids such as aporphine, acridone, benzophenanthridine and quinoline derivatives were found to be the main constituents of the stem bark, pericarps, roots and fruit. Flavonoids, lignans and isobutylamides have also been reported. Table 1.2 summarises the isolated compounds (Figure 1.19) from *Z. leprieurii*. α-pinene **(62)**, (E)-*β*-ocimene **(63)**, limonene **(64)** and myrcene **(65)** (Figure 1.19) were found to be the major constituents of the fruit essential oil of *Z. leprieurii* (Fogang *et al*., 2012).

Previous pharmacological investigations

Zanthoxylum leprieurii fruit essential oil showed antimicrobial and antibacterial activity, inhibiting the growth of several microorganisms and bacteria strains (Tatsadjieu *et al*., 2003). The oil also possesses antioxidant, anti-inflammatory, antidermatophitic and moderate cytotoxic properties (Misra *et al*., 2013; Tchabong *et al*., 2017). The aqueous-methanol stem bark extract was found to have wound healing properties as well as antimicrobial, cytotoxic and antioxidant activities (Kuete *et al*., 2011; Agyare *et al*., 2014). The aqueous

ethanolic extracts of the leaves, roots and stem bark have demonstrated moderate antifungal activity while the chloroform extract of the fruit showed moderate toxicity with the brine-shrimp assay (Ngane *et al*, 2000; Ngoumfo *et al*, 2010). Acridone alkaloids, 1-hydroxy-3-methoxy-*N*-methylacridone **(16)**, arborinine **(13),** 1,3-dihydroxy-2-methoxy-*N*-methylacridone **(19)** and tegerrardin A **(26)** isolated from the fruit of *Z. leprieurii* were found to be moderately active against lung carcinoma cells (A549), colorectal adenocarcinoma cells (DLD-1) and normal cells (WS1) with IC_{50} values ranging from 27 to 77 µM (Ngoumfo *et al*., 2010; Kuete *et al*., 2011). Nitidine **(45)** demonstrated strong antileukemic activities against L1210 and P388 and showed growth inhibition of Lewis lung carcinoma (Wall *et al*., 1987). 2-Hydroxy-1,3-dimethoxy-*N*-methyl-9-acridone **(25)** and 3-hydroxy-1,5,6-trimethoxyacridone **(22)** showed good activity against pan-sensitive and resistant strains of *Mycobacterium tuberculosis* (Bunalema *et al*., 2017). Arborinine **(23)** and xanthoxoline **(27)** demonstrated good *in vitro* antiplasmodial activity against *Plasmodium falciparum* 3D7 strains with IC_{50} values of 4.5±1.0 and 4.6± 0.6 µg/mL, respectively (Tchinda *et al*., 2009). The same study reported arborinine **(23)** and tegerrardin A **(26)** as good chelating agents with 90% and 61% radical scavenging activity, respectively (Tchinda *et al*., 2009).

Table 1.2 Secondary metabolites isolated from *Z. leprieurii*

Isolated compounds	Plant parts	References
Acridone alkaloids		
1-Hydroxy-3,4-dimethoxy-*N*-methylacridone **(15)**	Fruits, roots	(Fish and Waterman, 1972a; Tchinda *et al*., 2009)
1-Hydroxy-3-methoxy-*N*-methylacridone **(16)**	Fruits, roots and stem bark	(Adesina, 2005; Ngoumfo *et al*., 2010; Bunalema *et al*., 2017)

Table 1.2 *continued*

1-Hydroxy-*N*-methylacridone **(17)**	Fruits, roots and stem bark	(Adesina, 2005)
1,2-Dihydroxy-3-methoxy-*N*-methylacridone **(18)**	Fruits and roots	(Ngoumfo *et al*., 2010)
1,3-Dihydroxy-2-methoxy-*N*-methylacridone **(19)**	Fruits and roots	(Ngoumfo *et al*., 2010)
1,3-Dihydroxy-4-methoxy-*N*-methylacridone **(20)**	Roots	(Fish and Waterman, 1972b)
2-Hydroxy-1,3-dimethoxy-N-methyl-acridone **(21)**	Stem bark	(Bunalema *et al*., 2017)
3-Hydroxy-1,5,6-trimethoxy-acridone **(22)**	Fruits and stem bark	(Wouatsa *et al*., 2013a; Bunalema *et al*., 2017)
Arborinine **(23)**	Fruits and roots	(Tchinda *et al*., 2009; Ngoumfo *et al*., 2010)
Helebelicine A **(24)**	Fruits	(Ngoumfo *et al*., 2010)
Helebelicine B **(25)**	Fruits	(Ngoumfo *et al*., 2010)
Tegerrardin A **(26)**	Fruits and roots	(Tchinda *et al*., 2009; Ngoumfo *et al*., 2010)
Xanthoxoline **(27)**	Fruits, roots and stem bark	(Adesina, 2005; Tchinda *et al*., 2009; Ngoumfo *et al*., 2010)
Alkamides		
(2*E*,4*E*)-*N*-Isobutyleicosa-deca-2,4-dienamide **(28)**	Roots	(Adesina, 2005)
(2*E*,4*E*,8*E*,10*E*,12*E*)-*N*-Isobutyl-2,4,8,10,12-tetradecapentaenamide **(29)**	Roots	(Adesina, 2005)
N-Isopentyl-cinnamamide **(30)**	Roots	(Adesina, 2005)
N-Docosanoyltyramine **(31)**	Fruits and roots	(Ngoumfo *et al*., 2010)
Violyedoenamide **(32)**	Fruits and roots	(Ngoumfo *et al*., 2010)

Table 1.2 *continued*

Aporphine alkaloids		
Magnoflorine **(33)**	Roots and stem bark	Adesina, 2005
N-Methylcorydine **(34)**	Roots	Adesina, 2005
Tembetarine **(35)**	Roots and stem bark	(Fish and Waterman, 1972b)
Benzophenanthridine alkaloids		
10-*O*-Demethyl-12-*O*-methylarnottianamide **(36)**	Roots	(Ngoumfo *et al*., 2010)
10-*O*-Demethyl-12-*O*-methylisoarnottianamide **(37)**	Roots	(Ngoumfo *et al*., 2010)
Angoline **(38)**	Fruits and roots	(Ngoumfo *et al*., 2010)
Arnottianamide **(39)**	Roots	(Adesina, 2005)
Chelerythrine **(40)**	Roots and stem bark	(Adesina, 2005)
Decarine **(41)**	Fruits and roots	(Ngoumfo *et al*., 2010)
Dihydroavicine **(42)**	Roots	(Adesina, 2005)
Dihydronitidine **(43)**	Fruits and roots	(Ngoumfo *et al*., 2010)
Fagaronine **(44)**	Roots	(Adesina, 2005)
Nitidine **(45)**	Roots and stem bark	(Adesina, 2005; Ngoumfo *et al*., 2010)
Norchelerythrine **(46)**	Roots	(Adesina, 2005)
Coumarins		
6,7-Dimethylcoumarin **(47)**	Fruits and roots	(Ngoumfo *et al*., 2010)
6,7,8-Trimethoxycoumarin **(48)**	Bark	(Eshiet and Taylor, 1968)
7, 8-Dimethoxycoumarin **(49)**	Fruits	(Misra *et al*., 2013)

Table 1.2 *continued*

Scoparone **(50)**	Roots and stem bark	(Adesina, 2005; Tchinda *et al*., 2009)
Xanthotoxin **(51)**	Roots and stem bark	Adesina, 2005
Lignans		
Asarinin **(52)**	Roots	(Adesina, 2005)
Lirioresinol-B-dimethyl ether **(53)**	Roots	(Adesina, 2005)
Sesamin **(54)**	Fruits, roots and stem bark	(Adesina, 2005; Ngoumfo *et al*., 2010)
Quinoline alkaloids		
Skimmianine **(55)**	Roots	Adesina, 2005
Triterpenes		
β-Sitosterol **(9)**	Fruits	(Ngoumfo *et al*., 2010)
β-Sitosterol palmitate **(56)**	Bark	(Eshiet and Taylor, 1968)
Lupeol **(8)**	Fruits and roots	(Ngoumfo *et al*., 2010)
Other compounds		
Candicine **(57)**	Stem bark and roots	(Fish and Waterman, 1972a)
Glucose **(58)**	Fruits and roots	(Ngoumfo *et al*., 2010)
Hesperidin **(59)**	Fruits and roots	(Ngoumfo *et al*., 2010)
Sacchore **(60)**	Fruits and roots	(Ngoumfo *et al*., 2010)
Sinapic acid **(61)**	Fruits	(Misra *et al*., 2013)

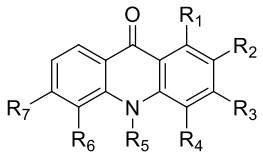

15 R_1= OH R_2= H R_3= R_4= OCH_3 R_5= CH_3 R_6= R_7= H
16 R_1= OH R_2= H R_3= OCH_3 R_4= H R_5= CH_3 R_6= R_7= H
17 R_1= OH R_2= R_3= R_4= H R_5= CH_3 R_6= R_7= H
18 R_1= OH R_2= OH R_3= OCH_3 R_4= H R_5= CH_3 R_6= R_7= H
19 R_1= OH R_2= OCH_3 R_3= OH R_4= H R_5= CH_3 R_6= R_7= H
20 R_1= OH R_2= H R_3= OH R_4= OCH_3 R_5= CH_3 R_6= R_7= H
21 R_1= OCH_3 R_2= R_3= R_4= H R_5= R_6= OCH_3 R_7= H
22 R_1= OCH_3 R_2= H R_3= OH R_4= R_5= H R_6= R_7= OCH_3
23 R_1= OH R_2= R_3= OCH_3 R_4= R_5= CH_3 R_6= R_7= H
24 R_1= OCH_3 R_2= H R_3= OH R_4= OCH_3 R_5= CH_3 R_6= R_7= H
25 R_1= R_2= OCH_3 R_3= OH R_4= H R_5= CH_3 R_6= R_7= H
26 R_1= OCH_3 R_2= H R_3= OH R_4= H R_5= CH_3 R_6= R_7= H
27 R_1= OH R_2= R_3= OCH_3 R_4= R_5= H R_6= R_7= H

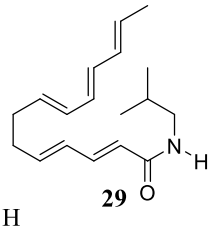

29

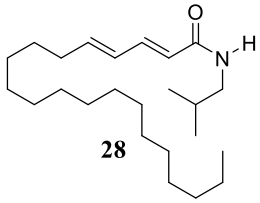

28

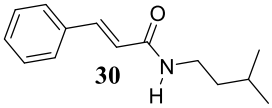

30

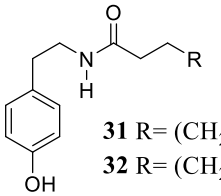

31 R= $(CH_2)_{18}CH_3$
32 R= $(CH_2)_{20}CH_3$

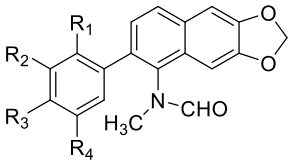

36 R_1= OCH_3 R_2= OCH_3 R_3= OH R_4= H
37 R_1= OCH_3 R_2= H R_3= OH R_4=OCH_3
38 R_1= OH R_2= OCH_3 R_3=OCH_3 R_4= H

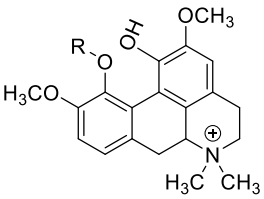

33 R= H
34 R= CH_3

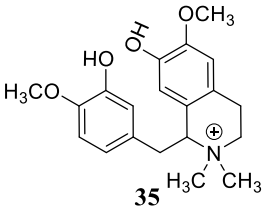

35

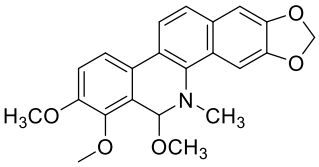

39

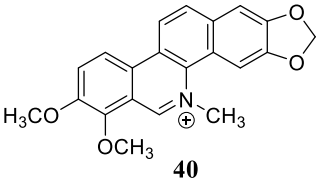

40

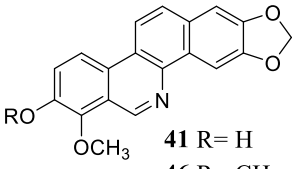

41 R= H
46 R= CH_3

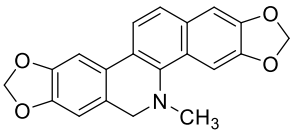

42

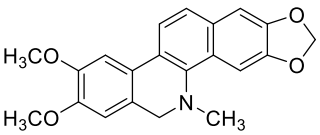

43

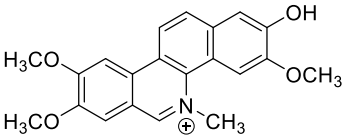

44

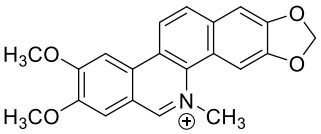

45

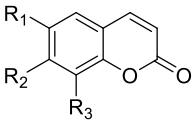

47 R_1= R_2= CH_3 R_3= H
48 R_1= R_2= R_3= OCH_3
49 R_1= H R_2= R_3= OCH_3
50 R_1= R_2= OCH_3 R_3= H

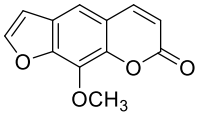

51

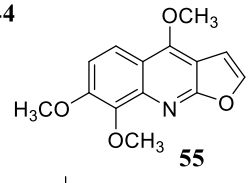

55

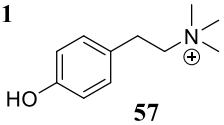

57

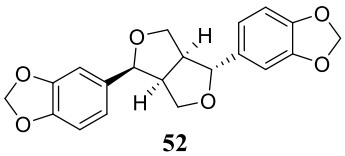

52

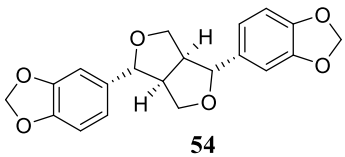

54

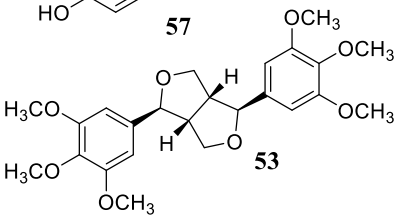

53

Figure 1.19 Isolated compounds from *Z. leprieurii*

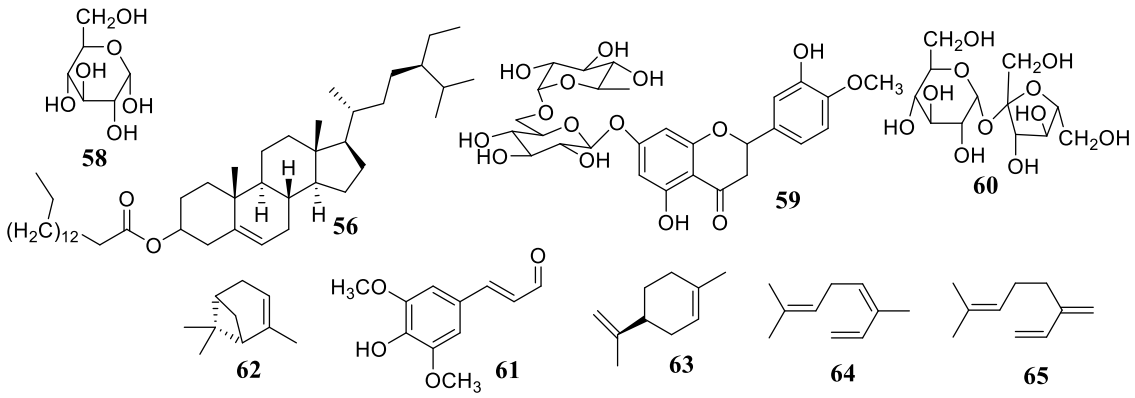

Figure 1.19 *continued*

1.5.5 *Zanthoxylum zanthoxyloides* (Lam.) Zepern. and Timler

Scientific name	*Zanthoxylum zanthoxyloides* (Lam.) Zepern. and Timler
Synonyms	*Fagara senegalensis* (DC.) A. Chev. *Fagara zanthoxyloides* Lam. *Zanthoxylum senegalense* DC *Zanthoxylum polyganum* Schum.
Family	Rutaceae
Subfamily	Toddalioideae **Tribe** Zanthoxyleae
English name	Candlewood
Vernacular name	Nwah che (Cameroon)

Botanical description

Zanthoxylum zanthoxyloides is a small tree of up to 6-12 m tall widespread in Africa savanna and dry forest vegetations (Matu, 2011). The trunk is spiny with straight, often short bole and rounded and a quite dense crown. The bark is grey to beige, rough, with fine vertical fissures, often with woody prickle-bearing protuberances; the slashes are yellow, odorous, orange-mottled beneath while the stems are glabrous, grey, with solitary prickles. The leaves are alternate, glabrous, impari-pinnate with 5-7(-11) opposite or

alternate leaflets, up to 12(-20) cm long; leaflets are obovate to elliptical, 5-10 cm x 2-4 cm, with cuneate to rounded base, obtuse or rounded apex, sometimes apiculate or notched, with many glandular dots, smelling of pepper and lemon when crushed, rigidly papery, pinnately veined with 10-14 pairs of lateral veins, barely prominent, fusing near the margin. The flowers are unisexual, regular, white or greenish, sessile; corolla barely open; Male flowers pentamerous. Petals imbricate. Rudiment of pistil subulate, upon a thickened central disk. The fruits (Figure 1.20) are rather crowded, in paniculate clusters shorter than the leaves, 1-carpellary, 1-seeded. Seeds are shining, blue-black; fruits contain an ovoid follicle, 5-6 mm in diameter, brown, with glandular dots, dehiscent, 1-seeded (Burkill, 1985).

Figure 1.20 Dried Fruits of *Z. zanthoxyloides*

Ethnobotanical uses

Zanthoxylum zanthoxyloides as the other African *Zanthoxylum* species has a broad spectrum of ethnopharmacological usage across Africa. In Ouganda, the root-bark extract is used in treating elephantiasis, toothache, impotence, gonorrhoea, malaria, dysmenorrhoea and abdominal pain (Adjanohoun *et al*., 1993). In Senegal, the plant is used in the treatment of enteritis, dysentery, diarrhoea, guinea worm, urethritis and as an

anti-odontalgic. In Cameroon, the leaves, stems and roots of these plants are used in the treatment of gonococci, urinary infections and dysentery (Noumi and Yomi, 2001). The seeds are used as spices. Leaves and bark are used for the treatment of cough, fever, colds, toothache and snake bites. The leaves are also used as scaring, antiseptic, astringent and laxative, while the stem bark is used as antirheumatic, anti-odontalgic, diuretic, urinary antiseptic, digestive aid and parasticide. The roots are used as antiseptic, antisickler, digestive aid and parasticide (Ngane *et al*., 2000; Kassim *et al*., 2004). In Ivory Coast, sap from the pulped bark is applied as eye drops to treat eye infections. In Ghana, roots and stem bark powder is taken to treat whooping cough (Arbonnier, 2004). In Nigeria, stem bark and roots decoction are drunk to treat cancer. Roots and stem bark of *Z. zanthoxyloides* are also used as chewing sticks for teeth cleaning (Arbonnier, 2004).

Previous phytochemical investigations

Zanthoxylum zanthoxyloides is a rich source of bioactive metabolites including alkaloids, aliphatic and aromatic amides, lignans, coumarins, sterols and carbohydrate residues (Figure 1.21). A list of isolated compounds from different parts of the plant as well as their activities is presented in Table 1.3. The main constituents of the fruit essential oils were found to be α-pinene **(62)**, (*E*)-*β*-ocimene **(63)**, citronellal **(143)**, citronellol **(144)**, citronellyl acetate **(145)**, geraniol **(146)**, limonene **(64)** and myrcene **(65)** (Figure 1.21) (Tatsadjieu *et al*., 2003; Fogang *et al*., 2012).

Previous pharmacological investigations

Zanthoxylum zanthoxyloides has demonstrated a panel of biological activities. The plant powder and extract have good insecticidal and antifeedant activities against a range of crop pests (Ojo *et al*., 2016). The fruit essential oil possesses antimicrobial, antibacterial, insecticidal and antioxidant properties (Tatsadjieu *et al*., 2003; Fogang *et al*., 2012).

Roots and stem bark methanolic extracts were found to be least toxic with LD_{50} 5.0 g/Kg and 1.5 mg/kg body weight, respectively in Wistar rats and the ethanolic extracts have moderate antifungal activity (Ngane *et al*., 2000; Misra *et al*., 2013). The crude alkaloid extracts obtained from the trunk bark demonstrated good antimalarial activity with IC_{50} ranging from 1.91 to 4.32 µg/mL (Gansane *et al*., 2010). The DCM extract of the stem and roots bark and the methanol extract of the stem bark have also been found to possess good antiplasmodial activity with IC_{50} ranging from 1 and 10 µg/mL. Extract of the root bark has also demonstrated significant anti-inflammatory, anti-sickling and analgesic activities and moderate antibacterial, antiprotozoal and antiviral activities against a range of pathogenic bacteria, *Herpes simplex* virus and *Leishmania major* (Kassim *et al*., 2005; Ahua *et al*., 2007; Barnabas *et al*., 2011). Extract of the root bark is also reported to have gastroprotective activity (Boye *et al*., 2012). Ethanolic extract of the leaves has shown antifungal, anthelmintic, antidiabetic, hypolipidaemic and antioxidant activities (Aloke *et al*., 2012; Adekunle *et al*., 2014). A moderate cytotoxic activity of the fruits ethanolic extract has also been reported (Choumessi *et al*., 2012).

The acridones 3,4,5,7-tetrahydroxy-1-methoxy-*N*-methylacridone **(67)** has been found to possess a moderate antibacterial activity against *Micrococcus luteus* and *Pseudomonas aeruginosa* and 3-hydroxy-1,5,6-trimethoxy-acridone **(22)** showed moderate cytotoxic effect against liver cancer cell line WRL-68 (Wouatsa *et al*., 2013a). Furoquinoline alkaloid atanine **(128)** possessed antiprostaglandin synthetase activity (Prempeh and Mensah-Attipoe, 2009). Fagaronine **(44)**, 2-hydroxymethylbenzoic acid **(109)**, burkinabins A, B and C **(111-113)** have demonstrated strong antileukaemic acid justifying of the usage of *Z. zanthoxyloides* plant in the traditional treatment of sickle cell anaemia (Adesina, 2005; Ouattara *et al*., 2009). Chelerythrine **(40)**, berberine **(90)** and 6-canthinone **(136)** possessed antimicrobial activity (Adesina, 2005).

Table 1.3 Secondary metabolites isolated from *Z. zanthoxyloides*

Isolated/identified compounds	Plant parts	References
Acridone alkaloids		
1-Hydroxy-3-methoxy-*N*-methylacridone **(16)**	Fruits	(Wouatsa *et al*., 2013a)
1,6-Dihydroxy-3-methoxy-acridone **(66)**	Fruits	(Wouatsa *et al*., 2013a)
3-Hydroxy-1,5,6-trimethoxy-acridone **(22)**	Fruits	(Wouatsa *et al*., 2013a)
3,4,5,7-Tetrahydroxy-1-methoxy-10-methyl-9-acridone **(67)**	Fruits	(Wouatsa *et al*., 2013a)
4-Hydroxyzanthacridone **(68)**	Fruits	(Wouatsa *et al*., 2013a)
4-Hydroxyzanthacridon-(2,4')-oxide **(69)**	Fruits	(Wouatsa *et al*., 2013a)
4-Methoxyzanthacridone **(70)**	Fruits	(Wouatsa *et al*., 2013a)
Helebelicine A **(24)**	Fruits	(Wouatsa *et al*., 2013a)
Alkamides		
(2*E*,4*E*)-*N*-Isobutyldeca-2,4-dienamide **(71)**	Roots	(Chaaib *et al*., 2003)
(2*E*,4*E*)-*N*-Isobutylhexadeca-2,4-dienamide **(72)**	Fruits, roots and bark	(Adesina, 2005)
(2*E*,4*E*)-*N*-isobutylocta-2,4-dienamide **(73)**	Roots	(Chaaib *et al*., 2003)
(2*E*,4*E*)-*N*-Isobutyltetradeca-2,4-dienamide **(74)**	Fruits	(Adesina, 2005)
(2*E*,4*E*,8*E*,10*E*,12*E*)-*N*-Isobutyl-2,4,8,10,12-tetradecapentaenamide **(29)**	Roots	(Adesina, 2005)
Cis-fagaramide **(75)**	Roots and stem bark	(Chaaib *et al*., 2003; Adesina, 2005)
N-Isopentylcinnamamide **(30)**	Roots	(Adesina, 2005
Pellitorine **(76)**	Roots	(Adesina, 2005)
Piperlonguminine **(77)**	Roots	(Adesina, 2005)
Rubebmamin **(78)**	Roots and stem bark	(Adesina, 2005; Oriowo, 1982)
Trans-fagaramide **(79)**	Roots	(Chaaib *et al*., 2003; Queiroz *et al*., 2006)

Table 1.3 *continued*

Aporphine alkaloids		
Berberine **(80)**	Roots	(Adesina, 2005)
Magnoflorine **(33)**	Roots	(Adesina, 2005)
N-Methylcorydine **(34)**	Roots	(Adesina, 2005)
N, *N*-Dimetylindicarpine **(81)**	Roots	(Queiroz *et al*., 2006)
Tembetarine **(35)**	Roots	(Adesina, 2005)
Benzophenanthridine alkaloids		
6-(2-Oxobutyl)-dihydrochelerythrine **(82)**	Roots	(Chaaib *et al*., 2003)
6-Acetonyldihydrochelerythrine **(83)**	Roots	(Chaaib *et al*., 2003)
6-Ethoxychelerythrine **(84)**	Roots bark	Torto *et al*., 1966
6-Hydroxydihydrochelerythrine **(85)**	Roots	(Wangensteen *et al*., 2017)
Bis-Dihydrochelerythrinyl ether **(86)**	Roots	(Adesina, 2005)
Arnottianamide **(38)**	Roots	(Adesina, 2005)
Buesgenine **(87)**	Roots	(Wangensteen *et al*., 2017)
Chelerythrine **(40)**	Roots	(Torto *et al*., 1966)
Dihydroavicine **(42)**	Roots	(Adesina, 2005)
Dihydrochelerythrine **(88)**	Stem bark	(Torto *et al*., 1973)
Fagaridine **(89)**	Stem bark	(Torto *et al*., 1973)
Fagaronine **(34)**	Roots and stem bark	(Queiroz *et al*., 2006)
Norchelerythrine **(36)**	Roots	(Queiroz *et al*., 2006)
Oxychelerythrine **(90)**	Roots	(Adesina, 2005)
Coumarins		
4-Methoxycoumarin **(91)**	Fruits	(Tine *et al*., 2017)
6-Methylcoumarin **(92)**	Fruits	(Tine *et al*., 2017)
6,7-Dimethylesculetin **(47)**	Fruits	(Tine *et al*., 2017)
6,7,8-Trimethoxycoumarin **(48)**	Roots	(Wangensteen *et al*., 2017)

Table 1.3 *continued*

7-Methylcoumarin **(93)**	Fruits	(Tine *et al*., 2017
Bergapten **(94)**	Fruits and stem bark	(Adesina, 2005)
Daphnetin-7-methylether **(95)**	Fruits and stem bark	(Tine *et al*., 2017)
Herniarin **(96)**	Fruits and stem bark	(Tine *et al*., 2017)
Isobergapten **(97)**	Fruits	(Tine *et al*., 2017)
Isopimpinellin **(98)**	Fruits and leaves	(Tine *et al*., 2017)
Imperatorin **(99)**	Stem bark	(Adesina, 2005)
Marmesin **(100)**	Fruits	(Adesina, 2005)
Pimpinellin **(101)**	Stem bark	(Adesina, 2005)
Psoralen **(102)**	Fruits	(Adesina, 2005)
Scoparone **(50)**	Fruits, roots and bark	(Adesina, 2005; Misra *et al*., 2013
Scopoletin **(103)**	Stem bark	(Adesina, 2005)
Umbelliferone **(104)**	Stem bark	(Adesina, 2005)
Xanthotoxin **(51)**	Fruits and stem bark	(Adesina, 2005)
Lignans		
Asarinin **(52)**	Roots	(Adesina, 2005)
Sesamin **(54)**	Roots	(Chaaib *et al*., 2003)
Xanthoxylol **(105)**	Roots	(Elujoba and Nagels, 1985)
Triterpenes		
β-Amyrin **(106)**	Roots	(Adesina, 2005)
β-Sitosterol **(9)**	Fruits and roots	(Chaaib *et al*., 2003; Misra *et al*., 2013)
Campesterol **(107)**	Roots	(Adesina, 2005)
Lupeol **(8)**	Fruits and roots	(Chaaib *et al*., 2003; Misra et al., 2013)
Squalene **(108)**	Roots	(Adesina, 2005)
Stigmasterol **(10)**	Fruits and roots	(Chaaib *et al*., 2003; Adesina, 2005; Misra *et al*., 2013)

Table 1.3 *continued*

Phenolic and flavonoids		
2-Hydroxymethylbenzoic acid **(109)**	Roots	(Adesina, 2005)
2,5-Dihydroxybenzoic acid **(110)**	Leaves	(Isaac *et al*., 2009
Burkinabin A **(111)**	Roots	(Ouattara *et al*., 2004; Queiroz *et al*., 2006)
Burkinabin B **(112)**	Roots	(Ouattara *et al*., 2004)
Burkinabin C **(113)**	Roots	(Ouattara *et al*., 2004; Queiroz *et al*., 2006)
Caffeic acid **(114)**	Leaves and stem bark	(Asante *et al*., 2009)
Chlorogenic acid **(115)**	Stem bark, roots	(Wangensteen *et al*., 2017)
Diosmin **(116)**	Roots	(Adesina, 2005)
Gallic acid **(117)**	Leaves	(Asante *et al*., 2009)
Hesperidin **(59)**	Roots	(Queiroz *et al*., 2006)
Kaempferol **(118)**	Stem bark	(Ogunbolude *et al*., 2014)
Neochlorogenic acid **(119)**	Roots	(Wangensteen *et al*., 2017)
para-Coumaric acid **(120)**	Leaves	(Asante *et al*., 2009)
para-Hydroxybenzoic acid **(121)**	Roots	(Elujoba and Nagels, 1985)
Quercetin **(122)**	Stem bark	(Ogunbolude *et al*., 2014)
Rosmaniric acid **(123)**	Leaves	(Asante *et al*., 2009)
Rutin **(124)**	Stem bark	(Ogunbolude *et al*., 2014)
Syringic acid **(125)**	Leaves	(Elujoba and Nagels, 1985; Asante *et al*., 2009)
Vanillic acid **(126)**	Leaves, roots	(Asante *et al*., 2009; Elujoba and Nagels, 1985)
Quinoline alkaloids		
Acronycine **(127)**	Fruits and roots	(Adesina, 2005)
Atanine **(128)**	Ptericarps, Stem bark and roots	(Torto *et al*., 1973; Adesina, 2005)

Table 1.3 *continued*

Dictamnine **(129)**	Roots	(Wangensteen *et al*., 2017)
Fagarine **(130)**	Roots	(Adesina, 2005)
Skimmianine **(55)**	Roots	(Adesina, 2005)
Other compounds		
(-)-*p*-Synephrine **(131)**	Roots	(Wangensteen *et al*., 2017)
4-Methylthiocanthin-6-one **(132)**	Fruits and roots	(Adesina, 2005)
4'-(3"-Methylbut-2"-enyloxy)-3-phenylpropanol **(133)**	Roots	(Chaaib *et al*., 2003)
4'-(4''-Hydroxy-3''-methyl-butyloxy)-2-phenylethyl **(134)**	Roots	(Chaaib *et al*., 2003)
5-Methoxycanthin-6-one **(135)**	Fruits and roots	(Adesina, 2005)
6-Canthinone **(136)**	Roots	(Adesina, 2005)
7,8-Di-*O*-(3-methoxy-4-hydroxybenzoyl)-2,5-dihydroxycyclooctane-1,6-endoperoxyde **(137)**	Roots bark	(Chaaib *et al*., 2003)
p-Mentha-1,8-dien-9-ol **(138)**	Fruits	(Misra *et al*., 2013)
Cuspidiol **(139)**	Roots	(Chaaib *et al*., 2003)
Dihydrocuspidiol **(140)**	Roots	(Chaaib *et al*., 2003)
Germacrone **(141)**	Roots	(Adesina, 2005)
Zantholic acid **(142)**	Fruits	(Wouatsa *et al*., 2013b)

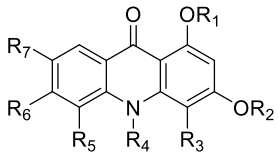

66 R_1= R_3= R_4= R_5= R_7= H R_2= CH_3 R_6= OH
67 R_1= R_4= CH_3 R_2= R_6= H R_3= R_5= R_7= OH

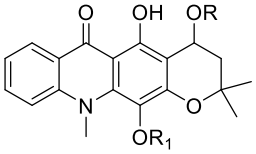

68 R= R_1= H
70 R= H R_1= Me

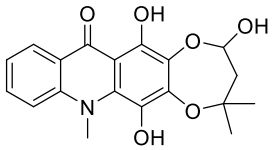

69

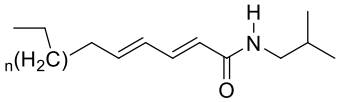

71 n= 2 **72** n= 8 **73** n= 10
74 n= 6 **76** n= 1

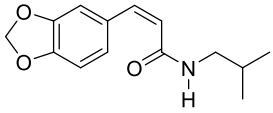

75

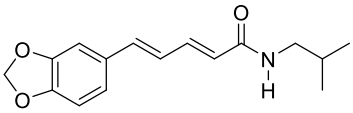

77

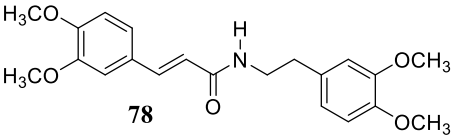

78

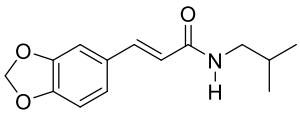

79

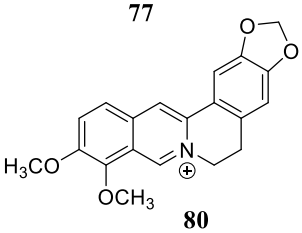

80

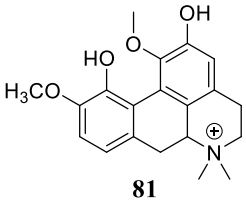

81

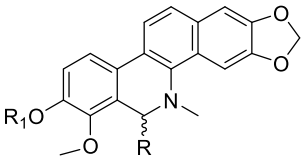

82 R= 2-oxobutyl R_1= CH_3
83 R= acetonyl R_1= CH_3
84 R= OCH_2CH_3 R_1= CH_3
85 R= OH R_1= CH_3
87 R= OH R_1= H
88 R= H R_1= CH_3
90 R= O R_1= CH_3

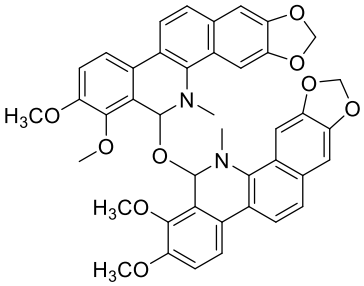

86

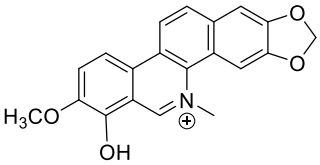

89

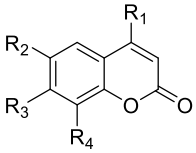

91 R_1= OCH_3 R_2= R_3= R_4= H
92 R_1= H R_2= OCH_3 R_3= R_4= H
93 R_1= R_2= H R_3= OCH_3 R_4= H
95 R_1= R_2= H R_3= OCH_3 R_4= OH
96 R_1= R_2= H R_3= OCH_3 R_4= H
103 R_1= R_4= H R_2= OCH_3 R_3= OH
104 R_1= R_2= H R_3= OH R_4= H

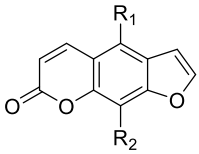

94 R_1= OCH_3 R_2= H
98 R_1= OCH_3 R_2= OCH_3
99 R_1= H R_2= isoprenyl
102 R_1= R_2= H

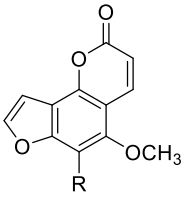

97 R= H
101 R= OCH_3

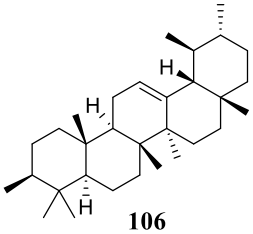

106

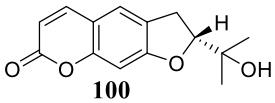

100

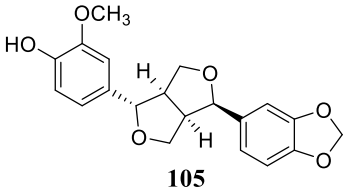

105

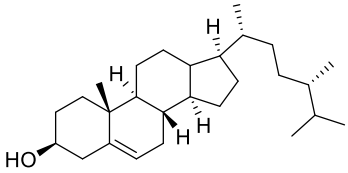

107

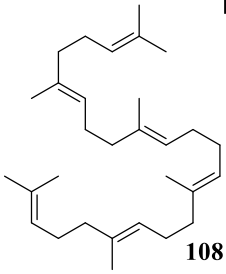

108

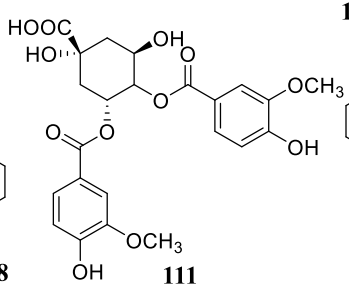

111

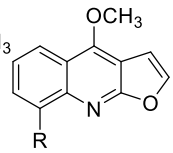

138 R= H
136 R= OCH_3

Figure 1.21 Identified and isolated compounds from *Z. zanthoxyloides*

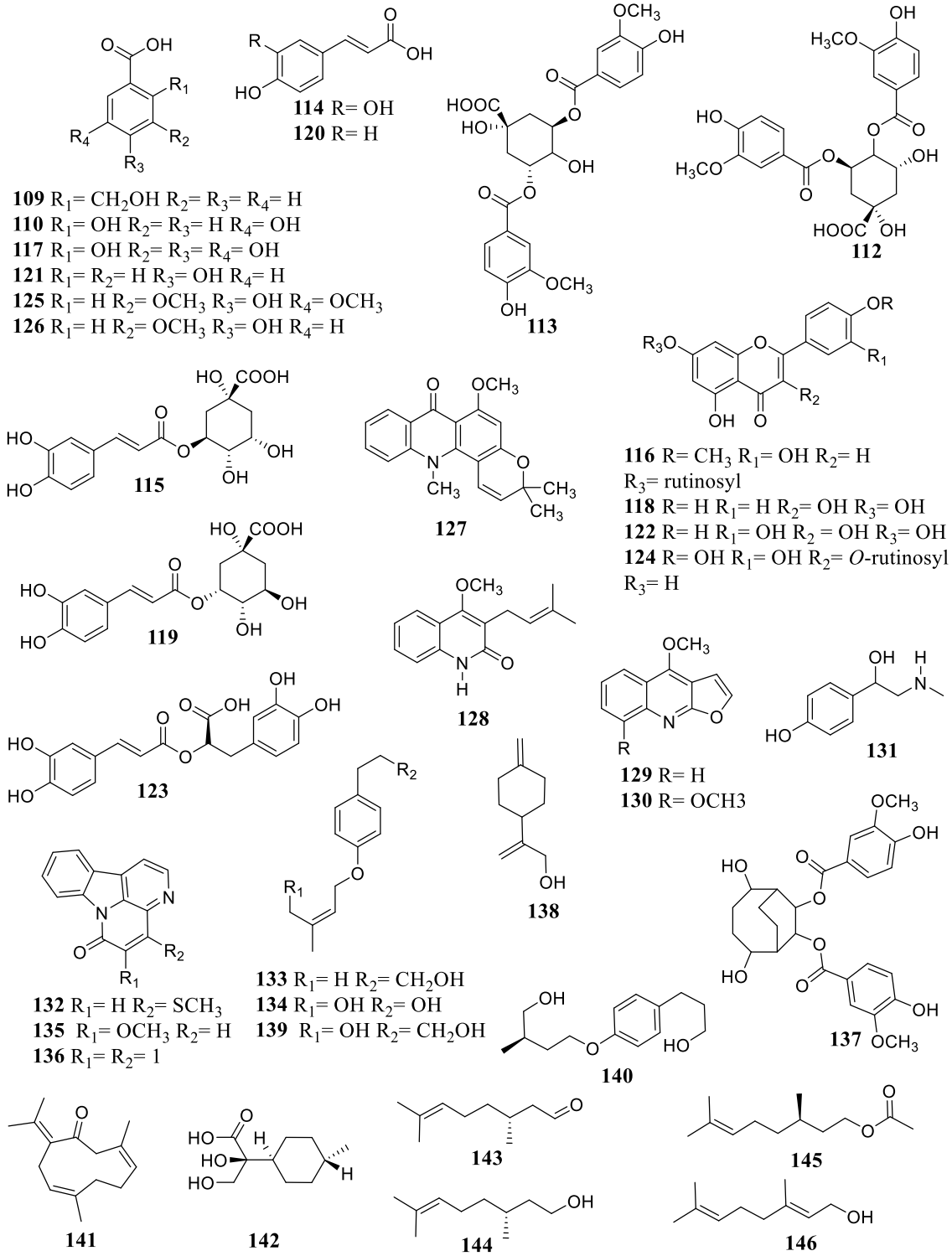

Figure 1.21 *Continued*

1.6 Aim and objectives

Despite important medical and technological advances made in the development of new drugs, as well as considerable efforts in the treatment and the campaign against cancer and malaria, they remain two of the most commoncauses of death worldwide. About 200 million cases of malaria are reported every year giving rise to an estimated 445,000-500,000 deaths yearly (WHO, 2017). The burden of the disease is boosted by the resistance of the parasites to existing antimalarial drugs and by the resistance of the mosquito vector to insecticides in endemic areas particularly in sub-Saharan Africa, where 91% of deaths from malaria are reported. As for cancer, it is the second leading cause of death worldwide claiming about 8.8 million deaths in 2015 (WHO, 2018a). Globally, one in six deaths are due to cancer and this number is projected to almost double by the year 2030. Therefore, more research on alternative prevention and treatment are needed.

Traditional medicine is important and indispensable in the development and discovery of new drug leads. Indeed, screenings of medicinal plants based on their ethnopharmacological applications, especially in the treatment of tumours and malaria, have led to some remarkable discoveries in the past.

Thus, the aim of the present investigation was to identify phytochemicals with antimalarial and/or chemopreventive properties from five medicinal plants based on their folklore use in the Cameroonian community for the treatment of different types of fever, malaria and tumours.

This aim comprised following objectives:

- To obtain crude extracts from the selected plants and to evaluate their potent chemopreventive and antimalarial activities.

- To carry out bioassay directed isolation of active compounds.
- To characterise these bioactive compounds by spectroscopic means.
- To evaluate the biological activities of the isolated compounds.

Chapter 2 Materials and Methods

2.1 Plant materials

Plants were collected from the Centre (Mount Eloundem, Mfoundi) and the West (Dschang Local Market) regions of the Republic of Cameroon, which is a tropical country located in sub-Saharan Africa at longitude 7.3697° N, and latitude 12.3547° E (Figure 2.1), with the assistance Mr Victor Nana, a botanist of the Cameroon National Herbarium (CNH), Yaoundé, Cameroon. Mr Nana also identified all the species collected by comparison with respective voucher specimens available at the CNH. Plant materials were collected during the months of June and November in 2015. Table 2.1 gives details on the different plants' parts collected, the voucher numbers, period and place of collection.

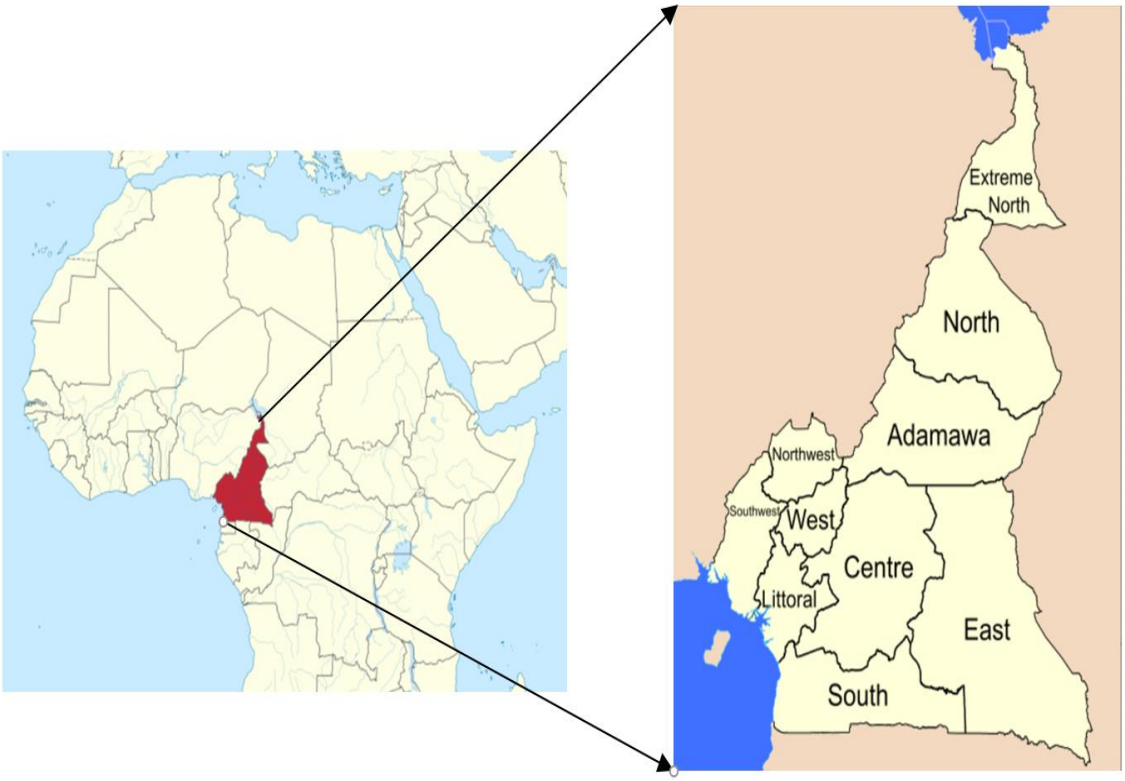

Figure 2.1 Map showing Cameroon geographical position and the different regions where the plants were collected

Table 2.1 List of medicinal plants studied

Plant name	**Family**	**Voucher Number**	**Part collected**	**Period/ Region**
Croton oligandrus Pierre ex Hutch	Euphorbiaceae	6687/SFR	Stem bark and leaves	June 2015/ Centre
Justicia hypocrateriformis (Vahl) Milne-Redh	Acanthaceae	37822/SFR	Leaves	June 2015/ Centre
Pseudospondias microcarpa (A. Rich.) Engl.	Anacardiaceae	41437/SFR	Fruits, leaves and stem bark	June 2015/ Centre
Zanthoxylum lepreurii Guill. and Perr.	Rutaceae	106669/SFR	Fruits	November 2015/ West
Zanthoxylum zanthoxyloides (Lam.) Zepern. and Timler	Rutaceae	21793/SFR	Fruits	November 2015/ West

2.2 Chemicals and reagents

2.2.1 Chemicals

All the solvents were purchased from Fisher Scientific Ltd. (Loughborough, UK). Deionized water used in the present work was obtained from a MiliQ water system (Merck, Germany). Deuterated NMR solvents including chloroform ($CDCl_3$), methanol (CD_3OD), acetone (acetone-d_6), pyridine (Pyr-d_5), DMSO (DMSO-d_6) and water (D_2O) were purchased from Cambridge Isotope Laboratories Inc. (Tewksbury, USA). Precoated aluminium plates of Silica gel 60 PF_{254} (0.2 mm thickness, 20 x 20 cm) for Thin Layer Chromatography (TLC) were sourced from Merck Ltd., Germany. Silica gel (70-230 mesh) and Silica Kieselgel 60H, purchased from Sigma-Aldrich Company Ltd. (Dorset, UK), were used for open column chromatography (CC) and vacuum liquid

chromatography (VLC), respectively. Sodium dodecyl sulphate (SDS), bovine hemin, sodium acetate buffer 3M, NaOH and 37% HCl solution were also purchased from Sigma-Aldrich Company Ltd.

2.2.2 Cell lines, cell culture media and reagents

Names and tissues of origin of each cell line used in this study are listed in Table 2.2. AREc32 cells were a generous gift of Prof Roland Wolf (University of Dundee, UK), while the other cell lines were obtained from Dr Andrews Evans cells bank (LJMU, Liverpool, UK).

Table 2.2 Cell lines used in bioassays

Name	Origin
AREc32	Human mammary MCF7-derived reporter cells
A549	Adenocarcinoma human alveolar basal epithelial cells
MCF7	Human breast adenocarcinoma cells
PC3	Human prostate cancer cell line
PNT2	Human normal prostate epithelium cells

Foetal bovine serum (FBS), penicillin/streptomycin, L-glutamine, Dulbecco's Modified Eagles Medium (DMEM), trypsin-EDTA and phosphate buffer saline (PBS), were purchased from Biosera (Neuville, France). Doxorubicin, gentamicin and trypan blue solution were obtained from Sigma Aldrich Company Ltd. (Dorset, UK). Luciferase assay kit reagent was from Promega Corp. (Loughborough, UK).

2.3 Phytochemical work

2.3.1 Plant preparation and Soxhlet extraction

The plant materials were individually cut into small pieces; air dried at room temperature and powdered using a maize grinder into a coarse powder. The powdered plant materials were extracted using Soxhlet extraction.

Individual plant material was placed in a thimble made of thick filter paper and placed in the extraction chamber, extraction solvent (0.9 L) was poured in and the condenser was placed on the extraction chamber (Figure 2.2). The solvent was brought to boil using an Electrothermal^{TM} electromantle (Fisher Scientific, Loughborough-UK). When solvent boiled, the extraction chamber was gradually filled with solvent and performed extraction until it reached the maximum level, when the solvent with the dissolved extracted components went back to the flask. This was one cycle of extraction. This cycle was repeated 10 times for each solvent used. In this way, the dissolved components remained in the flask, while clean solvent was evaporated and the plant material in the thimble was repeatedly extracted (Rostagno and Prado, 2013). The plant material was extracted, successively, with *n*-hexane, dichloromethane (DCM) and methanol (MeOH). The resulting extracts were concentrated to dryness under reduced pressure on a Cole-Palmer rotary evaporator (Stone, UK). Extracts were stored at 4°C and dissolved in appropriate solvent prior to usage.

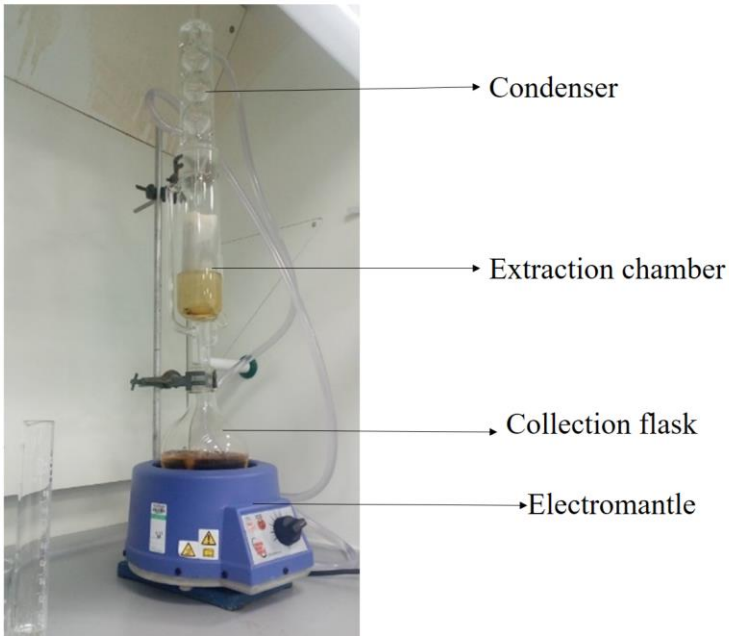

Figure 2.2 Soxhlet apparatus

2.3.2 Chromatographic techniques

2.3.2.1 Vacuum liquid chromatography

Vacuum liquid chromatography (VLC) was used for the rapid fractionation of active non-polar and medium polarity extracts. The technique was used as described by Pelletier *et al.* (1986). The system consisted of a sintered glass Buchner filter funnel with an attachment to a side arm flask connected to a vacuum pump (Figure 2.3). Approximately the two third of the VLC funnel was dry-packed with Kieselgel 60H, the stationary phase, under vacuum and the appropriate solvent was allowed to flow through the system (Reid and Sarker, 2012). A portion of the *n*-hexane or DCM extract were dissolved in a little amount of appropriate solvent, mixed with normal silica gel (70-230 mesh), taken to dryness either by air drying or under reduced pressure using rotary evaporator and the mixture was loaded on the top of the funnel as a uniform thin layer. Vacuum was applied, and the column was eluted with a stepwise gradient of mobile phase consisting of an increasing amount of ethyl acetate in *n*-hexane (Hex/EA 0%, 10%, 20%, 40%, 60% and

80%, H1-H6) or MeOH in DCM (DCM/MeOH 0%, 2%, 6%, 10%, 15% and 25%, D1-D6) for the *n*-hexane or DCM extract respectively to obtained six different fractions. Collected VLC fractions were concentrated to dryness under reduced pressure and analysed by TLC to get an idea of their composition. Fractions with similar TLC profiles were mixed together.

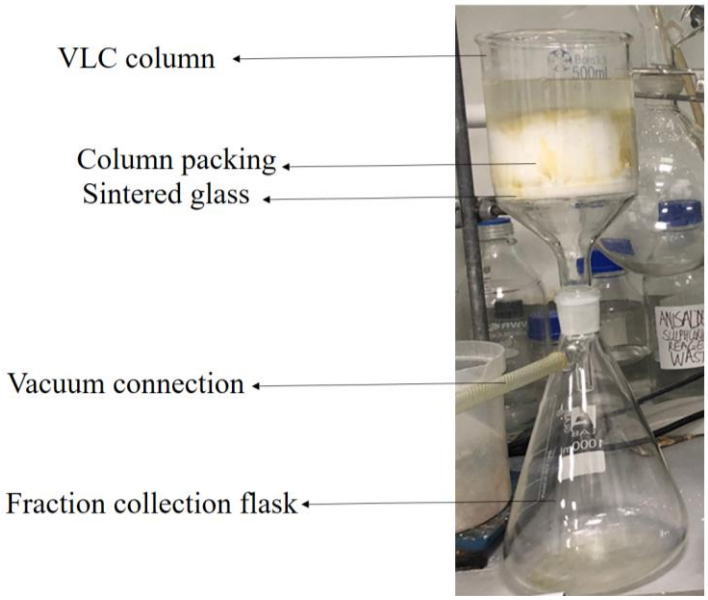

Figure 2.3 VLC system

2.3.2.2 Solid-phase extraction

Solid-phase extraction (SPE) was used for the fractionation of active methanolic extract and to clean-up DCM extract prior to preparative HPLC. The SPE is quite similar to VLC with the only difference being that a commercially available pre-packed SPE cartridge is used instead of a funnel prepacked with silica gel (Reid and Sarker, 2012) (Figure 2.4). A Strata C-18-E cartridge 20 g (Phenomenex, California-USA) was used for this study. A portion of the dried MeOH extract (2 g) was suspended in 10 mL of a 10% MeOH in water mixture and loaded into the cartridge, previously washed with MeOH (50 mL), followed by equilibration with water (100 mL). The cartridge was eluted with MeOH–

water mixture of decreasing polarity to obtain four fractions (F1-F4): 20, 50, 80 % MeOH in water and 100% MeOH (200 mL each). All four fractions were evaporated to dryness using a combination of a rotary evaporator and a freeze-dryer. A portion of each resulting fraction was dissolved in MeOH to obtain a solution of 1 mg/mL and analysed by HPLC-UV/DAD. For the clean-up of DCM extract, 2 g of the sample were dissolved in 10 mL 30% MeOH in water solution and the cartridge was eluted with 80% MeOH in water solution.

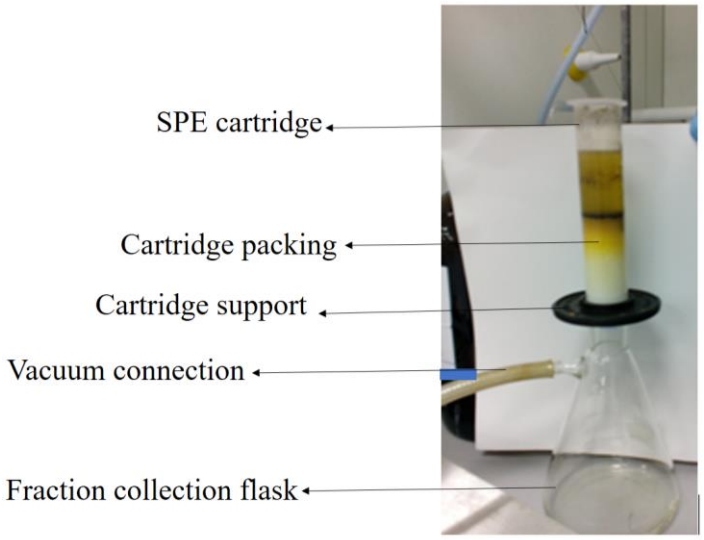

Figure 2.4 Solid Phase Extraction system

2.3.2.3 Thin layer chromatography

Thin layer chromatography (TLC) is a separation technique mainly used for the detection and monitoring of compounds through a separation process based on the criteria of adsorption, binding to silica and polarity (Gibbons, 2012). The technique was used in this study to screen the plant extracts for the presence of secondary metabolites, to determine the starting eluting solvent composition for column chromatography, to monitor fractions collection during chromatography, to check the purity of isolated compounds from CC and as isolation technique for the purification of compounds (preparative TLC). Precoated

silica gel 60 PF_{254} aluminium plates were used for this purpose. Samples were applied manually at the base, about 1 cm from the bottom edge of the TLC plate, using a glass capillary and developed in a chromatographic chamber using an appropriate solvent system. Multiple developments were sometime needed to improve resolution. After drying, the developed plates were visualised by irradiation with short-wave (254 nm) and long-wave (366 nm) using a Camag UV lamp (CAMAG, Hungerford-UK) and by spraying with a 1% anisaldehyde solution in aqueous H_2SO_4 followed by heating to 105 °C in Sciquip oven 30S (Sciquip, Shrewsbury-UK) for 5 min (Figure 2.5).

In the case of preparative TLC, only a small part (1/10 part) of TLC plate was spread with the anisaldehyde reagent after having covered the remaining part with aluminium foil. Bands of interest were identified and scratched with the help of spatula. The compounds of interest were extracted from the collected silica gel by cold maceration with a mixture of 10% MeOH in DCM.

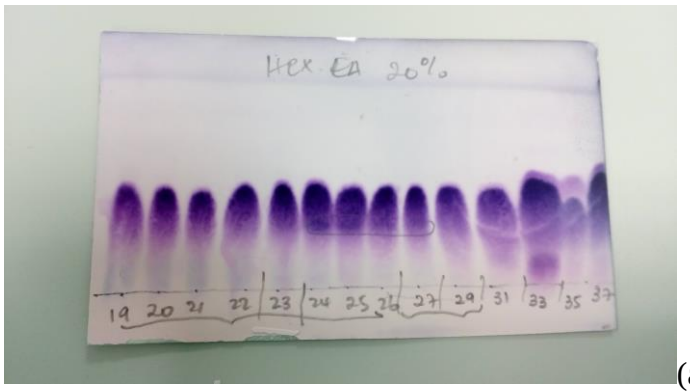

(a)

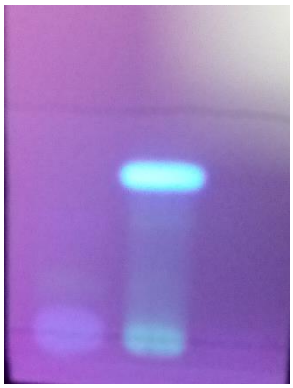
(b)

Figure 2.5 TLC plates of a) xylopic acid developed in Hex:EtOAC (8:2) and sprayed with 1% anisaldehyde and b) skimmianine developed in DCM:MeOH (9.2:0.8) visualised at 254 nm

2.3.2.4 Column chromatography

Column chromatography (CC) was used to isolate compounds from active *n*-hexane fraction. Silica gel (70-230 mesh) was used for this purpose. The sample and the column (Figure 2.6) were prepared in the same way as described for VLC, but in the case of CC the elution was carried out purely under the gravitational force, and no negative or positive pressure was applied. Wet packing technique was also used instead of dry packing as for the case of VLC. *n*-Hexane was used as packing solvent. Excess solvent was run through the column to allow the silica gel to settle well before introducing the sample on the top of the column. The column was eluted with a stepwise gradient of mobile phase of increasing polarity. The initial solvent composition was determined by TLC analysis. Depending on the column size, 10-50 mL of eluents were collected per fraction, and their contents were analysed by TLC.

Figure 2.6 CC system operated by manual fraction collection

2.3.2.5 High-performance liquid chromatography

High-performance liquid chromatography (HPLC) is a separation technique both used as analytical and preparative for the detection, separation, quantification and isolation of compound mixtures, including natural products.

2.3.2.5.1 Analytical high-performance liquid chromatography

Analytical HPLC was used to screen the plant extracts for the presence of secondary metabolites, to develop methods for isolation using preparative HPLC and to verify the purity of isolated compounds. The experiment was performed on an UPLC Dionex 3000 (Thermoscientific, UK) or Agilent 1260 infinity series (Agilent, UK) both equipped with a binary pump, an autosampler, a column chamber, a degasser and a UV/DAD detector from the same corresponding model and company. Samples were prepared in MeOH (1 mg/mL) and analysed on a Phenomenex Gemini-NX 5 U C18 column (150 × 4.6 mm, Phenomenex, USA) or a Hypersil 5 U C18 column (150 × 4.6 mm, Phenomenex, USA) with a gradient of 30-100% MeOH (containing 0.1% TFA), 70-0% H_2O (containing 0.1% TFA) over 30 min or of 30-100% ACN, 70-0% H_2O (containing 0.1% TFA). The column temperature was set at 25 °C. A volume of 10 µL of the prepared sample was injected and the chromatogram was monitored at 1 mL/min using variable UV/vis wavelengths comprising between 205 and 366 nm. Methods described above were always used to verify the purity of the collected fractions obtained from preparative HPLC analyses and as starting methods for the development of further methods (Table 2.3) to be used on preparative HPLC for isolation and purification of compounds.

2.3.2.5.2 Preparative high-performance liquid chromatography

Preparative HPLC was used for the isolation and purification of compounds from the DCM and MeOH fractions using developed methods from analytical HPLC. Table 2.3 below shows the different methods developed on the analytical HPLC and used on the prep-HPLC for the isolation of compounds. The experiment was carried out on an Agilent 1260 infinity series equipped with a binary pump, a degasser, a column chamber and a UV/DAD detector. An ACE Gemini-NX 5 U C18 column (150 × 21.2 mm, Hichrom Ltd, UK) maintained at 25 ºC and monitor at a flow rate of 10 mL/min was used for isolation. Manual peak collection was carried on using UV/DAD detector and repeated chromatography were needed to isolate a good amount of compound. The samples were all prepared in MeOH. MeOH and H_2O used for HPLC analysed contained 0.1% TFA.

Table 2.3 List of the different HPLC methods developed

	Time slot (min)	**%MeOH**	**%ACN**	**%H_2O**
Method A	0 - 30	30 - 100	-	70 - 0
	30 - 35	100	-	0
Method B	0 - 15	-	30 - 65	70 - 35
Method C	0 - 20	30 - 75	-	70 - 25
Method D	0 - 10	45 - 50	-	55 - 50
	10 - 30	50 - 60	-	50 - 40
Method E	0 - 30	30 - 65	-	70 - 35

2.3.3 Isolation of compounds

2.3.3.1 Isolation of compounds from *Croton oligandrus*

The air-dried and powdered stem bark (330.8 g) of *C. oligandrus* were extracted with *n*-hexane, DCM and MeOH to obtain 3.7, 2.1 and 7.4 g of beige oily, beige and brown extracts, respectively.

A portion of the *n*-hexane (3.3 g) and DCM (1.8 g) extracts were adsorbed on to normal silica gel (70-230 mesh) and fractionated using VLC to obtain six fractions each (H1- H6) and (D1-D6) for *n*-hexane and DCM extracts, respectively, following the VLC procedure as described earlier.

Fraction H3 (420.9 mg) of *n*-hexane extract was further purified using a CC over silica gel using a gradient of Hex-EtOAc 0-30% to give a mixture (18.2 mg) of **149** and **150**, and **147** (4.4 mg). Compounds **7** (16.1 mg) and **8** (19.0 mg) were obtained from H5, H6 and D4 by recrystallisation using Hex-EtOAc 15-30%. The mixture of **149** and **150** (3.2 mg) were also obtained from D2 and D3 of the DCM crude extract by recrystallisation with Hex-EtOAc 15%. D4, D5 and D6 showed similar TLC and HPLC profiles and were then mixed together for purification. The mixture of the two fractions (783.0 mg) was finally purified by preparative RP-HPLC using the method A (Table 2.3). Figure 2.7 showed the obtained chromatogram as well as the peaks corresponding to the different compounds (**148**, **151-162)** identified and characterised from the combined fractions.

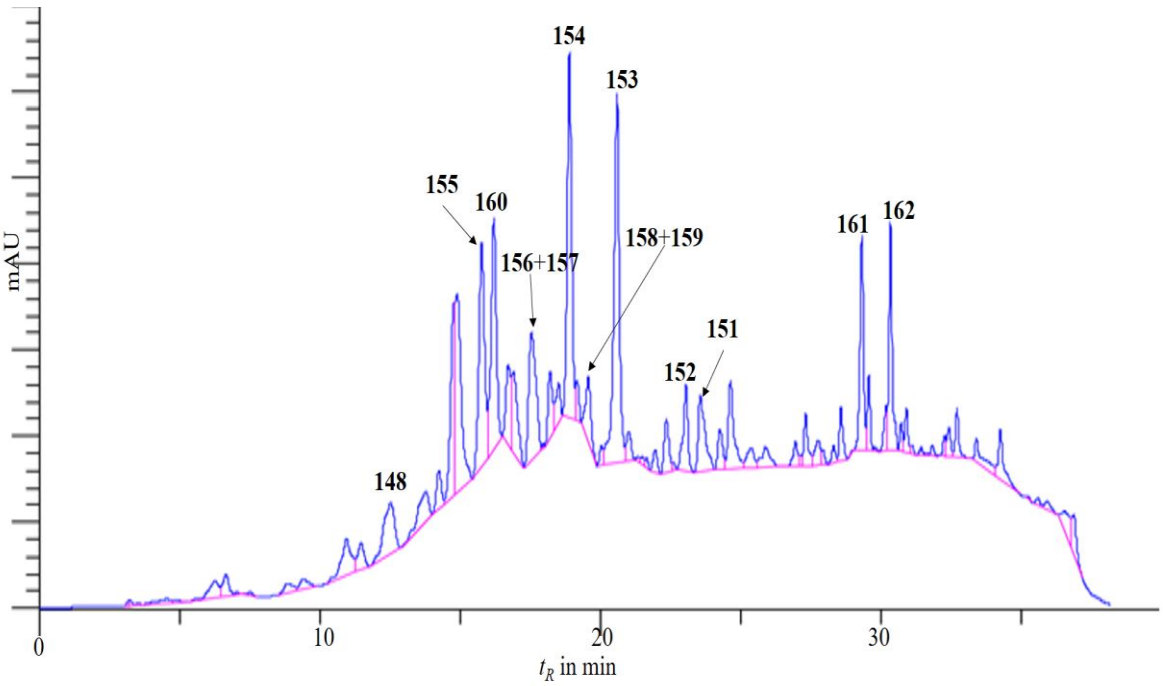

Figure 2.7 Chromatogram of *C. oligandrus* fractions D4+D6-method A, inj. vol. 130 µL, sample conc. 182.7 mg/mL, monitored at 215nm

Table 2.4 Isolation of compounds from *C. oligandrus*

Cpds	**Extract containing the cpds**	**VLC fraction containing the cpds**	**Mode of isolation**	**R_f or t_R in min**	**Visual aspect**	**Amount in mg**
7	*n*-hexane	H5, D4	-	0.47*	White powder	16.1
8	*n*-hexane	H6, D4	-	0.40*	White powder	19.0
147	*n*-hexane	H3	CC	0.56*	White powder	4.4
148	DCM	D4, D5 and D6	HPLC	12.51	White powder	8.3
149+150	DCM, *n*-hexane	H3, D2 and D3	CC	0.63*	White powder	21.4
151	DCM	D4, D5 and D6	HPLC	23.54	White powder	6.3
152	DCM	D4, D5 and D6	HPLC	23.03	White powder	3.3
153	DCM	D4, D5 and D6	HPLC	20.57	White powder	15.6
154	DCM	D4, D5 and D6	HPLC	18.89	White powder	13.9
155	DCM	D4, D5 and D6	HPLC	15.76	White powder	2.9
156+157	DCM	D4, D5 and D6	HPLC	17.54	White powder	7.8
158+159	DCM	D4, D5 and D6	HPLC	19.55	White powder	6.5
160	DCM	D4, D5 and D6	HPLC	16.19	White powder	7.3
161	DCM	D4, D5 and D6	HPLC	29.29	Yellow powder	4.1
162	DCM	D4, D5 and D6	HPLC	30.31	White powder	5.7

*TLC plate developed in Hex:EtOAc 40%

The MeOH extract was not processed further as it was found to be non-active. In addition, the same extraction procedure was carried out with 280.0 g of the dried leaves to obtain 6.9, 2.9 and 9.9 g of *n*-hexane, DCM and MeOH extracts, respectively. Only the *n*-hexane extract was found to be active. However, it was not processed further as preliminary ^{1}H NMR revealed a mixture of **7**, **8** and fatty acids.

2.3.3.2 Isolation of compounds from *Justicia hypocrateriformis*

The air-dried and powdered leaves (450.5 g) of *J. hypocrateriformis* were extracted with *n*-hexane, DCM and MeOH to obtain 13.6, 10.2 and 41.8 g of dark green, brown green and dark brown extracts, respectively. Preliminary screening revealed MeOH as the only active extract.

The MeOH extract (4 g) was dissolved in MeOH and cleaned using SPE eluted with MeOH/H_2O 50% to remove chlorophyll. After drying, 2 g of the obtained extract was subjected to standard SPE procedure described above. F1 (668.8 mg) was adsorbed on to normal silica gel and subjected to CC using of a gradient of EtOAc:MeOH 0-30%. Forty-one fractions of 50 mL were collected and grouped based on their TLC profiles to eight main subfractions (F1A-F1H). A white crystalline precipitate identified as sucrose (**60**) was obtained from F1H (CC fractions 30-41, collected with 24-30% MeOH in EtOAc). Compound **170-171** were obtained by PTLC of CC fractions 17-20 (EtOAc:MeOH 13%). The Plate was developed in DCM:MeOH 10%.

Fractions F2 (428.6 mg) and F3 (361.8 mg) were subjected to preparative RP-HPLC using method C and D (Table 2.3) respectively. Chromatograms of the fractions are shown on Figure 2.8. Seven compounds (**163-169**) were identified and characterised from the

collected peaks. Overall, ten compounds were isolated and characterised from the leaves of *J. hypocrateriformis* (Table 2.5).

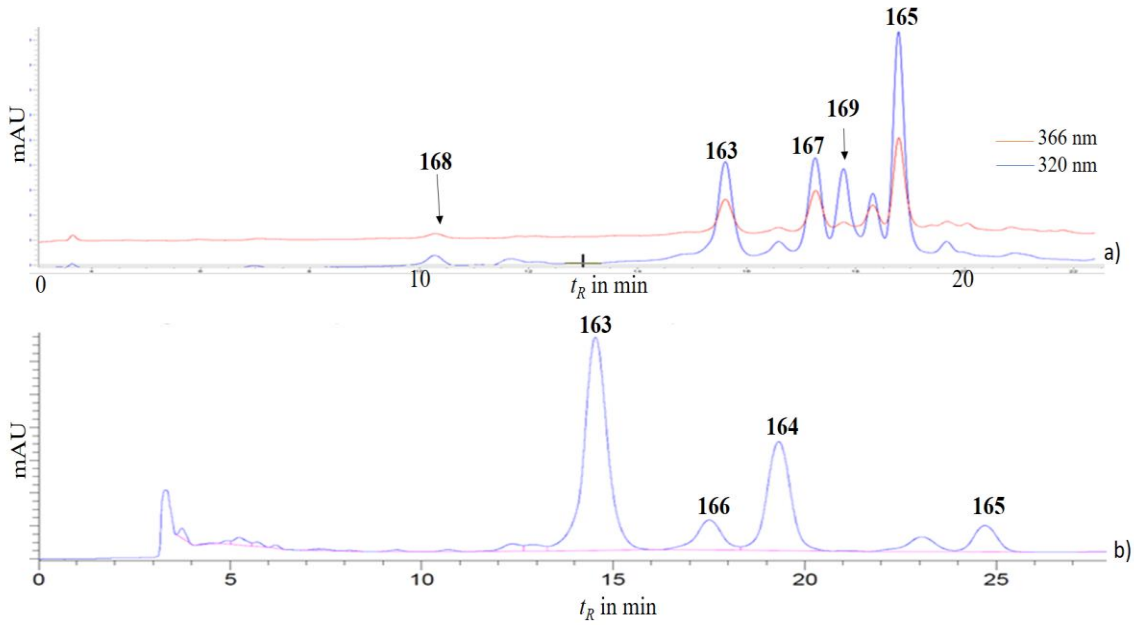

Figure 2.8 Chromatogram of *J. hypocrateriformis* fractions, a) F2, method C, injection vol. 500 µL, sample conc. 25 mg/mL, monitored at 320 and 366 nm b) F3, method D, injection vol. 100 µL, sample conc. 50 mg/mL, monitored at 205 nm

Table 2.5 Isolation of compounds from *J. hypocrateriformis*

Cpds	**SPE fractions containing the compounds**	**Mode of isolation**	**R_f or t_R in min**	**Visual aspect**	**Amount in mg**
163	F2, F3	HPLC	15.53	Yellow powder	8.4
164	F3	HPLC	19.34	Yellow powder	2.9
165	F2, F3	HPLC	24.71	Yellow powder	2.2
166	F3	HPLC	17.50	Yellow powder	3.3
167	F2	HPLC	16.75	Yellow powder	2.6
168	F2	HPLC	27.01	Yellow powder	4.4
169	F2	HPLC	17.75	Brown powder	1.6
170+171	F1	PTLC* of CC pooled fractions 17-20	0.37	Brown powder	3.4

* PTLC developed in DCM:MeOH 10%.

2.3.3.3 Isolation of compounds from *Pseudospondias microcarpa*

Stem bark (276.0 g), fruits (262.0 g) and leaves (437.0 g) of *P. microcarpa* were individually extracted to yield 2.2, 4.1 and 13.4 g of *n*-hexane; 1.0, 0.9 and 2.7 g of DCM; and 5.9, 7.1 and 12.5 g of MeOH extract, respectively. Only the stem bark DCM and MeOH extracts, and the leaves MeOH extract were subjected to chromatographic separation.

The bark DCM extract was cleaned up, while the MeOH extract was subjected to standard SPE prior to isolation of their phytochemicals by preparative RP-HPLC. F2 and F3 obtained from the SPE of the MeOH extract were found to have similar chromatograms after analytical HPLC and combined to a single fraction. The DCM extract (597.6 mg) and the MeOH fractions F2+F3 (194.3 mg) were chromatographed using methods A and E (Table 2.3), respectively. Both extracts afforded compounds **103**, **148** and **175** (Table 2.7) from the peaks collected.

The leaves MeOH extract was cleaned up and subjected to standard SPE method as described for *J. hypocarteriformis*. F2 (198.8 mg) and F3 (328.6 mg) were found to have similar analytical HPLC profiles and were mixed together for separation of their constituents. Separation was performed using HPLC method C (Table 2.3). Four compounds (**164**, **166**, **172** and **173**) were identified and characterised from the obtained chromatogram (Figure 2.10). F1 and F4 were not processed further. Table 2.6 lists all the compounds isolated and characterised from *P. microcarpa*.

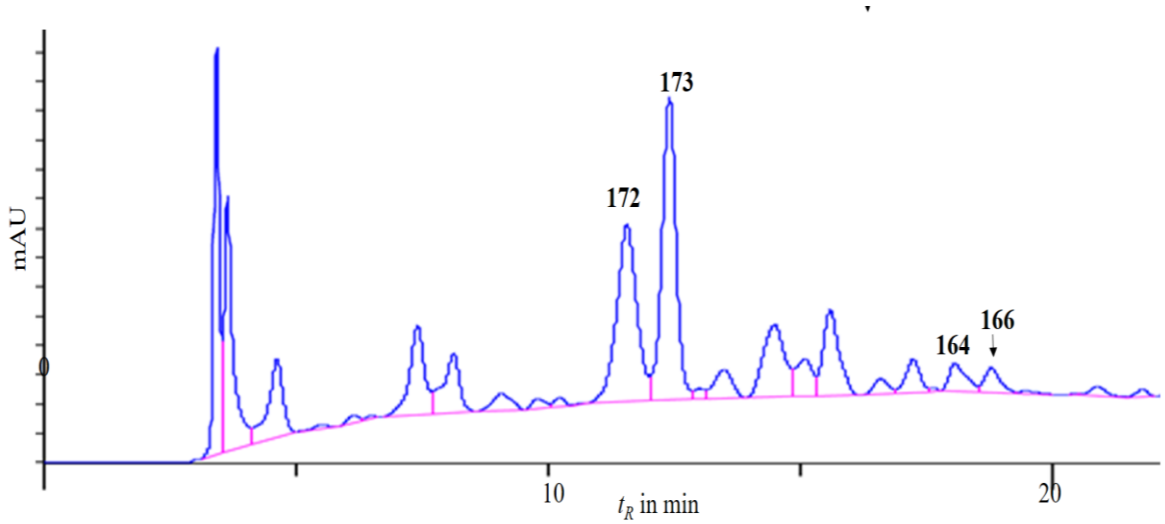

Figure 2.9 Chromatogram of *P. microcarpa* leaves fractions F2 + F3, method C, injection vol. 120 µL, sample conc. 75 mg/mL, monitored at 230 nm

Table 2.6 Isolation of compounds from *P. microcarpa*

Cpds	**Part of plant containing the cpds**	**Extract containing the cpds**	**SPE/VLC containing the cpds**	**Mode of isolation (method)**	**t_R in min**	**Visual aspect**	**Amount in mg**
103	Stem bark	DCM	-	HPLC (A)	4.55	Brown powder	3.1
		MeOH	F2 and F3	HPLC (E)	13.28		
148	Stem bark	DCM	-	HPLC (A)	4.28	Beige powder	3.6
		MeOH	F2 and F3	HPLC (E)	13.00		
164	Leaves	MeOH	F2 and F3	HPLC (C)	18.67	Brown powder	1.9
166	Leaves	MeOH	F2 and F3	HPLC (C)	19.23	Brown powder	2.1
172	Leaves	MeOH	F2 and F3	HPLC (C)	11.20	Yellow powder	6.1
173	Leaves	MeOH	F2 and F3	HPLC (C)	14.69	Brown powder	2.4
174	Stem bark	DCM	-	HPLC (A)	4.78	Brown powder	4.3
		MeOH	F2 and F3	HPLC (E)	13.33		

2.3.3.4 Isolation of compounds from *Zanthoxylum leprieurii*

The air-dried and powdered fruits (546.8 g) of *Z. leprieurii* were extracted with *n*-hexane, DCM and MeOH to obtain 32.7, 21.1 and 54.3 g of brown oily, light maroon and dark maroon extracts, respectively.

The brown oily *n*-hexane extract (20 g) was subjected to CC over silica gel 60 (230-400 mesh, 6.5 cm x 50 cm) using a gradient system of Hex:EtOAc (0-50%) and DCM-MeOH (10-30%) as eluents. Fifty-three sub-fractions (ca. 125 mL each) were collected and pooled on the basis of their analytical TLC profile to six main fractions A-F. Fraction B (3.8 g, pooled sub-fractions 9-20) was further chromatographed using silica gel 60 (230-400 mesh) CC with increasing amounts of EtOAc in *n*-hexane as eluent to afford **175** (120.5 mg) and **176** (230.2 mg). Fraction C (1.9 g, pooled sub-fractions 22-32) was subjected to repeated CC as previously described to yield **178** (7.4 mg), **179** (80.7 mg), along with a mixture of sterols. A white granular precipitate giving single pink spot on TLC and identified as **177** (43.1 mg) was obtained from fraction F (2.1 g, pooled sub-fractions 48-53).

Fractions D4 (2.46 g), D5 (533.5 mg) and D6 (892.3 mg) obtained by VLC of the DCM extract (7.11 g) were mixed together based on their TLC profiles. The mixture obtained (2 g) was cleaned up using SPE, dried, resuspended in MeOH and subjected to preparative RP-HPLC using HPLC method C (Table 2.3) for compounds isolation. From the peaks collected, compounds **114**, **180**-**182** were identified and characterised.

The MeOH extract was found to be inactive and was not purified. Table 2.7 lists all the compounds isolated from *Z. leprieurii* and their methods of isolation.

Table 2.7 isolation of compounds from *Z. leprieurii*

Cpds	**Extract containing the cpds**	**VLC fractions containing the cpds**	**Mode of isolation**	**R_f or t_R in min**	**Visual aspect**	**Amount in mg**
114	DCM	D4, D5 and D6	HPLC	10.62	Brown powder	4.4
175	*n*-hexane	-	CC of CC pooled fractions 9-20 (Hex:EtOAc 10-20%) eluted with EtOAc in *n*-hexane (5-15%)	0.47*	White powder	120.5
176	*n*-hexane	-		0.38*	White powder	230.2
177	*n*-hexane	-	Precipitates in CC pooled fractions 48-53 (DCM:MeOH 15%)	0.12*	White powder	43.1
178	*n*-hexane	-	CC of CC pooled fractions 22-32 (Hex:EtOAc 20-30%) eluted with EtOAc in *n*-hexane (1-20%)	0.18*	White powder	7.4
179	*n*-hexane	-		0.22*	White powder	80.7
180	DCM	D4, D5 and D6	HPLC	9.41	Brown powder	3.6
181	DCM	D4, D5 and D6	HPLC	7.70	Brown powder	1.3
182	DCM	D4, D5 and D6	HPLC	9.42	Yellow powder	3.3

*TLC developed in Hex:EtOAC 25% and sprayed with 1% anisaldehyde solution

2.3.3.5 Isolation of compounds from *Zanthoxylum zanthoxyloides*

The air-dried ground fruits (350.0 g) of *Z. zanthoxyloides* were extracted to give 34.6 g, 3.9 g and 19.6 g of *n*-hexane, DCM and MeOH extract, respectively.

The DCM extract (3.0 g) was subjected to VLC to obtained six fractions D1-D6 as describe above. Fractions D4 (336.0 mg), D5 (223.2 mg) and D6 (129.9 mg) were mixed based on their TLC profiles, cleaned up and subjected to RP-HPLC for separation. Compounds **54**, **55**, **79**, **128**, **184** and **187** were identified and characterised from the fractions collected from the obtained chromatogram (Figure 2.10).

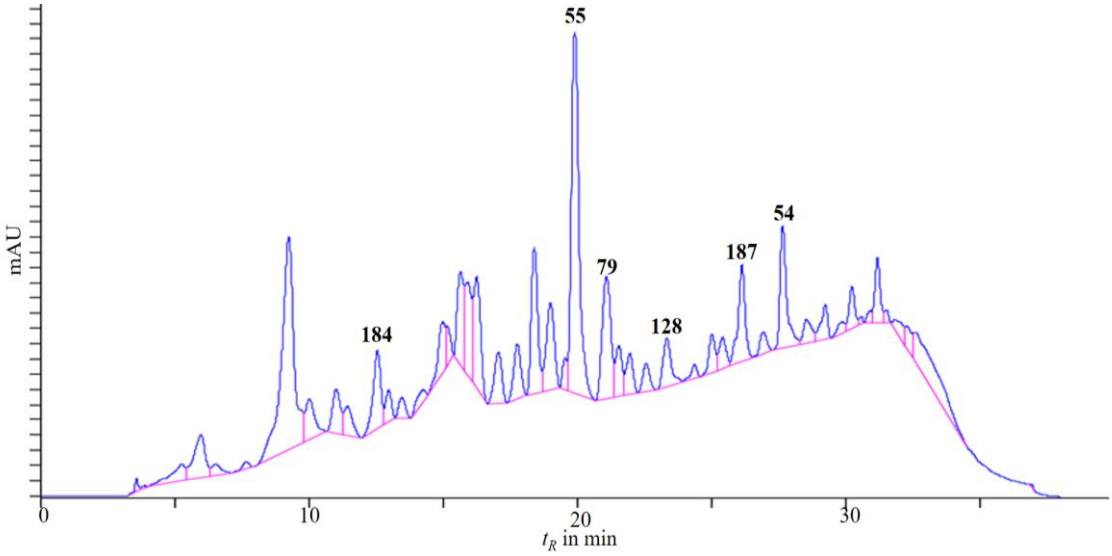

Figure 2.10 Chromatogram of *Z. zanthoxyloides* DCM fractions D4-D6, method A, injection vol. 300 µL, sample conc. 50 mg/mL, monitored at 220 nm

The MeOH extract was subjected to standard SPE and four fractions F1-F4 were obtained. The procedure was repeated twice to obtain a good amount of each fraction. F2 (704.8 mg) was subjected to preparative HPLC analysis (Figure 2.11a) using HPLC method B (Table 2.3) to yield **183** (3.5 mg) and **184** (3.6 mg) having the retention times (t_R) 4.35 and 5.95 min, respectively. Fraction F2-B (5.7 mg) collected at t_R = 5.28 min was further purified through preparative TLC to afford **189** (3.2 mg, EtOAc:MeOH 7:3, R_f 0.41).

Fraction F2-D (3.6 mg) collected at t_R = 6.55 min was also purified by preparative TLC to obtain **190** (1.9 mg, EtOAc:MeOH 7:3, R_f 0.46). Preparative TLC of fraction F2-E (3.8 mg) collected at t_R = 7.22 min provided **188** (1.8 mg, EtOAc:MeOH 7:3, R_f 0.41). Purification of fraction F2-F (10.2 mg) collected at t_R = 7.61 min using TLC with a mixture of EtOAc:MeOH (7:3) as eluent afforded more of **188** (2.5 mg, R_f 0.41) and **186** (3.6 mg, R_f 0.28).

F3 (845.8 mg) was also analysed by preparative HPLC using method A (Figure 2.11b). Compounds **54**, **55**, **59**, **128**, **183**, **185**, **187** and **191** were identified and characterised from the collected fractions.

Fractions F1 and F4 were not processed further. F1 was found to be rich in sugar while F4 were found to contain the same compounds as the DCM extract. Table 2.8 groups all the characterised compounds from *Z. zanthoxyloides*.

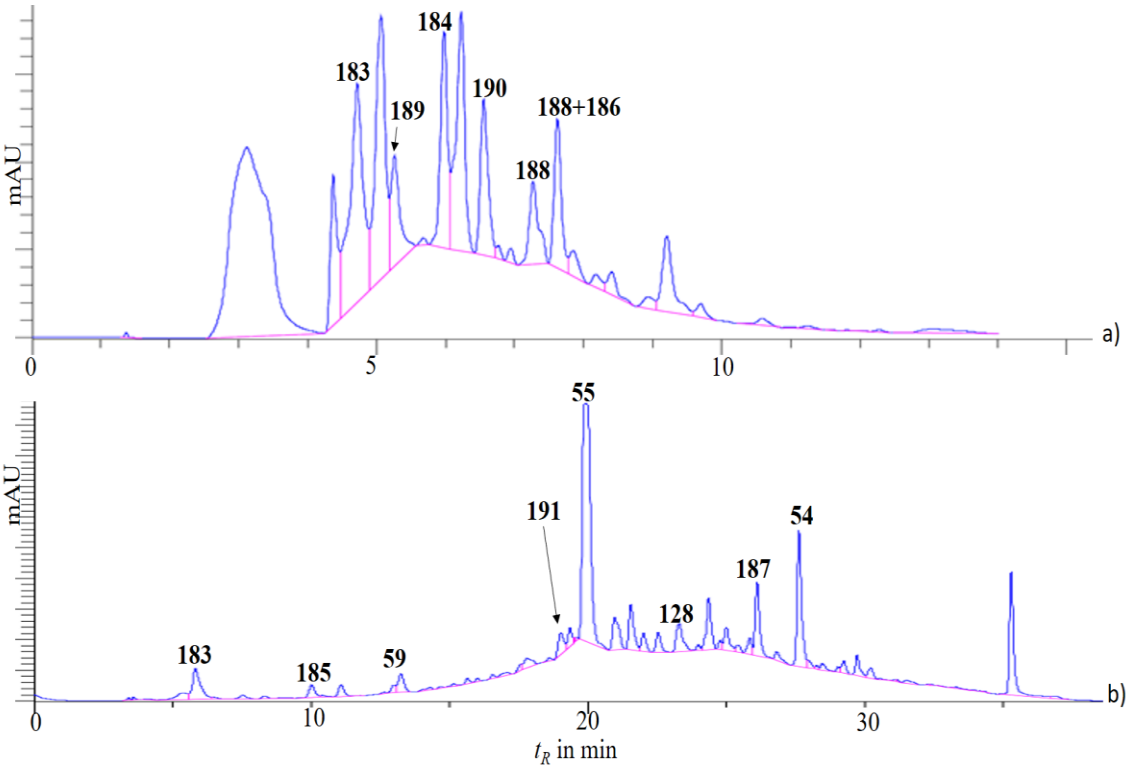

Figure 2.11 Chromatogram of *Z. zanthoxyloides* a) F2, method B, inj vol. 280 µL, sample conc. 182.5 mg/mL, monitored at 254 nm b) F3, method A, inj vol. 120 µL, sample conc. 100 mg/mL, monitored at 230 nm

Table 2.8 Isolation of compounds from *Z. zanthoxyloides*

Cpds	**Extract (s) containing the cpds**	**VLC/SPE fraction (s) containing the cpds**	**Mode of isolation (method)**	**R_f or t_R in min**	**Visual aspect**	**Amount in mg**
54	DCM, MeOH	D4-D6, F3	HPLC (A)	27.35	Brown powder	20.7
55	DCM, MeOH	D4-D6, F3	HPLC (A)	19.90	White needles	36.1
59	MeOH	F3	HPLC (A)	13.14	Yellow powder	1.9
79	DCM	D4-D6	HPLC (A)	20.43	Brown powder	5.4
128	DCM, MeOH	D4-D6, F3	HPLC (A)	24.01	Yellow powder	3.9
183	MeOH	F2, F3	HPLC (A and B)	4.88	Yellow powder	11.5
184	DCM, MeOH	D4-D6, F2	HPLC (B)	12.42	Beige powder	3.6
185	MeOH	F3	HPLC (A)	10.00	Brown powder	1.2
186	MeOH	F2	1. HPLC (B) 2. PTLC of HPLC fraction (t_R 7.61) in EtOAc:MeOH 7:3	0.28	Yellow powder	3.6
187	DCM, MeOH	D4-D6, F3	HPLC (A)	25.85	Yellow powder	11.2
188	MeOH	F2	1. HPLC (B) 2. PTLC of HPLC fraction (t_R 7.61) in EtOAc:MeOH 7:3	0.41	White liquid	4.3

Table 2.8 *continued*

189	MeOH	F2	HPLC (B)	0.41	White liquid	3.2
190	MeOH	F2	1. HPLC (B) 2. PTLC of HPLC fraction (t_R 7.61) in EtOAc:MeOH 7:3	0.46	White liquid	1.9
191	MeOH	F3	HPLC (A)	23.77	Yellow powder	1.7

2.3.4 Identification and characterisation of isolated compounds

Structure elucidation of all the isolated compounds was carried out by spectroscopic analyses including 1D (^{1}H and ^{13}C NMR) and 2D NMR (^{1}H-^{1}H COSY, DEPT 145, ^{1}H-^{13}C HSQC-DEPT, ^{1}H-^{13}C HMBC, ^{1}H-^{1}H NOESY and ^{1}H-^{1}H TOCSY) and mass spectrometry. Some compounds were also characterised by UV, FT-IR spectroscopy and polarimetry. Spectroscopic techniques are useful means for assessing the purity and the determination of the structures of natural substances (Boiteau *et al.*, 1964).

2.3.4.1 Nuclear magnetic resonance

Nuclear magnetic resonance (NMR) is a useful spectroscopic technique to obtain structural information about a given molecule. NMR spectra are plots of signals arising from absorption of radio frequency due to excitement of a nucleus or simultaneous excitement of two nuclei (Breitmaier and Sinnema, 1993; Crews *et al.*, 1998). Only ^{1}H and ^{13}C nuclei were excited during experiments. Experiments consist of 1D and 2D experiments. 1D experiments used in this study include proton (^{1}H) and carbon (^{13}C) NMR while 2D NMR experiments are ^{1}H-^{1}H COSY (Correlation SpectroscopY), DEPT 135º (Distortionless Enhancement by Polarization Transfer), ^{1}H-^{1}H NOESY (Nuclear Overhauser Effect SpectroscopY) and ^{1}H-^{1}H TOCSY (TOtal Correlation SpectroscopY),

HMBC (^{1}H-^{13}C Heteronuclear Multiple Bond Correlation Spectroscopy) and HSQC (^{1}H-^{13}C Heteronuclear Single Quantum correlation). NOESY was used to determine the relative stereochemistry of the molecule while TOCSY was used to identify protons belonging the same spin system for the structure elucidation of glycosylated molecules (Agrawal, 1992; Reggelin *et al*., 1992). Experiments were performed on either a Bruker AMX 600 or a Bruker AMX 300 instrument (Bruker, Germany). Chemical shifts (δ) are given in part by millions (ppm) and the coupling constants *J* in Hertz (Hz).

2.3.4.2 Ultraviolet-visible and Fourier transform infrared spectroscopies

Ultraviolet-visible (UV) and Fourier Transform Infrared (FT-IR) spectroscopies were recorded on Analytik Jena Specord 210 (Jena, Germany) and Agilent Cary 630 FT-IR (Agilent, UK) spectrophotometers respectively. Both methods are useful for the detection of functional groups in a molecule. Wavelengths scan for the UV was between 200-500 nm. Quartz cells were used for samples and blanks. The results were reported in nm as the wavelength of the maxima.

2.3.4.3 Optical rotation

Optical rotation was determined using Bellingham- Stanley ADP660 polarimeter with the sodium D line (589.3 nm) as the source of light. The measurements were made at 25 °C in a 10 cm cell. The results were calculated with the following formula: $[\alpha]^{25}_{D}$= 1000×α/l.c (in which α= observed rotation, l = cell length in dm and c = concentration in g/100 mL).

2.3.4.4 Mass spectrometry

Mass spectrometry (MS) is a technique useful in determination of the molecular weight of compounds, the possible molecular formula and fragmentation pattern (Hoffmann *et al*., 1996). High resolution mass spectra (HR MS) were recorded at the National Mass Spectrometry Facility (NMSF) (Swansea, UK) on a Xevo G2-S ASAP or LTQ Orbitrap XL1 spectrometers. Low and high resolution MS analyses were also performed at LJMU. HR MS was run on an Agilent 6200 Series Accurate-Mass Time-of-Flight (TOF) LC/MS using electro spray ionisation (ESI) in positive ion mode connected to an Agilent auto-sampler injection system. The analyte was prepared in MeOH and the mass spectrum was recorded relating to their mass to charge (*m/z*) at a capillary potential of 3,500 V. Low resolution analyses were performed on a Waters LCT Premier™ ESI-TOF Mass Spectrometer.

2.4 Bioactivity studies

2.4.1 Samples preparation for screening

Stock solutions of assayed samples were prepared in DMSO 100 mg/mL for crude extracts and fractions, and 100 mM for pure isolated compounds and stored at 4 ^{o}C. Prior to use, the stock solution was further diluted in the medium to final working concentrations ranging from 0-1000 µg/mL for extract and, 0-250 µM for pure compounds on the day of assay.

2.4.2 Cell culture

Dulbecco's Modified Eagles Medium (DMEM), Foetal bovine serum (FBS), penicillin/Streptomycin, and L-glutamine were warmed at 37 °C before making up a complete media. Penicillin/streptomycin (100 units/mL, 4 mL), L-glutamine (4 mL) and 50 mL of FBS were added into 500 mL of DMEM in a sterilised environment. The media was mixed and stored in a fridge at 4°C. Growth media was pre-warmed at 37°C for 20 min before each use. In the case of AREc2 cell line, 4 mL of 100 mg/mL of geneticin was also added to the growth medium. All cell lines were cultured at 37 °C in 95 % air and 5 % CO_2 in 25 or 75 cm^2 tissue culture flask (Corning, Staffordshire, UK) containing appropriate medium for the cell line.

When cells were 80-100 % confluent, they were passaged or used for the desired experiment. Firstly, the media was removed from the flasks and cells were washed with PBS twice to remove the residual medium and dead cells, as they are non-adherent to the flask surface. Small amount of pre-warmed trypsin-EDTA (0.2-0.5 mL) was added and incubated for 1-2 min at room temperature, then excess of trypsin was removed and the cells were incubated for an additional 2-4 min at 37 °C. The flasks were tapped gently to dislodge the cells and were visualised under a microscope.

After the cells were completely disassociated from the flask, the complete growth media was added into the flask. The medium was pipetted up and down several times to break up any cell clumps. The cell suspension was split into two fresh flasks and were labelled with new passage number and kept in an incubator at 37°C.

For the assays, after reaching 80-90% confluence, the cells were seeded into 96 well plates or 6 well plates at density 1.2×10^4 in a corresponding working volume of 180 µL/well and allowed to grow for 24 h before each experiment commenced.

2.4.3 Cell viability assays

Trypan blue assay using a haemocytometer was used during cell counting to determine cell numbers for setting up assays. Equal amount of trypan blue and cell solution were mixed by pipetting up and down for few times, and 10 μL of the obtained solution was transferred in each quadrant of the haemocytometer. Viable cells are typically round and refractile and exclude the stain, whilst non-viable cells are stained dark blue.

3-(4,5-dimethylthlthiazol-2-yl)-2,5-diphenyl tetrazolium bromide (MTT) assay based on the method described by Mosmann (1983) was used to assess the cytotoxicity of extracts and pure isolated compounds on the different cell lines used in this study. The MTT is converted by the NADPH present in viable cells to a purple formazan crystal (Figure 2.12) which has an absorbance maximum near 570 nm. When cells died, they lose the ability to convert the MTT into formazan and therefore, colour formation serves as a useful convenient manner of viable cells only.

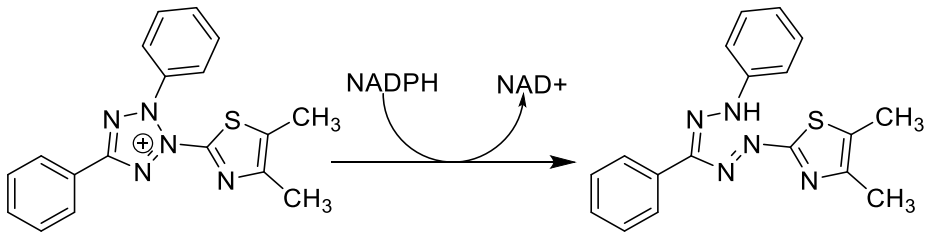

Figure 2.12 MTT transformation to formazan

Cells were seeded into 96 well plates at density 1.2×10^4 cells/well. After 24 h incubation, the medium was removed and replaced with fresh medium containing assayed sample (extract or pure compound) at the desired concentration. The final concentration of DMSO in each well was no more than 0.1%. A set of untreated control cells was included in each experiment, as well as a set of cells treated with 0.1% DMSO. Following

incubation with the extracts for 24 h (48 h for pure compounds except with AREc32 cell line), 20 µL of MTT solution (prepared in PBS at the concentration of 5 mg/mL) was added to each well. After 2 h of incubation at 37 °C, the medium was discarded and replaced with 100 µL of DMSO. The OD_{570} was determined with a microplate reader (CLARIO Star Microplate reader, BMG Labtech, UK). The percentage of cell viability was determined as percentage of control cells [(absorbance of treated cells/absorbance of untreated cells) × 100].

2.4.4 Luciferase reporter gene assay

The ability of the extracts, fractions and isolated compounds to activate the expression of ARE driven genes which are commonly activated by Nrf2 were evaluated by cell-based luciferase assay with a cell line which contains an ARE-driven luciferase reporter gene (AREc32, modified MCF-7 cell line). Luciferases are a class of oxidative enzymes found in several species that enable the host to bioluminesce in the presence of luciferin (Figure 2.13). The emission can be read using a luminometer and is directly correlated to the level of ARE activation (Wang *et al.*, 2006).

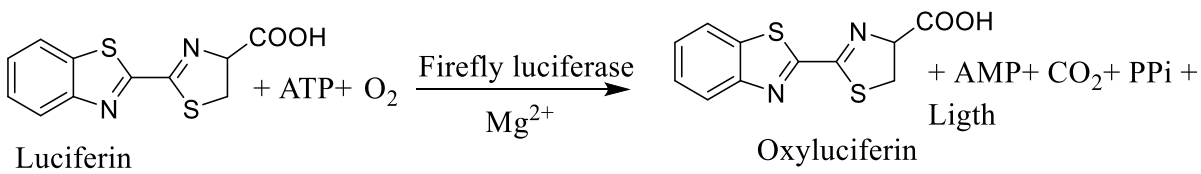

Figure 2.13 Formation of oxyluciferin

The Steady-Glo Luciferase assay kit from Promega was used for this purpose according to the manufacturer instructions. Briefly, AREc32 cells were seeded into 96 well plates at density 1.2×10^4 cells/well and treated for 24 h with the concentration of extract or

pure compound causing no more than a 10% reduction of cell viability as determined by the MTT assay. Wells were then washed twice with 100 µL of PBS and 20 µL of luciferase reporter lysis buffer (Promega, USA) was added to each well followed by a freeze thaw cycle (24 h) to achieve complete cell lysis. The 20 µL cell lysate was then aspirated and dispensed into a white opaque 96 well plates. 80 µL of Luciferase reporter substrate was added to each well and the luminescence immediately measured using a plate reader (ClarioStar microplate reader, BMG Labtech, UK). Levels of luciferase activity were expressed relative to the basal level of luciferase activity in control (no treatment) and presented as a fold increase (relative to control).

2.4.5 Haem polymerisation assay

The potential antimalarial activity of plant extracts was evaluated by the method described by Hussain *et al*. (2011). Briefly, varying concentrations (0-2 mg/mL in 10% DMSO) of the extracts were incubated with 300 µM of hematin (freshly dissolved in 0.1 M NaOH), 10 mM oleic acid and 10 µM HCl. The reaction volume was adjusted to 1000 µL using 500 mM sodium acetate buffer, pH 5. Chloroquine diphosphate was used as a positive control. The samples were incubated overnight at 37 ºC with regular shaking. After incubation, samples were centrifuged (14,000 x g, 10 min, at 21 °C) and the hemozoin pellet repeatedly washed with sonication (30 min, at 21 °C; FS100 bath sonicator; Decon Ultrasonics Ltd.) in 2.5% (w/v) SDS in phosphate buffered saline followed by a final wash in 0.1 M sodium bicarbonate, pH 9.0, until the supernatant was clear. After the final wash, the supernatant was removed, and the pellets were re-suspended in 1 mL of 0.1 M NaOH before determining the hemozoin content by measuring the absorbance at 405 nm using a 1 cm quartz cuvette. The results were recorded as % inhibition (I%) of haem polymerization/crystallization compared to

positive control (chloroquine) using the following formula: I% = [(AB–AA)/AB] x 100, where AB: absorbance of blank; AA: absorbance of test samples. All the solutions were pre-warmed at 60°C before initial mixing.

2.5 Statistical analysis

All bioassay experiments were carried out in triplicate with a minimum of three replicates per assayed concentration. Data were expressed as means ± SEM (standard error of mean). The graphs were plotted using Excel Microsoft office 2016. SEM is shown on the graph as an error bar. IC_{50}, LC_{10} and LC_{50} where calculated using Graph Prism 7.0 software. *P* value were calculated using unpaired student *t*-test and considered significant when $P \leq 0.01$.

Chapter 3 Results and Discussion

3.1 Yield of extraction

Different parts of the following medicinal plants viz. *Croton oligandrus* Pierre ex Hutch, *Ruspolia hypocrateriformis* (Vahl) Milne-Redh, *Pseudospondias microcarpa* (A. Rich.) Engl., *Zanthoxylum lepreurii* Guill. and Perr. and *Zanthoxylum zanthoxyloides* (Lam.) Zepern. and Timler (Figure 3.1) were collected, dried at room temperature, ground and successively extracted with a Soxhlet apparatus using *n*-hexane, DCM and MeOH. Eighteen extracts were obtained (Table 3.1). As the three solvents used have different polarity index, the constituents of the plant were gradually extracted according to their affinity with each solvent. The highest yield percentage of extraction was that of *Z. zanthoxyloides* with 23.9 % recovery percentage while *P. microcarpa* bark yielded the lowest extraction percentage of 3.3 %.

Figure 3.1 Pictures showing the different plant parts collected

a) *Croton oligandrus* Pierre ex Hutch stem bark; b) *Ruspolia hypocrateriformis* Vahl Milne-Redh leaves; c) *Pseudospondias microcarpa* (A. Rich.) Engl. stem bark; d) *Pseudospondias microcarpa* (A. Rich.) Engl. leaves; e) *Zanthoxylum lepreurii* Guill. and Perr. fruits; f) *Zanthoxylum zanthoxyloides* (Lam.) Zepern. and Timler fruits.

Table 3.1 Yield of extraction of the different plants collected

Plants	**Powder weight (g)**	**Extract weight (g)**			**Yield (%)**
		Hexane	DCM	MeOH	
C. oligandrus bark	330.8	3.7	2.1	7.4	4.0
R. hypocrateriformis leaves	450.0	13.6	10.2	41.8	14.6
P. microcarpa bark	276.6	2.2	1.1	5.9	3.3
P. microcarpa leaves	437.3	13.4	2.7	12.5	6.5
Z. leprieurii fruits	546.8	32.7	21.1	54.3	19.8
Z. zanthoxyloides fruits	350.0	59.58	5.9	18.25	23.9

3.2 Preliminary screening

3.2.1 Luciferase activity

The extracts obtained from the collected plant materials were screened for their potential cancer chemopreventive properties using the AREc32 cell line. AREc32 cells are stably transformed variant of the MCF-7 cells containing a luciferase reporter gene under the control of antioxidant promoters, and therefore, is an excellent cell model for the identification of potent activator of the Nrf2 signalling pathway (Wang *et al.*, 2006).

3.2.1.1 AREc32 cells viability

The cell viability of the AREc32 cells in the presence of each extract was first assessed by the MTT assay with the aim of determing the threshold dose nontoxic for the cells and the suitable dosage for the luciferase assay. The cells were incubated in the presence of the extracts and the effect of those extracts on cell viability measured after 24 h and compared to that of control (untreated cells). Results are shown on Figure 3.2. The DCM Extract of *P. microcarpa* bark was found to be the most toxic to the AREc32 cells killing

nearly 50% of cells at 62.5 µg/mL while the MeOH Extract of *Z. zanthoxyloides* fruits was found to be the least toxic with only 70% of cells death occurring at 1 mg/mL. JHL and PML were found to have a cytotoxic effect on AREc32 cells at very low concentrations. The concentration causing no more than 10% cells death (LC_{10}), was chosen as the assayed concentration for the luciferase assay (Table 3.2) as no significant cell death was observed below that concentration.

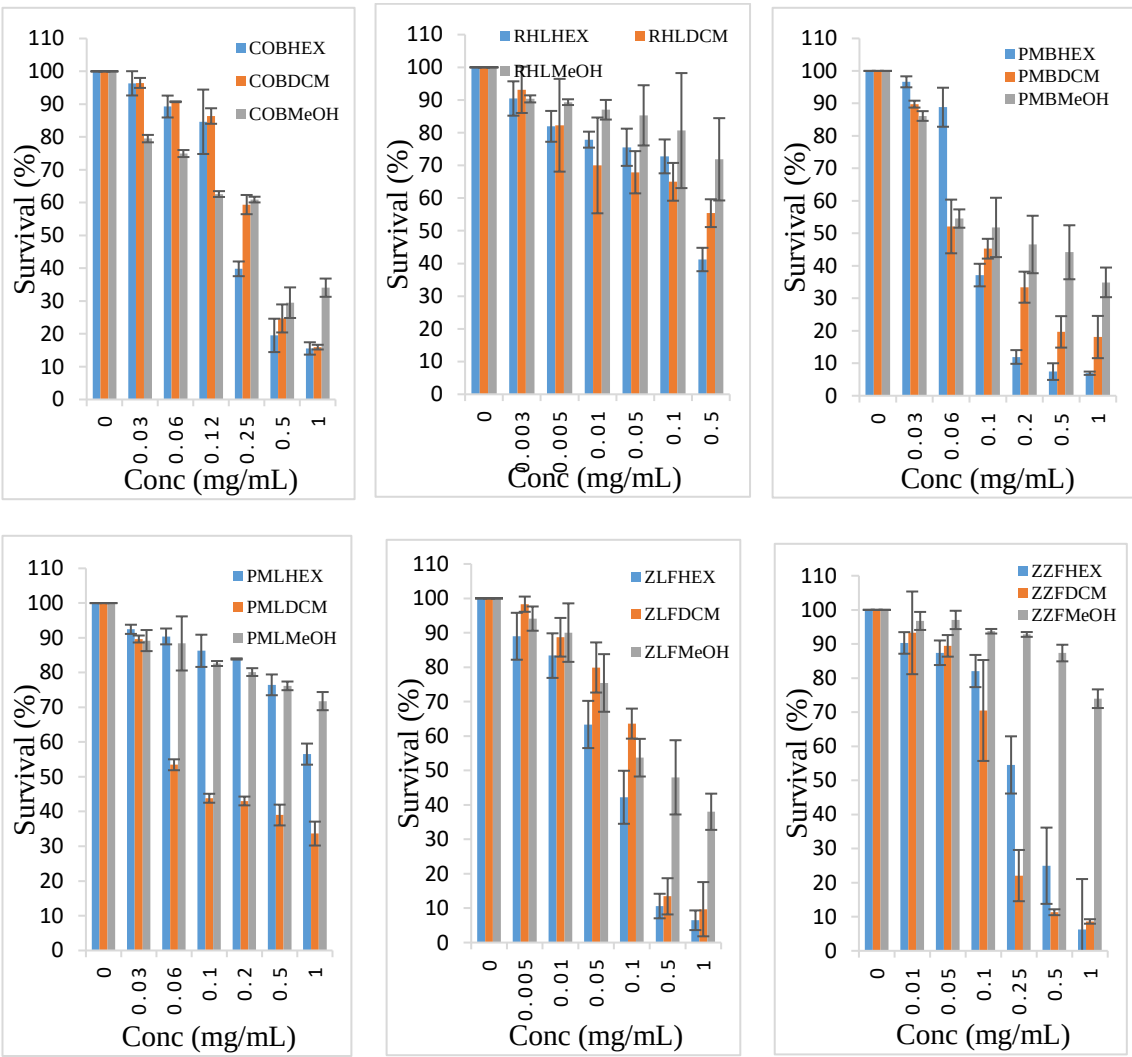

Figure 3.2 Effect of tested extracts on the viability of AREc32 cells.

Cells were treated for 24 h with 0.1% DMSO (control), or with various concentrations (0 – 1 mg/mL) of extracts. Cell viability was determined by MTT assay. Each measured parameter is plotted as mean ± SEM of three independent experiments (5 replicates/ experiment). COB: *C. oligandrus* bark; RHL: *R. hypocrateriformis* leaves; PMB: *P. microcarpa* bark; PML: *P. microcarpa* leaves; ZLF: *Z. leprieurii* fruits; ZZF: *Z. zanthoxyloides* fruits, HEX: *n*-Hexane extract; DCM: DCM extract; MeOH: MeOH extract.

Table 3.2 Concentrations of extracts causing no more than 10% toxicity

Extract	**Least toxic concentration (LC_{10} in µg/mL)**					
	COB	JHL	PMB	PML	ZLF	ZZF
HEX	60	4	60	60	4	5
DCM	60	3	30	30	5	50
MeOH	10	5	30	30	5	500

Cells were treated for 24 h with various concentrations (0 – 1 mg/mL) of extracts. Cell viability was determined by MTT assay. LC_{10} was determined using GraphPad Prism software of three independent experiments (5 replicates/ experiment). COB: *C. oligandrus* bark; RHL: *R. hypocrateriformis* leaves; PMB: *P. microcarpa* bark; PML: *P. microcarpa* leaves; ZLF: *Z. leprieurii* fruits; ZZF: *Z. zanthoxyloides* fruits, HEX: *n*-Hexane extract; DCM: DCM extract; MeOH: MeOH extract.

3.2.1.2 Luciferase assay

Luciferase assay was carried out as describe in the experimental section (Chapter 2, 2.4.4). The results are shown on Figure 3.3. Among the tested extracts, COBHEX, COBDCM, ZZFDCM and ZZFMeOH extracts were found to induce luciferase activity. ZZFMeOH was the most active with a 36-fold induction follow by its DCM extract with 33-fold induction. The activities of *Z. zanthoxyloides* DCM and MeOH extracts were similar to that of *t*BHQ (50 µM) used as positive control. *t*BHQ is a well characterized chemopreventive compound which exert its activity by inducing Nrf2-regulated genes (Wang *et al.*, 2006). The fact that only DCM and MeOH extracts induced high levels of the luciferase activity (greater than 30-fold) might be linked to presence of polar compounds in the plant.

Several *Zanthoxylum* species are traditionally used in Asia and Central America to treat and prevent cancer (Epifano *et al.*, 2011). Phytochemical studies of *Z. zanthoxyloides* have led to the isolation of alkaloids with good cytotoxicity against a panel of cancer cell lines (Wouatsa *et al.*, 2013). It is interesting to note that *Z. leprieuri* extracts did not show

any significant increase of the luciferase activity compared to the closely related species *Z. zanthoxyloides*. A comparative study carried out by Wouatsa *et al*. (2013a) has revealed that the two plants only have few phytochemicals in common.

In contrast to *Z. zanthoxyloides*, for which polar extracts were active, only nonpolar and medium polar extracts of *C. oligandrum* showed good luciferase induction. COBHEX and COBDCM extracts were found to induce the luciferase activity by 18 and 21-fold, respectively. *Croton* is a rich source of diterpenes (Xu *et al.*, 2018), and some isolated diterpenes from plants have been reported to have cancer chemopreventive activity (Dhanasekaran *et al.*, 2009; Endringer *et al.*, 2014).

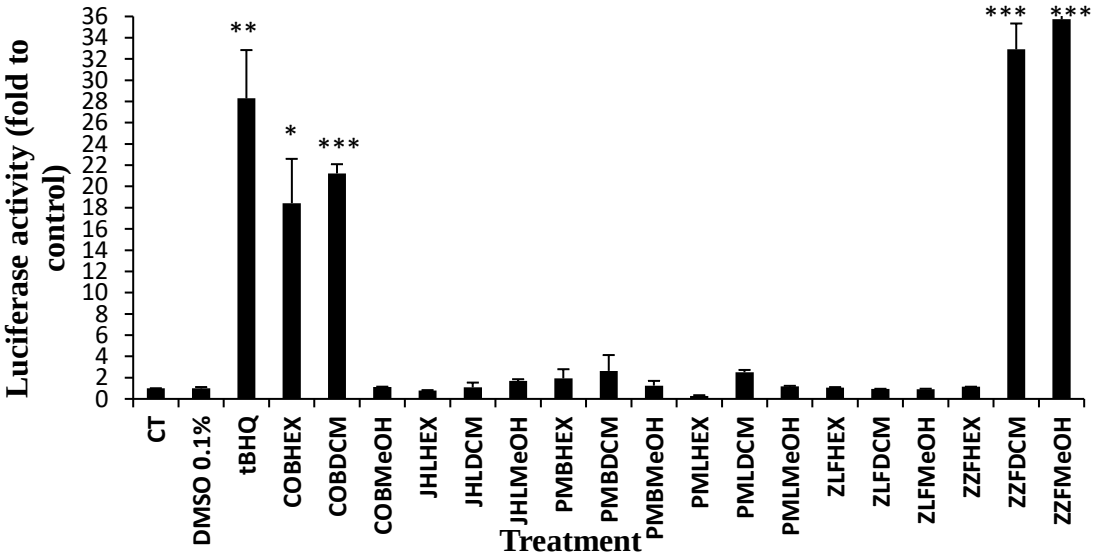

Figure 3.3 Luciferase activity of the screened extracts

AREc32 cells were seeded in 96-well plates at 1.2 x 10^4 cells/well. After 24 h, *t*BHQ (50 μM) and the extracts were added to the medium. The cells were then incubated for another 24 h and assayed for luciferase activity as detailed in Chapter 2, 2.4.4. The value of luciferase activity of untreated cells (CT) was set at 1. Values shown are mean ± SEM of three experiments. *$p < 0.1$; **$p < 0.01$, ***$p < 0.001$ significantly increased versus control. DMSO 0.1%: (cells treated with 0.1% DMSO medium).

The most active crude extracts were fractionated using VLC for *n*-hexane and DCM extracts, and SPE for MeOH extract. For each *n*-hexane or DCM extract, six fractions were obtained and four fractions only for MeOH extract. The effect of the fractions on

the viability of AREc32 cells was assessed by the MTT assay to determine their least toxic concentration (Concentrations causing no more than 10% cells death), and the obtained concentration (Table 3.3) was used as dosage to evaluate the luciferase activity of the fractions.

Table 3.3 Concentrations of fractions causing no more than 10% toxicity

Extract	**Least toxic concentration (LC_{10} in µg/mL)**					
	F1	F2	F3	F4	F5	F6
COBHEX	5	5	10	1	0.5	1
COBDCM	5	10	0.5	5	0.5	5
ZZFDCM	0.5	1	1	5	5	0.1
ZZFMeOH	5	1	0.5	5	-	-

Cells were treated for 24 h with various concentrations (0 – 1 mg/mL) of extracts. Cell viability was determined by MTT assay. LC_{10} was determined using GraphPad Prism software of three independent experiments (5 replicates/ experiment). F1-F6 are fractions obtained from VLC and SPE of active crude extracts COB: *C. oligandrus* bark; ZZF: *Z. zanthoxyloides* fruits, HEX: *n*-Hexane extract; DCM: DCM extract; MeOH: MeOH extract.

The level of induction of the luciferase activity by each fraction tested is depicted in Figure 3.4. Overall, fractionation considerably reduced the activity, as most of the fractions did not show significant fold induction of the luciferase activity as the mother crude extract. The only plausible explanation could be that the activities observed from the corresponding crude extract were due to synergistic action of the different compounds present in the plant. In addition, the fractionation techniques used, VLC and SPE separated the constituents of the plant based on their affinity with the eluent used. Thus, each fraction is a mixture of several compounds with similar polarity in different proportions conferring a unique phytochemical profile. Moreover, plant extracts contain complex mixtures of compounds in which most of the time a single constituent is not responsible for the overall activity (Williamson, 2001).

Among the tested fractions, COBHEX F1 and ZZFMeOH F3 showed induction of 3.24- and 2.4-fold, respectively. The activity of ZZFMeOH F3 was comparable to that of *t*BHQ 6 µM (2.5- fold induction) while COBHEX F1 was more active than *t*BHQ 6 µM. The remaining fractions showed fold induction below 2. According to McMahon and coworkers (2014), chemicals causing fold increase of luciferase activity greater than 2 are considered as active.

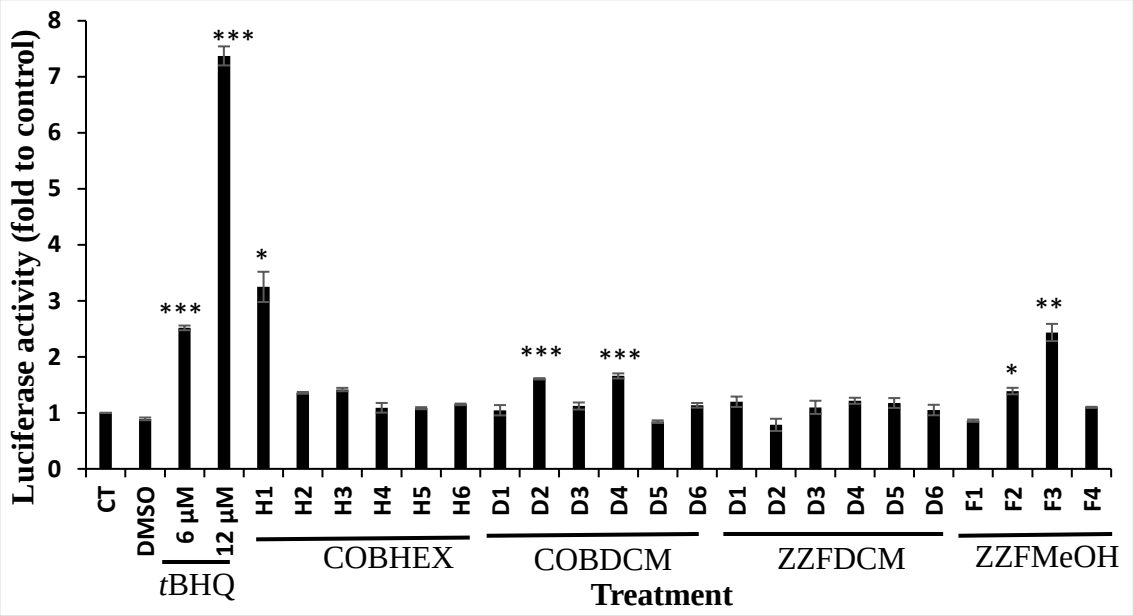

Figure 3.4 Luciferase activity of the fractions

AREc32 cells were seeded in 96-well plates at 1.2 x 10^4 cells/well. After 24 h, *t*BHQ (6 and 12 µM) and the fractions were added to the medium. The cells were then incubated for another 24 h and assayed for luciferase activity as detailed in Chapter 2, 2.4.4. The value of luciferase activity of untreated cells (CT) was set at 1. Values shown are mean ± SEM of three experiments. *$p < 0.01$; **$p < 0.001$, ***$p < 0.0001$ significantly increased versus control. DMSO, cells treated with 0.1% DMSO medium.

3.2.2 Haem polymerisation assay

Hemozoin, also called malaria pigment, is essential for the survival of the malaria parasite in red blood cells (Coronado *et al.*, 2011). The pigment is a polymer of haem units, which is biocrystallised during haem detoxification in the erythrocytic life of the parasite.

Inhibition of the haem polymerisation is therefore targeted for the search of antimalarial substances. Several screening techniques have been developed for the purpose. In the present study, we have performed the assay using the method published by Hussain *et al*. (2011) as described in the experimental section. Chloroquine diphosphate was used as positive control. Results are shown in Table 3.4.

Table 3.4 Haem polymerisation inhibitory concentration (IC_{50} in µg/mL)

Extract	**IC_{50} (µg/mL) ± SEM**		
	HEX	DCM	MeOH
COB	180.0 ± 6.0	164.8 ± 53.0	> 1
JHL	206.7 ± 52.0	> 1	170.3 ± 77.9
PMB	73.9 ± 25.8	2.5 ± 1.5	4.0 ± 1.7
PML	> 1	> 1	13.0 ± 9.0
ZLF	> 1	45.8 ± 25.0	> 1
ZZF	> 1	> 1	> 1
Chloroquine	0.43 ± 0.08		

IC_{50} was determined using GraphPad Prism of three independent experiments (3 replicates/experiment). COB: *C. oligandrus* bark; RHL: *R. hypocrateriformis* leaves; PMB: *P. microcarpa* bark; PML: *P. microcarpa* leaves; ZLF: *Z. leprieurii* fruits; ZZF: *Z. zanthoxyloides* fruits, HEX: *n*-Hexane extract; DCM: DCM extract; MeOH: MeOH extract.

Among the five plants screened, *P. microcarpa* extracts were found to be the most active. Inhibition of the haem polymerisation was observed for the DCM and MeOH extracts of the stem bark with IC_{50} values 2.5 ± 1.5 and 4.0 ± 1.7 µg/mL, respectively. MeOH extract produced 50% inhibition at 13.0 µg/mL. The PMB hexane extract was less active (IC_{50} 73.9 ± 25.8 µg/mL), while PML hexane and MeOH were found to have no effect at the highest concentration tested. The IC_{50} obtained for PMB DCM and MeOH extracts were comparable to the result obtained when the stem bark ethanol extract (IC_{50} 1.13± 0.16 µg/mL) was screened *in vitro* against multi-drug resistant *Plasmodium falciparum* K1

strain (Malebo *et al.*, 2009). The IC_{50} of the MeOH extract was close to the result published by Mbatchi et *al.* (2006) (IC_{50} 26 ± 10 µg/mL) when the ethanol extract was tested in *vitro* against human erythrocytes infected by FcM29 originated from Cameroon. *Z. zanthoxyloides* fruits extracts were found to be not active at the highest concentration tested. However, previous screenings have demonstrated a moderate antimalarial activity for the root and trunk bark extracts (Kassim *et al.*, 2005; Gansane *et al.*, 2010).

This is the first report on the evaluation of the antimalarial activity *C. oligandrus* and *J. hypocrateriformis*. Overall, extracts with IC_{50} < 200 µg/mL, i.e. COBHEX, COBDCM, JHLMeOH, PMBHEX, PMBDCM, PMBMeOH, PMLMeOH and ZLFDCM were selected for further studies.

3.3 Characterisation and structure elucidation of isolated compounds

3.3.1 Phytochemistry of *Croton oligandrus*

The *n*-hexane and DCM extracts of *C. oligandrus* exhibited good antimalarial and chemopreventive properties. CC and RP-HPLC analyses of the *n*-hexane and DCM extracts led to the isolation and characterization of eighteen compounds, which were identified as 3-*β*-*O*-acetyl aleuritolic acid (**7**), lupeol (**8**), vanillin (**147**), *trans*-ferulic acid (**148**), a mixture of ferulate derivatives: cluytyl ferulate (**149**) and hexacosanoyl ferulate (**150**), crotocorylifuran (**151**), crotonzambefuran A (**152**), megalocarpoidolide D (**153**), 12-*epi*-megalocarpoloide D (**154**), crotonolin E (**155**), the epimeric mixtures of crotonolin A (**156**) and crotonolin B (**157**), and crotonolin C (**158**) and crotonolin D (**159**), crotonolin F (**160**), 7-*α*-hydroxydehydroabietic acid (**161**) and 7-oxo-dehydroabietic acid (**162**) (Figure 3.5). This is the first report on the occurrence of the compounds **147-162** in *C. oligandrus*. Compounds **154-160** are new clerodane diterpenes from any natural

source. Diterpenes are the most abundant secondary metabolites found in the genus *Croton*, representing about 85% of all the isolated metabolites with clerodane being the most abundant subclass (Xu *et al.*, 2018).

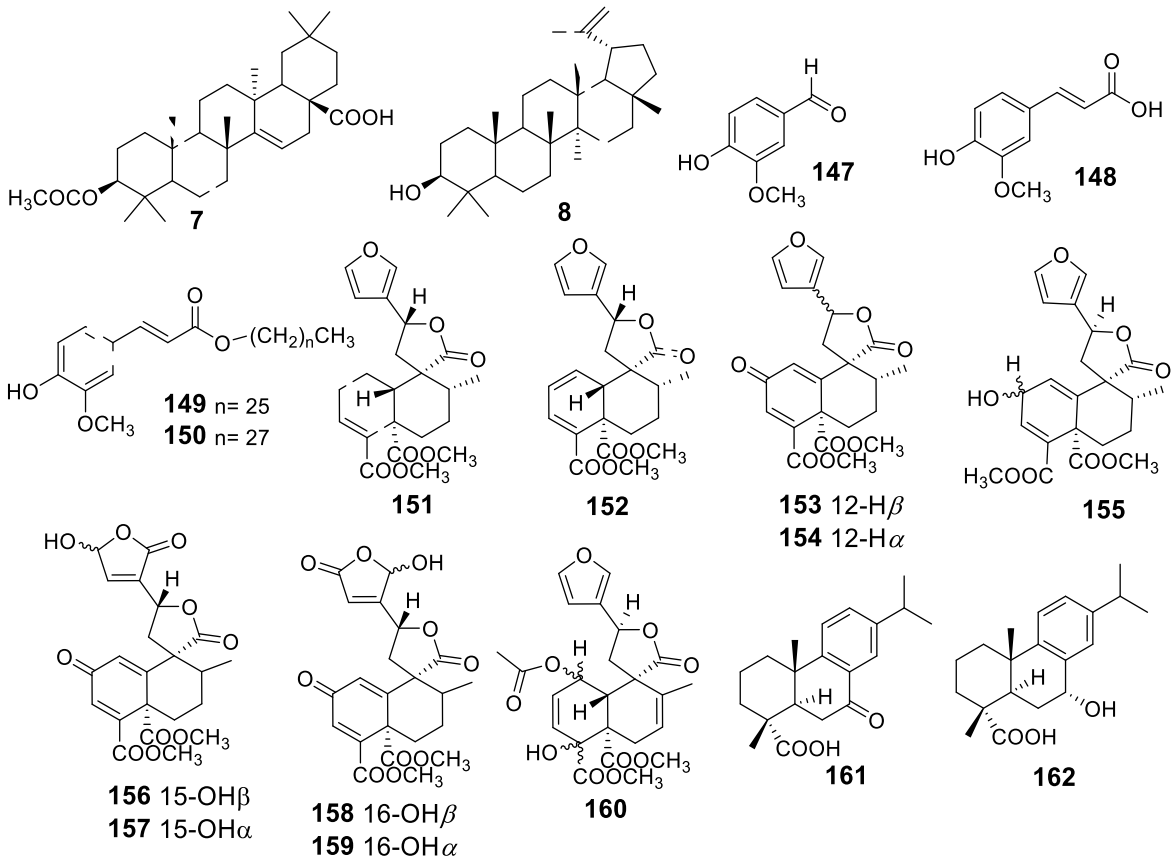

Figure 3.5 Structures of isolated compounds from the bark of *C. oligandrus*

3.3.1.1 Structure elucidation of 3-*β*-*O*-acetyl aleuritolic acid (**7**)

Compound **7** was obtained as a white powder, which precipitated in a mixture of Hex-EtOAc (7:1). Its molecular formula $C_{32}H_{50}O_4$ was deduced from the ESI-MS spectrum in positive ion mode (Figure 3.6) by the sodiated molecular ion peak at *m/z* 521 $[M+Na]^+$. Its ^1H NMR spectrum (Figure 3.7, Table 3.5), showed seven methyl singlets at δ_H 0.88, 0.90, 0.96, 0.97, 0.97, 0.98, 0.99, 1.95 and 2.06; a doublet of doublets at δ_H 5.52 (J = 3.4, 7.9 Hz) indicating the presence of an olefinic proton (Misra and Khastgir, 1970) and

another doublet of doublets at δ 4.48 (J = 5.3, 10.9 Hz), attributable to an oxymethine proton. All these preliminary observations suggested the presence of a triterpenoid skeleton in the molecule. This was further confirmed by the presence of thirty-two carbon signals in the ^{13}C NMR spectrum of **7** (Figure 3.8, Table 3.5) corresponding to eight methyls, ten methylenes, five methines including an oxymethine at δ_C 80.9 (C-3) and an olefinic methine at δ_C 116.7 (C-15), nine quaternary carbons including an olefinic carbon at δ_C 160.6 (C-14) and two carbonyls signals at δ_C 184.0 and 170.9 indicating the presence of a carboxylic acid and an acetoxy function, respectively. The signals at δ_C 160.5 and 116.8 could be assigned to the double-bonded carbons (C=C), which are typical of that of C14-C15 double bond signals of a taraxerane skeleton (Rasool *et al.*, 1989). The position of the double bond could be confirmed by the different ^{1}H-^{13}C long-range correlations (Figure 3.8) observed in the HMBC spectrum. The methyl signal at δ_H 2.06 was attributed to the methyl of the acetoxy group based on its correlation to the carbonyl at δ_C 170.9 observed in the HMBC. The acetoxy group could be placed on C-3 of the triterpene skeleton as there was a ^{3}J correlation from the 3-oxymethine (δ_H 4.48) to the acetoxy carbonyl (δ_C 170.9), observed in the HMBC spectrum. The assignment of all ^{1}H and ^{13}C NMR signals (Table 3.5) of **7** was achieved by a combination of COSY, HSQC and HMBC spectral analyses, and in comparison, with the published data for 3-*β*-*O*-acetyl aleuritolic acid (Mahato and Kundu, 1994; Prabowo *et al.*, 2013). Thus, compound **7** was identified conclusively as 3-*β*-*O*-acetyl aleuritolic acid. Acetyl aleuritolic acid (**7**) was first isolated from the bark of *Aleurites montana* (Euphorbiaceae) and is widespread in all genera of the Euphorbiaceae including the genus *Croton* (Misra and Khastgir, 1970; Salatino *et al.*, 2007).

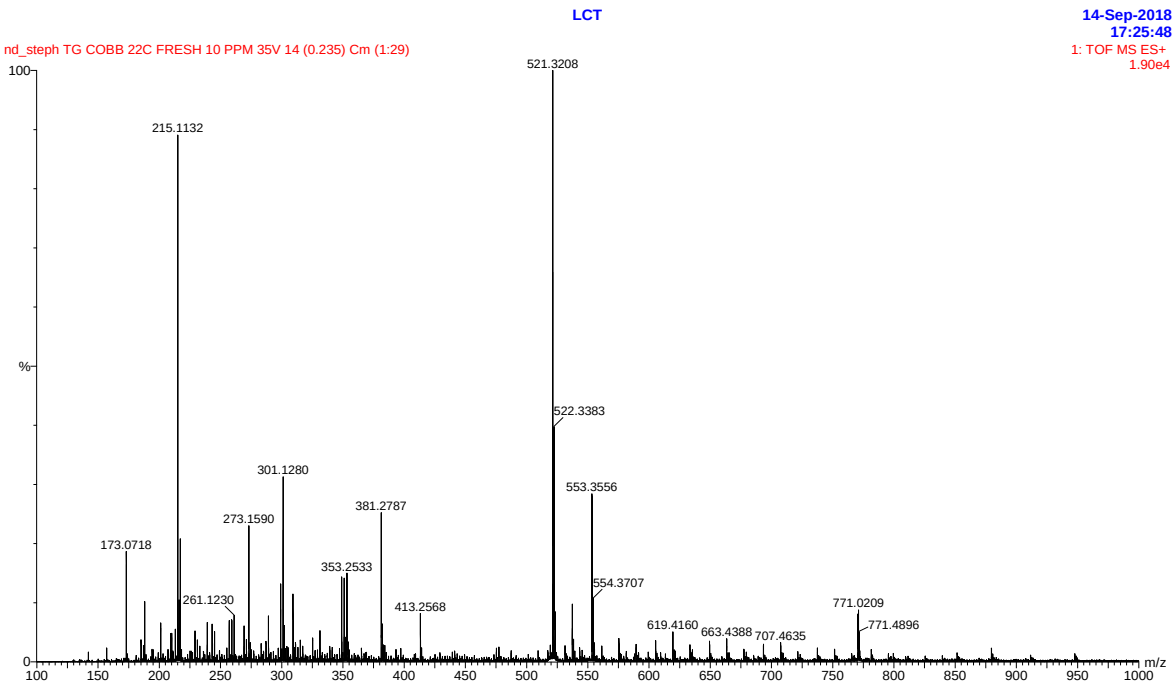

Figure 3.6 ESI-MS spectrum of **7**

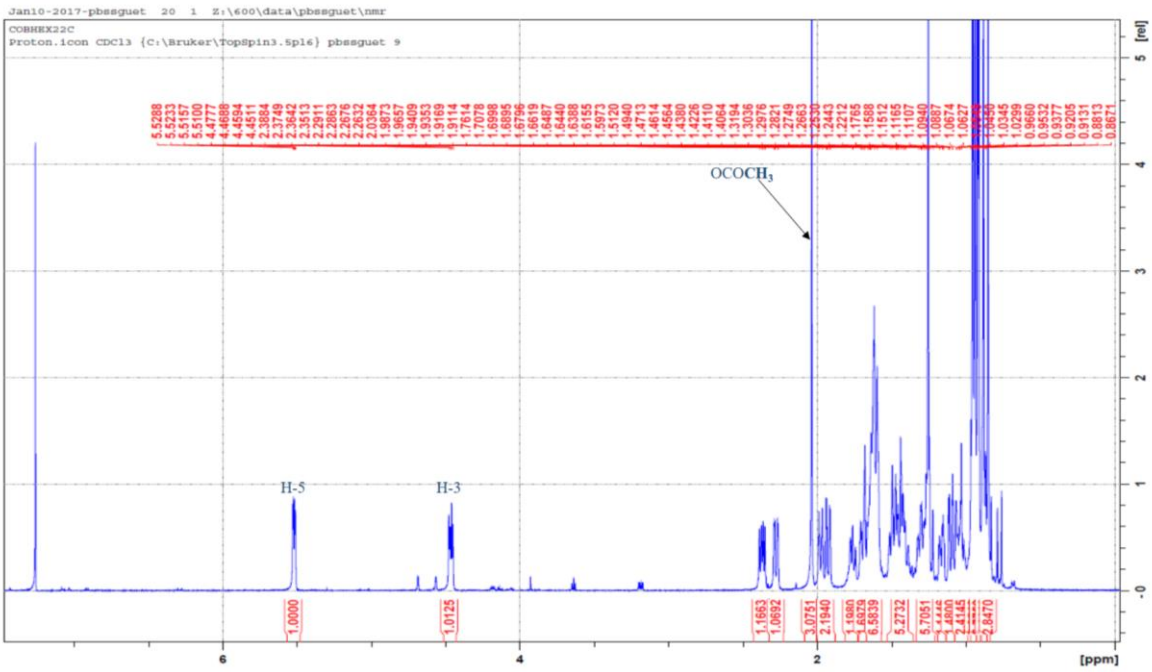

Figure 3.7 ^{1}H NMR (600 MHz, $CDCl_3$) of **7**

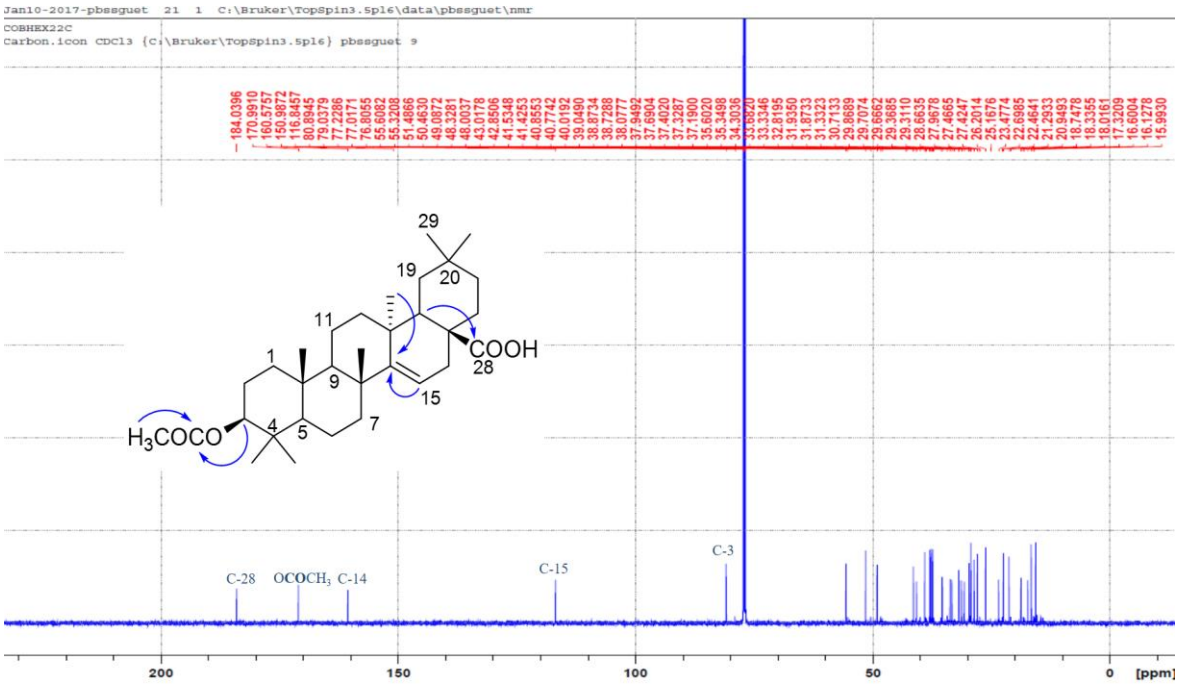

Figure 3.8 ^{13}C NMR (150 MHz, $CDCl_3$) and key HMBC correlations of **7**

Table 3.5 ^{1}H (600 MHz, $CDCl_3$) and ^{13}C NMR (150 MHz, $CDCl_3$) data of **7**

Position	δ_H m (*J* in Hz)	δ_C	Position	δ_H m (*J* in Hz)	δ_C	Position	δ_H m (*J* in Hz)	δ_C
1	1.05	37.7	11	1.52	17.3	20	29.7	-
	1.65			1.67		21	33.6	1.09
2	1.65	23.4	12	1.65	33.3	22	1.43	30.7
3	4.48 dd (*5.3, 10.9*)	80.9		1.76			1.71	
4	-	37.4	13	-	37.3	23	0.88 s	27.9
5	0.92	55.6	14	-	160.6	24	0.99 s	16.5
6	1.20	18.7	15	5.52 dd (*3.4, 7.9*)	116.7	25	0.96 s	15.6
	1.65		16	1.95	31.4	26	0.98 s	26.1
7	1.32	40.8		2.39		27	0.97 s	22.4
	2.00		17	-	51.3	28	-	184.0
8	-	39.0	18	2.29	41.5	29	0.97 s	31.9
9	1.45	49.0	19	1.14	35.3	30	0.90 s	28.7
10	-	37.9		1.30				
CH_3CO	-	170.9	$OCCH_3$	2.06 s	21.3			

3.3.1.2 Structure elucidation of cluytyl ferulate (**149**) and hexacosanoyl ferulate (**150**) as a mixture

Compounds **149** and **150** were obtained as a mixture and as a white powder. These were identified as the main constituents of the *n*-hexane extract along with acetyl aleuritolic acid (**7**) and lupeol (**8**). The HR ESI-MS spectrum in negative ion mode (Figure 3.9) of the white powder revealed a mixture composition of two homologous substances showing $[M-H]^-$ peaks at *m/z* 557.4571 and 585.4881, with a relative abundance of 52 and 45%, respectively, corresponding to the formulas $C_{36}H_{61}O_4$ and $C_{38}H_{65}O_4$, respectively, calculated for $[C_{36}H_{61}O_4]^-$, 557.4575 and $[C_{38}H_{65}O_4]^-$, 585.4888, respectively. The ^1H NMR spectrum (Figure 3.10, Table 3.6) exhibited signals for a methoxy group (δ_H 3.95, s), two *trans* olefinic protons (δ_H 7.63 and 6.31, J =16.0 Hz), and three aromatic hydrogens forming an ABX system (δ_H 6.93, d, J = 8.1 Hz;, 7.09, d, J = 1.8 Hz and 7.10 , dd, J = 1.8, 8.1 Hz) that could be assigned to a ferulic acid moiety (Balde *et al.*, 1991). The signals at δ_H 4.21 (2H, t, J = 6.7 Hz), 1.27-1.71 (2H, brs, m) and 0.90 (3H, t, J = 6.9 Hz) could be attributed to an oxymethylene, a long saturated aliphatic chain and a terminal methyl functionality, respectively, suggesting the presence an aliphatic alcohol moiety in the molecule. The ^{13}C NMR spectrum (Figure 3.11, Table 3.6) confirmed the presence of a saturated fatty alcohol moiety, an ester linkage and a ferulic moiety. Assignment of the ^1H and ^{13}C NMR data of **149** and **150** (Table 3.6) were confirmed by the ^1H-^{13}C long-range correlations (Figure 3.11) observed in the HMBC spectrum. All assignments of ^1H and ^{13}C NMR signals of these compounds are in good agreement with those published for cluytyl ferulate and hexacosenoyl ferulate, respectively (Wandji *et al.*, 1990; Balde *et al.*, 1991). Thus, compounds **149** and **150** were identified as cluytyl ferulate (**149**) and hexacosenoyl ferulate (**150**), respectively.

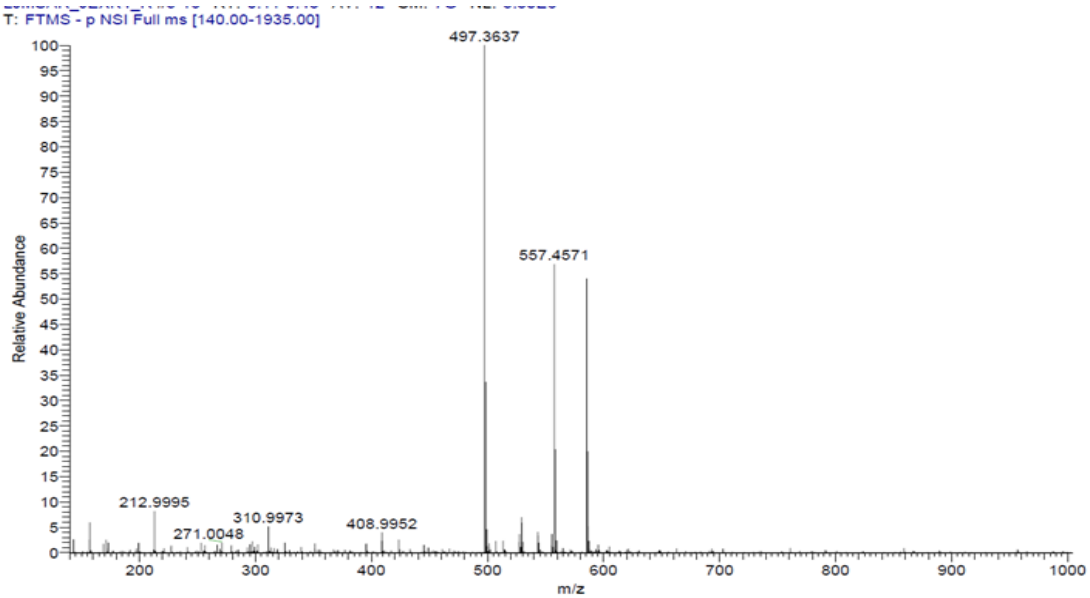

Figure 3.9 ESI-MS spectrum of **149** and **150**

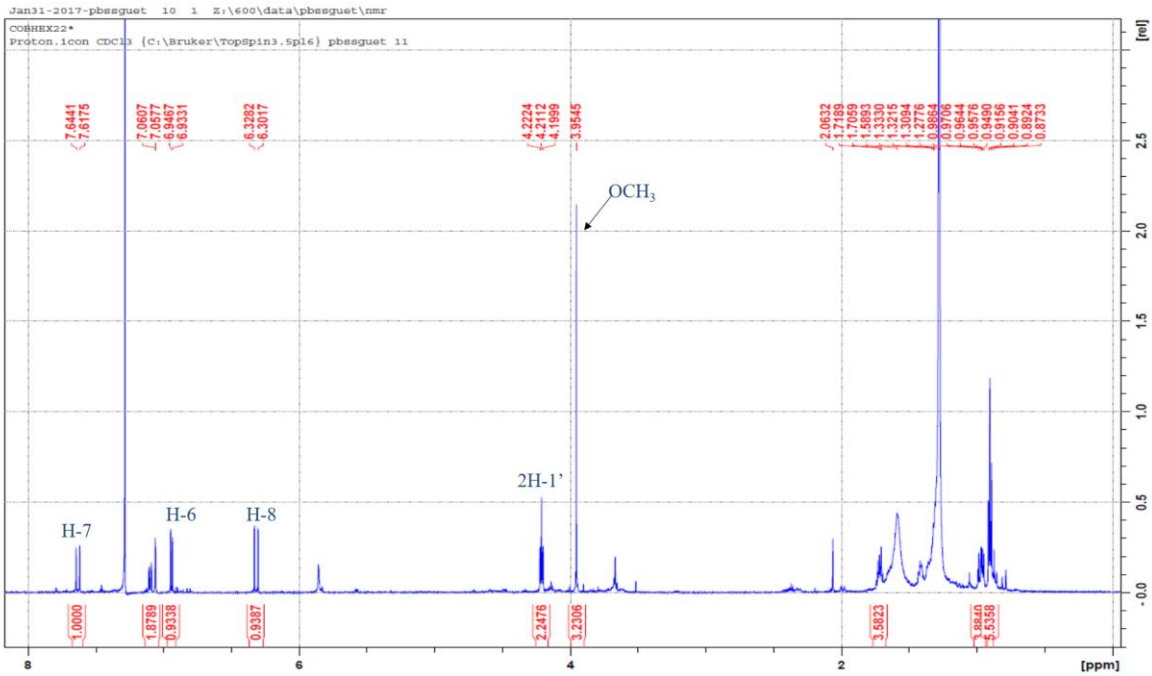

Figure 3.10 ^{1}H NMR (600 MHz, $CDCl_3$) of **149** and **150**

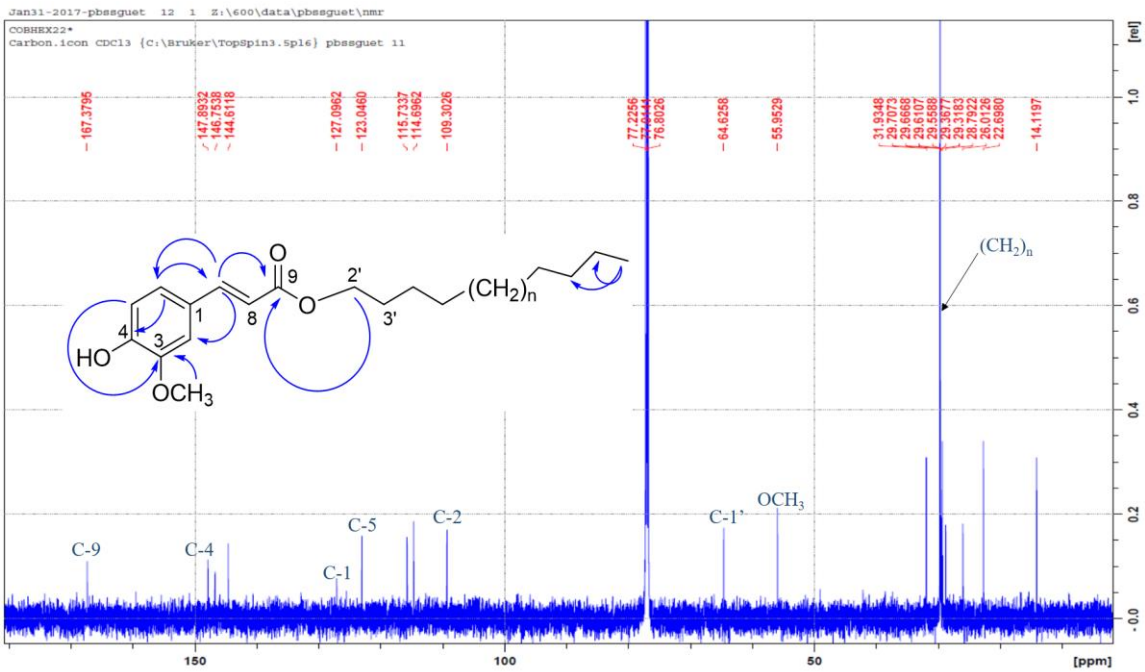

Figure 3.11 ^{13}C NMR (150 MHz, $CDCl_3$) and key HMBC correlations of **149** and **150**

Table 3.6 ^{1}H (600 MHz, $CDCl_3$) and ^{13}C NMR (150 MHz, $CDCl_3$) data of **149** and **150**

Position	δ_H m (*J* in Hz)	δ_C	Position	δ_H m (*J* in Hz)	δ_C
1	-	127.1	1’	4.20 t (*6.7*)	64.6
2	7.06 d (*1.8*)	109.3	2’	1.42 m	26.0
3	-	146.7	3’	1.71 m	28.8
4	-	147.9	4’-23’/25’	1.27 brs	29.3
5	7.10 dd (*1.8*, *8.1*)	123.0	24’/26’	1.27 brs	31.9
6	6.93 d (*8.1*)	114.7	25’/27’	1.27 brs	22.7
7	7.63 d (*16.0*)	144.6	26’/28’	0.90 t (*6.9*)	14.1
8	6.31 d (*16.0*)	115.7	OCH_3	3.95 s	55.9
9	-	167.4			

3.3.1.3 Structure elucidation of crotocorylifuran (**151**)

Compound **151** was obtained as a white amorphous powder. Its molecular formula $C_{22}H_{26}0_7$ was determined by ESI-MS analysis (Figure 3.12) in positive ion mode, where the sodiated ion peak was observed at *m/z* 425 $[M+Na]^+$. Its ^{1}H NMR spectrum (Figure 3.13, Table 3.7) indicated the presence of a secondary methyl group at δ_H 1.02 (3H, d, *J* = 6.4 Hz), two methoxy singlet functions at δ_H 3.71 and 3.76, characteristic signals of a *β*-substituted furan ring at δ_H 6.41 (1H, brd, *J* = 0.9 Hz), 7.44 (1H, ov) and 7.45 (1H, brs) (Tchissambou *et al.*, 1990), an oxymethine proton at δ_H 5.40 (1H, t, *J* = 8.5 Hz) and an olefinic proton belonging to a trisubstituted double bond at δ_H 6.84 (1H, dd, *J* = 4.3, 7.5 Hz) were also observed. The ^{13}C NMR spectrum (Figure 3.14, Table 3.8) of **151** showed 22 carbon resonances suggesting a diterpene skeleton. The ^{13}C NMR and HSQC DEPT analyses supported the observations made on the ^{1}H NMR spectrum and also indicated the presence of five methylenes at δ_C 19.2 (C-1), 26.4 (C-2), 32.3 (C-6), 27.9 (C-7) and 42.4 (C-11) and two methines at δ_C 40.2 (C-8) and 51.9 (C-10), which on the HSQC spectrum correlated with the proton signals appearing at δ_H 1.58 (m) and 1.76 (dd, *J* = 2.4, 13.2 Hz), respectively. All these data together with the different correlations observed in the COSY and HMBC spectra suggested a *neo*-clerodane (ex *ent*-clerodane)-type diterpene skeleton (Li *et al.*, 2016). The ^{1}H and ^{13}C NMR data (Tables 3.7-3.8) of **151** were similar to those of crotocorylifuran (Tchissambou *et al.*, 1990). The absolute configuration of the C-12 carbon was determined using the NOESY experiment. For a C-12*R* configuration, a correlation would be seen between H-12 and 3H-17, while a correlation seen between H-12 and H-1*α* will imply C-12*S* configuration (Bautista *et al.*, 2012; Ndunda *et al.*, 2016). For compound **151**, a correlation observed in the NOESY spectrum between the H-12 and H-1*α* proton (δ_H 1.92) suggested a C-12*S* configuration. All the ^{1}H and ^{13}C NMR data of **151** supported by the ^{1}H-^{13}C long-range correlations

observed (Figure 3.14) led to its identification as crotocorylifuran, a clerodane diterpene first isolated from the trunk bark of *Croton haumanianus* (Tchissambou *et al.*, 1990).

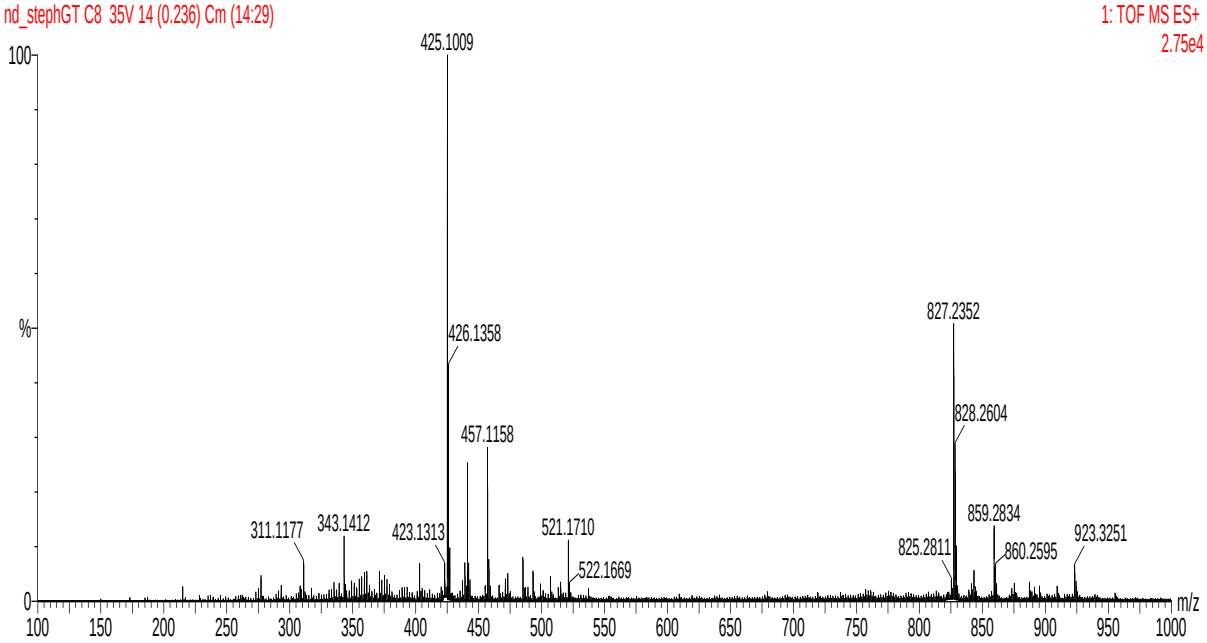

Figure 3.12 ESI-MS spectrum of **151**

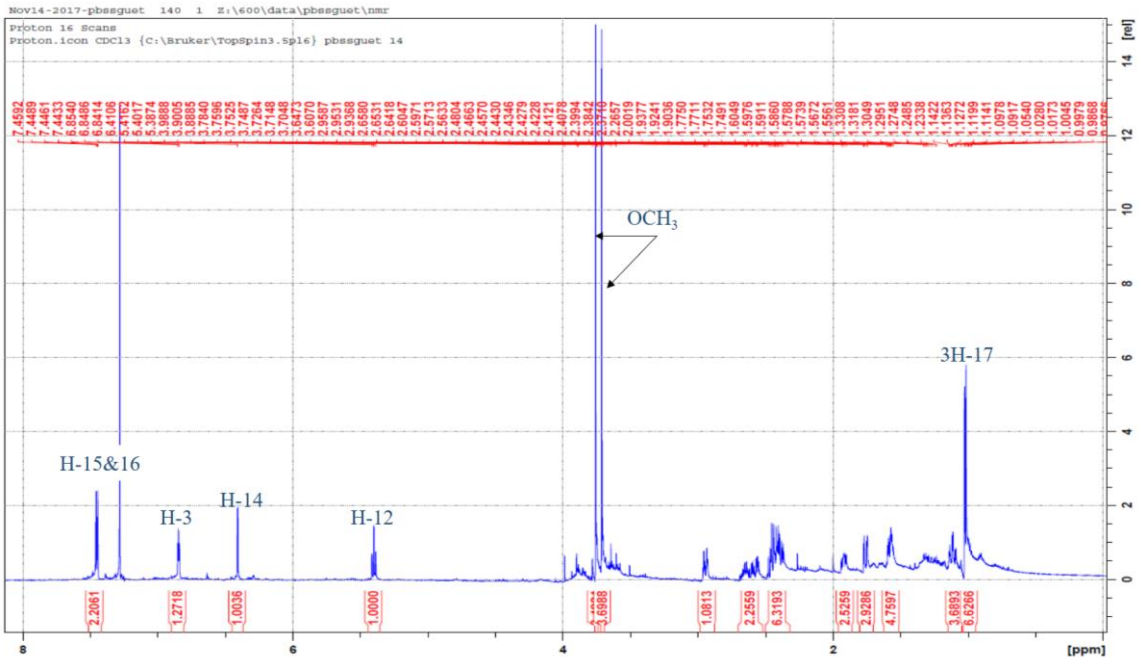

Figure 3.13 ^{1}H NMR (600 MHz, $CDCl_3$) of compound **151**

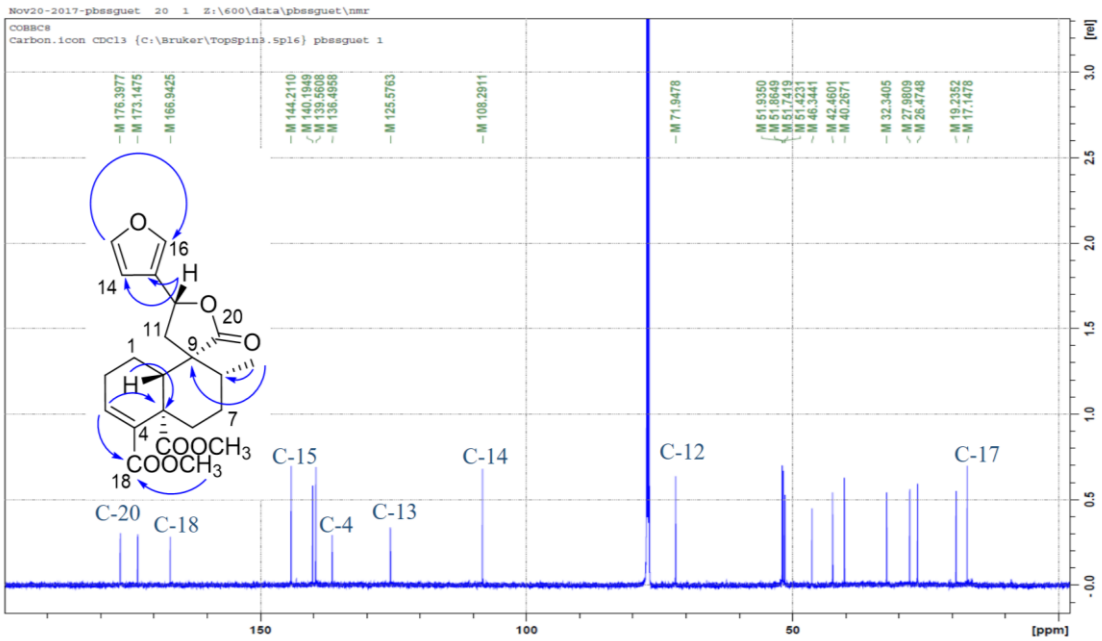

Figure 3.14 ^{13}C NMR (150 MHz, $CDCl_3$) and key HMBC correlations of **151**

3.3.1.4 Structure elucidation of megalocarpoidolide D (**153**)

Compound **153** was isolated as a white amorphous powder, $[\alpha]_D^{25}$ -88.8 (c 0.001, MeOH). Its molecular formula $C_{22}H_{22}O_8$ was determined from the *pseudo*molecular ion peak at *m/z* 437 $[M+Na]^+$ from its ESI-MS spectrum (Figure 3.15) obtained in positive ion mode. The IR spectrum of **153** displayed absorption stretching bands at 1715, 1767 and 1663 cm^{-1} that could be attributed to the carbonyl of ester, lactone and ketone groups, respectively. The ^{1}H NMR spectrum (Figure 3.16, Table 3.7) revealed characteristic signals of a *β*-substituted furan ring at δ_H 6.45 (m, H-14), 7.47 (br dd, *J* = 1.5, 3.1 Hz, H-15) and 7.54 (brs, H-16), two olefinic protons at δ_H 6.47 (d, *J* = 1.3 Hz) and 6.78 (d, *J*= 1.3 Hz), an oxymethine at δ_H 5.55 (dd, *J* = 5.2, 11.1 Hz), as well as three methyl signals including two methoxy singlets at δ_H 3.65 and 3.84 and a doublet methyl at δ_H 1.17 (d, *J* = 6.4 Hz). Its ^{13}C NMR spectrum (Figure 3.17, Table 3.8) exhibited the resonances of 22 carbons suggesting a diterpene skeleton. The carbon signals appearing at δ_C 108.1 (C-14),

123.5 (C-13), 140.5 (C-16) and 144.6 (C-15) and correlating on the HSQC spectrum (Figure 3.18) with the protons at δ_H 6.47 (d, J = 1.3 Hz) and 6.78 (d, J = 1.3 Hz) could be attributed to those of the substituted furan ring. One oxymethine at δ_C 71.2 as well as seven quaternary carbons including three carbonyl ester groups at δ_C 165.3, 166.3 and 172.1 and a ketone carbonyl at δ_C 185.7 were also observed in the ^{13}C NMR spectrum. Assignment of the ^{1}H and ^{13}C NMR data of **153** supported by its 2D NMR correlations (Figures 3.18-3.21) suggested an *ent*-clerodane diterpene skeleton (Li *et al.*, 2016). The HMBC spectrum revealed that the two carbonyls at δ_C 165.3 and 166.3 correlating with the methoxy signals at δ_H 3.84 and 3.65, respectively, could be at C-18 and C-19, while the carbonyl at δ_C 172.1 could be attributed to that of a lactone moiety and assigned the position C-20. The other carbonyl at δ_C 185.8 could be identified to that of a conjugated carbonyl and assigned to position C-2 by comparison of the NMR data of **153** with those published for megalocarpoidolide D (Ndunda *et al.*, 2016). All the ^{1}H and ^{13}C NMR data of **153** and the ^{1}H-^{13}C long-range correlations (Figure 3.16) were in good agreement with those of the *β*-substituted furanoclerodane, megalocarpoidolide D, isolated from the roots of *Croton megalacarpoides* (Ndunda *et al.*, 2016). Furthermore, analysis of the NOESY spectrum (Figure 3.20) showed a strong correlation between H-12 and H-1 confirming the *β*-orientation of H-12 (Bautista *et al.*, 2012). Thus, compound **153** was identified as megalocarpoidolide D**.**

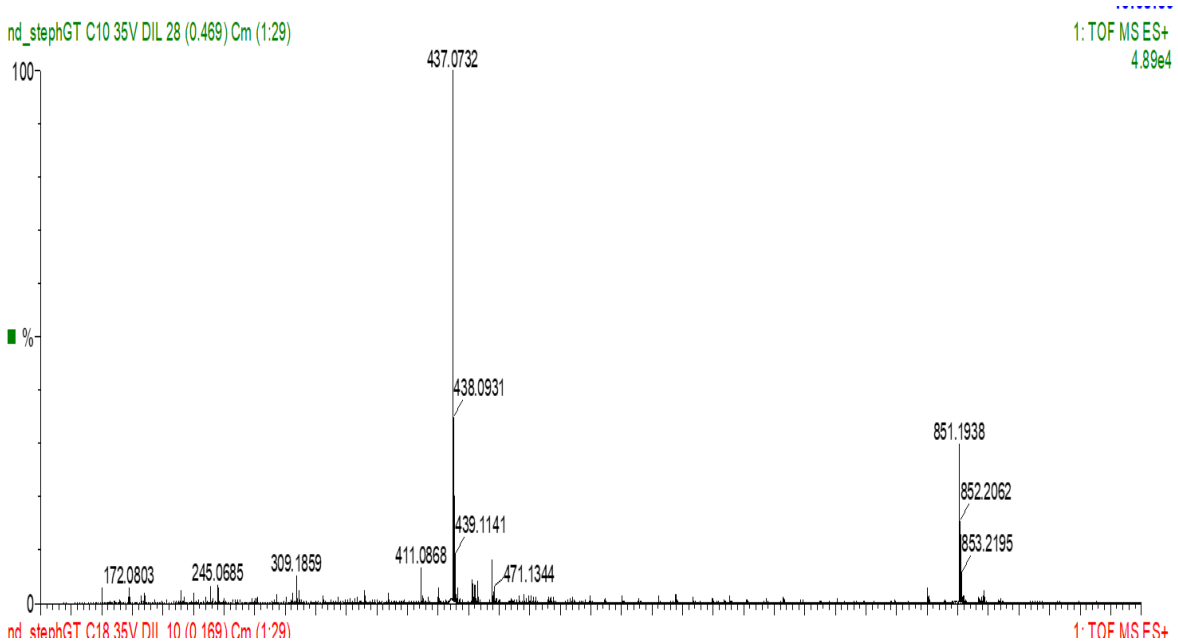

Figure 3.15 ESI-MS spectrum of **153**

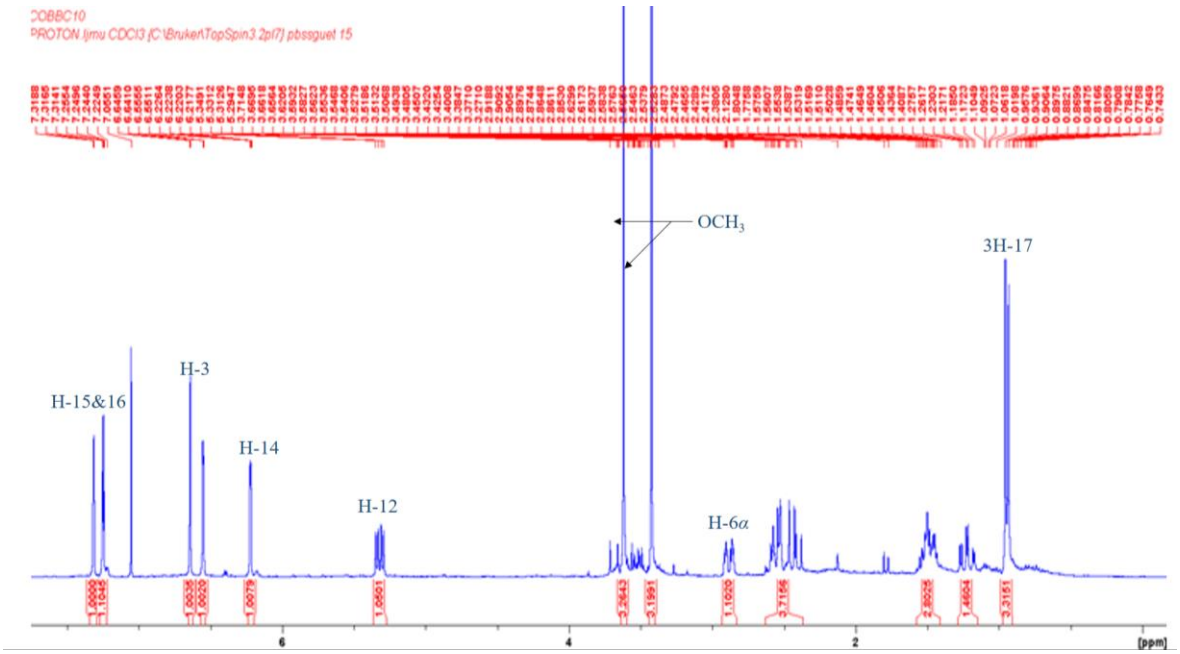

Figure 3.16 ^{1}H NMR (300 MHz, $CDCl_3$) of **153**

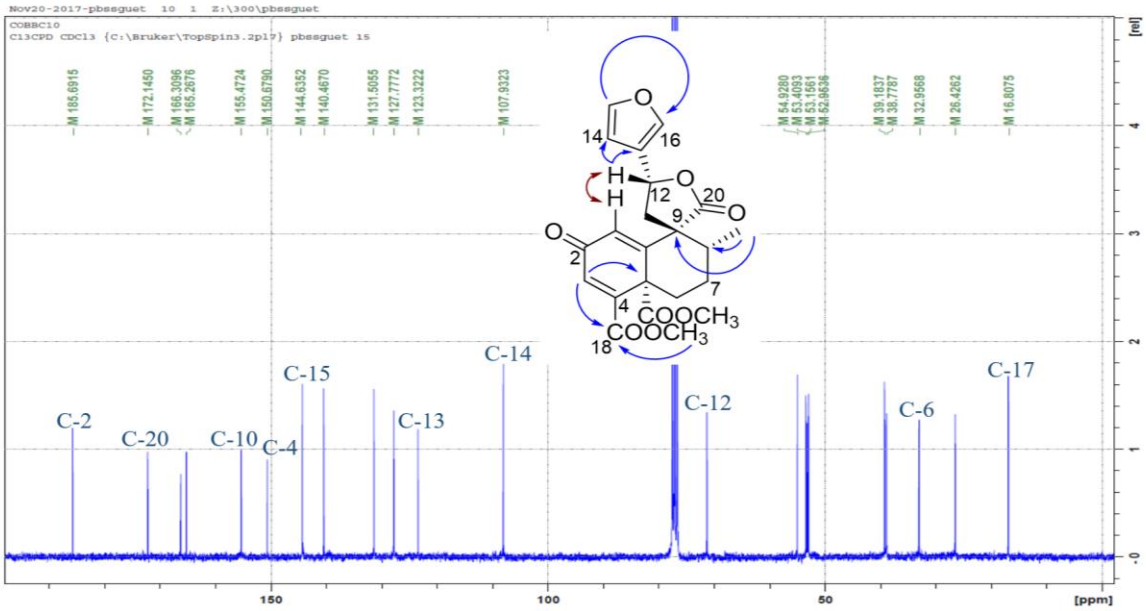

Figure 3.17 ^{13}C NMR (75 MHz, $CDCl_3$) and key ^{1}H-^{1}H NOESY (↔) and HMBC (→) correlations of **153**

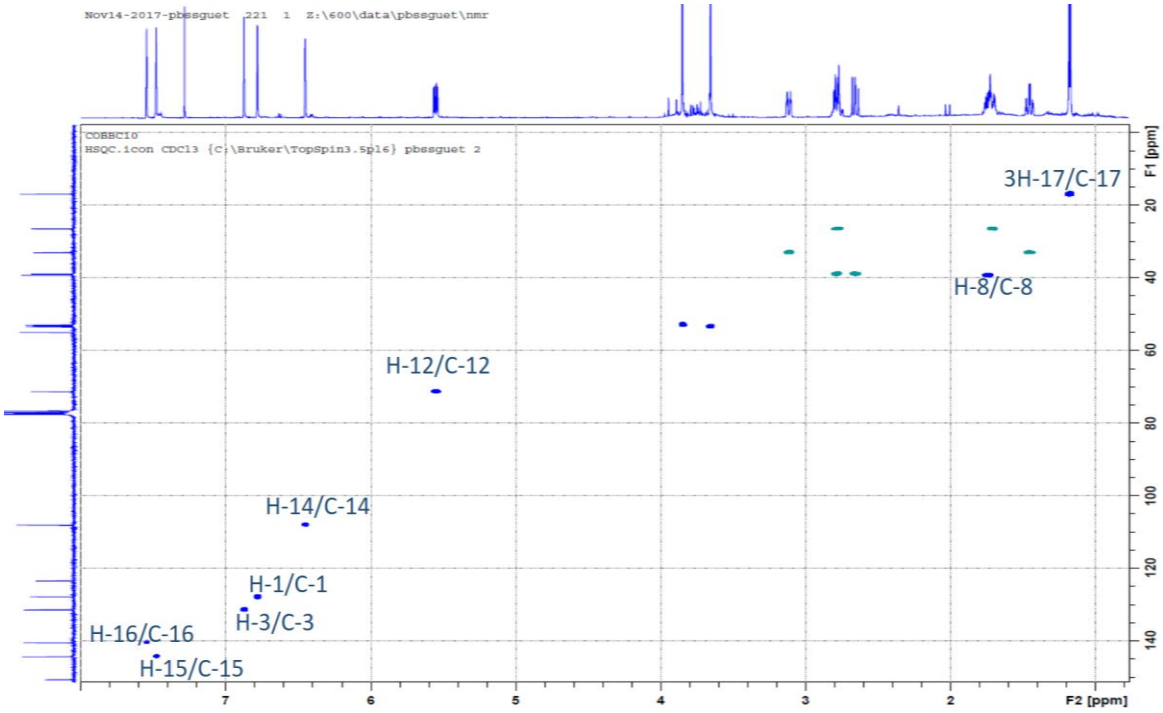

Figure 3.18 HSQC spectrum of **153**

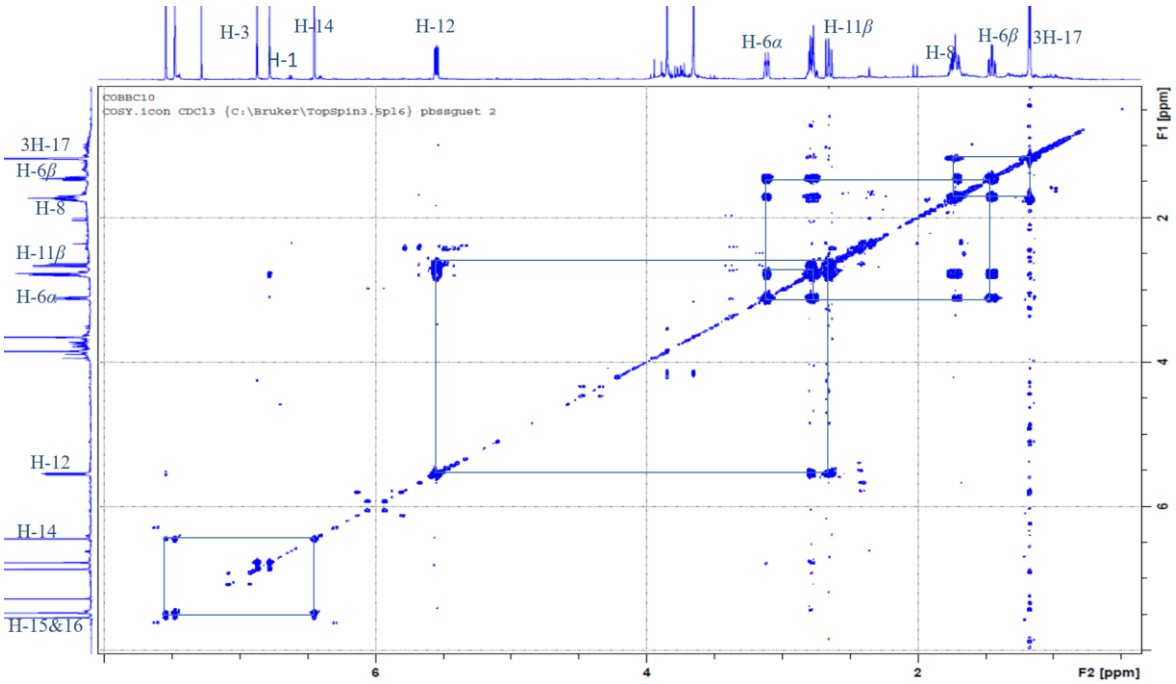

Figure 3.19 ^{1}H-^{1}H COSY spectrum of **153**

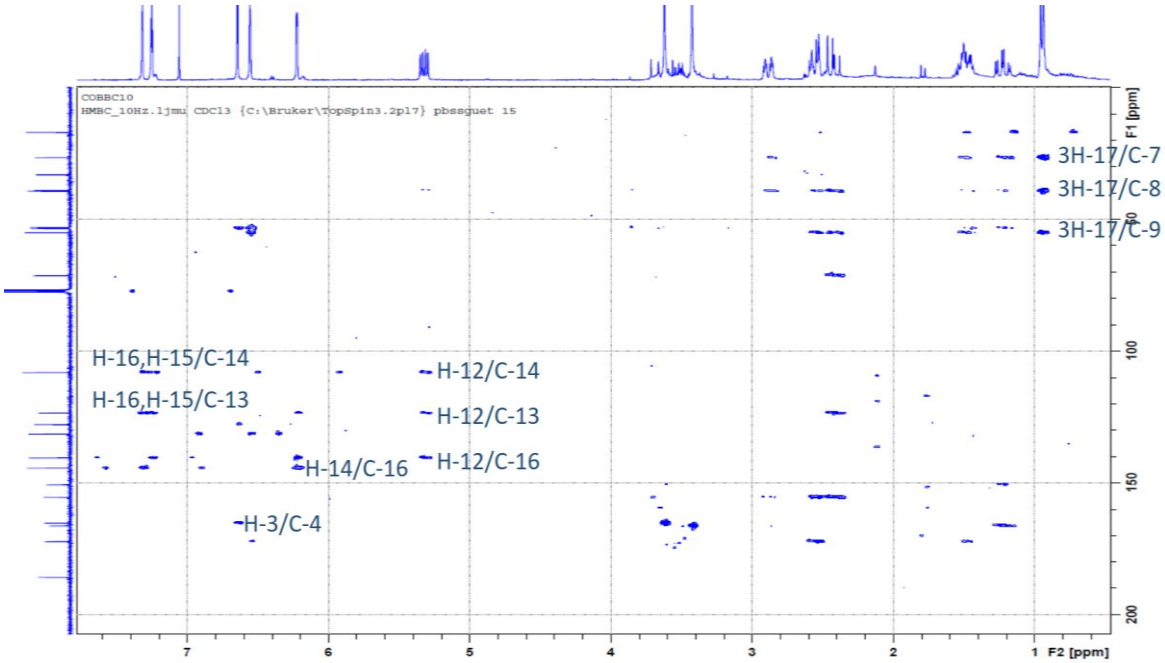

Figure 3.20 HMBC spectrum of **153**

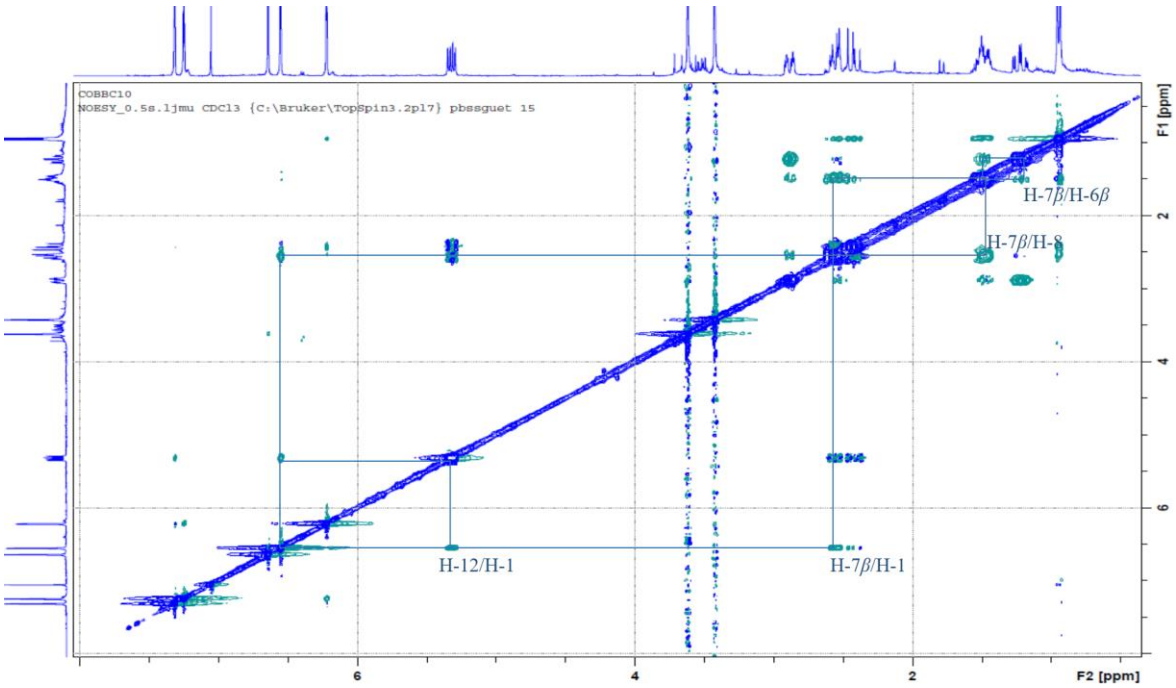

Figure 3.21 ^{1}H-^{1}H NOESY spectrum of **153**

3.3.1.5 Structure elucidation of 12-*epi*-megalocarpoloide D (**154**)

Compound **154** was isolated as a white amorphous powder, $[\alpha]_D^{25}$ +81.7 (c 0.0018, MeOH). Its molecular formula $C_{22}H_{22}O_8$ was determined from the *pseudo*molecular ion peak at *m/z* 432.1650 calculated for $C_{22}H_{22}O_8NH_4$ $[M+NH_4]^+$, 432.1653 from its HR ESI-MS spectrum obtained in positive ion mode. The IR spectrum of **154** quite identical to that of **153**, also displayed absorption stretching bands at 1715, 1767 and 1663 cm^{-1} attributable to the carbonyl of ester, lactone and ketone groups, respectively. The ^{1}H and ^{13}C NMR spectra (Figures 3.22-3.23) of compound **154** as well as its 2D NMR spectra including COSY, HSQC and HMBC were all similar to those of **153** with only slight differences in terms of chemical shifts (Tables 3.7-3.8). Analysis of its ^{1}H, ^{13}C, COSY, HSQC and HMBC spectral data concluded its core structure to be identical to that of **153**. However, in the NOESY spectrum (Figure 3.24), a strong correlation observed between H-12 and H-17 suggested an *α*-orientation of H-12 and thus, established a 12*R*

configuration for **154** opposite to the 12*S* configuration found for **153** (Ndunda *et al.*, 2016). Therefore, the structure of compound **154** supported by its NOESY and HMBC key correlations (Figure 3.23) was established to be the C-12*R* epimer of **153** and named 12-*epi*-megalocarpoidolide D, a new clerodane from natural source.

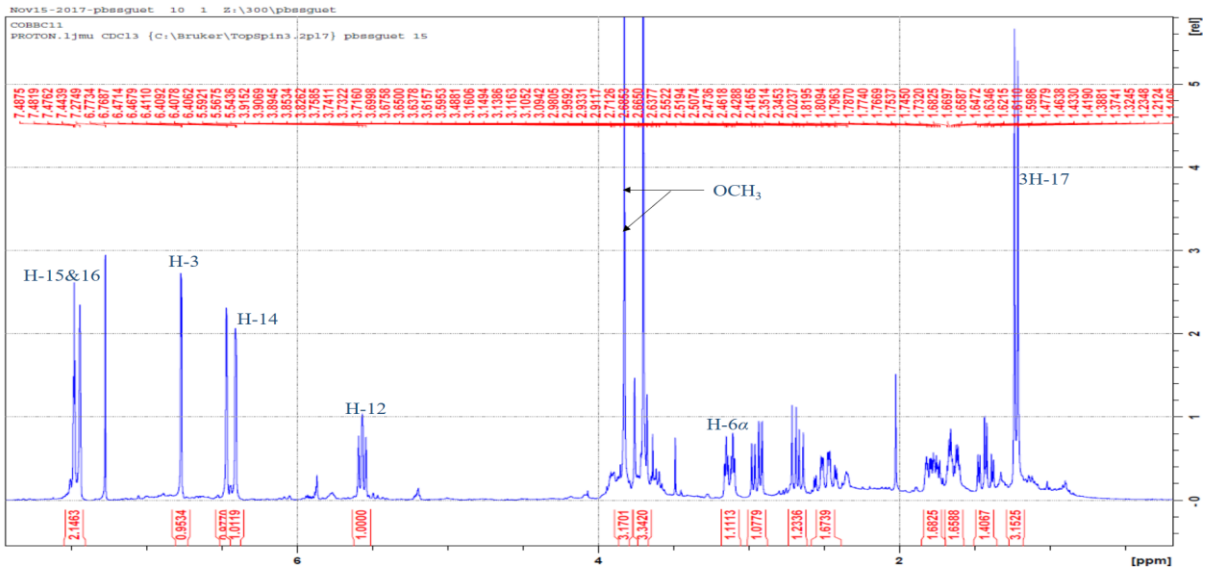

Figure 3.22 ^{1}H NMR (300 MHz, $CDCl_3$) of **154**

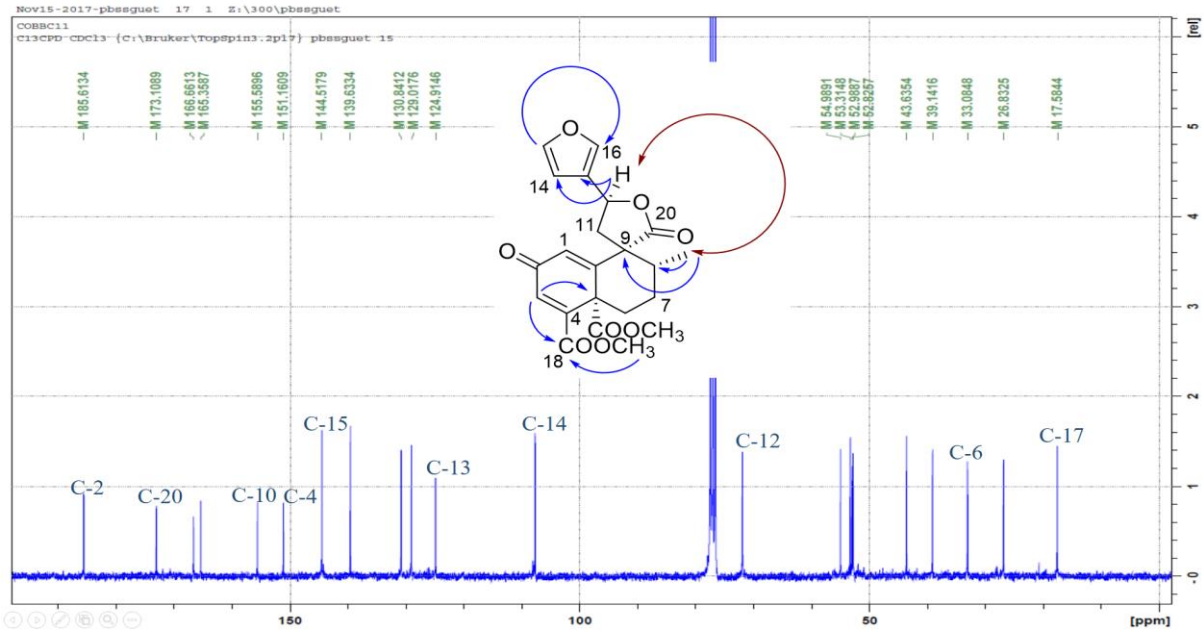

Figure 3.23 ^{13}C NMR (75 MHz, $CDCl_3$) and key ^{1}H-^{1}H NOESY (↔) and HMBC (→) correlations of **154**

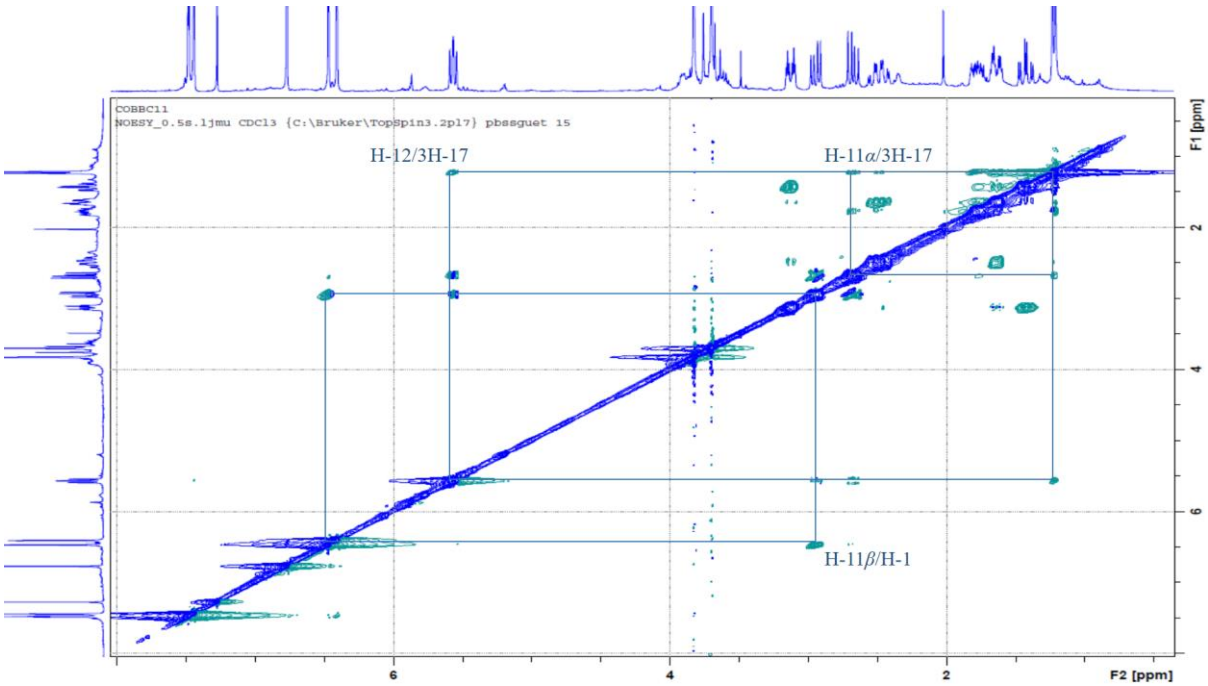

Figure 3.24 ^{1}H-^{1}H NOESY spectrum of **154**

3.3.1.6 Structure elucidation of crotonolin A (**156**) and crotonolin B (**157**) as a mixture

Compounds **156** and its 15-epimer **157** were isolated as a white amorphous powder mixture ($[\alpha]_D^{25}$ 0.0 (c 0.009, MeOH) with molecular formula of $C_{22}H_{22}O_{10}$ as determined from their HR ESI-MS spectrum obtained in the negative ion mode, where the peak at *m/z* 445.1142 $[M-H]^-$ could be calculated 445.1140 for $C_{22}H_{21}O_{10}$. Their FT-IR spectrum showed absorption bands at 3465, 1775, 1712 and 1661 cm^{-1} assignable to the stretch signals of hydroxyl and the carbonyls of ester, lactone and ketone groups, respectively. The ^{1}H (Figure 3.25) and ^{13}C NMR (Figure 3.26) spectra of the mixture of **156** and **157** similar to those of compound **153**, also suggested a clerodane skeleton (Li *et al.*, 2016). The only difference between the ^{1}H NMR of the mixture of **156** and **157** and that of compound **153** was the absence of the signals corresponding to the *β*-substituted furan ring protons in the ^{1}H NMR spectrum of **156** and **157**. Those furan ring protons were replaced by two methines doublets at δ_H 6.19 and 7.40 showing cross peak correlations

in the HSQC spectrum with carbon signals at δ_C 99.3 and 149.8, respectively. These two methines, in the HMBC spectrum showed a strong correlation with a deshielded carbon signal at δ_C 170.9. The above NMR data were similar to those of the unsaturated *γ*-hydroxy-*α,β*-unsaturated-*γ*-lactone moiety present in salvidinin B, a clerodane diterpene isolated from *Salvia divinorum* (Shirota *et al.*, 2006). The hemiacetal carbon C-15 was then attributed to the signal at δ_C 99.3, the olefinic carbon C-14 at δ_C 149.8, the carbonyl C-16 at δ_C 170.9 and C-13 at δ_C 135.0. These attributions were supported by the ^3J correlation between the proton signal at δ_H 7.40 (H-14) and the carbon C-12, and correlations between protons H-12 and H-11*β* with C-13 observed in the HMBC experiment. However, the signals attributed to protons H-14 and H-15 were not broad singlets like in the case of similar molecular (Blas *et al.*, 2004; Shirota *et al.*, 2006; Maldonado *et al.*, 2016). In addition, the two protons were not showing any correlation in the COSY experiment and the coupling constants of two doublets were different (6.5 and 9.4 Hz). Therefore, it was clear that two broad singlets instead of doublets were present; this led to the conclusion that the obtained powder was a mixture of 15*α*-OH and 15*β*-OH isomers. Furthermore, analysis of the NOESY spectrum showed a strong correlation between H-12 and H-1 suggesting a C-12*S* configuration. In addition, the optical inactivity of the mixture indicated that it was a racemic mixture. Based on their ^{1}H and ^{13}C NMR (Table 3.7-3.8) and the ^{1}H-^{13}C long-range correlations observed in the HMBC spectrum (Figure 3.26), compounds **156** and **157** were identified as 2,16-dioxo-15*β*-hydroxy-18,19-dimethoxycarbonyl-15,16-epoxy-*ent*-cleroda-1(10),3,13-trien-20,12-olide and 2,16-dioxo-15*α*-hydroxy-18,19-dimethoxycarbonyl-15,16-epoxy-*ent*-cleroda-1(10),3,13(16),14-tetraen-20,12-olide, two new clerodane diterpenes and were given the trivial names crotonolins A (**158**) and B (**159**), respectively.

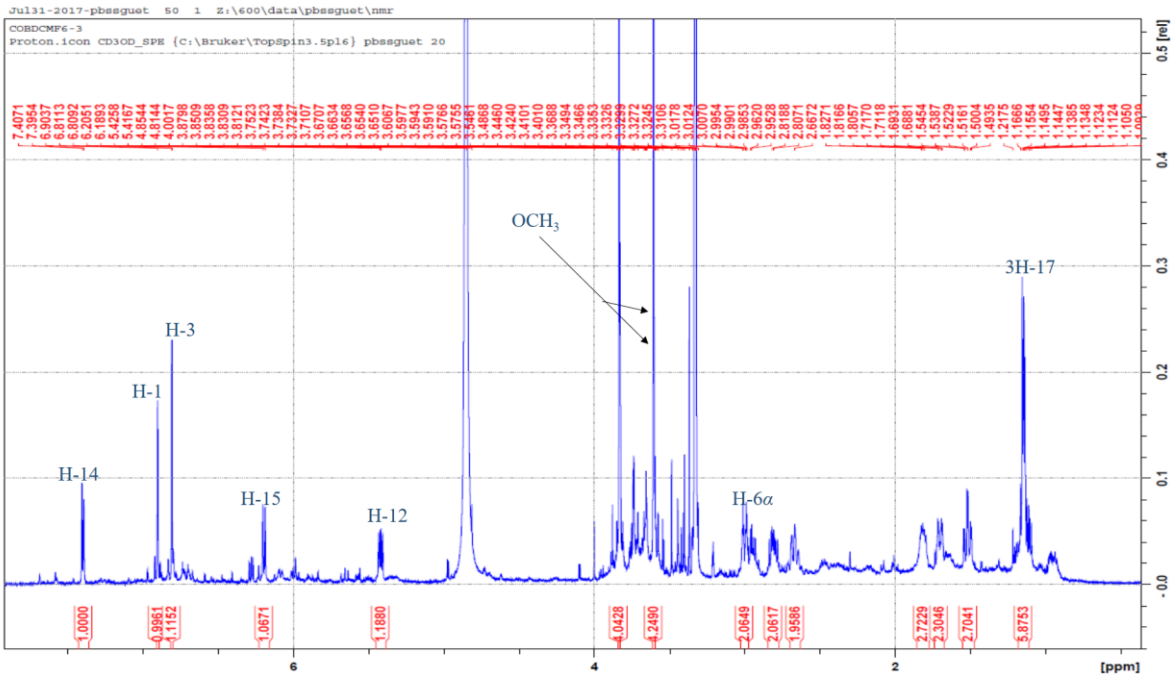

Figure 3.25 ^{1}H NMR (600 MHz, CD_3OD) of **156** and **157**

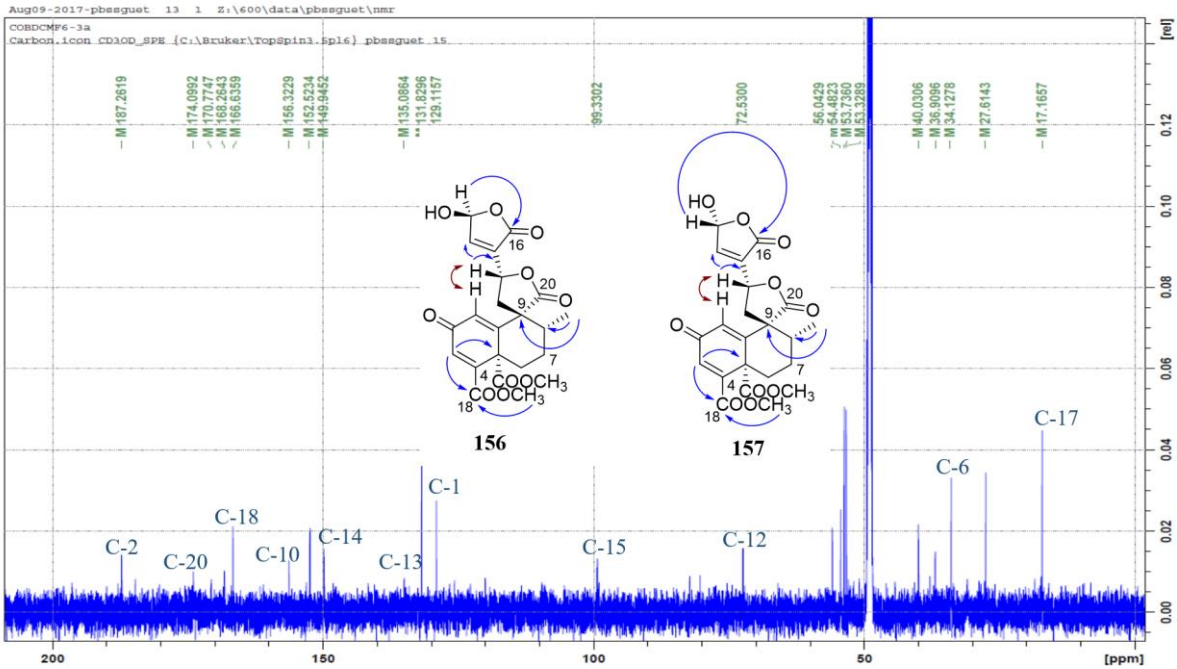

Figure 3.26 ^{13}C NMR (150 MHz, CD_3OD) and key ^{1}H-^{1}H NOESY (↔) and HMBC (→) correlations of **156** and **157**

3.3.1.7 Structure elucidation of crotonolin C (**158**) and crotonolin D (**159**) as a mixture

Compounds **158** and its epimer **159** were isolated as a white amorphous powder mixture ($[\alpha]_D^{25}$ -16.5 (c 0.0002, MeOH) with molecular formula of $C_{22}H_{22}O_{10}$ as determined from their HR-ESI-MS spectra obtained in the positive ion mode, where the sodiated ion peak was observed at *m/z* 469.1120 $[M+Na]^+$, calculated 469.1111 for $C_{22}H_{22}O_{10}Na$. Their FT-IR spectrum showed absorption bands at 3465, 1775, 1712 and 1670 cm^{-1} that could be assigned to the stretch signals of hydroxyl and the carbonyls of ester, lactone and ketone groups, respectively. Their ^1H NMR and ^{13}C NMR spectra (Figures 3.27-3.28) similar with those of compounds **156** and **157**, also suggested a clerodane skeleton containing a *γ*-hydroxy-*α,β*-unsaturated-*γ*-lactone moiety (Shirota *et al.*, 2006). However, the observed chemical shifts corresponding to the proton and carbon resonances of the lactones units in **158** and **159** were different from those observed for **156** and **157**. The lactone units **158** and **159** were identified as 16-hydroxy-13-en-15,16-olides from their NMR data (Blas *et al.*, 2004; Shirota *et al.*, 2006; Maldonado *et al.*, 2016). In this case, the combination of the different signals and correlations observed in the 1D and 2D NMR spectra confirmed the suggested structure elements. The resonances at δ_C 163.6 could be attributed to the *β*-carbon (C-13), δ_H 6.22 and δ_C 119.2 to the *α*-methine (C-14), δ_C 169.1 to the lactone carbonyl (C-15), and δ_H 6.28 and δ_C 96.7 to the hemiacetalic methine (C-16). The configuration of C-12 carbon in the compounds **158** and **159** were determined by NOESY experiment (Figure 3.28). A strong correlation observed in this spectrum between the H-12 protons and the H-1 protons suggested a C-12*S* orientation for both molecules. The ^1H and ^{13}C NMR data (Tables 3.7-3.8) of **158** and **159**, in addition to the key HMBC correlations (Figure 3.28) observed led to their characterisation as 2,15-dioxo-16*β*-hydroxy-18,19-dimethoxycarbonyl-15,16-epoxy-*ent*-cleroda-1(10),3,13(16),14-tetraen-20,12-olide and 2,15-dioxo-16*α*-hydroxy-18,19-dimethoxycarbonyl-15,16-epoxy-*ent*-cleroda-1(10),3,13(16),14-tetraen-20,12-olide

respectively, two clerodane diterpenes not previously described and were given the trivial names crotonolins C (**158**) and D (**159**), respectively.

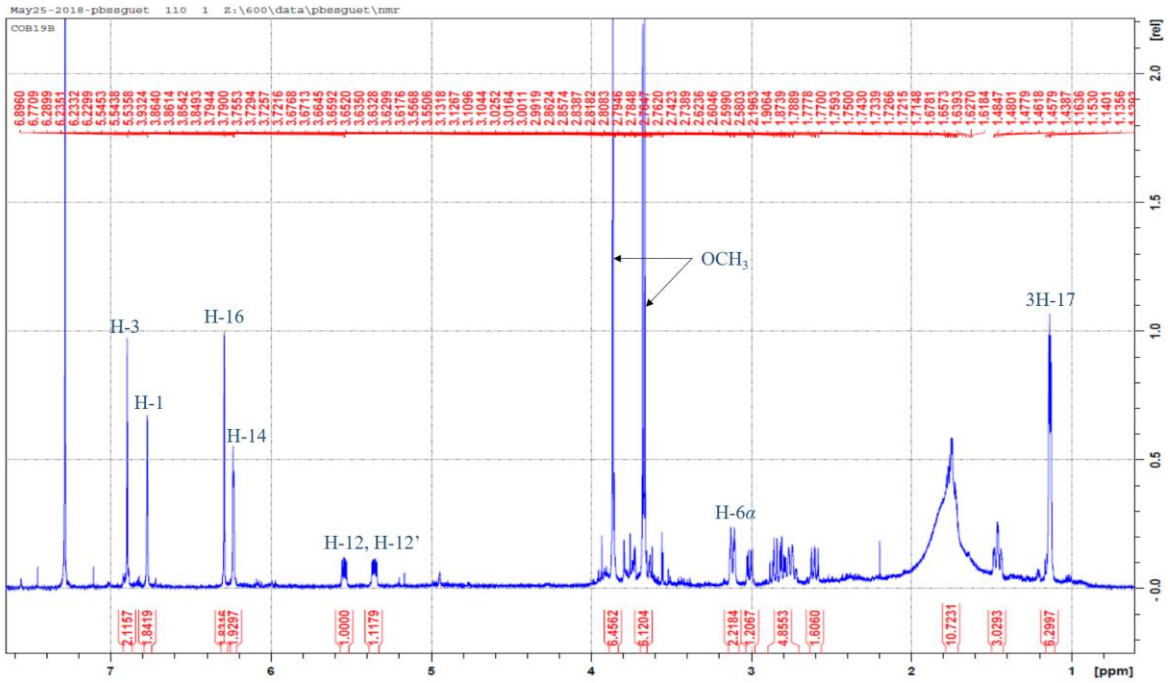

Figure 3.27 ^{1}H NMR (600 MHz, $CDCl_3$) of **158** and **159**

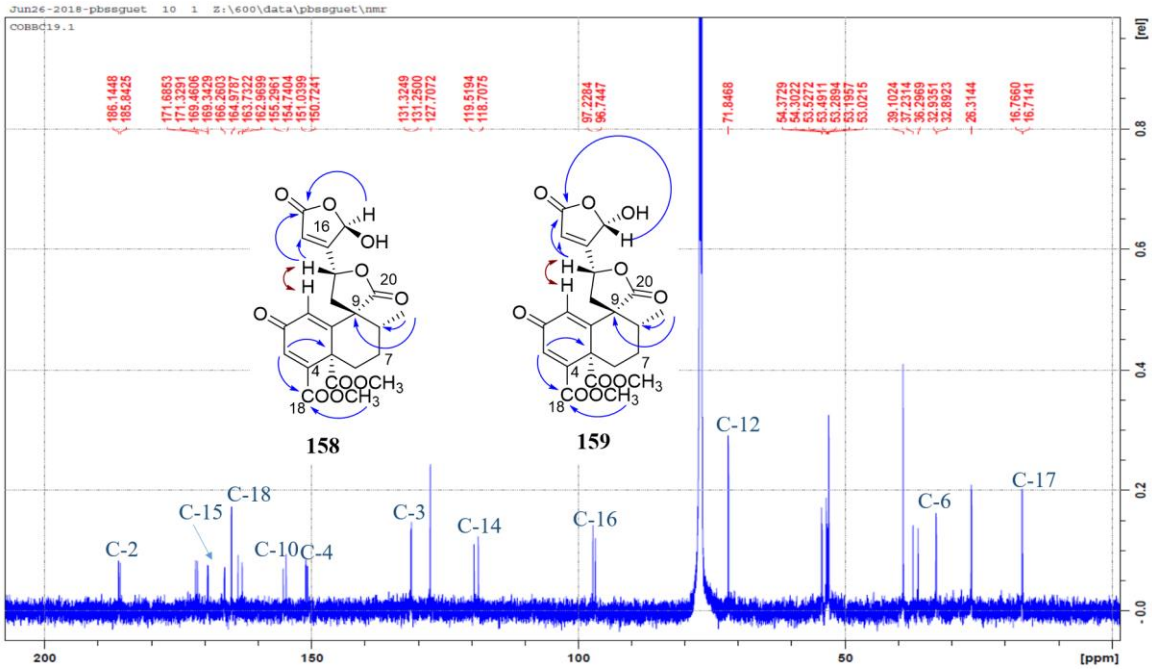

Figure 3.28 ^{13}C NMR (150 MHz, $CDCl_3$) and key ^{1}H-^{1}H NOESY (↔) and HMBC (→) correlations of **158** and **159**

3.3.1.8 Structure elucidation of crotonolin F (**160**)

Compound **160** was isolated as a white amorphous powder, $[\alpha]_D^{25}$ +58.4 (c 0.00025, MeOH. Its molecular formula $C_{24}H_{26}O_{10}$ was determined from its HR ESI-MS spectra obtained in the positive ion mode where the peak at *m/z* 497.1443 $[M+Na]^+$ was calculated for $C_{24}H_{26}O_{10}Na$, 497.1418 Compound **160** could be identified as a *β*-substituted furan clerodane from its ^1H, ^{13}C NMR and HSQC spectra (Figures 3.29-3.31) which showed some similar features with those of previously identified clerodanes (Tchissambou *et al.*, 1990). The ^1H NMR spectrum of **160** showed a couple of olefinic protons at δ_H 5.88 (H-3) and 5.89 (H-2), which showed scalar coupling in the COSY spectrum, an oxymethine proton at δ_H 5.21 (H-1) as well as a vinyl methyl proton resonance at δ_H 1.84 (3H, t, *J* = 1.2 Hz, H-17), which showed correlations in the HMBC spectrum (Figure 3.31) with the olefinic carbons at δ_C 126.0 (C-7) and 129.3 (C-8) and the quaternary carbon at δ_C 51.9 (C-9). The ^{13}C NMR spectrum revealed characteristic signals of *γ*-lactone (δ_C 175.7, C-20; 71.8, C-12) and a *β*-substituted furan moiety (δ_C 124.8, C-13; 108.1, C-14; 144.2, C-15; 139.6, C-16). The signals at δ_C 172.0, 170.1 and 170.7 were attributed to the carbonyls of two methyl esters (C-18 and C-19) and an acetoxy function respectively. In the HMBC spectrum, ^3J long-range ^1H-^{13}C correlations could be observed between the oxymethine proton at δ_H 5.21 (H-1) and the carbonyl of the acetoxy at δ_C 170.7 suggesting an acetylation on that position C-1. Correlations were also observed between the carbon δ_C 77.9 (C-4) and the protons at δ_H 5.21 (H-1), 3.14 (H-10) and 2.36 (H-6). In the NOESY spectrum, a strong correlation observed between H-12 and 3H-17 suggested that H-12 is on the same side as 3H-17. The correlation observed between H11*β*/H10 established the *β*-orientation of H-10. The NOESY experiment was not helpful to determine the position of the 1-acetoxy and 4-OH groups. The ^1H and ^{13}C NMR data of **160** (Tables 3.7-3.8), supported by its key HMBC correlations (Figure 3.30) led to its characterisation as 1*-acetoxy-4*-hydroxy-18,19-dimethoxycarbonyl-15,16-epoxy-*ent*-cleroda-2,7,13(16),14-

tetraen-20,12-olide, a new *ent*-clerodane diterpene not previously described and given the trivial name crotonolin F.

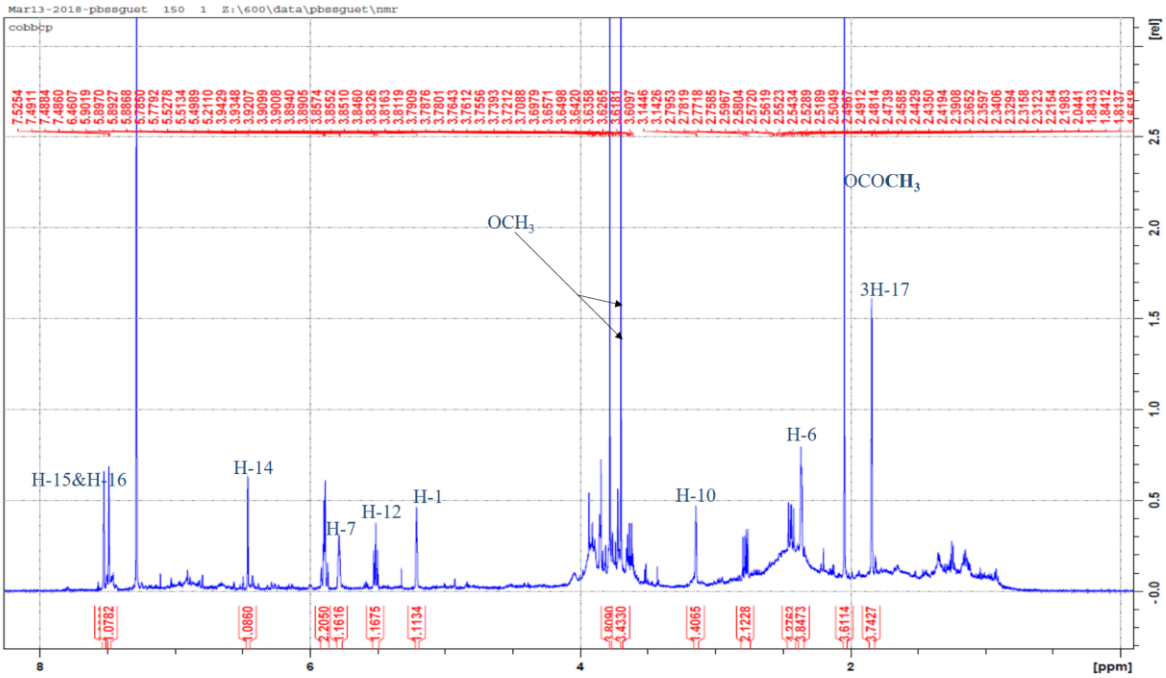

Figure 3.29 ^{1}H NMR (600 MHz, $CDCl_3$) of **160**

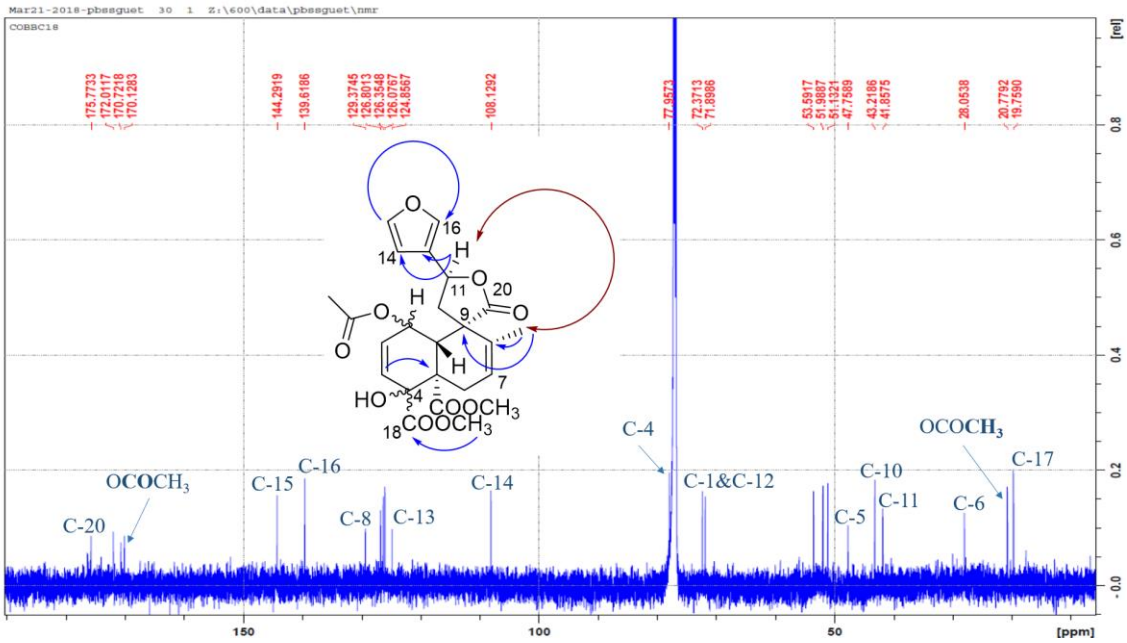

Figure 3.30 ^{13}C NMR (150 MHz, $CDCl_3$) and key ^{1}H-^{1}H NOESY (↔) and HMBC (→) correlations of **160**

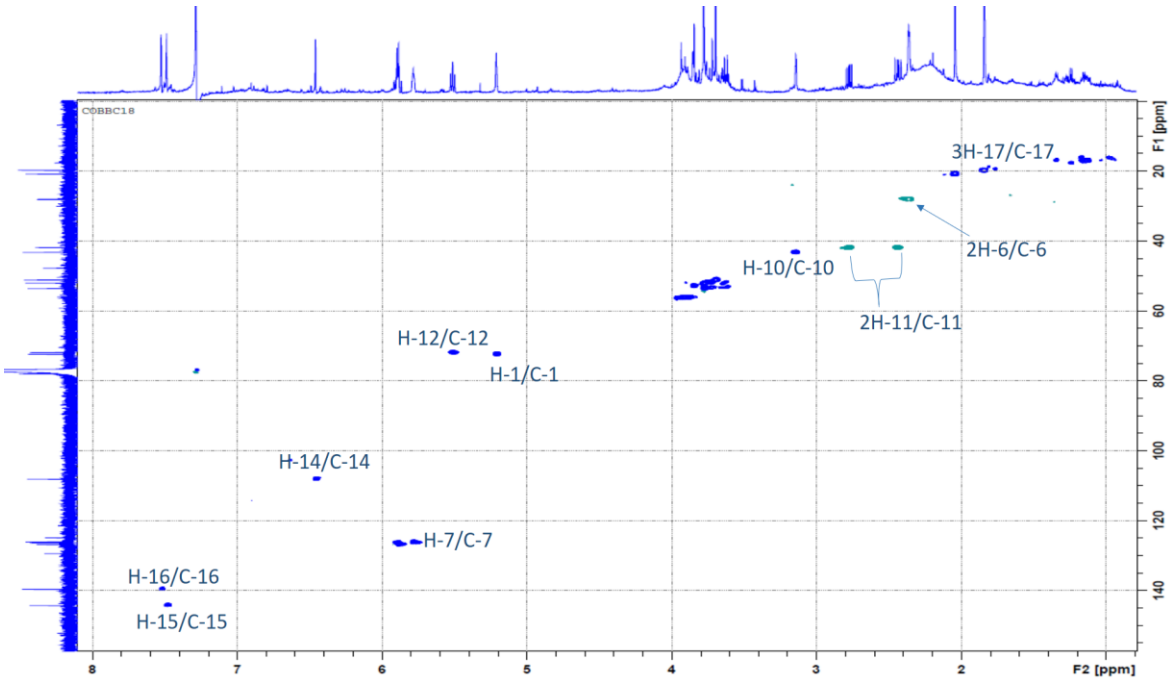

Figure 3.31 HSQC spectrum of **160**

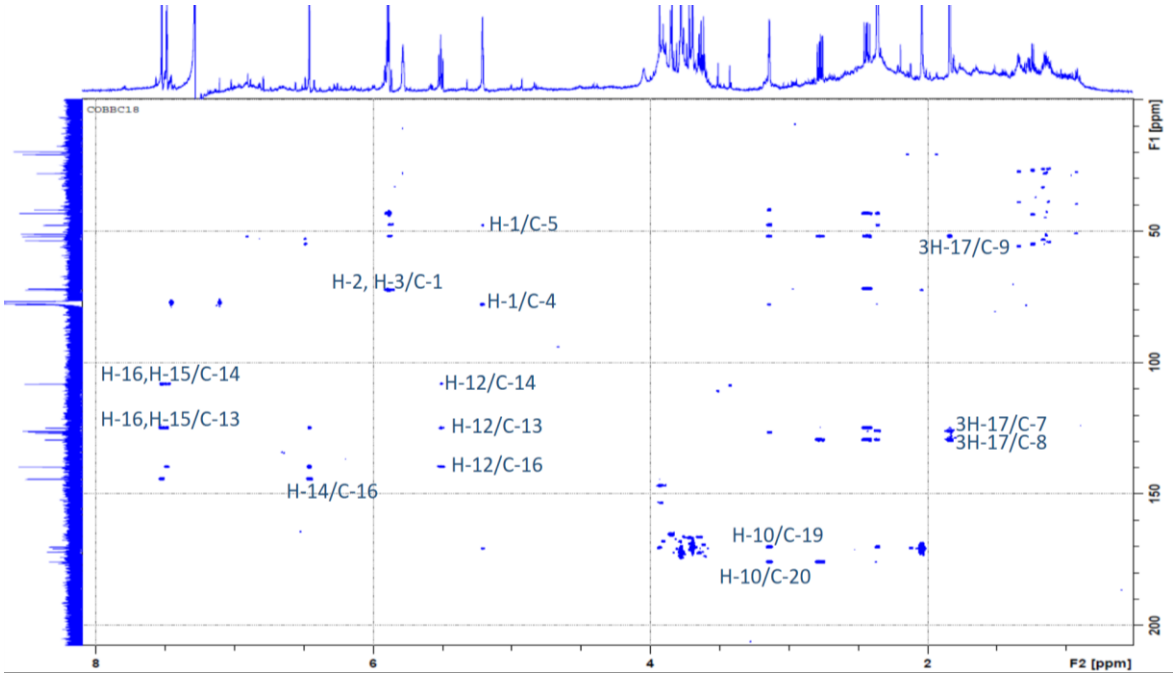

Figure 3.32 HMBC spectrum of **160**

3.3.1.9 Structure elucidation of 7-oxodehydroabietic acid (**161**)

Compound **161** was obtained as a yellow powder and assigned the molecular formula of $C_{20}H_{26}O_3$ on the basis of the *pseudo*molecular ion peak at *m/z* 315.1963 $[M + H]^+$ calculated for $[C_{20}H_{26}O_3 + H]^+$, 315.1966 from the HR ESI-MS spectrum. Its ^{1}H NMR spectrum (Figure 3.33; Table 3.7) indicated the presence of four methyls including two singlets at δ_H 1.38 and 1.29 and two doublets at δ_H 1.26 (J = 1.7 Hz) and 1.27 (J = 1.7 Hz). Four methylenes and five methines including three aromatic methines at δ_H 7.32 (d, J = 8.2 Hz), 7.42 (dd, J = 2.0, 8.2 Hz) and 7.89 (d, J = 2.0 Hz) as well as a septuplet methine at δ_H 2.95, which coupled with the two methyl doublets in the COSY spectrum, were also observed. These observations were supported by the different correlations observed on the HSQC-DEPT. The ^{13}C NMR spectrum (Figure 3.34; Table 3.8) also indicated the presence of seven quaternary carbons including two carbonyls at δ_C 198.7 and 181.4, which could be attributed to ketone and carboxylic acid functions respectively. In the HMBC spectrum, long-range correlations could be observed between the methine proton at δ_H 2.95 (H-14) and the carbons at δ_C 132.6 (C-12), 125.1 (C-16), 23.8 (C-15) and 23.7 (C-17). The proton at δ_H 2.51 (H-6α) showed correlations with the carbons at δ_C 198.7 (C-7) and 37.2 (C-10), while the H-6β proton at δ_H 2.76 showed correlations with the carbons on position C-4 (δ_C 46.3), C-5 (δ_C 43.6), C-7(δ_C 198.7), C-10 (δ_C 37.2) and C-19 (δ_C 16.2). The ^{1}H and ^{13}C NMR data (Tables 3.7-3.8), supported by the key HMBC correlations (Figure 3.33), were in good agreement with those published for 7-oxodehydroabietic acid (Tanaka *et al.*, 1997). Therefore, compound **161** was identified as 7-oxo-dehydroabietic acid.

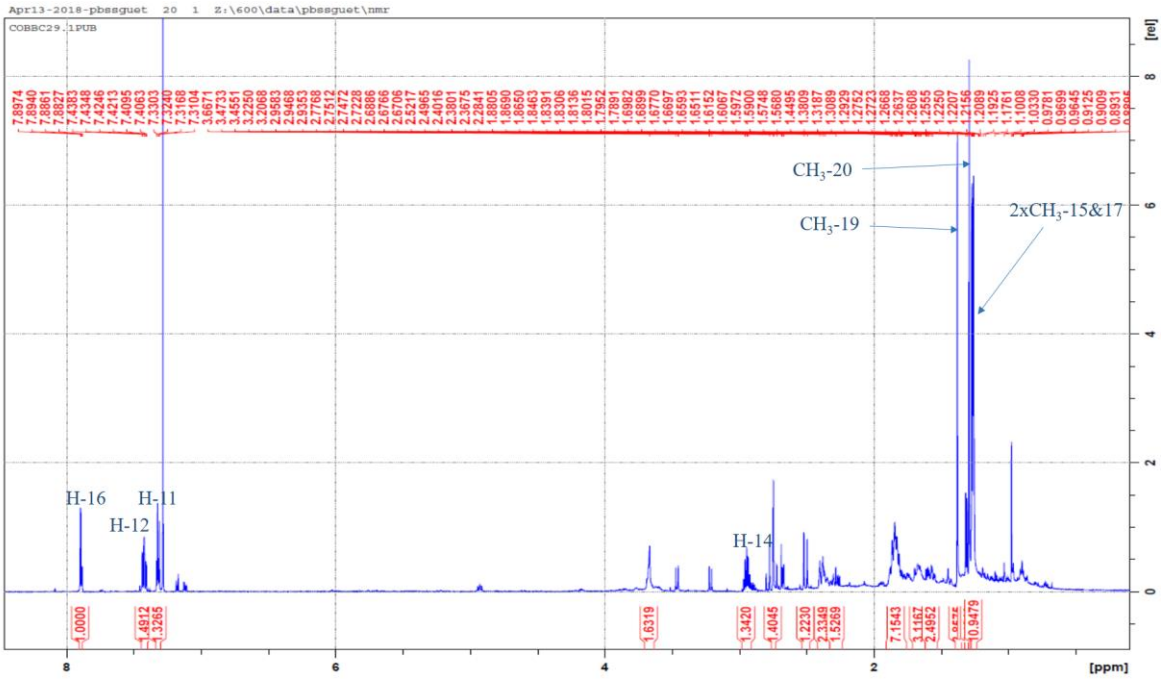

Figure 3.33 ^{1}H NMR spectrum (600 MHz, $CDCl_3$) of **161**

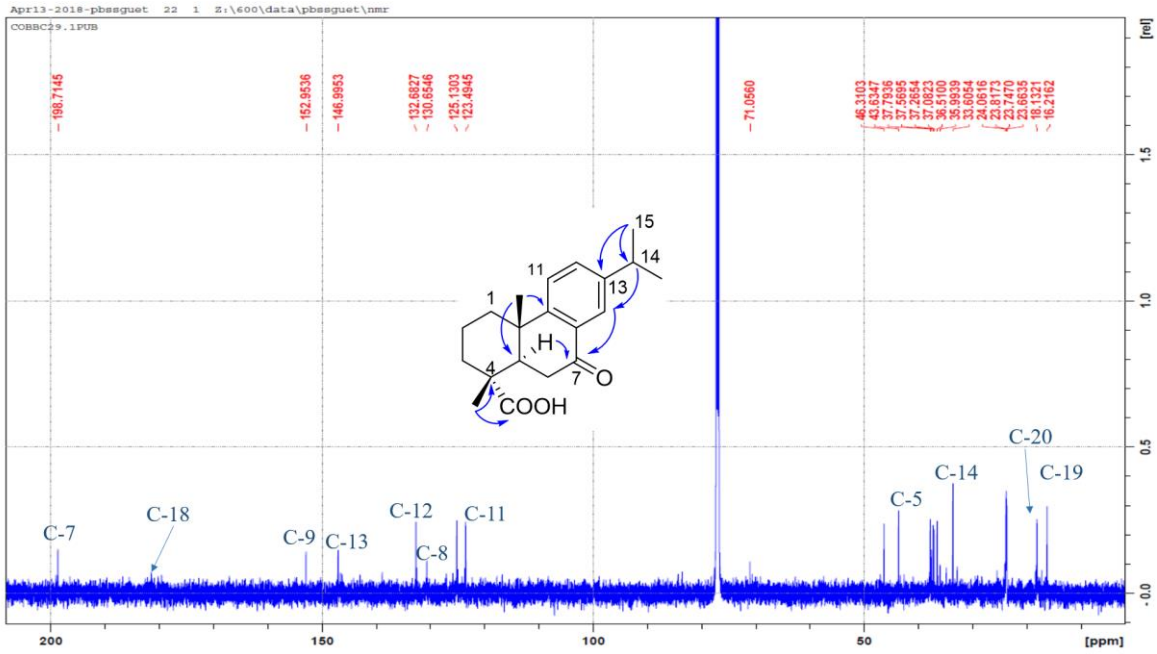

Figure 3.34 ^{13}C NMR (600 MHz, $CDCl_3$) and key HMBC correlations of **161**

Table 3.7 ^{1}H NMR data of compounds **151-162**

Position						δ_H (*J* in Hz)					
	151	**152**	**153**	**154**	**155**	**156/157**[a]	**158**	**159**	**160**	**161**	**162**
1	1.92 m	6.00 dd (*3.5*, *9.3*)	6.47 d (*1.3*)	6.47 d (*1.0*)	6.04 brt (*1.9*)	6.91 d (*1.2*)	6.76 s	6.76 s	5.21 m	1.84 m	1.49 m
	2.65 m	-	-	-	-	-	-	-	-	-	2.31 m
2	2.43 m	6.20 dd (*3.1*, *4.9*)	-	-	4.87 t (*2.4*)	-	-	-	5.89 ov	1.67 m	1.83 m
	2.58 *m*	-	-	-	-	-	-	-	-	2.39 m	-
3	6.84 dd (*4.3*, *7.5*)	7.00 d (*5.2*)	6.78 d (*1.3*)	6.78 d (*1.0*)	6.70 dd (*1.8*, *2.3*)	6.80 d (*1.2*)	6.88 s	6.88 s	5.88 ov	1.84 m	1.62 m
						-	-	-	-	-	1.83 m
5						-	-	-	-	2.74	2.48 *m*
6	1.12 ddd (*3.6*, *13.4*, *16.9*)	1.32 m	1.45 ddd (*3.7*, *13.3*)	1.44 ddd (*13.5*, *9.3*, *17.7*)	1.31 m	1.51 ddd (*4.0*, *13.5 17.5*)	1.45 ddd (*3.2*, *13.1*, *16.9*)	1.45 ddd (*3.2*, *13.1*, *16.9*)	2.36 m	2.51 d (*15.2*)	1.72 m
	2.95 dt (*3.3*, *6.4*)	2.95, dt (*3.7*, *13.0*)	3.11 dt (*3.0*, *6.1*)	3.13 dt (*13.3*, *3.3*)	3.04 dt (*3.3*, *13.3*)	3.00 m	3.10, dt (*3.1*, *13.0*)	3.10, dt (*3.1*, *13.0*)	5.78 brt (*3.4*)	2.76 d (*15.2*)	2.12 m
7	1.58 m	1.56 m	1.71 m	1.65 m	1.57 dd (*3.6*, *14.2*)	1.66 m	1.74 m	1.74 m	-	-	4.79 d (*3.4*)
	2.43 m	2.28 m	2.78 *m*	2.49 ddd (*4.2*, *13.9*, *17.1*)	2.40 m	2.66 m	2.77 m	2.77 m	-	-	-
8	1.58 m	1.70 m	1.75 *m*	1.78 m	1.69 m	1.82 m	1.78 *m*	1.78 m	-	-	-

Table 3.7 *continued*

Position						δ_H (*J* in Hz)					
	151	**152**	**153**	**154**	**155**	**156/157**[a]	**158**	**159**	**160**	**161**	**162**
10	1.76 dd (*2.4*, *13.2*)	2.89 t (*3.2*)	-	-	-	-	-	-	3.14 m		-
11	2.43 m	2.48 m	2.78 m	2.69 dd (*8.2*, *14.3*)	2.62 dd (*8.8*, *14.3*)	2.80 m	2.59 dd (*11.2*, *14.6*)	2.81 m	2.43 dd (*9.4*, *14.1*)	7.32 d (*8.2*)	7.18 d (*8.3*)
	-	-	2.65 dd (*11.1*, *14.5*)	2.94 dd (*6.3*, *14.2*)	2.94 dd (*6.2*, *14.3*)	2.93 m	2.99 dd (*5.3*, *14.6*)		2.77 dd (*7.9*, *14.1*)	-	-
12	5.40 t (*8.5*)	5.48 t (*8.7*)	5.55 dd (*5.2*, *11.1*)	5.57 t (*7.0)*	5.53 dd (*6.4*, *8.7*)	5.72 dd (*5.5*, *11.1*)	5.34 dd *(5.3*, *11.2*)	5.53 dd (*6.7*, *10.7*)	5.50 m	7.42 dd (*2.0*, *8.2*)	7.12 dd (*1.9*, *8.2*)
14	6.41 brd (*0.9*)	6.45 d (*0.9*)	6.45 m	6.41 m	6.44 d (*0.9*)	7.40/ 7.39, brs	6.22 s	6.22 s	6.46 brs	7.89 d (*2.0*)	7.20 d (*1.9*)
15	7.44 ov	7.49 brt (*1.6*)	7.47 dd (*1.5*, *3.1*)	7.49 brd (*1.6*)	7.49 dd (*0.9*, *1.6*)	6.18 /6.20, *brs*	-	-	7.48 brt (*1.6*)	2.95 m	2.86 m
16	7.45 brs	7.51 brs	7.54 brs	7.45 m	7.48 brs		6.28 s	6.28 s	7.52 brs	1.26 d (*6.4*)	1.23 d (*6.4*)
17	1.02 d (*6.4*)	1.15 d (*6.9*)	1.17 d (*6.4*)	1.23 d (*6.7*)	1.17 d (*6.7*)	1.15 d (*5.8*)	1.12 d (*6.5*)	1.11 d (*6.3*)	-	1.27 d (*6.4*)	1.23 *d* (*6.4*)
19						-	-	-	-	1.38 s	1.28 s
20						-	-	-	-	1.29 s	1.16 s
18-OCH_3	3.71 s	3.74 s	3.84 s	3.84 s	3.76 s	3.71 s	3.85 s	3.85 s	3.78 s	-	-
19-OCH_3	3.76 s	3.62 s	3.65 s	3.71 s	3.71 s	3.60 s	3.66 s	3.65 s	3.69 s	-	-
$COCH_3$						-	-	-	2.04 s	-	-

Table 3.8 ^{13}C NMR data of compounds **151-162**

Position	δ_C										
	151	**152**	**153**	**154**	**155**	**156,157**	**158**	**159**	**160**	**161**	**162**
1	19.2	132.7	127.8	129.1	129.4	129.0	127.7	127.7	72.3	18.4	37.8
2	26.4	125.9	185.8	185.7	64.4	187.2	186.1	185.8	126.8	37.0	18.6
3	140.1	135.5	131.4	130.9	136.2	131.7	131.3	131.2	126.3	36.5	36.5
4	136.5	136.3	150.7	151.3	156.1	152.4	150.7	151.0	77.9	46.3	47.1
5	46.3	47.0	53.5	55.1	48.3	54.3	53.4	53.2	47.7	43.6	39.8
6	32.3	31.9	33.1	33.2	31.4	33.9	32.9	32.9	28.0	37.7	31.1
7	27.9	28.1	26.5	27.2	27.2	27.5	26.4	26.4	126.0	198.7	68.3
8	40.2	43.1	39.7	43.7	41.7	40.0	39.1	39.1	129.3	130.6	135.9
9	51.4	50.7	55.0	53.6	53.3	55.9	54.3	54.3	51.9	152.9	146.7
10	51.9	50.0	155.4	155.7	151.9	156.2	155.2	154.7	43.2	37.2	37.5
11	42.4	41.8	38.9	39.2	40.0	36.9	37.1	36.3	41.8	123.4	124.3
12	71.9	72.1	71.2	72.0	71.8	72.4	71.5	71.5	71.8	132.6	126.7
13	125.5	125.4	123.5	125.0	125.8	135.0	163.7	162.9	124.8	146.9	146.7
14	108.2	108.3	108.1	107.8	107.9	149.8	119.5	118.7	108.1	125.1	128.3
15	144.2	144.5	144.4	144.6	144.2	99.3	169.3	169.4	144.2	33.6	33.6
16	139.5	139.4	140.5	139.7	139.3	170.9	96.7	97.2	139.6	23.8	23.9
17	17.1	17.5	16.9	17.7	17.8	17.1	17.1	17.1	19.7	23.7	23.9
18	166.9	166.9	165.3	165.5	166.2	166.7	164.9	164.9	172.0	181.4	182.2
19	173.0	173.4	166.3	166.7	170.7	168.4	166.3	166.2	170.0	16.2	16.4
20	176.3	176.6	172.1	173.1	174.8	174.0	171.1	171.6	175.7	23.6	24.1
18-OCH_3	51.7	51.8	53.0	52.9	52.0	53.3	53.0	53.0	53.5		
19-OCH_3	51.8	51.7	53.2	53.1	52.6	53.7	53.5	53.2	51.1		
$COCH_3$									170.7		
$COCH_3$									20.7		

3.3.2 Phytochemistry of *Ruspolia hypocrateriformis*

Combination of CC, SPE, preparative TLC and RP-HPLC analyses of the methanol extract of the leaves of *R. hypocrateriformis* afforded ten compounds including six glycosylated flavonoids, a quindoline, two pyrrolidine alkaloids and a disaccharide. The compounds were identified as luteolin-7-*O*-*β*-D-apiofuranosyl-(1→2)-*β*-D-xylopyranoside (**163**), chrysoeriol-7-*O*-*β*-D-apiofuranosyl-(1→2)-*β*-D-xylopyranoside (**164**), chrysoeriol-7-*O*-[4'''-*O*-acetyl-*β*-D-apiofuranosyl-(1→2)]-*β*-D-xylopyranoside (**165**), luteolin-7-*O*-*α*-L-rhamnopynosyl-(1→2)-*β*-D-xylopyranoside (**166**), chrysoeriol-7-*O*-*α*-L-rhamnopynosyl-(1→2)-*β*-D-xylopyranoside (**167**), luteolin 7-O-[*β*-D-glucopyranosyl-(1→2)-*α*-L-rhamnosyl-(1→6)]-*β*-D-glucopyranoside (**168**), 10*H*-quindoline (**169**), secundallerones B and C (**170-171**) and sucrose (**60**) (Figure 3.35).

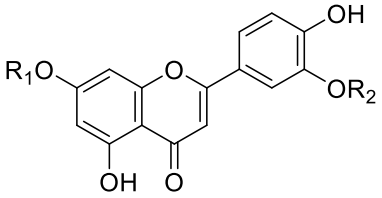

163 R_1= *β*-D-apiofuranosyl-(1'''→2'')-*β*-D-xylopyranosyl R_2= H
164 R_1= *β*–D-apiofuranosyl-(1''→2'')-*β*-D-xylopyranosyl R_2= CH_3
165 R_1= 4'''-*O*-acetyl-*β*-D-apiofuranosyl-(1'''→2'')-*β*-D-xylopyranosyl R_2= CH_3
166 R_1= *α*-L-rhamnopyranosyl-(1''→2'')-*β*-D-xylopyranosyl R_2= H
167 R_1= *α*-D-rhamnopyranosyl-(1'''→2'')-*β*-D-xylopyranosyl R_2= CH_3
168 R_1= *β*-D-glucopyranosyl-(1''''→2''')-*α*-L-rhamnosyl-(1''→6'')-*β*-D-glucopyranosyl R_2= H

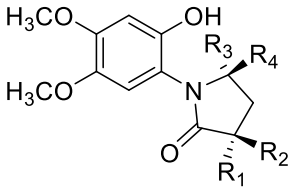

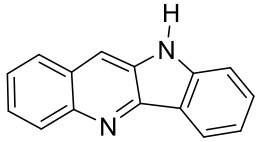

169

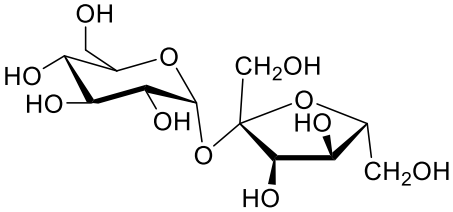

60

170 R_1= OH R_2= H R_3= OH R_4= H
171 R_1= OH R_2= R_3= H R_4= OH

Figure 3.35 Structures of isolated compounds from the leaves of *R. hypocrateriformis*

3.3.2.1 Structure elucidation of luteolin-7-*O*-*β*-D-apiofuranosyl-(1→2)-*β*-D-xylopyranoside (**163**)

Compound **163** was isolated as a yellow amorphous powder. Its molecular formula $C_{25}H_{26}O_{14}$ was determined by the peak at *m/z* 551.1392 calculated for $[C_{25}H_{26}O_{14}+H]^+$, 551.1395 and consistent with thirteen RDB, from its HR ESI-MS spectrum (Figure 3.36) in positive mode ion. The ^{1}H NMR spectrum (Figure 3.38; Table 3.9) revealed 17 peaks belonging to a glycosylated molecule bearing two sugar moieties. The aglycone part of the compound was identified as luteolin by the presence of an ABX system resonating at δ_H 7.26 (d, *J* = 8.2 Hz), 7.49 (dd, *J* = 2.1, 8.2 Hz) and 7.87 (d, *J* = 2.1 Hz), characteristic of a 3,4-dihydroxylated B ring; an AX system appearing as two doublet signals at δ_H 6.92 and 6.95 (*J* = 2.0 Hz), typical of a *meta*-dihydroxylated A ring, and one singlet at δ_H 6.89 attributable to the H-3 proton of the luteolin C ring. The sugar moieties were identified by the presence of two anomeric proton signals at δ_H 5.58 (d, *J* = 7.4 Hz) and 6.52 (d, *J* = 0.9 Hz). 2D NMR experiments, mainly COSY and HSQC (Figures 3.39-3.40), helped to assign the resonance signals belonging to the sugar moieties. COSY and TOCSY were useful to construct each sugar moiety and to identify proton signals belonging to the same sugar. This led to the identification of two pentose residues, one as *β*-D-apiofuranoside and the second as and *β*-D-xylopyranose by comparison of their NMR spectroscopic data with those reported in the literature (Koffi *et al.*, 2013; Tagousop *et al.*, 2017). Analysis of the HMBC spectrum (Figure 3.41) revealed that the two sugars were linked together. ^3J long-range correlations were observed between the proton H-1''' (δ_H 6.52) of the apiose and the carbon C-2'' of the xylose (δ_C 77.0 ppm), and between the proton H-2'' (δ_H 4.49) of the xylose and the carbon C-1''' (δ_C 110.5) of the apiose. Other long-range correlations observed between the proton H-1'' (δ_H 5.58) of the xylose and the carbon C-7 (δ_C 163.3) of the luteolin aglycone and between the proton H-8 (δ_H 6.95) of the aglycone and the anomeric carbon (δ_C 100.3, C-1'') of the xylose confirmed the attachment of the

diglycoside unit on the carbon C-7 of the aglycone. All the ^{1}H and ^{13}C NMR data of **163** (Tables 3.9-3.10), as well as the key HMBC correlations (Figure 3.37) identified **163** as luteolin 7-O-[*β*-D-apiofuranosyl-(1→2)]-*β*-D-xylopyranoside, a glycosylated flavone previously isolated from two Acanthaceae species i.e. *Graptophyllum grandulosum* and *Justicia secunda* (Koffi *et al.*, 2003; Tagousop *et al.*, 2017).

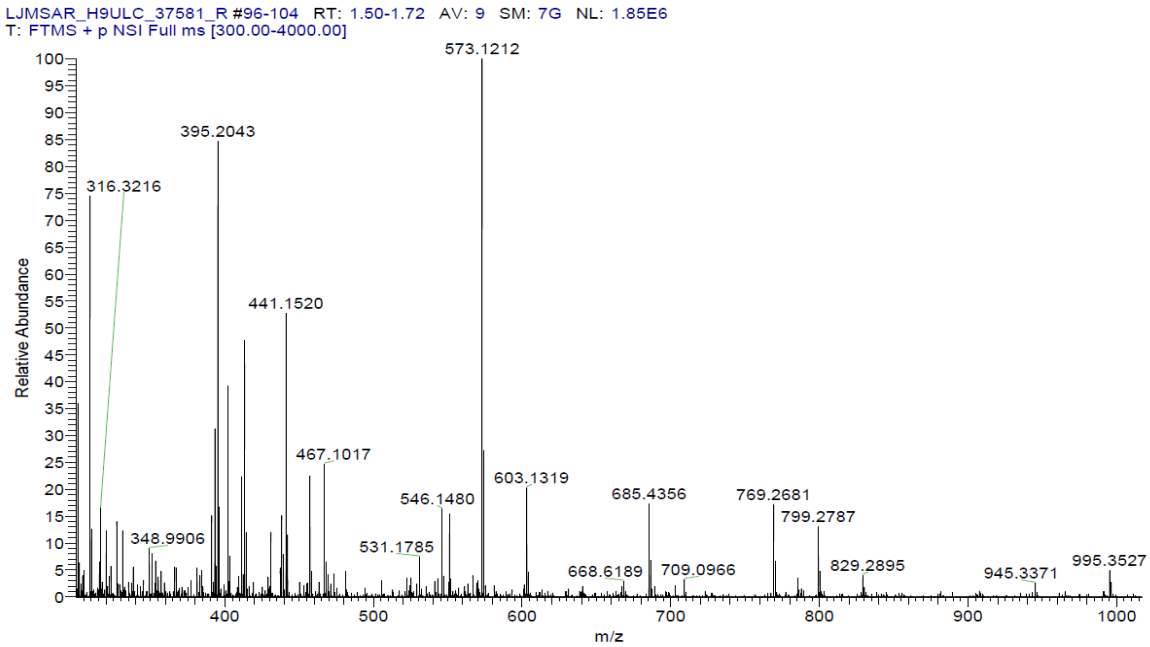

Figure 3.36 ESI-MS spectrum of **163**

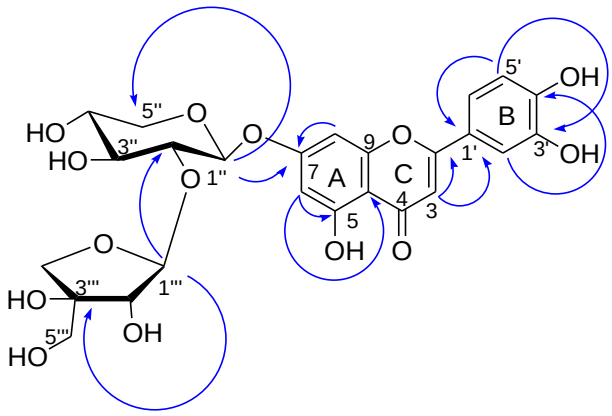

Figure 3.37 Key HMBC correlations of **163**

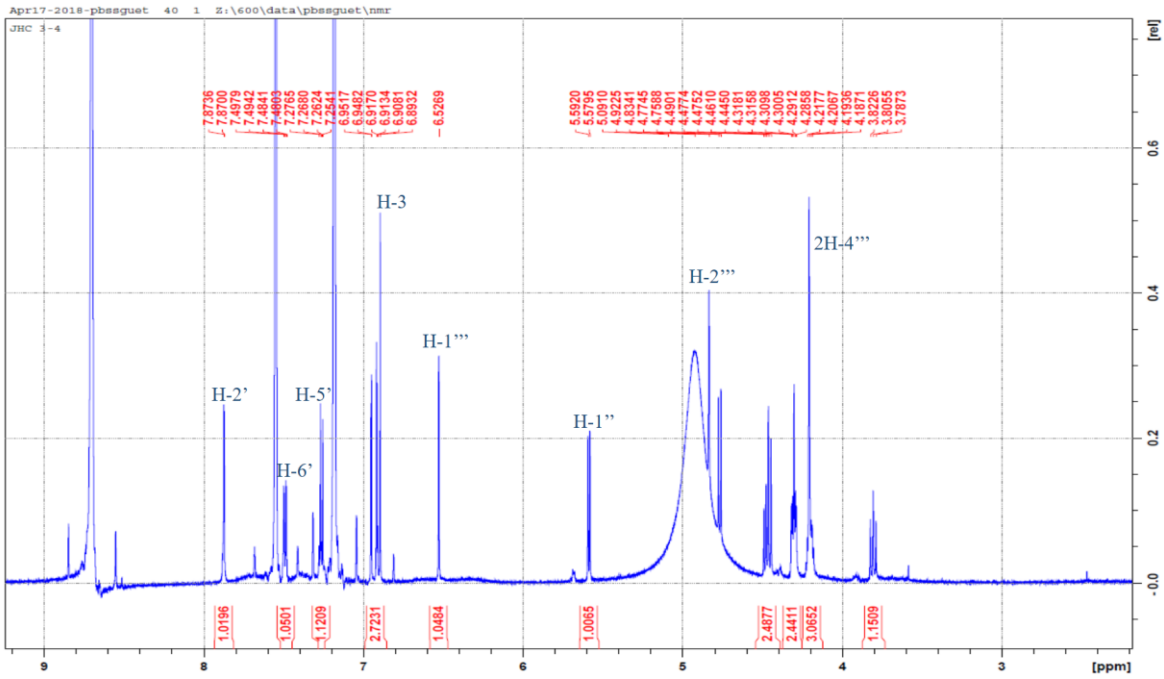

Figure 3.38 ^{1}H NMR (600 MHz, Pyr-d_5) of **163**

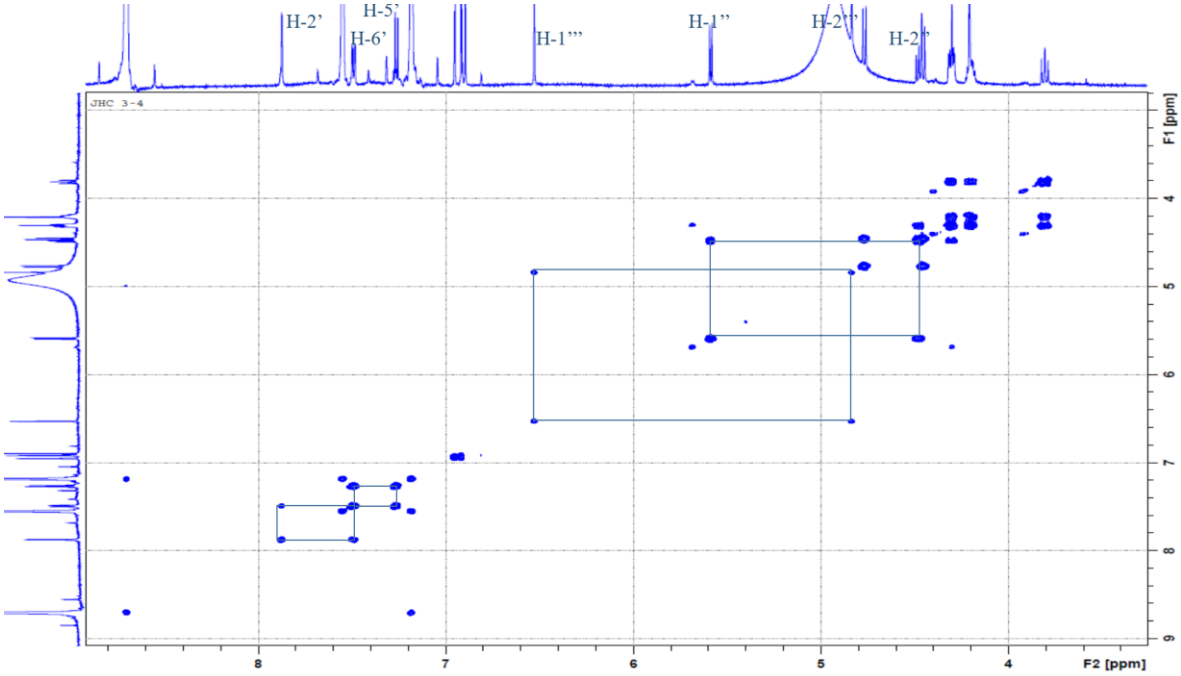

Figure 3.39 ^{1}H-^{1}H COSY spectrum of **163**

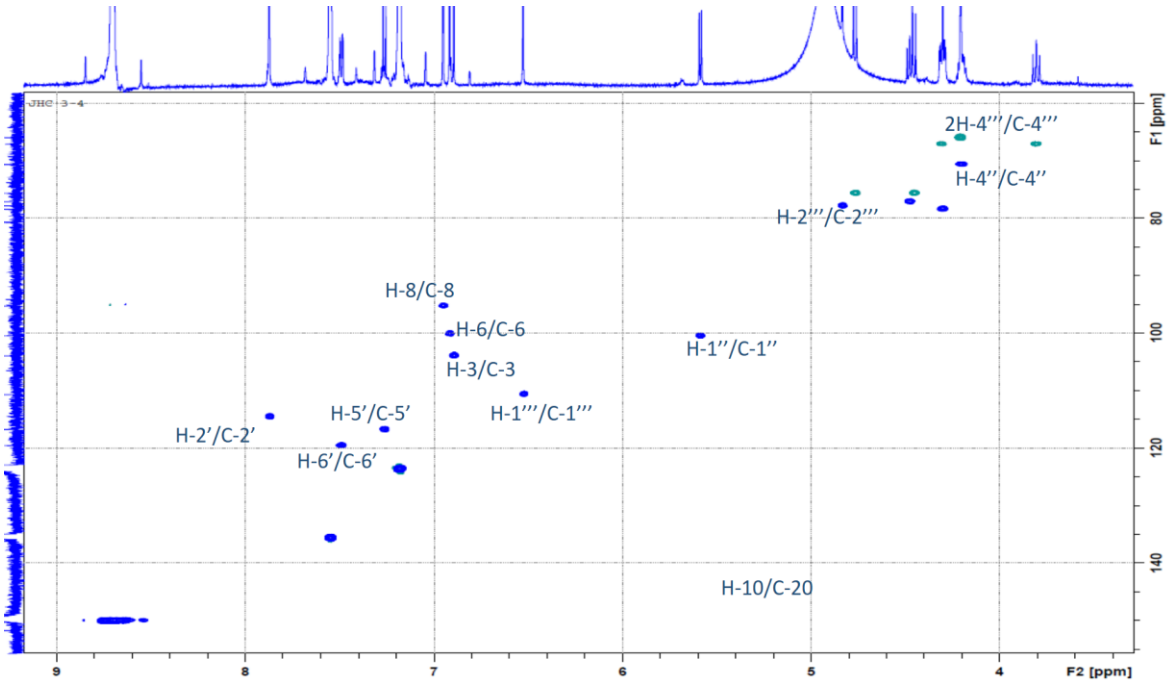

Figure 3.40 HSQC spectrum of **163**

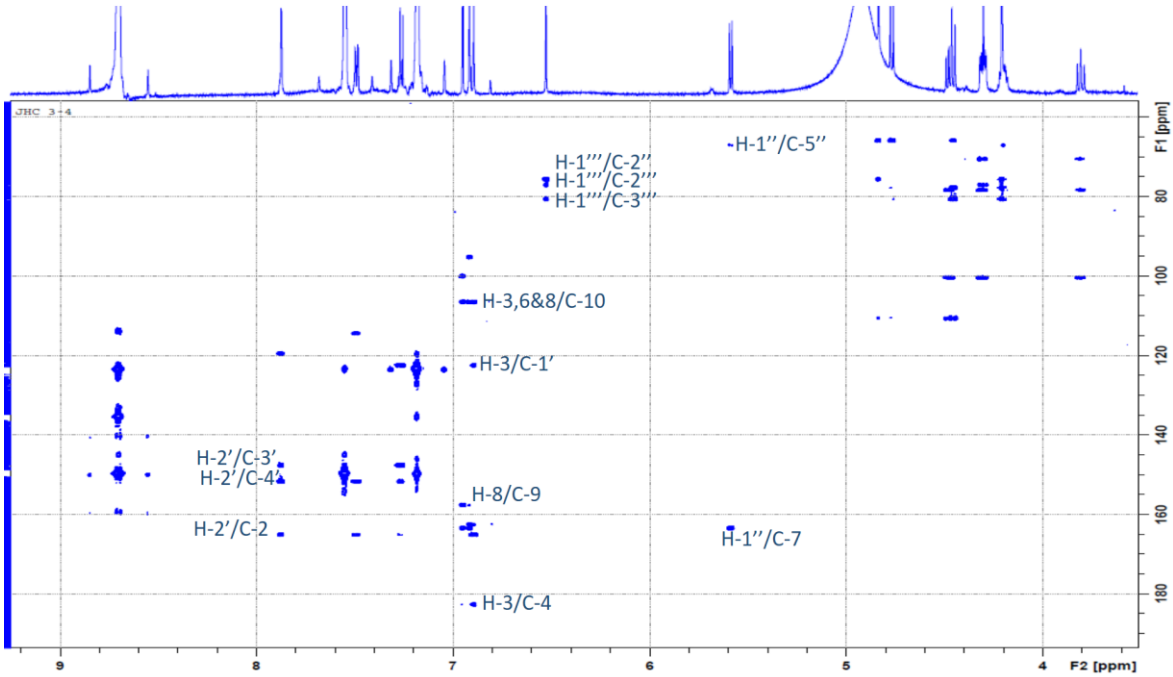

Figure 3.41 HMBC spectrum of **163**

3.3.2.2 Structure elucidation of chrysoeriol-7-*O*-*β*-D-apiofuranosyl-(1→2)-*β*-D-xylopyranoside (**164**)

Compound **164** was isolated as a yellow amorphous powder. Its molecular formula $C_{26}H_{28}O_{14}$ was determined from the sodiated ion peak at *m/z* 587 $[M+Na]^+$ in its ESI-MS spectrum in positive mode ion. Its 1D and 2D NMR spectra similar to those of **163** suggested a luteolin diglycoside skeleton. The only difference was the presence of an additional signal on the ^{1}H NMR (Figure 3.42, Table 3.9) of **164** of a singlet attributable to a methoxy group at δ_H 3.78. This was confirmed by the cross peak correlation observed on its HSQC spectrum between this signal and the carbon resonating at δ_C 55.8. In the HMBC spectrum, a ^3J long-range correlation was observed between the signal of the methoxy proton and a carbon resonating at δ_C 148.5 corresponding to the carbon C-3' of the luteolin skeleton. Therefore, the aglycone in compound **164** was identified as 3'-methoxyluteolin or chrysoeriol. All the ^{1}H and ^{13}C NMR data of **164** (Tables 3.9-3.10), and the key long-range correlations observed in the HMBC spectrum (Figure 3.42) led to its identification as chrysoeriol-7-*O*-*β*-D-apiofuranosyl-(1→2)-*β*-D-xylopyranoside or granduloside A, a flavonoid previously isolated from *Graptophyllum grandulosum* (Tagousop *et al.*, 2017).

3.3.2.3 Structure elucidation of chrysoeriol-7-*O*-[4'''-*O*-acetyl-*β*-D-apiofuranosyl-(1→2)]-*β*-D-xylopyranoside (**165**)

Compound **165** was also isolated as a yellow amorphous powder. Its molecular formula $C_{28}H_{30}O_{15}$ was determined by the peak at *m/z* 629 $[M+Na]^+$ in its ESI-MS spectrum in positive mode ion. Its 1D and 2D NMR spectra similar to those of **164** also suggested a chrysoeriol diglycoside skeleton. The only difference was the presence of an additional

signal on the ^{1}H NMR (Figure 3.43, Table 3.9) of **165** of a singlet at δ_H 1.93 (3H) attributable to the methyl protons of an acetoxy function. This was confirmed by the cross peak correlation observed on its HSQC spectrum between this methyl signal and the carbon resonating at δ_C 19.2. These observations were supported in the HMBC spectrum (Figure 3.43), by the ^{2}J correlations observed between the methyl signal at δ_H 1.93 and the deshielded carbon signal at δ_C 171.1 attributable the carbonyl of the acetoxy function. Another correlation observed between the 2H-4''' protons (δ_H 4.08) of the apiose and the carbonyl carbon (δ_C 171.1) established an acetylation of the alcohol function on position C-4''' of the apiose moiety. Thus, all the ^{1}H and ^{13}C NMR data of **167** (Tables 3.9-3.10), in addition to the key HMBC correlations observed (Figure 3.43) led to its identification as chrysoeriol-7-*O*-[4'''-*O*-acetyl-*β*-D-apiofuranosyl-(1→2)]-*β*-D-xylopyranoside or granduloside B, previously isolated from *Graptophyllum grandulosum* (Tagousop *et al.*, 2017).

3.3.2.4 Structure elucidation of luteolin-7-*O*-*α*-D-rhamnopynosyl-(1→2)-*β*-D-xylopyranoside (**166**)

Compound **166** was isolated as a yellow amorphous powder. Its molecular formula $C_{26}H_{28}O_{14}$ was confirmed from its HR ESI-MS spectrum (Figure 3.44) in positive mode ion, where the sodiated ion peak was observed at *m/z* 587.1378, calculated for $[C_{26}H_{28}O_{14}+Na]^{+}$, 587.1377, consistent with thirteen RDB. The ^{1}H NMR spectrum (Figure 3.45, Table 3.9) of **166** revealed a glycosylated flavone skeleton with the aglycone moiety clearly identifiable as luteolin. The only difference between the ^{1}H NMR spectrum of **166** with that of **163** was the resonance signals attributable to the sugar moieties. The ^{1}H NMR spectrum of **166** exhibited characteristic peaks belonging to two anomeric protons at δ_H 5.62 (d, J = 7.5 Hz) and 6.38 (d, J = 1.6 Hz) and a doublet methyl at δ_H 1.78

(J = 6.1 Hz) showing a cross peak correlation in the HSQC spectrum (Figure 3.46) with the carbon signal resonating at δ_C 18.6 suggesting a rhamnose as one of the glycosylic unit. Complete assignment of the protons and carbons of the sugar units was achieved by analysis of COSY, HSQC, HMBC and TOCSY spectra of **166**. The sugars were identified *β*-D-xylopyranose and *α*-L-rhamnose with their anomeric protons resonating at δ_H 5.62 (d, J = 7.5 Hz) and 6.38 (d, J = 1.6 Hz) respectively, by comparison of their chemical shifts with those reported in the literature (Osterdahl, 1979; Beier and Mundy, 1980; Agrawal, 1992). The HMBC spectrum (Figure 3.47) showed a correlation between the proton H-1'' (δ_H 5.62) of the xylose and the carbon C-7 (δ_C 163.2) of the aglycone, confirming its direct attachment to the luteolin skeleton. Other correlations observed between the proton H-1''' (δ_H 6.38) of the rhamnose and the carbon C-2'' of the xylose (δ_C 77.4) and between the proton H-2'' (δ_H 4.47) of the xylose and the carbon C-1''' (δ_C 102.3) of the rhamnose confirmed attachment of the rhamnosyl unit on the carbon C-2'' of the xylose. Thus, all the ^{1}H and ^{13}C NMR data of **166** (Tables 3.9-3.10), in addition to the keys 2D correlations observed (Figure 3.45) led to its characterisation as luteolin-7-*O*-*α*-L-rhamnopynosyl-(1→2)-*β*-D-xylopyranoside, a new flavone diglycoside from natural source and was given the trivial name justicialoside A.

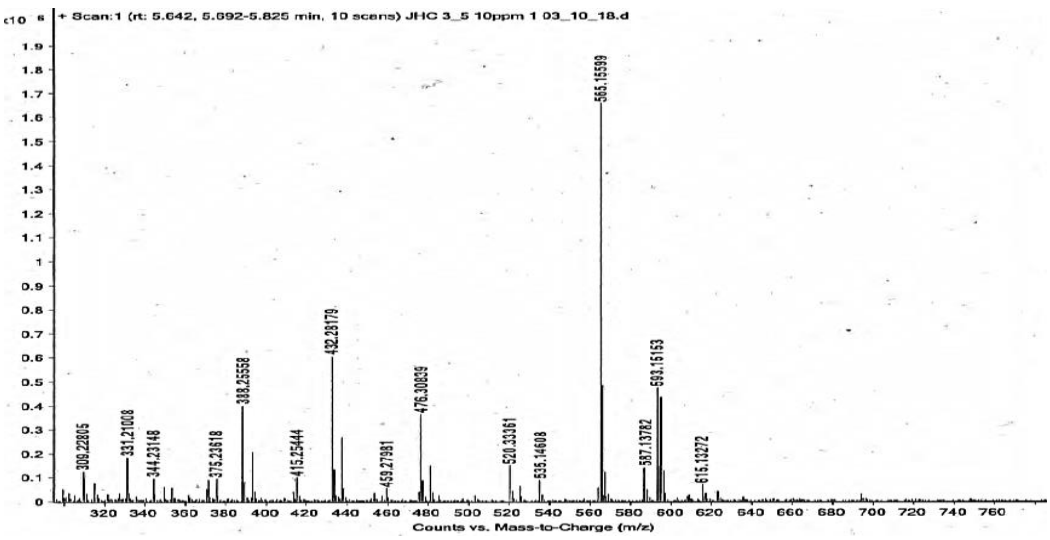

Figure 3.44 ESI MS spectrum of **166**

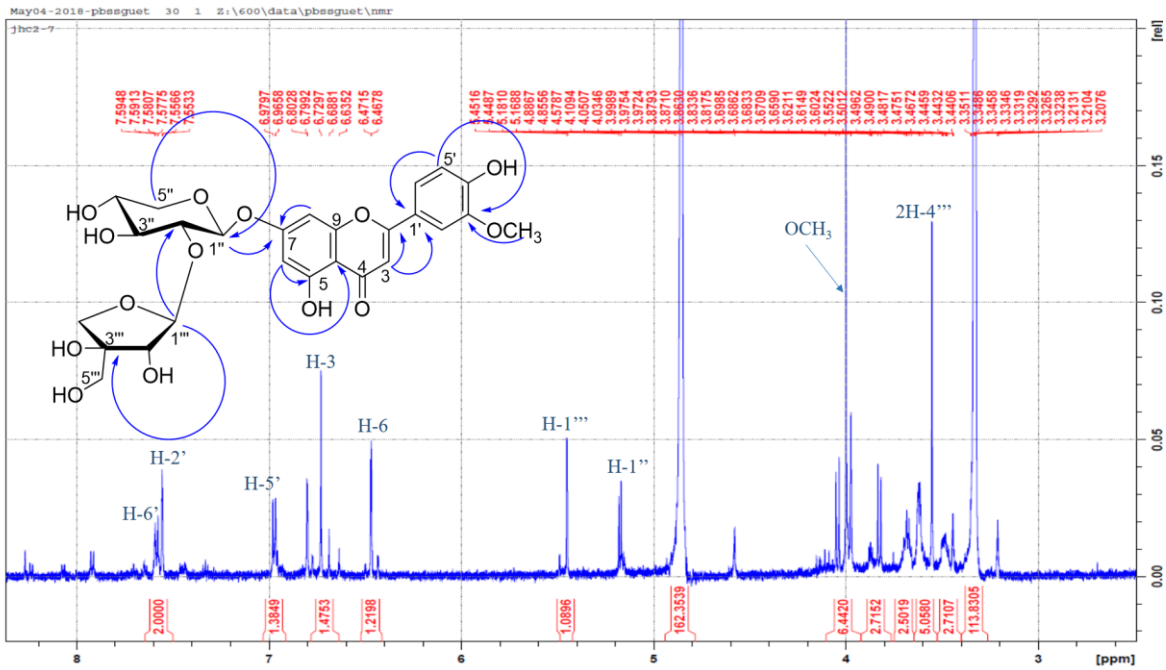

Figure 3.42 ^{1}H NMR (600 MHz, CD_3OD) and key HMBC correlations of **164**

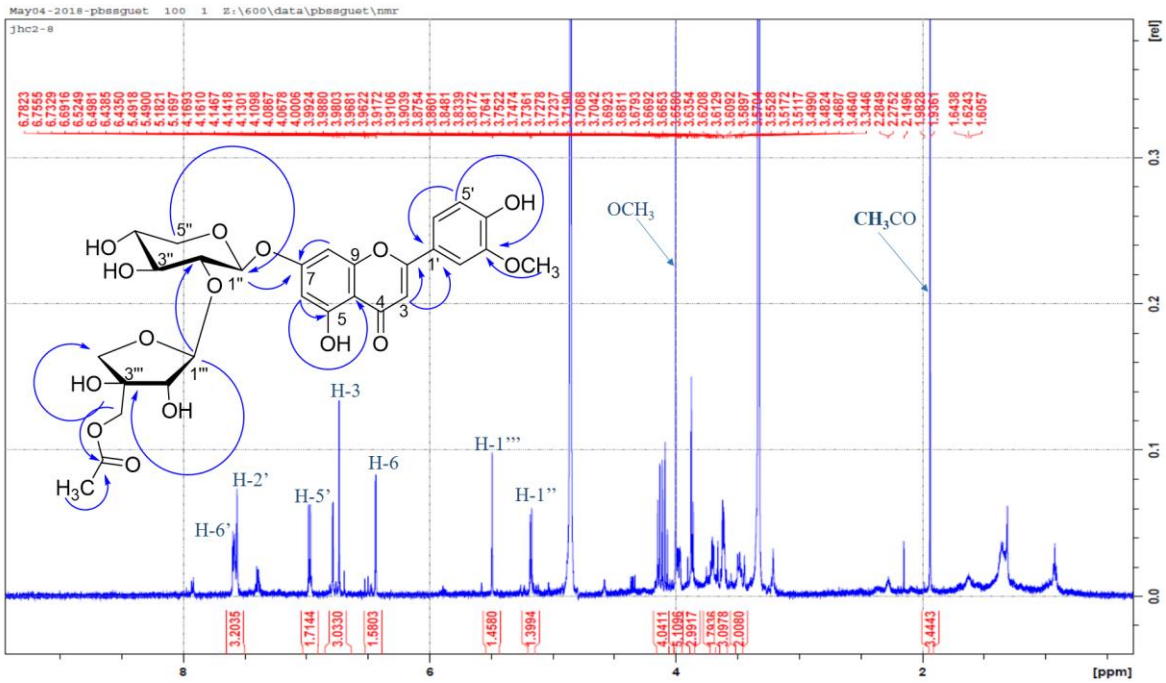

Figure 3.43 ^{1}H NMR (600 MHz, CD_3OD) and key HMBC correlations of **165**

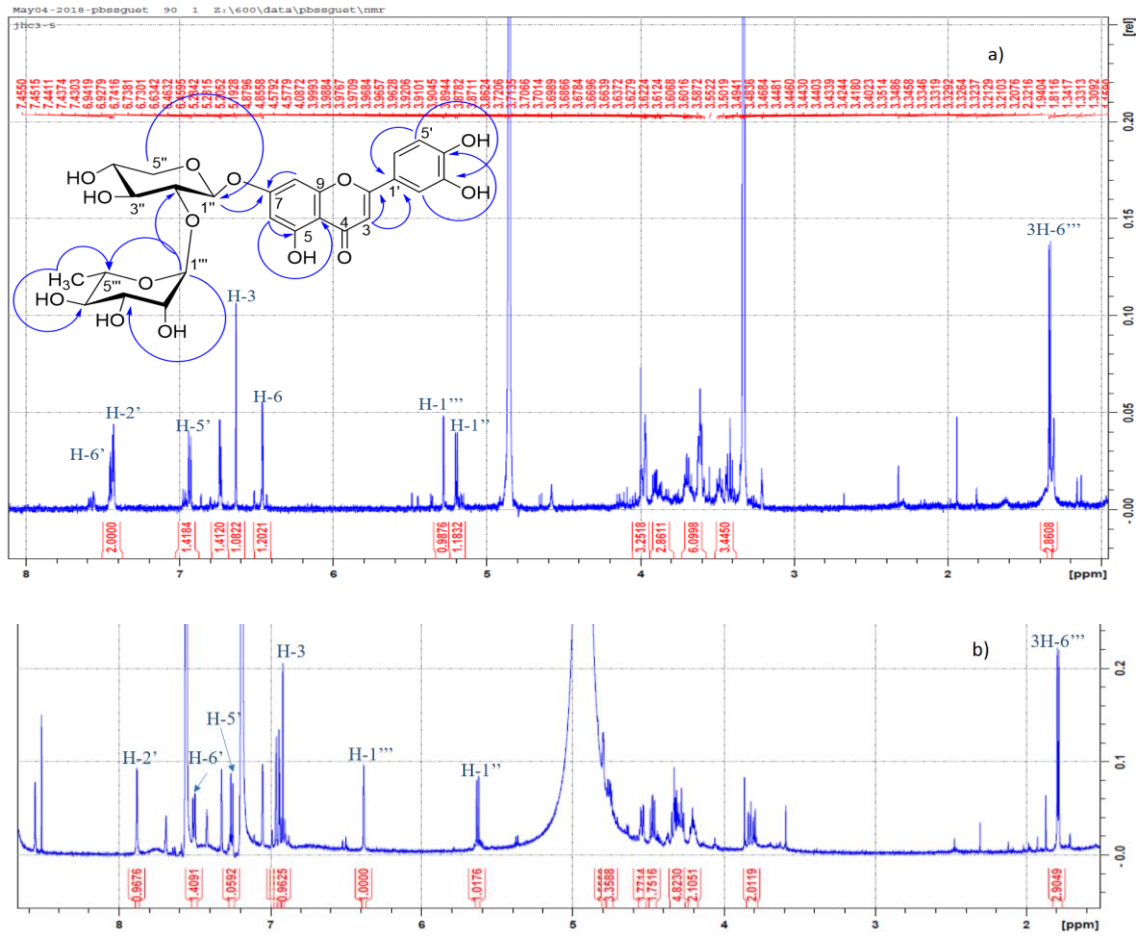

Figure 3.45 ^{1}H NMR (600 MHz, a-CD_3OD, b-Pyr-d_5) and key HMBC correlations of **166**

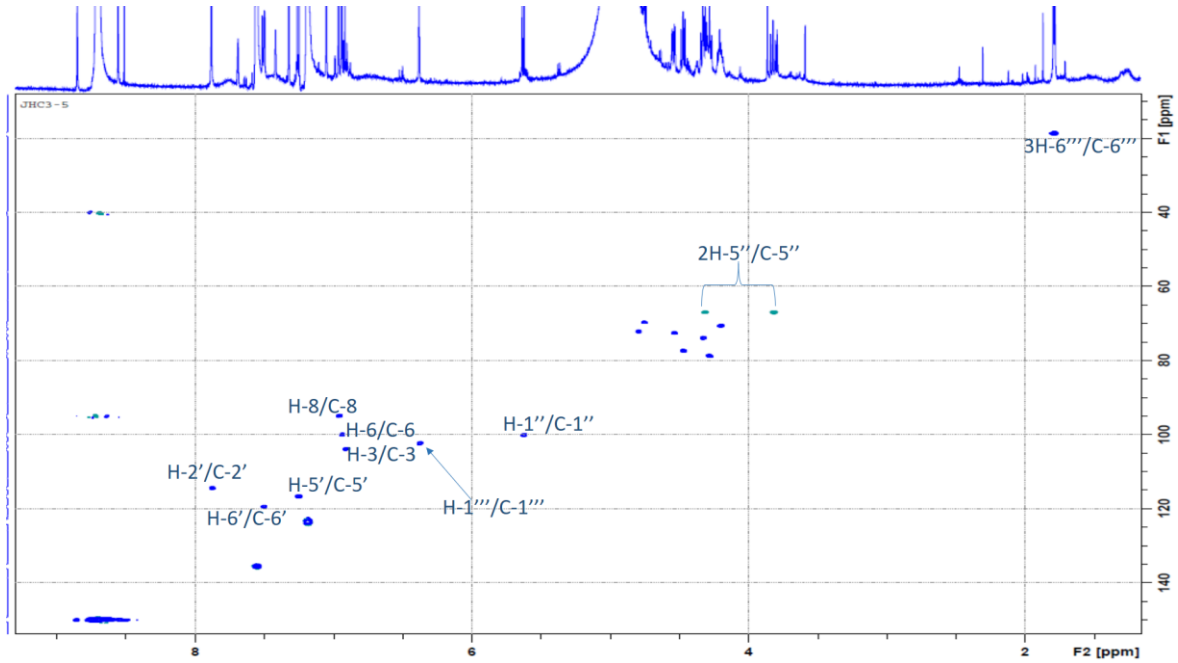

Figure 3.46 HSQC spectrum of **166**

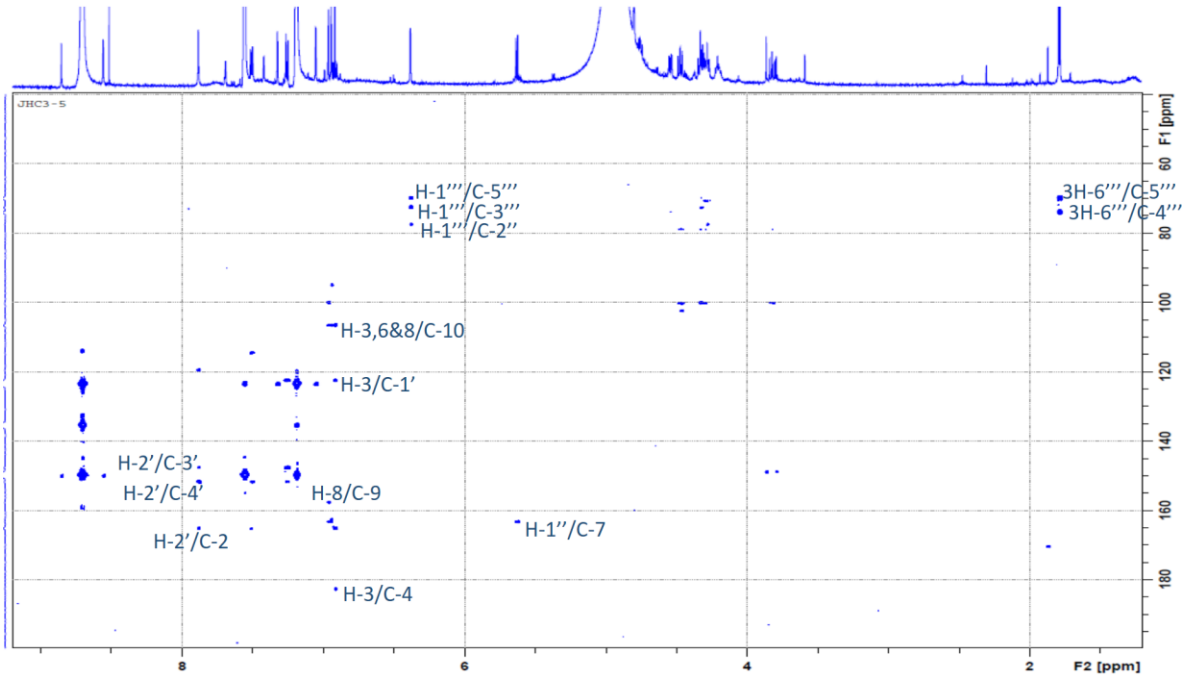

Figure 3.47 HMBC spectrum of **166**

3.3.2.5 Structure elucidation of chrysoeriol-7-*O*-*α*-L-rhamnopynosyl-(1→2)-*β*-D-xylopyranoside (**167**)

Compound **167** was isolated as a yellow amorphous powder. Its molecular formula $C_{27}H_{30}O_{14}$ was determined from its HR ESI-MS spectrum in positive mode ion by the peak at *m/z* 601.1533 calculated for $[C_{27}H_{30}O_{14}+Na]^+$, 601.1528 consistent with thirteen RDB. Its 1D and 2D NMR spectra, similar to those of **166,** also suggested a luteolin diglycoside skeleton. The only difference was the presence of an additional signal in the ^{1}H NMR (Figure 3.48, Table 3.9) of **167** of a singlet attributable to a methoxy group at δ_H 3.99 (3H). This was confirmed by the cross peak correlation observed on its HSQC spectrum between this signal and the carbon resonating at δ_C 55.4. In the HMBC spectrum (Figure 3.48), a cross peak correlation observed between the signal of the methoxy proton and a carbon resonating at δ_C 147.7 confirmed its position on the C-3' carbon of the luteolin skeleton. Thus, all the ^{1}H and ^{13}C NMR data (Tables 3.9-3.10), and the key

HMBC correlations of **167** (Figure 3.47) led to its identification as chrysoeriol-7-*O*-*α*-L-rhamnopynosyl-(1→2)-*β*-D-xylopyranoside, a new flavone diglycoside from natural source and was given the trivial name justicialoside B.

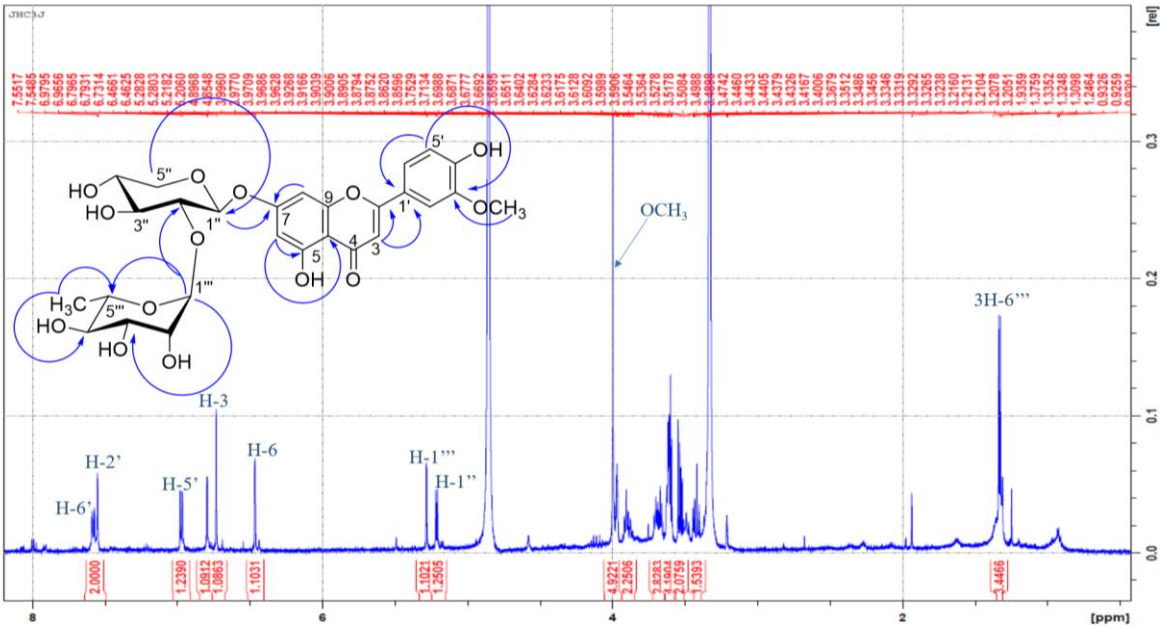

Figure 3.48 ^{1}H NMR (600 MHz, CD_3OD) and key HMBC correlations of **167**

3.3.2.6 Structure elucidation of luteolin 7-*O*-[*β*-D-glucopyranosyl-(1→2)-*α*-L-rhamnosyl-(1→6)]-*β*-D-glucopyranoside (**168**)

Compound **168** was isolated as a yellow amorphous powder. Its molecular formula $C_{33}H_{40}O_{20}$ was determined by the peak at *m/z* 779.2001 calculated for $[C_{33}H_{40}O_{20}+Na]^+$, 779.2005 and consistent with fourteen RDB, from its HR NSI-MS spectrum in positive mode ion. Its ^{1}H NMR spectrum (Figure 3.49, Table 3.9) revealed that **168** was a glycosylated luteolin. There were three sugar moieties recognizable by the three anomeric proton signals appearing at δ_H 4.69 (d, *J* = 7.9 Hz), 4.72 (d, *J* = 1.1 Hz) and 5.27 (d, *J* = 7.1 Hz). One of the sugar moieties could be identified as rhamnose by the presence of the characteristic methyl doublet at δ_H 1.19 (d, *J* = 6.1 Hz) (Osterdahl, 1979; Beier and

Mundy, 1980; Agrawal, 1992). TOCSY and COSY spectra of **168** were used to identify proton signals belonging to the same sugar moiety and for the construction of each sugar unit based on the direct ^{1}H-^{1}H coupling of their respective protons. Their corresponding carbon resonances was assigned using the HSQC spectrum. The two other sugar moieties could be identified as *β*-D-glucopyranoses based on their chemical shifts (Beier *et al.*, 1980). In the HMBC spectrum, correlations were observed between the anomeric proton at δ_H 5.27 (H-1'') and the carbon signal at δ_C 163.0 attributable to the carbon C-7 of the luteolin aglycone. Other correlations could also be observed between the anomeric protons at δ_H 4.69 (H-1''') and 4.72 (H-1'''') with the carbons at δ_C 82.0 (C-2'') and 66.1 (C-6''), respectively, of the glucopyranose unit attached to the aglycone. Thus, all the ^{1}H and ^{13}C NMR data of **168** (Tables 3.9-3.10), and the key HMBC correlations (Figure 3.49) confirmed its identification as luteolin 7-*O*-[*β*-glucopyranosyl-(1→2)-*β*-rhamnosyl-(1→6)]-*β*-glucopyranoside, a glycosylated flavone previously isolated from the leaves of *Justicia secunda* (Koffi *et al.*, 2013).

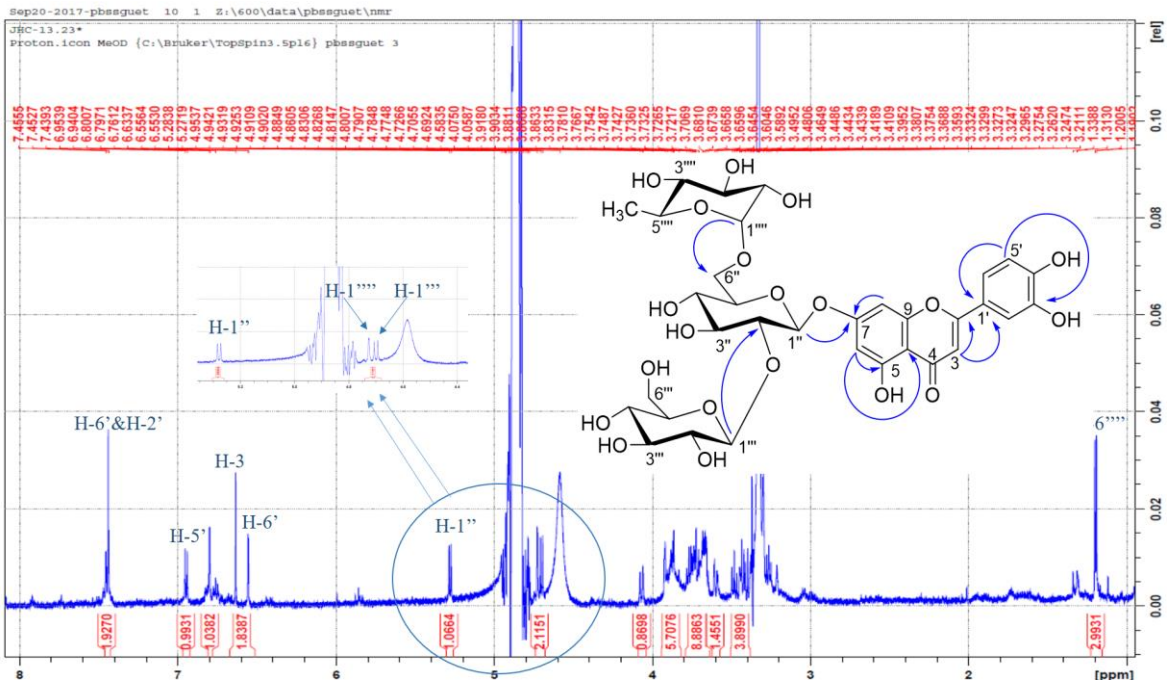

Figure 3.49 ^{1}H NMR (600 MHz, CD_3OD) and key HMBC correlations of **168**

3.3.2.7 Structure elucidation of secundallerones B and C (**170-171**) as a mixture

Compounds **170** and its diastereoisomer **171** were isolated as brown amorphous powder mixture with molecular formula of $C_{12}H_{15}NO_6$ determined from their HR ESI-MS spectrum (Figure 3.50) obtained in negative ion mode by the peak at *m/z* 268.0828 calculated for $[C_{12}H_{15}NO_6\text{-}H]^-$, 268.0827. The ^{1}H NMR spectrum (Figure 3.51, Table 3.11) of the mixture showed two set of signals each attributable to four methines including two aromatic singlets suggesting a 1,2,4,6-tetrasubstituted benzene ring and two oxymethines, one methylene and two methoxyls. These attributions were supported by the different correlations observed on the HSQC-DEPT spectrum of the mixture as well as the chemical shift of the corresponding carbons. The ^{1}H and ^{13}C NMR spectra of **170** and **171** were quite similar to those published for secundellarones B and C, two diastereoisomeric pyrrolidone alkaloids isolated from the leaves of *J. secunda* (Theiler *et al.*, 2014). In addition, their ^{1}H and ^{13}C NMR data (Table 3.11) were in good agreement with the data published for secundallerone B and C (Theiler *et al.*, 2014). Thus, compounds **170** and **171** were identified as secundarellone B and C, respectively.

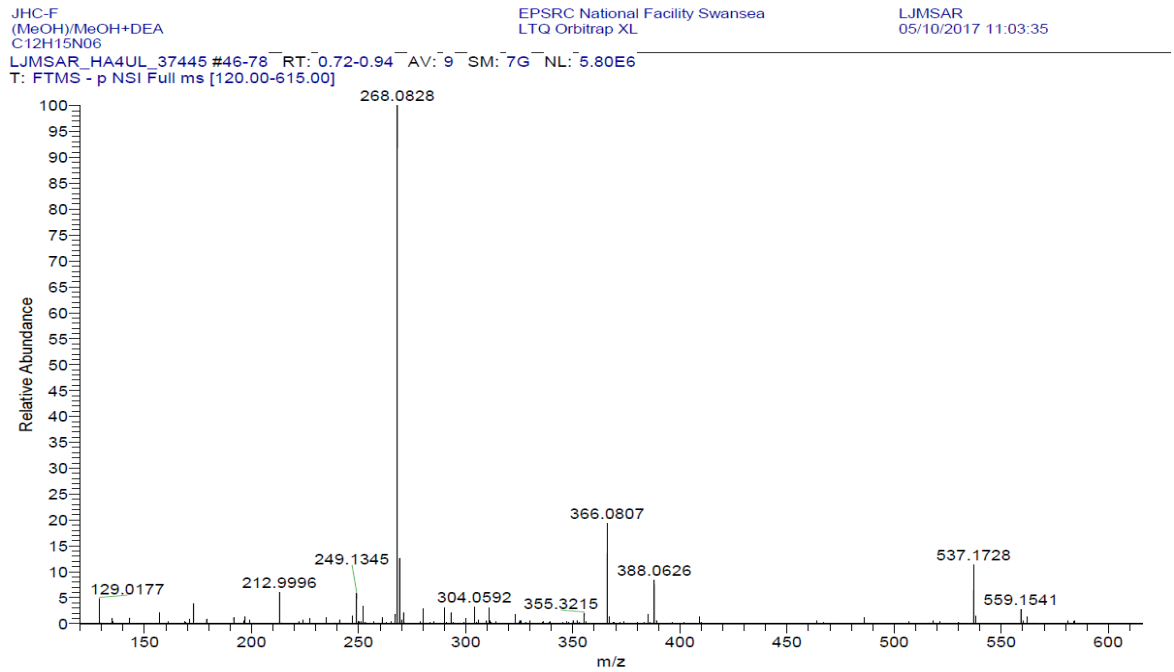

Figure 3.50 ESI-MS spectrum of **170** and **171**

Table 3.9 ^{1}H NMR data of compounds **163-168**

Position	δ_H m (*J* in Hz)					
	163[a]	**164**[a]	**165**[b]	**166**[a]	**167**[b]	**168**[b]
3	6.89 s	6.93 s	6.76 s	6.91 s	6.73 s	6.63 s
6	6.92 d (*2.0*)	6.94 d (*2.1*)	6.43 d (*2.1*)	6.94 d (*2.1*)	6.46 d (*2.1*)	6.55 d (*2.0*)
8	6.95 d (*2.0*)	7.11 d (*2.1*)	6.78 d (*2.1*)	6.96 d (*2.1*)	6.79 d (*2.1*)	6.79 d (*2.0*)
2’	7.87 d (*2.1*)	7.58 d (*2.2*)	7.56 d (*2.0*)	7.88 d (*2.2*)	7.55 d (*1.9*)	7.43 d (*1.6*)
5’	7.26 d (*8.2*)	7.25 d (*8.3*)	6.97 d (*8.2*)	7.25 d (*8.3*)	6.97 d (*8.4*)	6.94 d (*8.1*)
6’	7.49 dd (*2.1*, *8.2*)	7.60 dd (*2.2*, *8.3*)	7.58 dd (*2.0*, *8.2*)	7.50 dd (*2.2*, *8.3*)	7.58 dd (*1.9*, *8.4*)	7.45 dd (1.6, *8.1*)
1’’	5.58 d (*7.4*)	5.60 d (*7.5*)	5.17 d (*7.3*)	5.62 d (*7.5*)	5.21 d (*7.3*)	5.27 d (*7.1*)
2’’	4.49 m	4.47 dd (*7.6*, *9.0*)	3.70 m	4.47 dd (*7.6*, *9.0*)	3.69 m	3.76 m
3’’	4.30 ov	4.29 m	3.61 m	4.28 m	3.61 m	3.69 m
4’’	4.21 m	4.19 m	3.61 m	4.75 m	3.60 m	3.48 m
5’’	3.80 t (*10.6*)	3.78 m	3.48 m	3.80 m	3.49 m	3.72 m
	4.30 ov	4.30 m	3.97 dd (*4.0*, *11.8*)	4.31 m	3.98 m	
6’’						3.66 m
						4.05 m
1’’’	6.52 d (*1.8*)	6.52 d (*1.2*)	5.49 d (1.4)	6.38 d (*1.6*)	5.28 d (*1.5*)	4.69 d (*7.9*)
2’’’	4.83 brs	4.84 brs	3.87 ov	4.80 m	3.96 *m*	3.25 *m*
3’’’	-	-	-	4.54 dd (*3.3*, *9.3*)	3.61 m	3.42 m
4’’’	4.21 s	4.21 brs	4.08 brs	4.32 m	3.41 t (*9.6*)	3.39 m

Table 3.9 *continued*

Position	δ_H **m (*J* in Hz)**					
	163[a]	**164**[a]	**165**[b]	**166**[a]	**167**[b]	**168**[b]
5’’’	4.45 d (*9.6*)	4.43 d (*9.5*)	3.87 ov	4.75 m	3.89 m	3.30 m
	4.77 d (*9.6*)	4.76 d (*9.5*)	4.13 ov			
6’’’		-		1.78 d (*6.1*)	1.32 d (*6.2*)	3.59 m
						3.67 m
1’’’’						4.72 d (*1.1*)
2’’’’						3.91 m
3’’’’						3.73 m
4’’’’						3.35 m
5’’’’						3.65 m
6’’’’						1.19 d (*6.1*)
OCH_3		3.78 s	4.00 s	-	3.99 s	

a- ran in Pyr-d_5; b- ran in CD_3OD

Table 3.10 ^{13}C NMR data of compounds **165-170**

Position	δ_C					
	163[a]	**164**[a]	**165**[b]	**166**[a]	**167**[b]	**168**[b]
1	-	-	-	-	-	-
2	165.2	164.7	165.3	165.1	165.0	165.7
3	106.5	104.0	103.5	104.0	103.2	102.9
4	182.6	182.5	183.1	182.5	182.1	182.9
5	162.6	157.6	161.3	162.4	160.9	161.5
6	100.3	100.3	99.9	99.9	99.5	99.1
7	163.3	163.0	162.6	163.2	162.5	163.0
8	95.3	95.3	94.2	95.0	94.5	95.1
9	157.6	157.6	157.6	157.4	156.8	157.6
10	106.5	106.6	105.7	106.5	105.1	105.8
1’	122.3	122.3	122.0	122.3	121.5	122.2
2’	114.4	110.1	109.7	114.1	109.5	113.0
3’	147.5	148.5	148.0	147.6	147.7	149.9
4’	151.6	152.4	150.9	151.0	150.2	145.7
5’	116.6	116.7	115.4	116.5	115.3	115.9
6’	119.3	121.1	120.7	119.4	120.5	119.3
1’’	100.3	100.3	99.3	100.2	99.0	98.5
2’’	77.0	77.0	76.6	77.4	77.6	82.0
3’’	78.3	78.2	69.7	78.6	70.7	75.7
4’’	70.5	70.4	76.8	70.5	77.2	69.5
5’’	67.0	66.7	65.7	67.0	65.6	76.7
6’’						66.1
1’’’	110.5	110.4	108.9	102.3	101.2	104.0
2’’’	77.6	77.7	77.2	72.1	70.7	74.6
3’’’	80.6	80.7	nd	72.4	69.7	76.4
4’’’	65.8	65.8	66.9	74.0	72.6	69.7
5’’’	75.6	75.4	74.1	69.9	68.6	76.7
6’’’				18.6	16.9	60.7
1’’’’						100.9
2’’’’						70.7
3’’’’						71.2
4’’’’						72.6
5’’’’						68.4
6’’’’						16.4
OCH_3		55.8	55.0		55.4	
CH_3CO			19.2			
$COCH_3$			171.1			

Table 3.11 ^{1}H and ^{13}C NMR data of **170** and **171**

Position	**170**		**171**	
	δ_H m (*J*)	δ_C	δ_H m (*J*)	δ_C
1	-	-	-	-
2	-	176.0	-	177.4
3	5.30 t (*6.0*)	81.8	5.42 d (*6.4*)	83.4
4	1.80 ddd (*5.9*, *8.3*, *14.3*)	39.6	2.28 m	39.6
	2.91 ddd (*6.2*, *8.5*, *14.3*)		2.42 dd (*7.9*, *8.4*)	
5	4.36 t (*8.4*)	69.5	4.67 t (*8.2*)	69.2
1’	-	115.9	-	116.5
2’	-	148.8	-	148.9
3’	6.61 s	101.7	6.63 s	102.0
4’	-	151.4	-	151.5
5’	-	142.5	-	142.6
6’	6.86 s	116.3	6.81 s	115.0
4’-OCH3	3.74 s	56.6	3.76 s	56.6
5’-OCH3	3.83 s	56.7	3.81 s	57.3

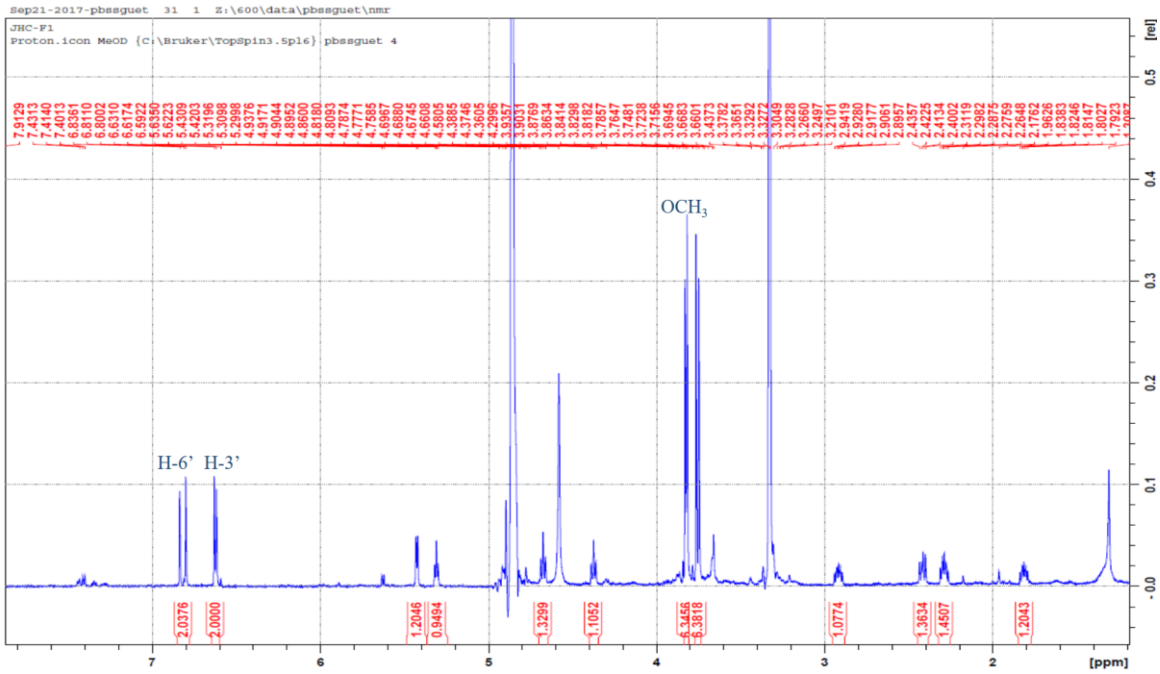

Figure 3.51 ^{1}H NMR (600 MHz, CD_3OD) of **170** and **171**

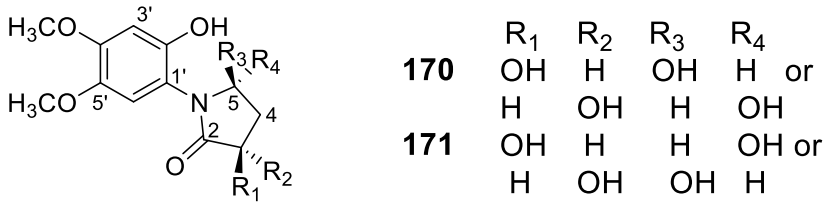

Figure 3.52 Key ^{1}H-^{1}H NOESY (↔) and HMBC (→) correlations **170** and **171**

3.3.3 Phytochemistry of *Pseudospondias microcarpa*

Chromatographic separation of the phytochemical constituents of the methanol and DCM extracts of the stem bark and leaves of *P. microcarpa* led to isolation of seven compounds (Figure 3.53). The compounds were characterised by spectroscopic means and by comparison of their spectral data with those of previously isolated compounds from our laboratory or with the literature. They were identified as *trans*-ferulic acid (**148**), chrysoeriol-7-*O*-*β*-D-apiofuranosyl-(1→2)-*β*-D-xylopyranoside (**164**), luteolin-7-*O*-*α*-L-rhamnopynosyl-(1→2)-*β*-D-xylopyranoside (**166**), isovetexin (**172**), apigenin 7-O-*β*-D-neohesperidoside (**173),** scopoletin (**103**) and pithecellobiumol B (**174**). All the isolated compounds belong to the class of phenolic compounds and their derivatives. To the best of our knowledge, this is the first report on the phytochemical studies of the genus *Pseudospondias* and the species *P. microcarpa*. The genus *Pseudospondias* derived from *Spondioidae* tribe of the Anarcadiaceae family (Mitchel and Daly, 2015), known to be a rich source of phenolic compounds including flavonoids, phenolic acid derivatives and tannins (Umadevi *et al.*, 1988; Sameh *et al.*, 2018).

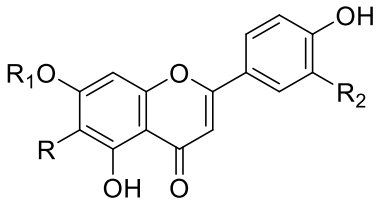

164 R= H R_1= β–D-apiofuranosyl-(1"→2")-β-D-xylopyranosyl R_2= OCH_3
166 R= H R_1= α-L-rhamnopyranosyl-(1"→2")-β-D-xylopyranosyl R_2= OH
172 R= β-D-glucopyranosyl R_1= H R_2= H
173 R= H R_1= α-L-rhamnosyl-(1"→2")-β-D-glucopyranosyl R_2= H

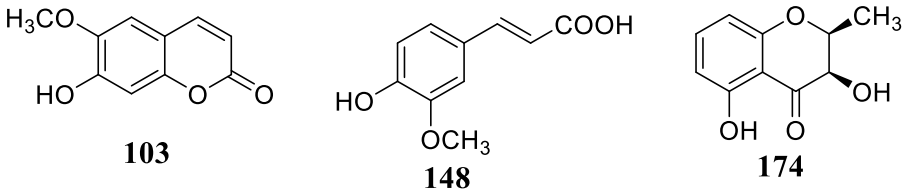

Figure 3.53 Structures of isolated compounds from *P. microcarpa*

3.3.3.1 Structure elucidation of scopoletin (**103**)

Compound **103** was isolated as a light brown powder. Its molecular formula $C_{10}H_8O_4$ was determined by the peak at *m/z* 215 $[M+Na]^+$, from its ESI-MS spectrum obtained in positive mode ion. Its ^{1}H NMR spectrum (Figure 3.54, Table 3.12) showed characteristic signal of H-3 (δ_H 6.20, d, J = 9.4 Hz) and H-4 (δ_H 7.90, d, J = 9.4 Hz) protons of the pyrone ring of coumarins (Kayser and Kolodziej, 1995), two aromatic singlet methines at δ_H 6.77 and 7.19 consistent with a tetrasubstituted aromatic ring and a methoxy signal at δ_H 3.80. In the HMBC spectrum (Figure 3.54), long-range correlations were observed between the olefinic proton at δ_H 7.90 (H-1') and the carbons at δ_C 109.9 (C-2) and 149.8 (C-6) and between the methoxy proton at δ_H 3.80 and the carbon at δ_C 145.7 (C-3). The ^{1}H and ^{13}C NMR data (Table 3.12) of **103** were in good agreement with those published for scopoletin (Darmawan *et al.,* 2012). Thus, compound **103** was characterised as scopoletin, a coumarin with a range of biological activities including antidiabetic, antimicrobial, anti-oxidant and antitumor (Zhao *et al.*, 2015; Napiroon *et al.*, 2018).

Table 3.12 ^{1}H (600 MHz, DMSO-d_6) and ^{13}C NMR (150 MHz, DMSO-d_6) data of **103**

Position	δ_H *m* (*J* in Hz)	δ_C	Position	δ_H *m* (*J* in Hz)	δ_C
2	-	161.5	7	-	151.5
3	6.20 d (*9.4*)	112.0	8	7.19 s	109.9
4	7.90 d (*9.4*)	145.1	9	-	111.2
5	6.77	103.1	10	-	145.7
6	-	149.8	OCH_3	3.80 s	56.4

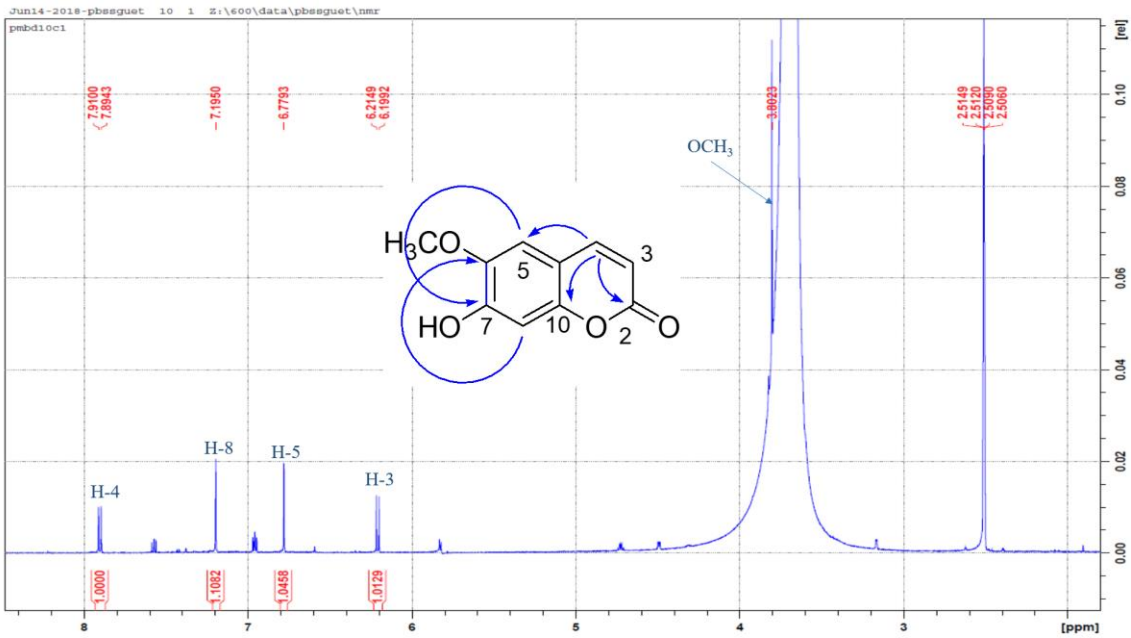

Figure 3.54 ^{1}H NMR (600 MHz, DMSO-d_6) and key HMBC correlations of **103**

3.3.3.2 Structure elucidation of isovetexin (**172**)

Compound **172** was isolated as a dark yellow amorphous powder. Its molecular formula $C_{21}H_{20}O_{10}$ was confirmed by the peak at *m/z* 455 $[M+Na]^+$, in its ESI-MS spectrum obtained in positive ion mode. The ^{1}H NMR spectrum (Figure 3.55, Table 3.13) showed

12 peaks belonging to a glycosylated molecule bearing one sugar moiety. The aglycone part of the compound was identified as apigenin by the presence of an A_2B_2 system resonating at δ_H 7.87 (2H, d, *J* = 8.8 Hz) and 6.95 (2H, d, *J* = 8.8 Hz) characteristic of the 1,4-disubstituted B ring; a singlet at δ_H 6.63 attributable to the H-3 proton of the C ring and another singlet at δ_H 6.54 ppm attributable to the H-6 or H-8 proton of the A ring suggesting an additional substituent on that ring at one of those positions. The sugar moiety was characterised by the presence of the methylene protons at δ_H 3.75 (dd, *J* = 5.3, 12.1 Hz) and 3.90 (dd, *J* = 2.3, 12.1 Hz) and four methines including the anomeric proton at δ_H 4.92 (d, *J* = 9.9 Hz), which on the HSQC spectrum (Figure 3.56) correlated with the carbon at δ_C 75.3 suggesting the direct C-C attachment of the sugar moiety to the aglycone ring. The observed ^{1}H and ^{13}C NMR data (Table 3.13) associated with the sugar moiety were in agreement with those published for *β*-D-glucose (Agrawal, 1992). In the HMBC spectrum (Figure 3.57), the singlet at δ_H 6.54 showed long-range correlations with the carbons at δ_C 105.2 (C-10), 158.7 (C-9) and 164.9 (C-7) and was therefore assigned to the proton at C-8 of the A ring. A ^3J long-range correlations were observed between the anomeric proton of the glucosyl moiety (δ_H 4.92, H-1’’) and the carbon at δ_C 109.3 (C-6), 162.0 (C-5) and 164.9 (C-7) confirming the direct attachment of the sugar carbon C-1’’at C-6 by a C–C linkage. All the observed NMR data (Table 3.13) were consistent with those published for apigenin-6-C-*β*-D-glucoside or isovitexin (Krafczyk *et al.*, 2008; Ganbaatar *et al.*, 2015). Thus, compound **172** was identified as isovitexin. Isovitexin has been identified and isolated from several genus of Anarcadiaceae and possesses a range of biological properties including anti-inflammatory, antispasmodic, antimicrobial and antinociceptive (Picerno *et al.*, 2006; Correa *et al.*, 2012; Abu-Reidah *et al.*, 2015).

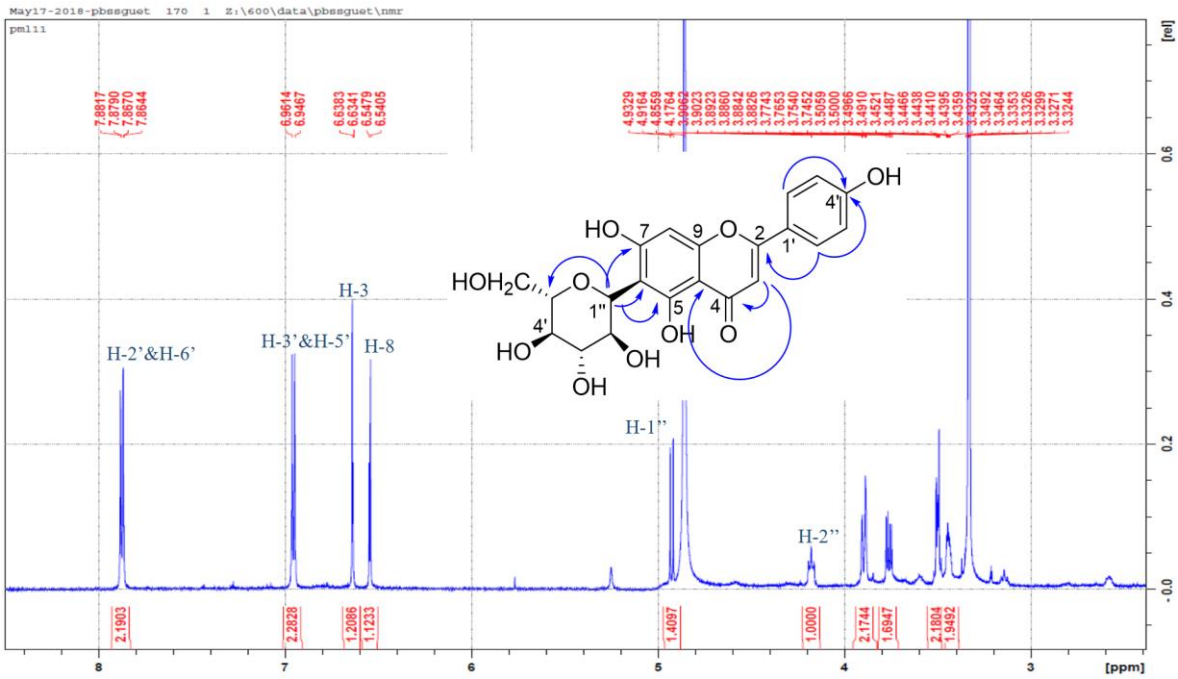

Figure 3.55 ^{1}H NMR (600 MHz, CD_3OD) and key HMBC correlations of **172**

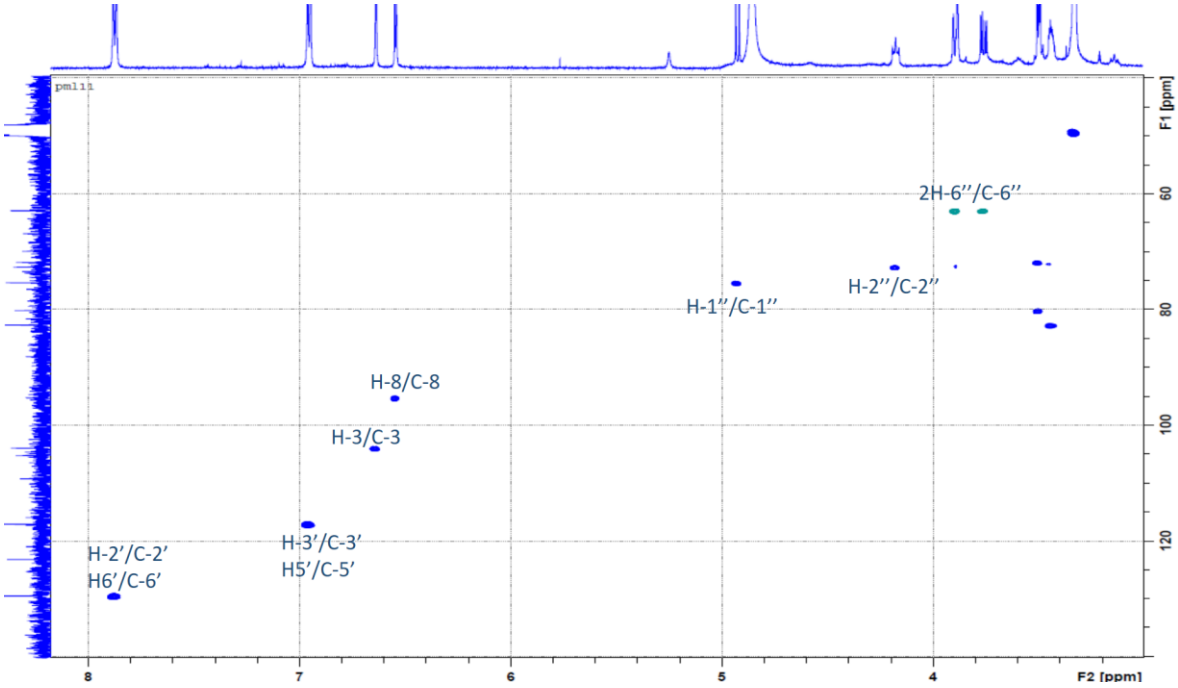

Figure 3.56 HSQC spectrum of **172**

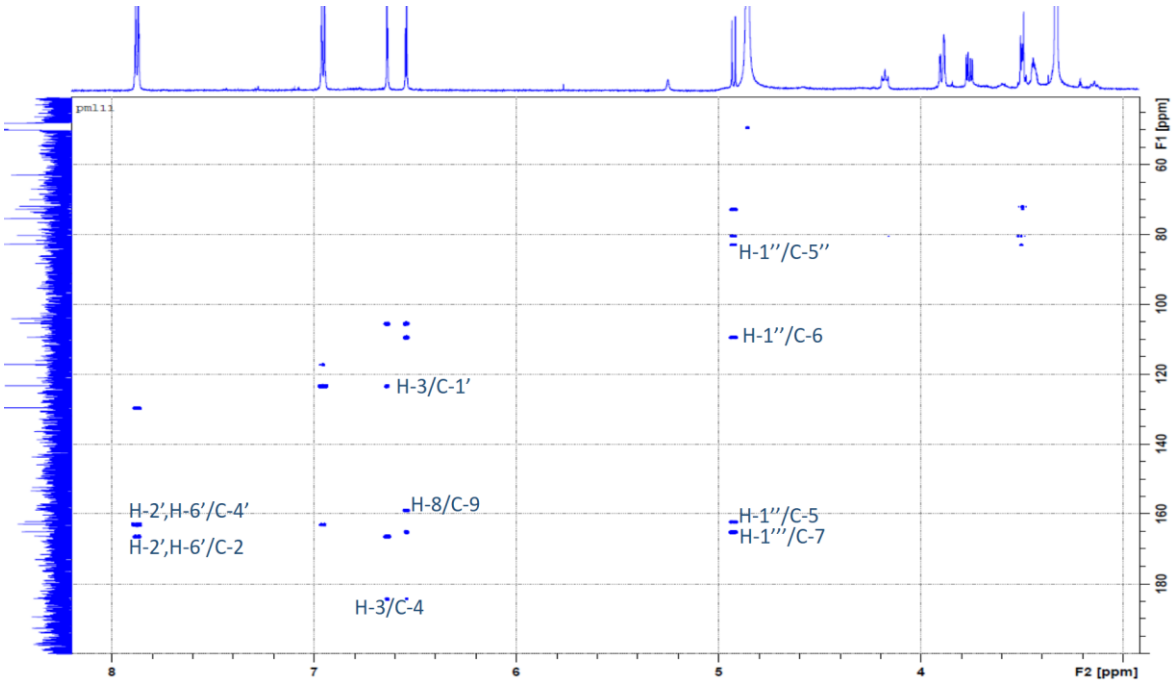

Figure 3.57 HMBC (600 MHz, CD_3OD) of **172**

3.3.3.3 Structure elucidation of apigenin 7-*O*-*β*-D-neohesperidoside (**173**)

Compound **173** was isolated as a dark brown amorphous powder. Its molecular formula $C_{27}H_{30}O_{14}$ was determined from the peak at *m/z* 601 $[M+Na]^+$, in its ESI-MS spectrum in positive mode ion. Its ^1H NMR spectrum (Figure 3.58, Table 3.13) suggested a glycosylated apigenin bearing two sugar moieties payable to the presence of two anomeric protons at δ_H 5.30 (d, J = 1.7 Hz) and 5.22 (d, J = 7.6 Hz) and the proton signals at δ_H 7.91 (2H, d, J = 8.8 Hz), 6.95 (2H, d, J = 8.8 Hz), 6.82 (1H, d, J = 2.2 Hz), 6.68 (1H, s) and 6.48 (1H, d, J = 2.2 Hz) attributable to the apigenin aglycone. The two sugar moieties were identified as *α*-L-rhamnose and *β*-D-glucose by comparison of the observed data with those published for the respective molecules (Osterdahl, 1979; Beier and Mundy, 1980). In the HMBC spectrum (Figure 3.58), a correlation observed between the anomeric proton of the glucosyl unit (δ_H 5.22, H-1'') and the carbon at δ_C 162.5 (C-7) confirmed its direct attachment to the aglycone. While, the correlation of the rhamnosyl

anomeric proton (δ_H 5.30, H-1’’’) with the carbon C-2’’ of the glycosyl at δ_C 77.6 led to the fixation of the rhamnosyl unit on the carbon C-2’’ of the glycoside. The ^{1}H and ^{13}C NMR data (Table 3.13) of **173** and the key HMBC correlations (Figure 3.58) were in good agreement with those published for apigenin 7-O-*β*-D-neohesperidoside (Osterdahl, 1979; Zhang *et al.*, 2016). Thus, compounds **173** was identified as apigenin 7-O-*β*-D-neohesperidoside, a flavone glycoside with antioxidant properties (Zhang *et al.*, 2016).

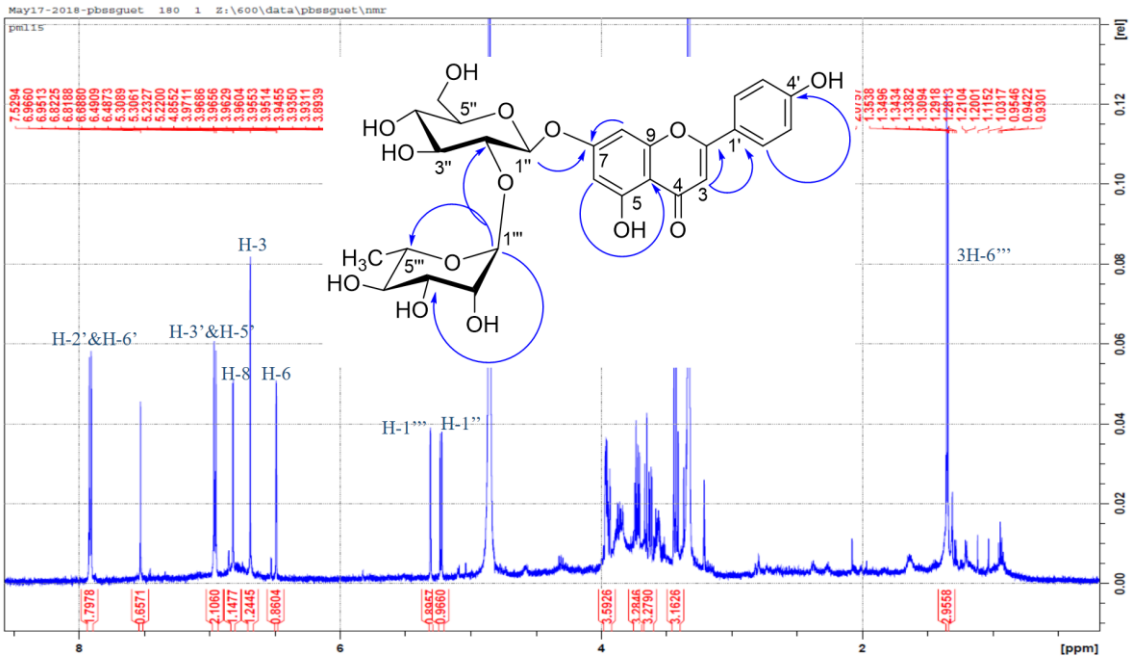

Figure 3.58 ^{1}H NMR (600 MHz, CD_3OD) and key HMBC correlations of **173**

3.3.3.4 Structure elucidation of pithecellobiumol B (**174**)

Compound **174** was isolated as a brown amorphous powder. Its molecular formula $C_{10}H_{10}O_4$ was determined from the *pseudo*molecular peak at *m/z* 217 $[M+Na]^+$, in its ESI-MS spectrum. Its ^{1}H NMR spectrum (Figure 3.59, Table 3.14) depicted seven peaks which could be attributed to five methines including three aromatic methine at δ_H 7.58 (dd, *J* = 7.3, 8.3 Hz), 6.97 (dd, *J* = 0.9, 8.3 Hz) and 6.96 (dd, *J* = 0.9, 7.3 Hz) and two

oxymethines at δ_H 4.75 (dq, J = 2.1, 6.6 Hz) and 4.50 (dd, J = 2.1, 6.3 Hz); a doublet methyl at δ_H 1.40 (J = 6.6 Hz) and a doublet proton at δ_H 5.71 (d, J = 6.3 Hz) which was attributed to the proton of a hydroxyl group as no cross peak correlation was observed for this signal in the HSQC-DEPT spectrum. In the HMBC (Figure 3.59), long-range correlations were observed between the methine at δ_H 4.50 (H-3) and the carbon at δ_C 107.7 (C-10) and 142.8 (C-9) and between the methine at δ_H 7.58 (H-7) and the carbons at δ_C 142.8 (C-8a) and 160.6 (C-5). The ^{1}H and ^{13}C NMR data (Table 3.14) of compound **174** were similar to those published for pithecellobiumol B (Wang *et al.*, 2017). In addition, pithecellobiumol B and **174** were found to have quite identical ^{1}H NMR spectra when ran in DMSO. Thus, **174** was recognised as pithecellobiumol B, a chromanone previously isolated from the leaves and twigs of *Pithecellobium clypearia* (Fabaceae) (Wang *et al.*, 2017).

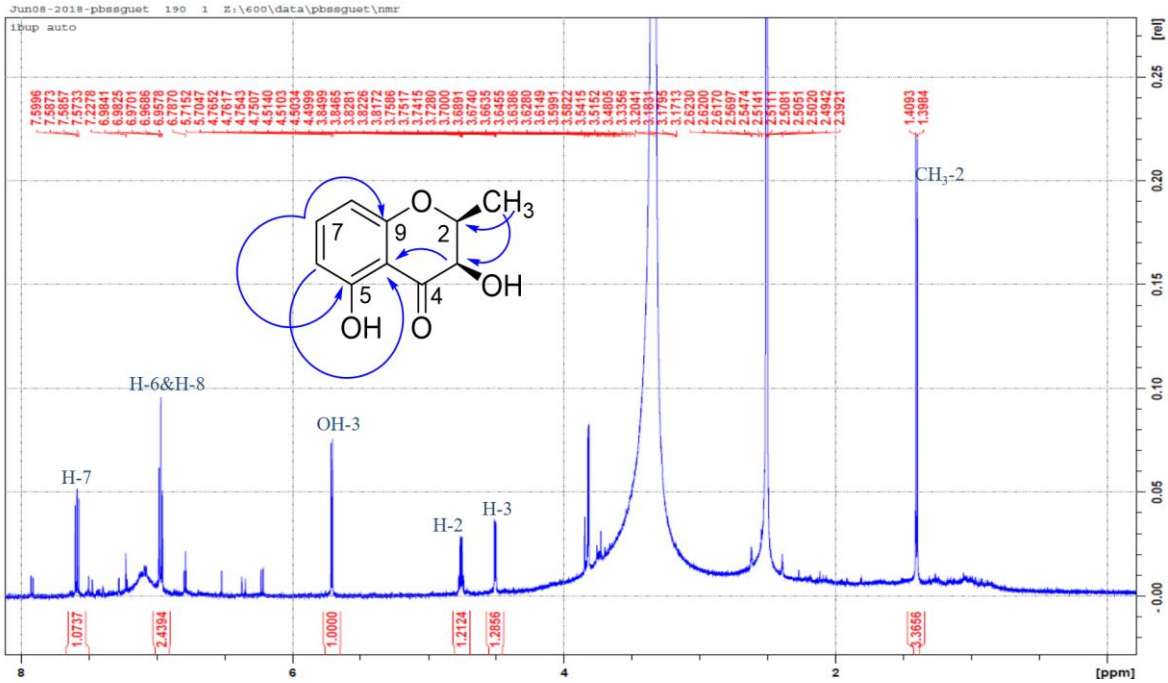

Figure 3.59 ^{1}H NMR (600 MHz, DMSO-d$_6$) and key HMBC correlations of **174**

Table 3.13 ^{1}H (600 MHz, CD_3OD) and ^{13}C NMR (75 MHz, CD_3OD) data of **172** and **173**

Position	δ_H *m* (*J* in Hz)		δ_C	
	172	**173**	**172**	**173**
1	-	-	-	-
2	-	-	166.3	164.8
3	6.63 s	6.68 s	103.9	102.7
4	-	-	183.9	182.1
5	-	-	162.0	nd
6	-	6.48 d (*2.2*)	109.3	99.5
7	-	-	164.9	162.5
8	6.54 s	6.82 d (*2.2*)	95.4	94.7
9	-	-	158.7	157.0
10	-	-	105.2	105.5
1’	-	-	123.1	121.4
2’	7.87 d (*8.8*)	7.91d (*8.8*)	129.4	128.6
3’	6.95 d (*8.8*)	6.95 d (*8.8*)	117.0	115.9
4’	-	-	162.8	161.3
5’	6.95 d (*8.8*)	6.95 d (*8.8*)	117.0	115.9
6’	7.87 d (*8.8*)	7.91d (*8.8*)	129.4	128.6
1’’	4.92 d (*9.9*)	5.22 d (*7.6*)	75.3	98.4
2’’	4.17 brt (*9.3*)	3.71 ov	72.6	77.6
3’’	3.49 ov	3.65 ov	80.1	77.6
4’’	3.47 ov	3.42 m	71.8	72.6
5’’	3.44 m	3.55 m	82.8	76.9
6’’	3.75 dd (*5.3*, *12.1*)	3.73 m	62.8	61.1
	3.90 dd (*2.3*,*12.1*)	3.94 m		
1’’’		5.30 d (*1.7*)		101.3
2’’’		3.97 m		70.7
3’’’		3.62 m		70.7
4’’’		3.43 m		70.1
5’’’		3.96 m		68.4
6’’’		1.34 d (*6.2*)		16.8

nd not determined

Table 3.14 ^{1}H (600 MHz, DMSO-d_6) and ^{13}C NMR (150 MHz, DMSO-d_6) data of **174**

Position	δ_H m (*J* in Hz)	δ_C	Position	δ_H m (*J* in Hz)	δ_C
1	-	-	8	6.97 dd (*0.9*, *8.3*)	117.6
2	4.75 dq (*1.9*, 6.*6*)	79.2	9	-	142.8
3	4.50 dd (*2.1*, *6.3*)	65.8	10	-	107.7
4	-	nd	2-CH3	1.40 d (*6.6*)	16.1
5	-	160.6	3-OH	5.71 d (*6.3*)	-
6	6.96 dd (*0.9*, *7.3*)	119.6	5-OH	10.9 brs	-
7	7.58 dd (*7.3*, *8.3*)	137.3			

nd not determined

3.3.4 Phytochemistry of *Zanthoxylum leprieurii*

Silica gel CC and RP-HPLC analyses of the *n*-hexane and DCM extracts of the fruits of *Z. leprieurii* afforded nine compounds including five kaurane diterpenes i.e., kaurenoic acid (**175**), xylopic acid (**176**), *ent*-kauran-16*β*-ol-19-oic acid (**177**), *ent*-kauran-16*β*-ol-19-al (**178**) and *ent*-kauran-16*β*-ol (**179**); two flavanes i.e., dulcisflavane (**180**) and epicatechin (**181**); caffeic acid (**114**) and icariside D2 (**182**) (Figure 3.60) along with a mixture of sterols. All the above listed compounds are here reported from the first time from *Z. leprieurii*. Compounds **114** and **180-182** have previously been reported from other *Zanthoxylum* species including *Z. piperitum, Z. schinifolium* (Kusuda *et al.*, 2006; Fang *et al.*, 2010). This is the first report on the occurrence kaurane diterpenoids (**175-179**) in the genus *Zanthoxylum*. Kaurane diterpenes are mainly found in the Asteraceae, Annonaceae and Euphorbiaceae families among others (Garcia *et al.*, 2007). First occurrence of kaurane diterpenes in the Rutaceae was the isolation of kaurenoic acid and its 15*β*-hydroxylated derivative from the genus *Phebalium* (Cannon *et al.*, 1966). Several kauranes were later isolated from the genus *Fortunella* (El-Shafae and Ibrahim, 2003).

Diterpenes are rather rare in the Rutaceae and only a few have been reported from the genus *Citrus*, *Evodia*, *Glycosmis* and *Pamburus* (Dreyer and Park, 1975; Seger *et al.*, 1998; Garcia *et al.*, 2007).

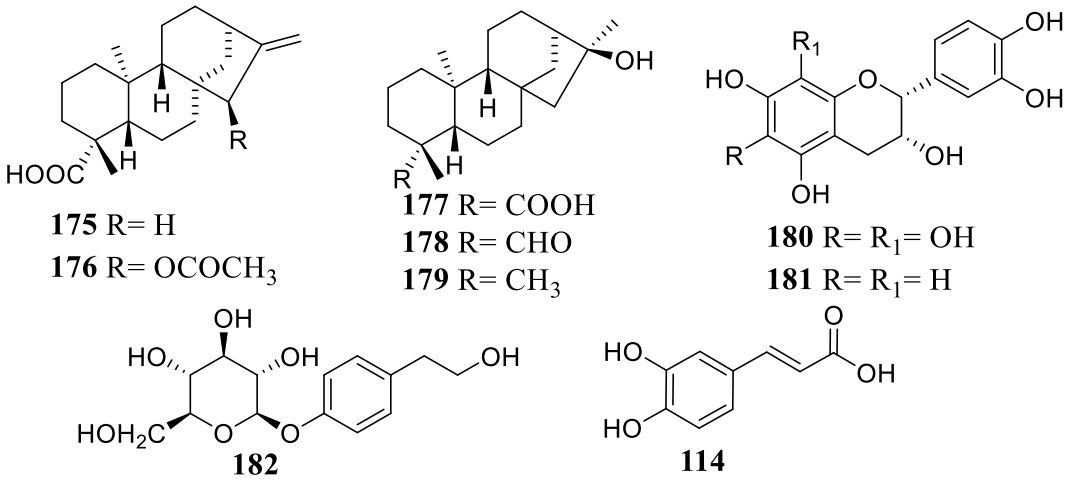

Figure 3.60 Isolated compounds from the fruits of *Z. leprieurii*

3.3.4.1 Structure elucidation of kaurenoic acid (**175**)

Compound **175** was isolated as white crystalline powder from the hexane extract of *Z. leprieurii*. Its molecular formula $C_{20}H_{30}O_2$ was determined from its HR ESI-MS spectrum (Figure 3.61) obtained in negative ion mode where the peak at *m/z* 301.2170 $[M-H]^-$ calculated for $C_{20}H_{29}O_2$, 301.2173 was observed. The ^1H NMR spectrum (Figure 3.62, Table 3.15) of **175** showed characteristic signals of two tertiary methyls at δ_H 0.92 (s, H-20) and 1.25 (s, H-18), two singlets at δ_H 4.67 and 4.72 (1H each) typical of the methylene protons (H-17) of an exocyclic double bond and one methine proton at δ_H 2.56 (brs, H-13). The ^{13}C NMR spectrum (Figure 3.62, Table 3.15) depicted 20 peaks which could be attributed to two methyls at δ_C 15.6 (C-20) and 28.9 (C-18); ten methylenes at δ 103.0 (C-17), 48.9 (C-15), 41.3 (C-7), 40.7 (C-1), 39.7 (C-14), 37.8 (C-3), 33.1 (C-12), 21.8 (C-6), 19.1 (C-2) and 18.4 (C-11); three methines at δ_C 57.0 (C-5), 55.1 (C-9) and 43.7

(C-13) and five quaternary carbons including a carboxylic acid function at δ_C 184.6 (C-19) and an olefinic carbon at δ_C 155.9 (C-16) suggesting **175** was a diterpene (Pacheco *et al.*, 2009). In the HMBC spectrum (Figure 3.64), long-range correlations could be observed between the olefinic protons H-17 and the carbons C-13, C-15 and C-16 and between the methine proton H-13 and the carbons C-8, C-12, C-15, C-16 and C-17. The ^{1}H and ^{13}C NMR data (Table 3.15) of **175** and the key correlations observed (Figure 3.64) were in good agreement with those published for *ent*-kaurenoic acid (Mitscher *et al.*, 1983; Viera *et al.*, 2002). Thus, compound **175** was identified as *ent*-kaurenoic acid, a kaurene diterpene with a range of biological activities including analgesic, antidiabetic, anti-inflammatory, antioxidant and neurological activities (Villa-Ruano *et al.*, 2016).

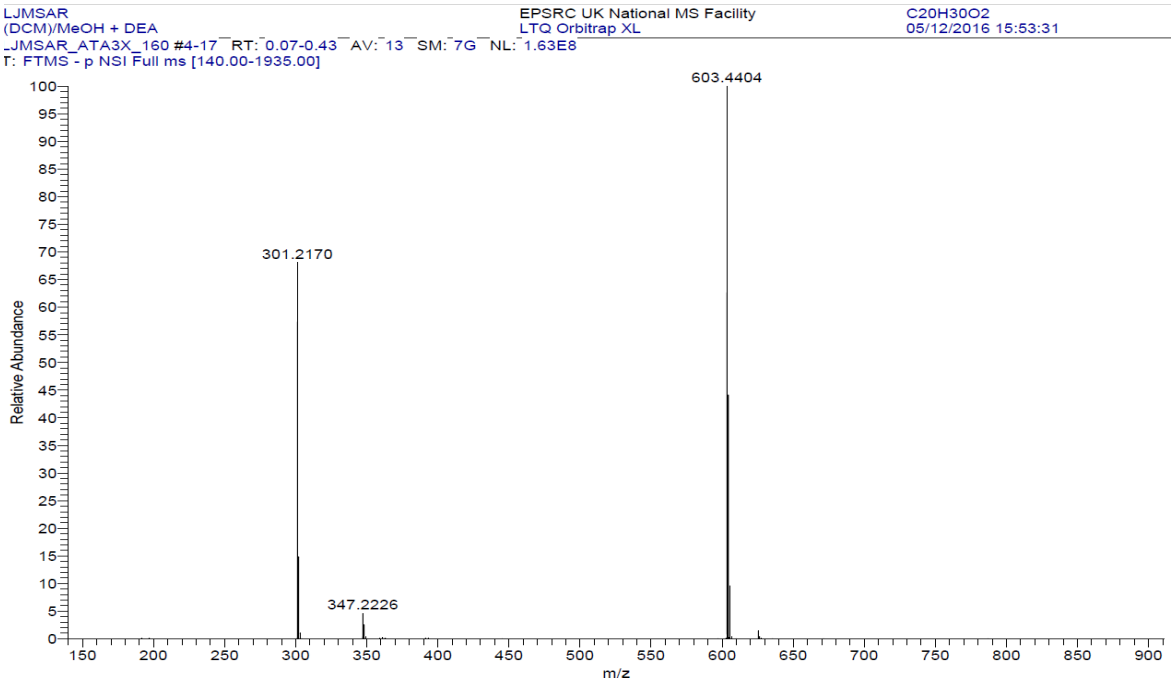

Figure 3.61 ESI-MS spectrum of **175**

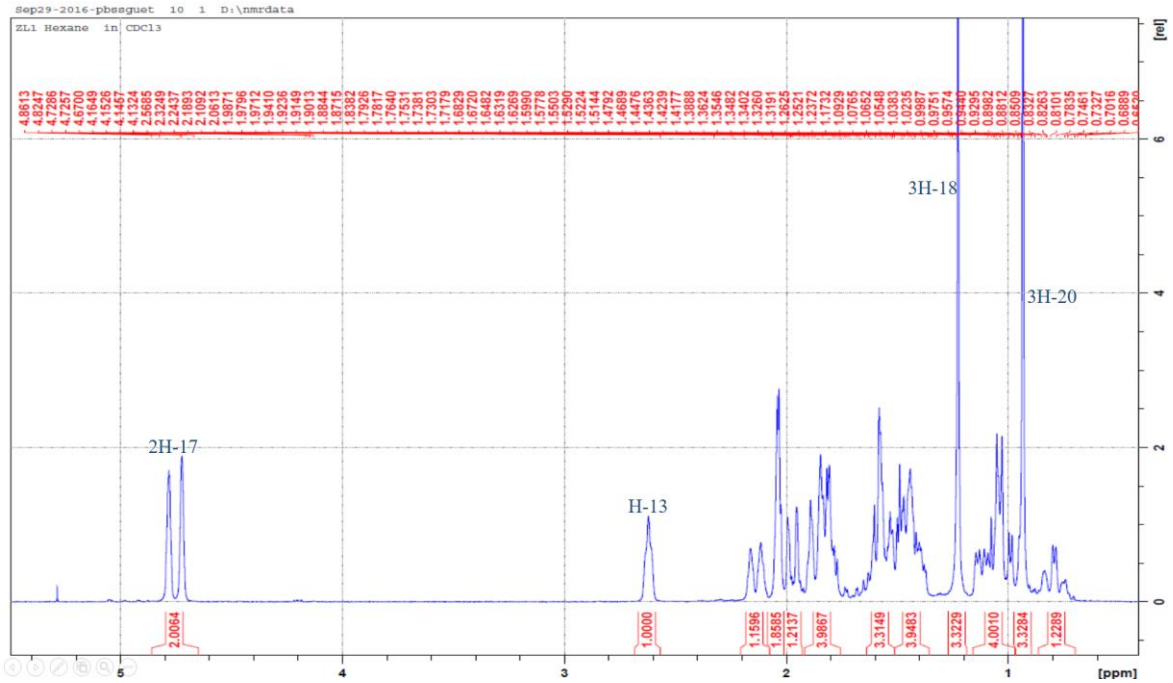

Figure 3.62 ^{1}H NMR (300 MHz, $CDCl_3$) of **175**

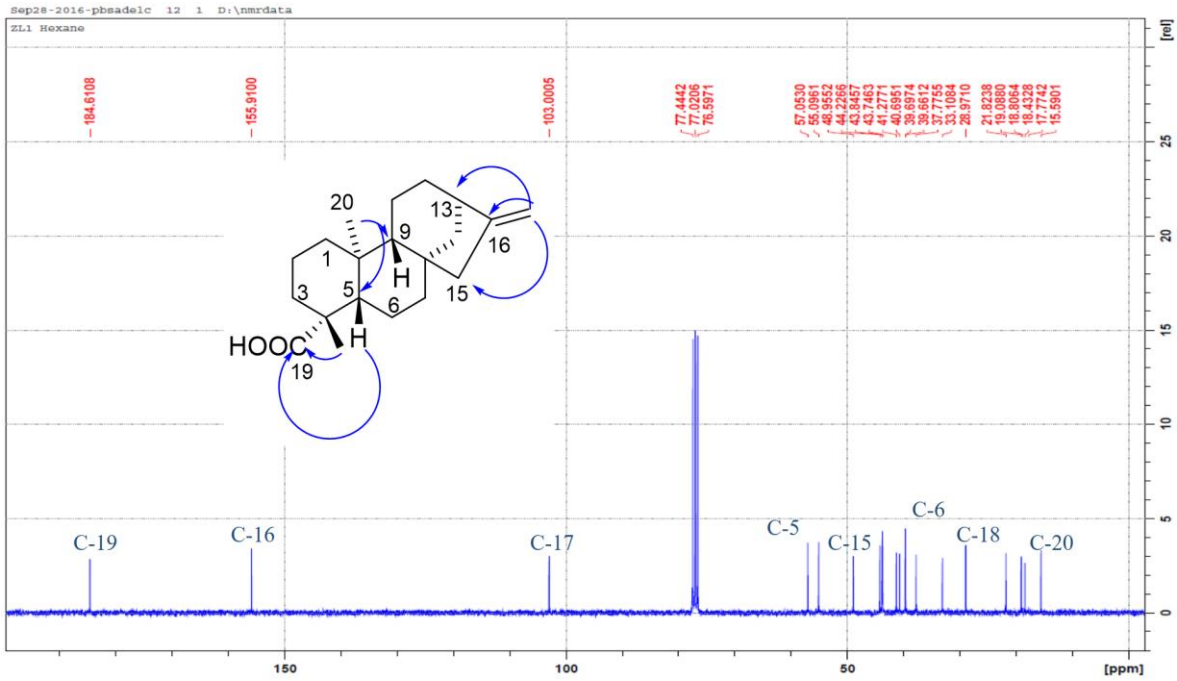

Figure 3.63 ^{13}C NMR (75 MHz, $CDCl_3$) and key HMBC correlations of **175**

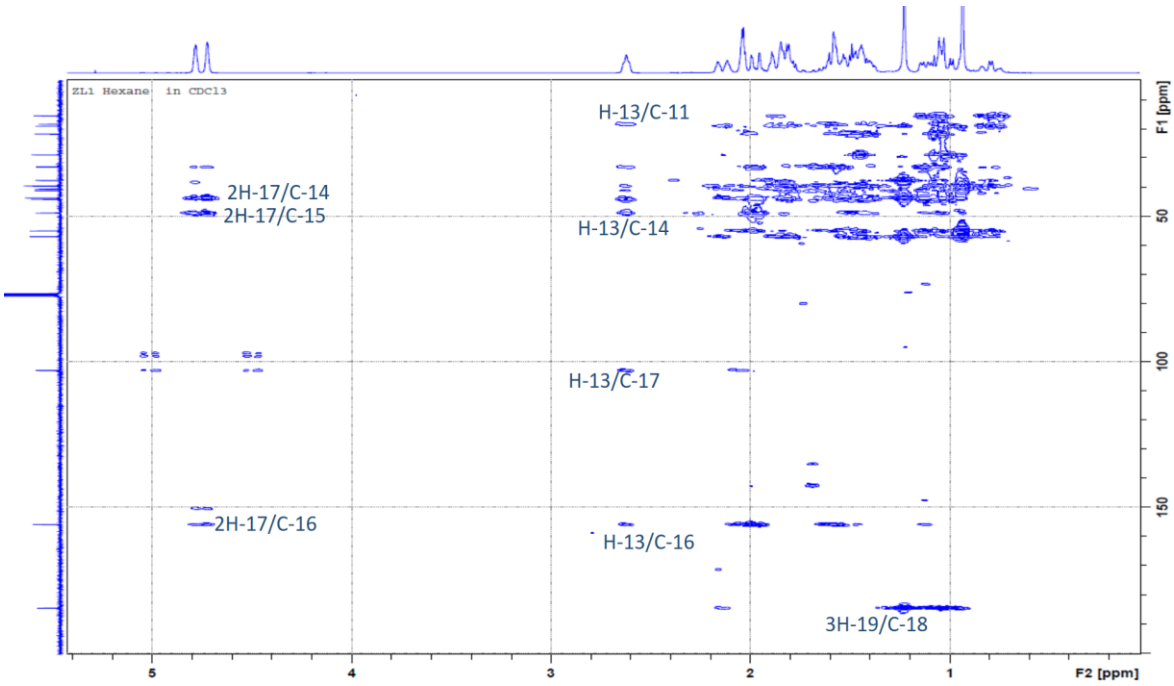

Figure 3.64 HMBC spectrum of **175**

3.3.4.2 Structure elucidation of xylopic acid (**176**)

Compound **176** was also isolated as white crystalline powder. Its molecular formula $C_{22}H_{32}O_4$ was determined from its HR ESI-MS spectrum by the peak at *m/z* 361.2375 $[M+H]^+$ calculated for $C_{22}H_{33}O_4$, 361.2379. Its ^{1}H NMR spectrum (Figure 3.65, Table 3.15) was similar to that of **175**. The only difference was the presence in the ^{1}H NMR spectrum of **176** of an additional methyl singlet at δ_H 2.26 suggesting the presence of an acetoxy function in the molecule, and an oxymethine at δ_H 5.16 (t, J = 2.5, 4.9 Hz). This was supported in the ^{13}C NMR spectrum (Figure 3.66, Table 3.15) by the peaks at δ_C 171.4 and 21.3 corresponding to the carbonyl and methyl of the acetoxy respectively and the oxymethine carbon at δ_C 81.6. In the HMBC spectrum (Figure 3.66), correlations observed between the olefinic methylene protons (H-17) and the carbons at δ_C 40.6 (C-13), 81.6 (C-15) and 153.7 (C-16) and between the oxymethine H-15 and the carbons at δ_C 45.9 (C-8), 106.1 (C-17), 153.7 (C-16) and 171.4 led to the fixation of the acetoxy

function on the carbon C-15 at δ_C 81.6. The orientation of the acetoxy function on C-15 was determined to be *β*-oriented using the NOESY experiment. All the ^{1}H and ^{13}C NMR data (Table 3.15) of **176** supported by the key HMBC correlations observed were in agreement with those published for *ent*-15*β*-acetoxy-kaur-16-en-19-oic acid or xylopic acid (Takahashi *et al.*, 2001). This was further confirmed in the MS spectrum of **176** by the peak at *m/z* 301.2245 which correspond to the loss of the acetoxy function $[M-OAc+H]^{+}$. Thus, compound **176** was identified as xylopic acid, a kaurene diterpene widespread in the *Xylopia* genus of the Annonaceae family (Takahashi *et al.*, 2001; Silva *et al.*, 2015).

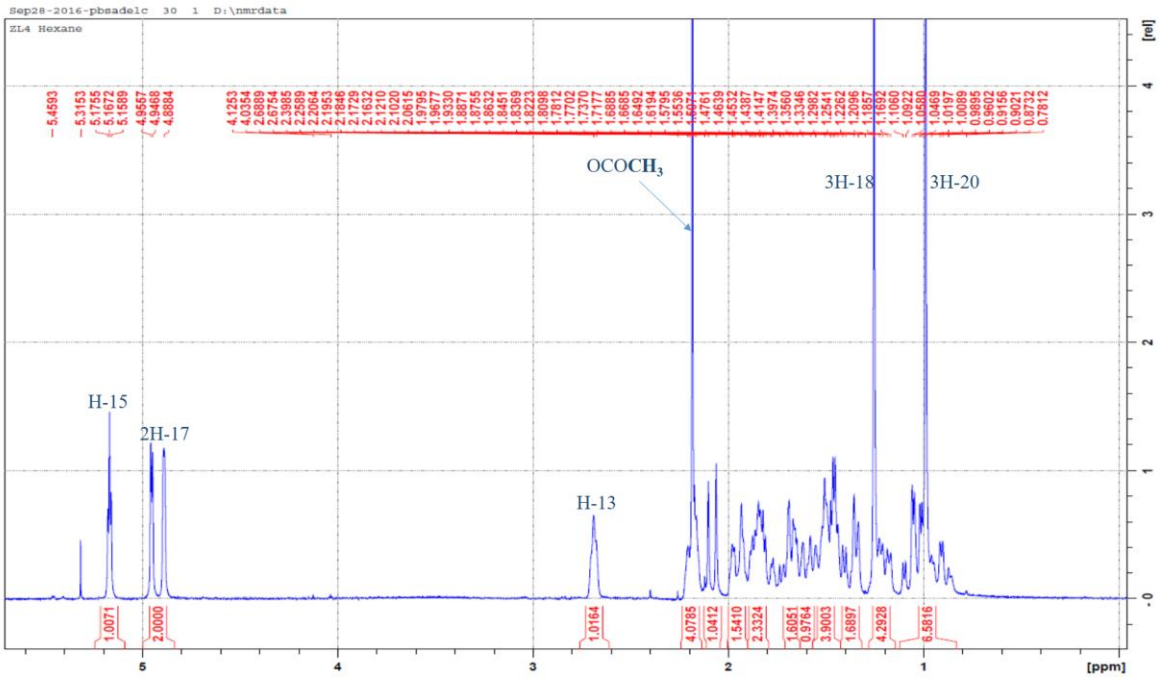

Figure 3.65 ^{1}H NMR (300 MHz, $CDCl_3$) of **176**

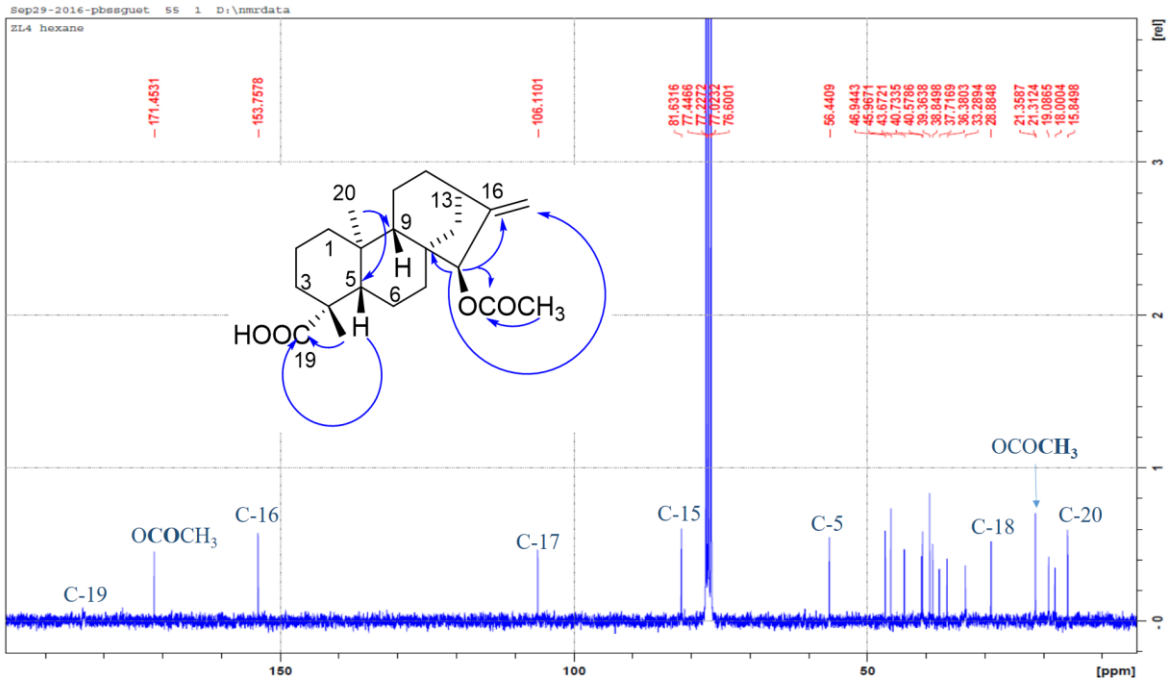

Figure 3.66 ^{13}C NMR (75 MHz, $CDCl_3$) and key HMBC correlations of **176**

3.3.4.3 Structure elucidation of *ent*-kauran-16*β*-ol-19-oic acid (**177**)

Compound **177** was isolated as a white granular powder. Its molecular formula $C_{20}H_{32}O_3$ was confirmed from its HR ESIMS spectrum obtained in negative ion mode by the peak at *m/z* 319.2273 $[M-H]^-$ calculated for $C_{20}H_{31}O_3$, 319.2279. Its ^{1}H NMR spectrum (Figure 3.67, Table 3.15) was similar to that of **175**. The only difference was the absence in the ^{1}H NMR spectrum of **177** of the olefinic methylene protons suggesting an oxidation, and the presence of an additional tertiary methyl singlet at δ_H 1.46. This was supported in its ^{13}C NMR spectrum (Figure 3.68, Table 3.15) by the absence of the olefinic carbons and the presence of a quaternary oxygenated carbon at δ_C 78.5 and a methyl at δ_C 23.2 which show in the HSQC spectrum cross peak correlation with the proton at δ_H 1.46. In the HMBC spectrum (Figure 3.68), long-range correlations could be observed between the methyl signal at δ_H 1.46 (H-17) and the carbons at δ_C 48.8 (C-13), 58.0 (C-15) and 78.5 (C-16) and between the methine proton at δ_H 1.76 (H-13) and the carbons δ_C 78.5 (C-16),

58.0 (C-15), 45.4 (C-8), 26.2 (C-12) and 23.2 (C-17). The orientation of the hydroxy function on C-16 was determined to be *β*-oriented using the NOESY experiment. All the ^{1}H and ^{13}C NMR data (Table 3.15) of **177** supported by the key HMBC correlations observed were in good agreement with those published for *ent*-16*β*-hydroxykauran-19-oic acid (Takahashi *et al.,* 1995). Thus, compound **177** was identified as *ent*-16*β*-hydroxykauran-19-oic acid, previously isolated from *Xylopia frutescens* (Takahashi *et al.,* 1995).

3.3.4.4 Structure elucidation of *ent*-kauran-16*β*-ol (**179**)

Compound **179** was isolated as white powder. Its molecular formula $C_{20}H_{35}O$ was determined from its HR ESI-MS spectrum obtained in positive ion mode by the peak at *m/z* 290.2843 $[M-H_2O+NH_4]^+$ calculated for $C_{20}H_{32}NH_4$, 290.2848. Its ^{1}H NMR spectrum (Figure 3.69, Table 3.15) was similar to that of **177**. The only difference was the presence of an additional tertiary methyl singlet at δ_H 0.78 in the ^{1}H NMR spectrum of **179**. In its ^{13}C NMR spectrum (Figure 3.70, Table 3.15), the presence of an additional methyl signal at δ_C 21.5 and the absence of the carboxylic acid carbon were clearly visible. In the HMBC spectrum (Figure 3.70), long-range correlations could be observed between the methyl signal at δ_H 0.78 (H-19) and the carbons at δ_C 18.6 (C-2), 33.2 (C-4), 33.6 (C-18), 42.0 (C-3) and 56.2 (C-5). All the ^{1}H and ^{13}C NMR data (Table 3.15) of **179,** supported by its key HMBC correlations, were in agreement with those published for *ent*-kauran-16*β*-ol (Morris *et al.,* 2005). This was further confirmed in the MS spectrum of **179** by the peak at *m/z* 273.2578 $[M-H_2O+H]^+$ arising from the loss of a water molecule due to the dehydration of the tertiary alcohol function. Thus, compound **179** was identified as *ent*-kauran-16*β*-ol, a kaurane diterpene previously isolated from sunflowers (Morris *et al.,* 2005).

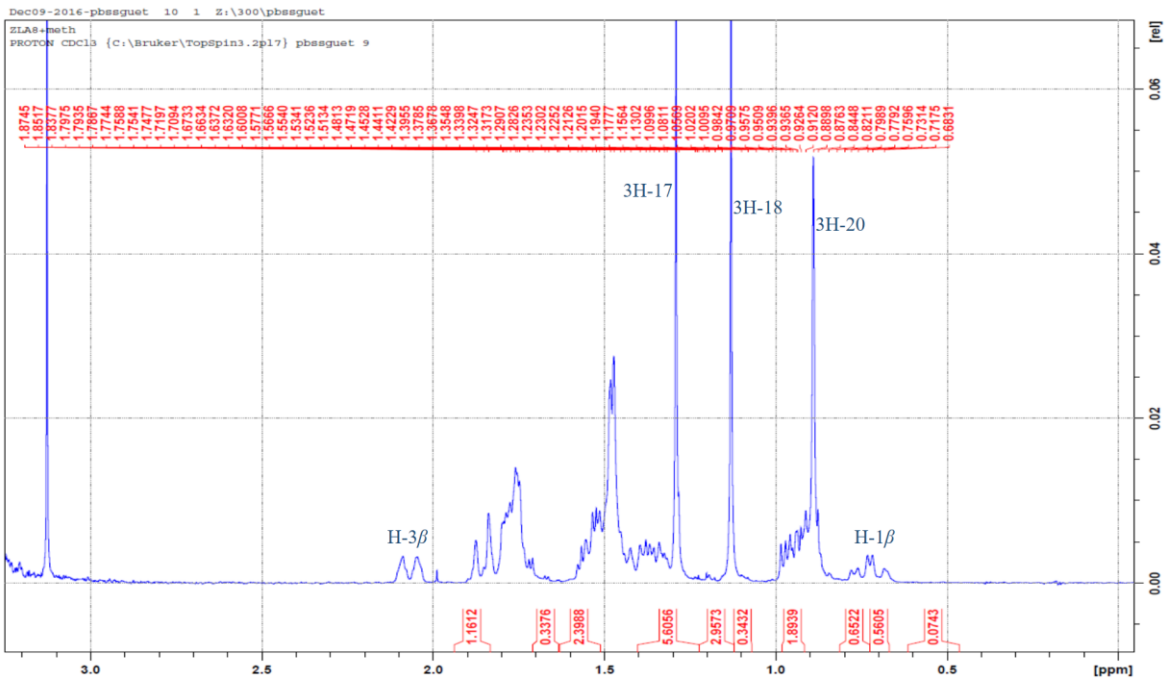

Figure 3.67 ^{1}H NMR (300 MHz, $CDCl_3$+ drops MeOH) of **177**

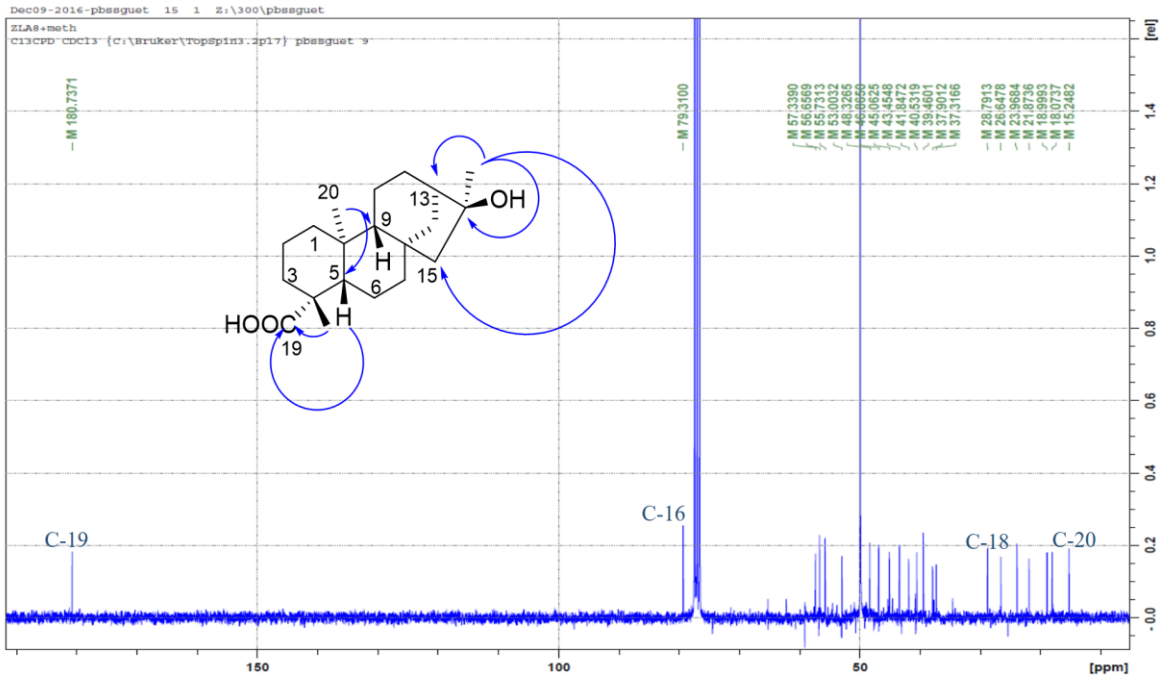

Figure 3.68 ^{13}C NMR (75 MHz, $CDCl_3$+ drops MeOH) and key HMBC correlations of **177**

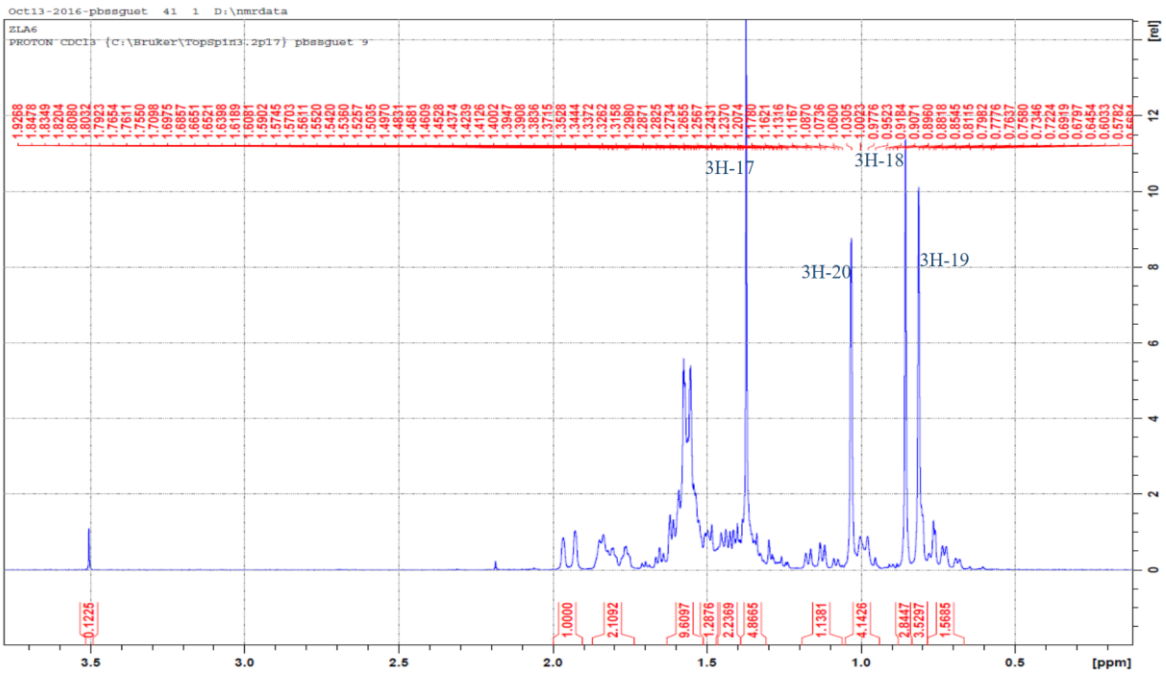

Figure 3.69 ^{1}H NMR (300 MHz, $CDCl_3$) of **179**

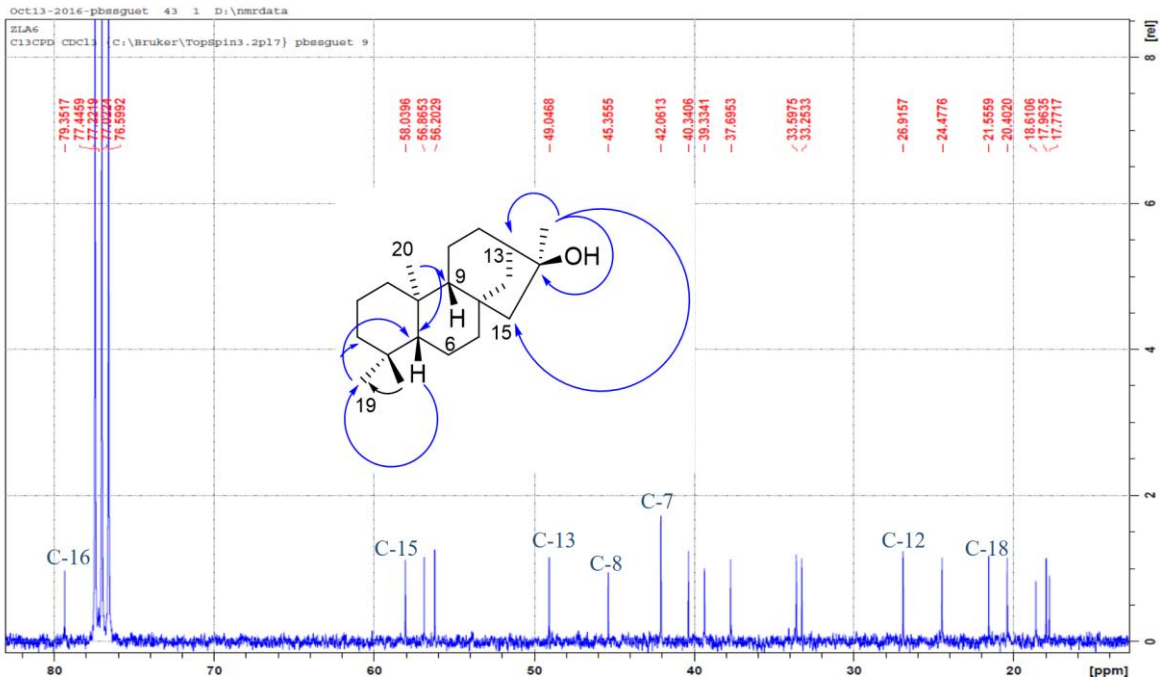

Figure 3.70 ^{13}C NMR (75 MHz, $CDCl_3$) and key HMBC correlations of **179**

Table 3.15 ^{1}H NMR ($CDCl_3$, 300 MHz) and ^{13}C NMR ($CDCl_3$, 75 MHz) data of **175-179**

Position	δ_H m (*J* in Hz)					δ_C				
	175	**176**	**177[a]**	**178[b]**	**179**	**175**	**176**	**177[a]**	**178[b]**	**179**
1	0.75 ddd (*13.0, 12.9, 5.5*)	0.91 ddd (*13.1, 8.8, 6.2*)	0.69 ddd (*15.0, 12.0, 3.0*)	0.84 ddd (*17.0, 13.6, 4.1*)	0.67 m	40.7	40.7	40.5	39.7	40.3
	1.76 m	1.97 m	1.76 m	1.86 m	1.76 m					
2	1.32 m	1.49 m	1.35 m	1.48 m	1.40 m	19.1	19.0	18.9	18.3	18.6
	1.79 m	1.93 m	1.83 m	1.66 m	1.63 m					
3	0.94 m	1.08 m	0.96 m	1.05 m	1.08 m	37.8	38.8	37.3	34.2	42.0
	2.06 dm	2.18 m	2.08 dm	2.16 dm	1.46 m					
4						43.8	43.6	48.3	48.4	33.2
5	1.03 m	1.04 m	0.96 m	1.17 dd (*2.5, 2.1*)	0.97 m	57.0	56.4	56.6	56.6	56.2
6	1.71 m	1.87 m	1.76 m	1.72 m	1.28 m	21.8	21.3	21.8	20.0	20.4
		2.26 m		1.91 m	1.59 m					
7	1.40 m	1.50 m	1.39 m	1.52 d (*3.8*)	1.31 m	41.3	39.9	43.4	41.9	42.0
			1.46 m	1.72 m	1.65 m					
8						44.2	45.9	45.0	45.1	45.3
9	0.97 m	1.35 m	0.93 m	1.05 m	0.75 m	55.1	46.9	55.7	55.4	56.8
10						39.6	36.3	39.4	39.3	39.3
11	1.43 m	1.55 m	1.46 m	1.60 m	1.57 m	18.4	18.0	18.0	18.0	17.9
		1.66 m								

Table 3.15 *continued*

Position			δ_H m (*J* in Hz)					δ_C		
	175	**176**	**177[a]**	**178[b]**	**179**	**175**	**176**	**177[a]**	**178[b]**	**179**
12	1.38 m	1.61 m	1.46 m	1.53 m	1.61 m	33.1	33.2	26.6	26.6	26.9
	1.47 m	1.73 m		1.62 m						
13	2.56 bs	2.68 bm	1.76 m	1.88 m	1.84 m	43.7	40.6	48.3	48.8	49.0
14	1.09 m	1.29 m	1.46 m	1.64 m	1.61 m	39.7	37.7	37.9	37.7	37.6
	1.90 d (*3.7*)	2.16 d (*3.5*)	1.83 m	1.94 m	1.93 m					
15	1.98 bs	5.16 t (2.5, 4.9)	1.46 bs	1.60 bs	1.55 bs	48.9	81.6	57.3	57.6	58.0
16						155.9	153.7	79.3	79.3	79.3
17	4.67 s	4.88 bs	1.12 s	1.39 s	1.38 s	103.0	106.1	23.9	24.5	24.4
	4.72 s	4.94 d (*2.6*)								
18	1.25 s	1.33 s	0.93 s	1.05 s	0.83 s	28.9	28.8	28.7	24.2	33.6
19	-	-	-	9.75 d (*1.4*)	0.78 s	184.6	184.2	180.7	205.9	21.5
20	0.93 s	1.01 s	0.69 s	0.89 s	1.03 s	15.6	15.8	15.2	16.4	17.7
CH_3CO		2.26 s					21.3			
CH_3CO							171.4			

[a] recorded in $CDCl_3$+drops of MeOH; [b] recorded at 600 MHz for ^1H and 150 MHz for ^{13}C

3.3.4.5 Structure elucidation of dulcisflavan (**180**)

Compound **180** was isolated as a brown amorphous powder. Its molecular formula $C_{15}H_{14}O_8$ was determined from its ESI-MS spectrum obtained in positive ion mode, where the sodiated ion peak was observedat *m/z* 345 $[M+Na]^+$. Its ^1H NMR spectrum (Figure 3.71, Table 3.16) revealed the presence of three aromatic protons at δ_H 6.77 (d, *J* = 8.1 Hz), 6.81 (dd, *J* = 1.6, 8.1 Hz) and 6.99 (d, *J* = 1.6 Hz) members of a 1,3,4-trisubstituted benzene as well as two oxygenated methines at δ_H 4.19 and 4.83 and a set of methylene protons at δ_H 2.75 (dd, *J* = 2.8, 16.5 Hz) and 2.88 (dd, *J* = 4.5, 16.5 Hz). The ^{13}C NMR spectrum (Figure 3.72, Table 3.16) of **180** depicted thirteen peaks which could be assigned based on the correlation observed in the HSQC and HMBC spectra (Figures 3.73-3.74) to one methylene, five methines and nine quaternary carbons. In the HMBC spectrum (Figure 3.72), correlations could be observed between the methylene protons (H-4) and the carbons at δ_C 67.5 (C-3), 79.8 (C-2), 100.2 (C-10) and 157.6 (C-5) and between the oxymethine at δ_H 4.83 (H-2) and the carbons at δ_C 29.3 (C-4), 67.5 (C-3), 115.3 (C-2'), 119.5 (C-6'), 132.5 (C-1') and 157.3 (C-9). The ^1H and ^{13}C NMR data (Table 16) of **180** were in good agreement with those published for dulcisflavan (Deachathai *et al.*, 2005). Thus, compound **180** was identified as dulcisflavan, a flavan with antioxidant activity previously isolated from the fruit of *Garcinia dulcis* (Deachathai *et al.*, 2005).

3.3.4.6 Structure elucidation of icariside D2 (**182**)

Compound **182** was isolated as a dark brown amorphous powder. Its molecular formula $C_{15}H_{14}O_8$ was determined from its pseudomolecular ion peak at *m/z* 345 $[M+Na]^+$ in the ESI-MS spectrum obtained in positive ion mode Its ^1H NMR spectrum (Figure 3.75,

Table 3.17) suggested a glycosylated compound bearing a sugar moiety by the presence of an anomeric proton at δ_H 4.90 (d, *J* = 7.5 Hz). Four aromatic protons forming an A_2B_2 system at δ_H 7.18 (d, *J* = 8.7 Hz) and 7.06 (d, *J* = 8.7 Hz) suggesting a 1,4-disubstituted benzene, five oxygenated methines as well as three methylenes including two oxygenated ones at δ_H 4.69 (t, *J* = 7.0 Hz) and 3.90 (dd, *J* = 2.2, 12.1 Hz) and 3.71 (dd, *J* = 5.5, 12.1 Hz) were also observed. In the COSY spectrum, a chain of correlation from the anomeric proton at δ_H 4.90 to the methylenes at δ_H 3.90 and 3.71 led to the identification of the sugar moiety as *β*-D-glucoside. Their corresponding carbons were determined by analysis of the ^{13}C (Figure 3.76, Table 3.17) and HSQC-DEPT spectra. The obtained NMR data of the sugar moiety (Table 3.17) were consistent with those published for *β*-D-glucopyranoside (Agrawal, 1992). In the HMBC spectrum (Figure 3.76), correlations could be observed between the anomeric proton at δ_H 4.90 (H-1') and the carbon at δ_C 158.3 (C-4), 78.1 (C-5'), 78.0 (C-3') and 71.4 (C-10) and between the methylene at δ_H 3.24 (t, *J*=7.0 Hz) and the carbons at δ_C 131.7 (C-1), 130.7 (C-2, C-6) and 77.5 (C-*β*). All the ^1H and ^{13}C NMR data (Table 3.17) of **182** supported by the observed key HMBC correlations, were comparable with those published for 4-(2-hydroxyethyl)phenyl-*β*-D-glucopyranoside or icariside D2 (Miyase *et al.,* 1989). Thus, compound **182** was identified as icariside D2, a lignan glycoside with cytotoxic properties first isolated from *Epimedium diphyllum* (Berberidaceae) (Miyase *et al.,* 1989; Hien *et al.,* 2015).

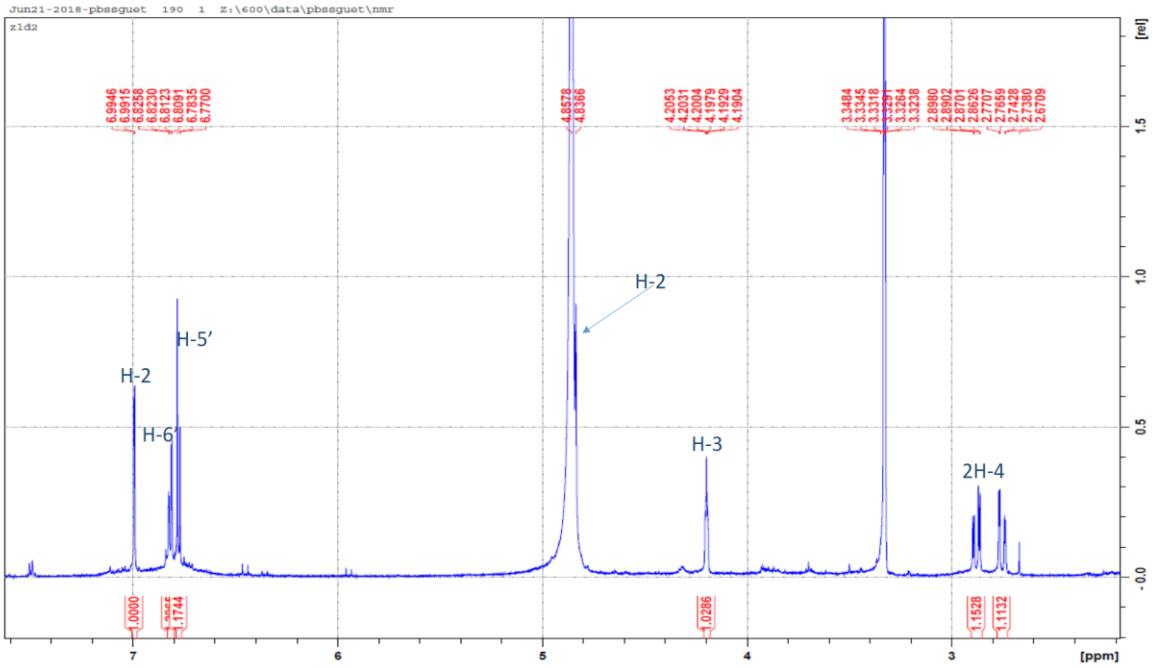

Figure 3.71 ^{1}H NMR (300 MHz, CD_3OD) of **180**

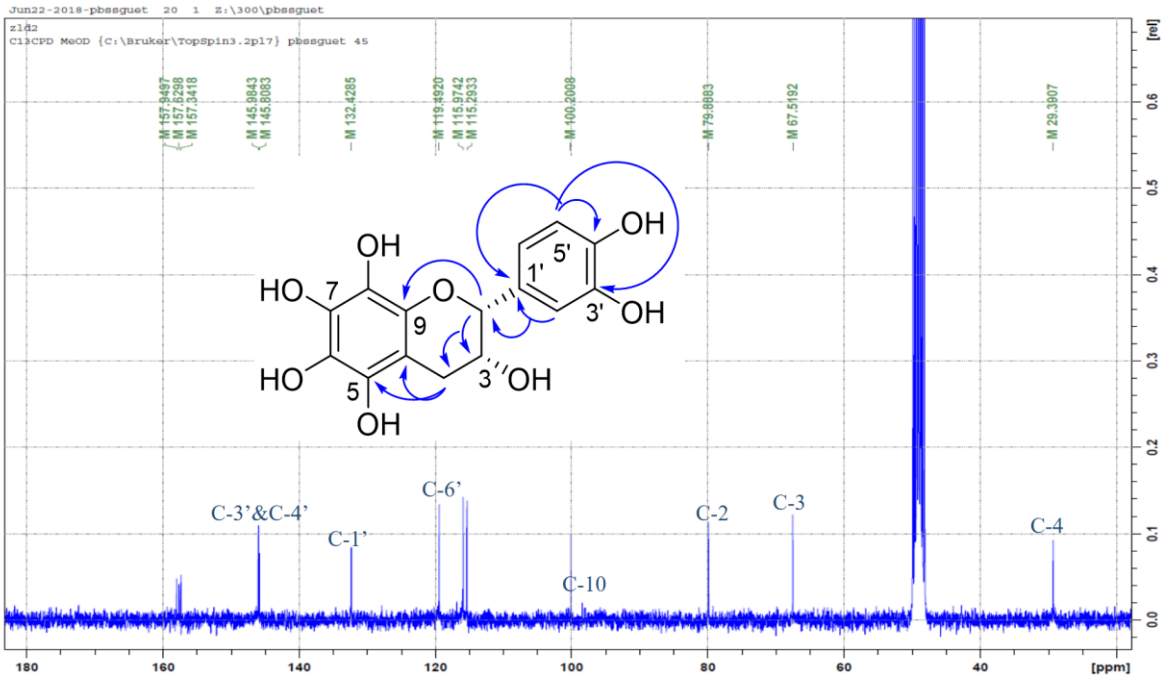

Figure 3.72 ^{13}C NMR (75 MHz, CD_3OD) and key HMBC correlations of **180**

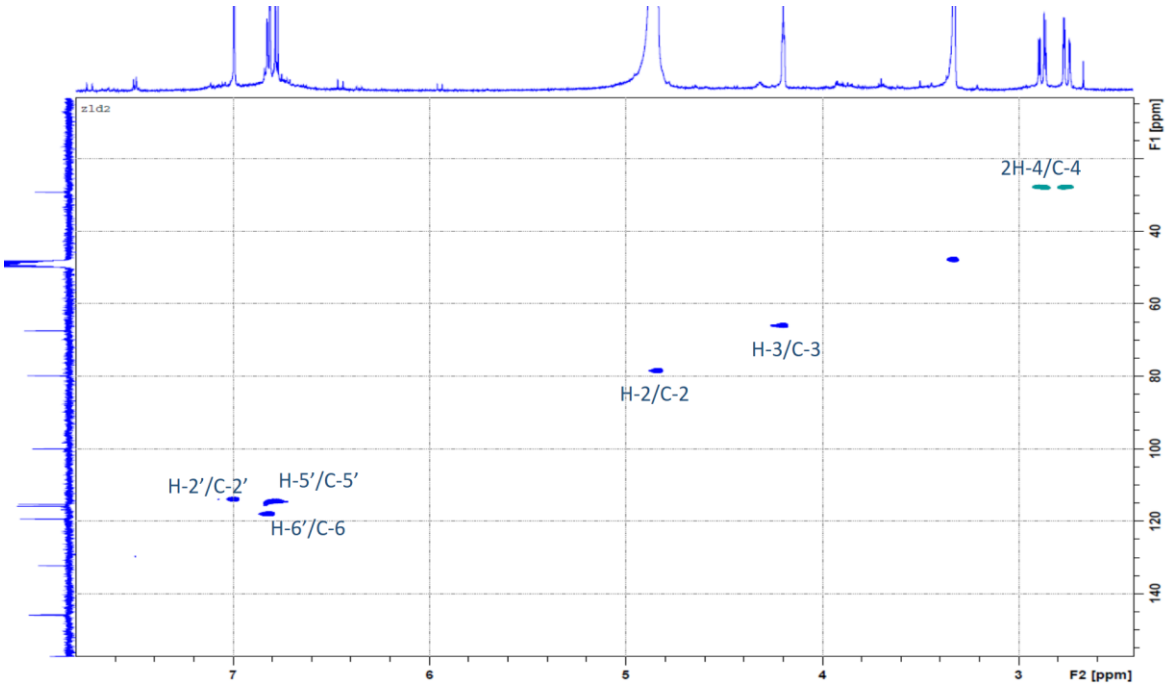

Figure 3.73 HSQC spectrum of **180**

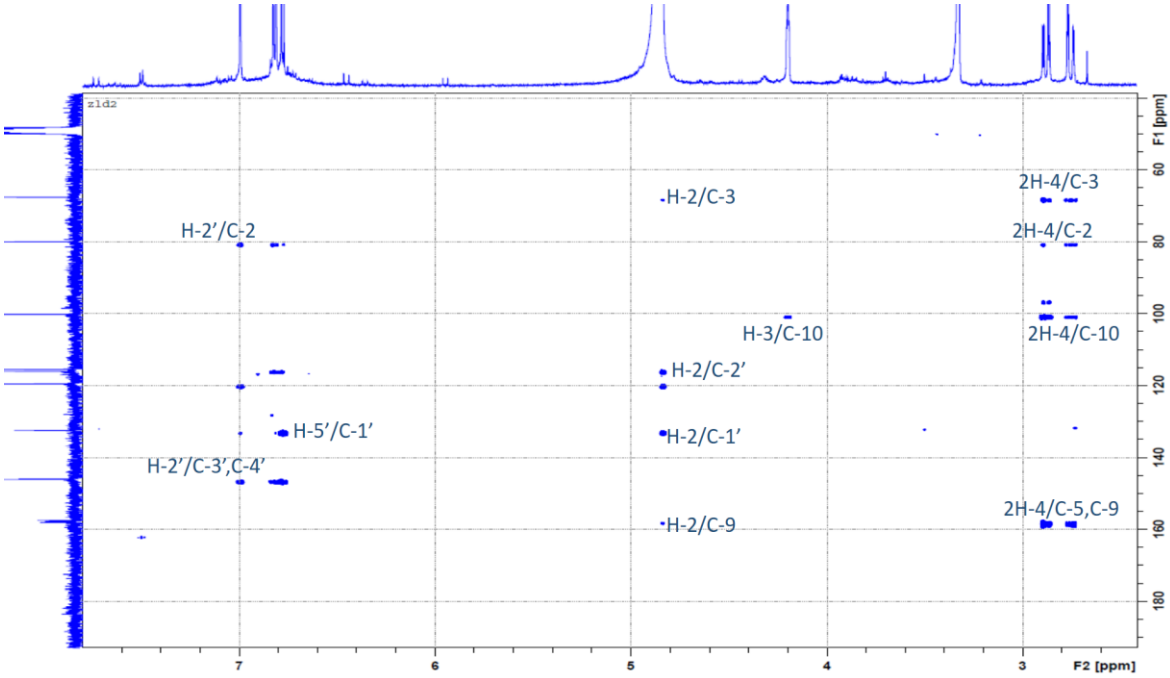

Figure 3.74 HMBC spectrum of **180**

Table 3.16 ^{1}H (600 MHz, CD_3OD) and ^{13}C NMR (75 MHz, CD_3OD) data of **180**

Position	δ_H m (*J* in Hz)	δ_C	Position	δ_H m (*J* in Hz)	δ_C
1	-	-	9	-	157.3
2	4.86 ov	79.8	10	-	100.2
3	4.19 m	67.5	1’	-	132.4
4	2.75 dd (*2.8*, *16.5*)	29.3	2’	6.99 d (*1.6*)	115.3
	2.88 dd (*4.5*, *16.5*)		3’	-	145.8
5	-	157.3	4’		145.9
6	-	132.4	5’	6.77 d (*8.1*)	115.9
7	-	157.6	6’	6.81 dd (*1.6*, *8.1*)	119.5
8	-	157.9			

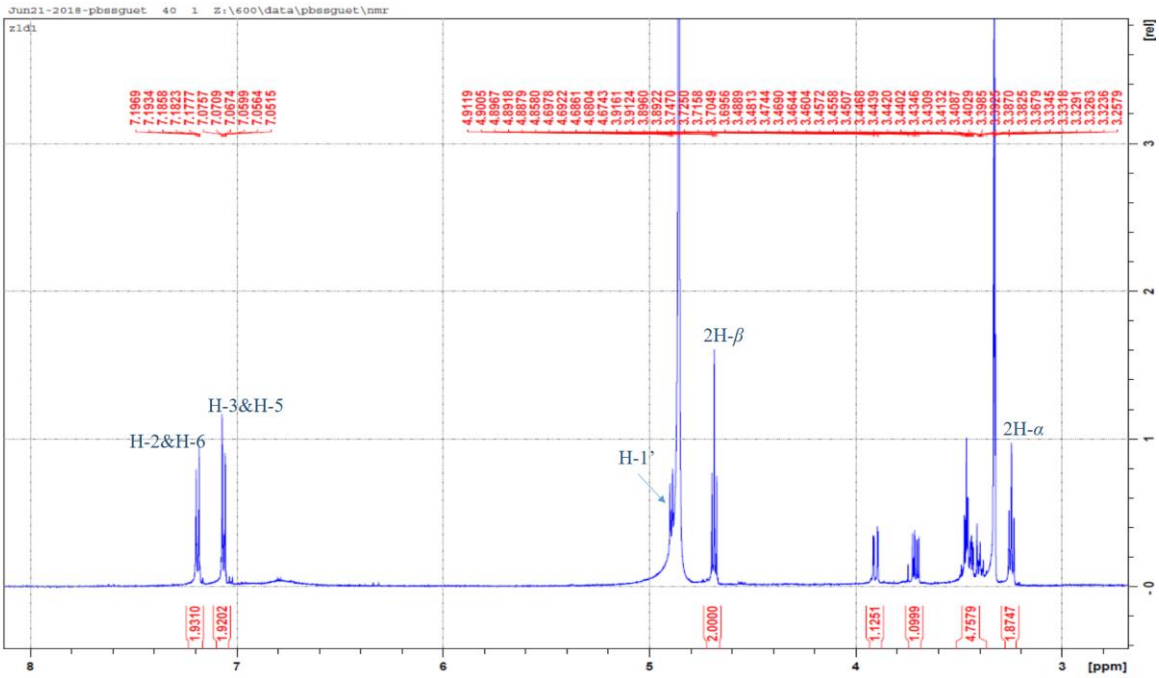

Figure 3.75 ^{1}H NMR (600 MHz, CD_3OD) of **182**

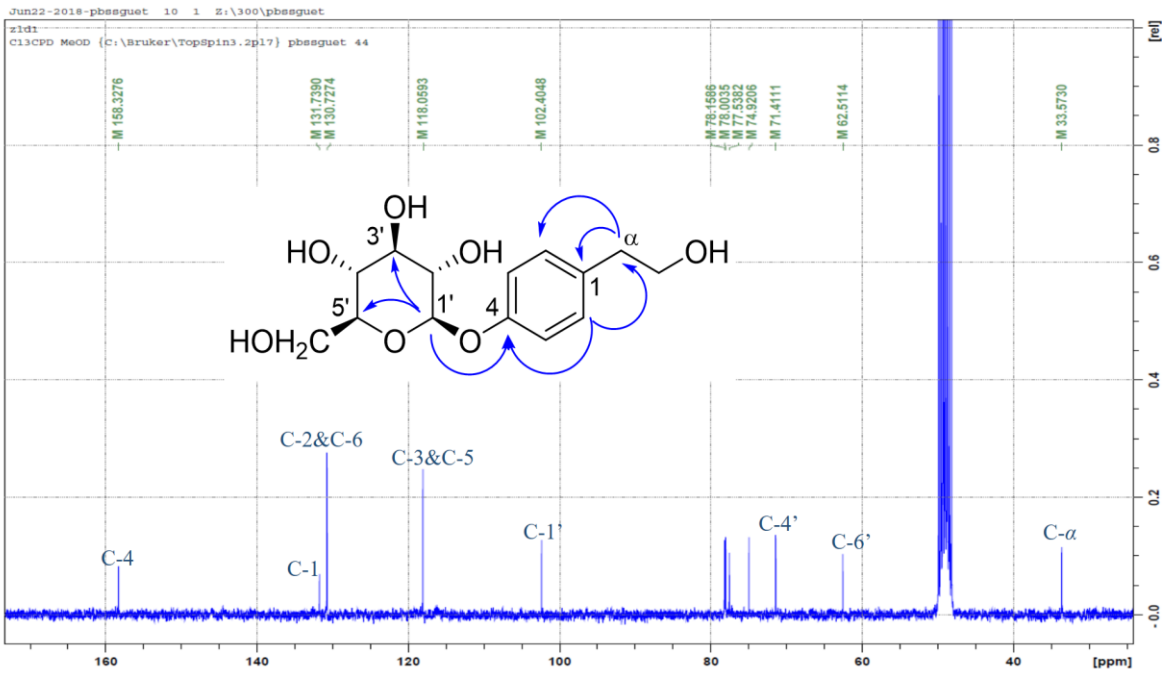

Figure 3.76 ^{13}C NMR (75 MHz, CD_3OD) and key HMBC correlations of **182**

Table 3.17 ^{1}H (600 MHz, CD_3OD) and ^{13}C NMR (75 MHz, CD_3OD) data of **182**

Position	δ_H m (*J* in Hz)	δ_C	Position	δ_H m (*J* in Hz)	δ_C
1		131.7	3’	3.47 ov	78.0
2	7.18 d (*8.7*)	130.7	4’	3.40 ov	71.4
3	7.06 d (*8.7*)	118.0	5’	3.44 ov	78.1
4		158.3	6’	3.71 dd (*2.2*, *12.1*)	62.5
5	7.06 d (*8.7*)	118.0		3.90 dd (*5.5*, *12.1*)	
6	7.18 d (*8.7*)	130.7	C-*α*	3.24 t (*7.0*)	33.5
1’	4.90 d (*7.5*)	102.4	C-*β*	4.69 t (*7.0*)	77.5
2’	3.46 ov	74.9			

3.3.5 Phytochemistry of *Zanthoxylum zanthoxyloides*

Preparative RP-HPLC and TLC analyses of the DCM and MeOH extracts of the fruits *Z. xanthoxyloides* afforded fourteen compounds including eight quinoline alkaloids, skimmianine (**55**), atanine (**128**), *N*-methylplatydesminium cation (**183**), isoplatydesmine (**184**), myrtopsine (**185**), ribalinine (**186**) and *N*-methylatanine (**187**); five alkamides, *trans*-fagaramide (**79**), zanthoamides G-I (**188-190**) and; a lignan, sesamin (**54**); and two flavanones, hesperidin (**59**) and hesperetin (**191**) (Figure 3.77). Compounds **188-190** are new alkamides, whilst compounds **183-187** are here reported for the first time from *Z. zanthoxyloides*.

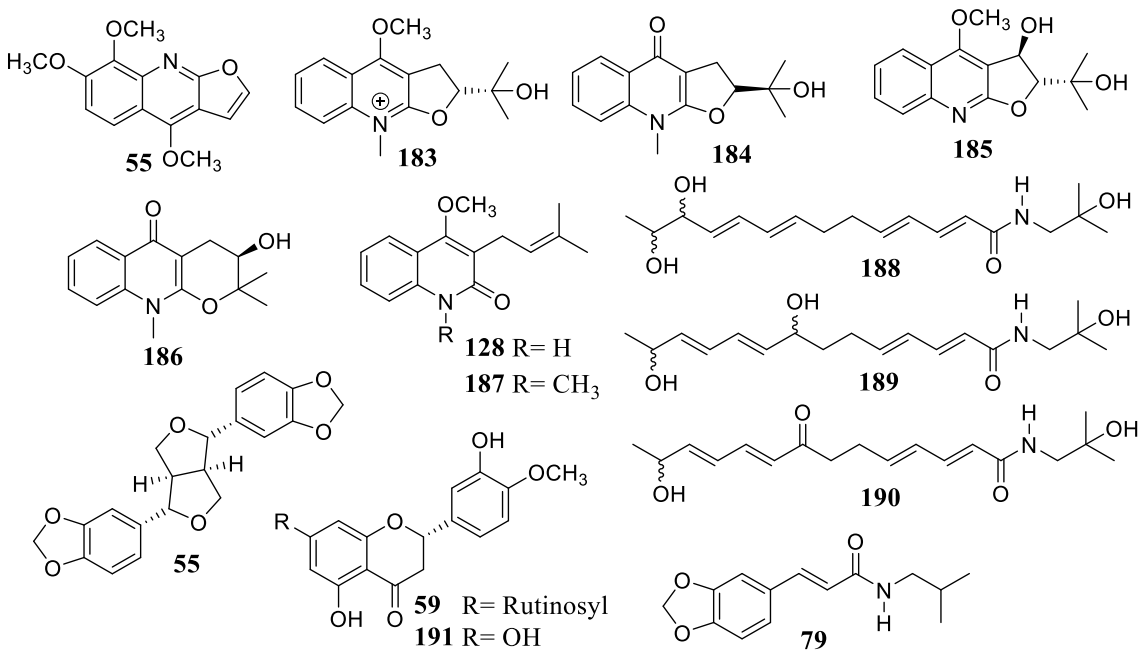

Figure 3.77 Structures of isolated compounds from the fruits of *Z. zanthoxyloides*

3.3.5.1 Structure elucidation of skimmianine (**55**)

Compound **55** was isolated as white needles. Its molecular formula $C_{14}H_{13}NO_4$ was determined from its HR ESI-MS spectrum (Figure 3.78) obtained in positive ion mode,

where the *pseudo*molecular ion peak was observed at *m/z* 260.0919 $[M+H]^+$ calculated for $C_{14}H_{13}NO_4H$, 260.0917. Its ^1H NMR spectrum (Figure 3.79, Table 3.18) showed characteristic signals of three methoxy groups at δ_H 3.89 (OCH_3-8), 4.02 (OCH_3-7) and 4.49 (OCH_3-4) and four aromatic methines at δ_H 7.28 (d, *J* = 2.6 Hz, H-1'), 7.36 (d, *J* = 9.4 Hz, H-6), 7.75 (d, *J* = 2.6 Hz, H-2') and 8.05 (d, *J* = 9.4 Hz, H-5). Its ^{13}C NMR (Figure 3.80, Table 3.18) revealed 14 signals attributable to three methoxy, four methines and seven quaternary carbons including the deshielded signal at δ_C 164.6 suggesting the presence of an amide in the molecule. Analysis of the different correlations present in the HMBC spectrum (Figure 3.80) revealed the core structure of the molecule to be quinoline alkaloid. The ^1H and ^{13}C NMR data (Table 3.18) of **55** were in good agreement with those published for skimmianine (Chakravarty *et al.*, 1999). Thus, compound **55** was identified as skimmianine, a common quinoline alkaloids in the Rutaceae family (Adamska-Szewczyk *et al.*, 2016).

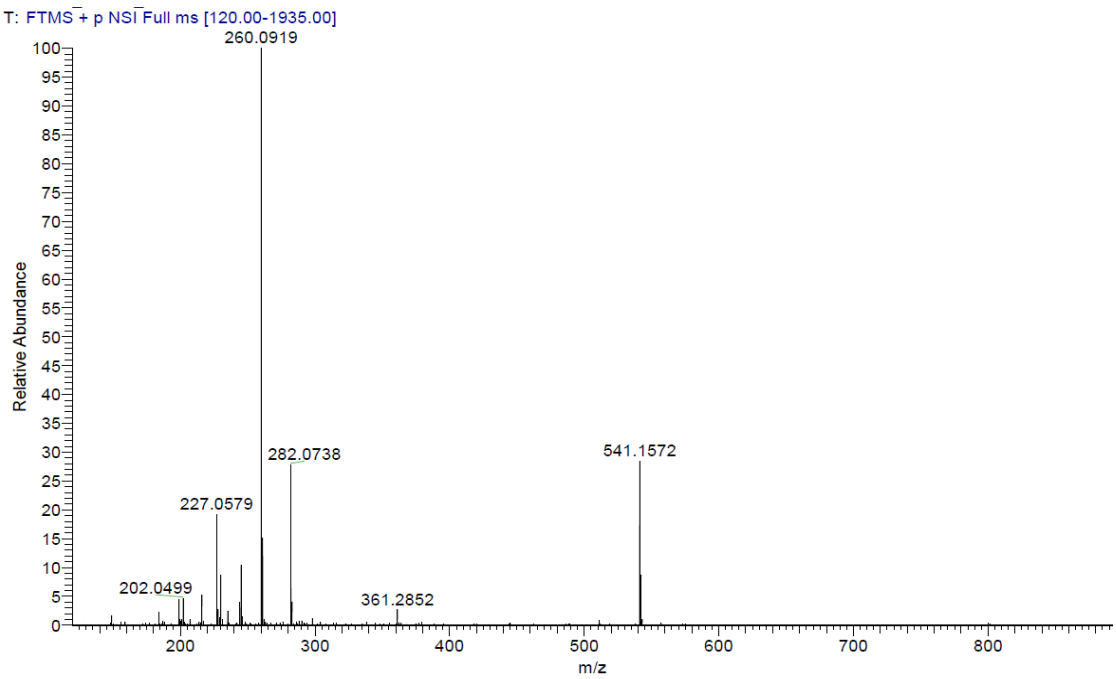

Figure 3.78 ESI-MS spectrum of **55**

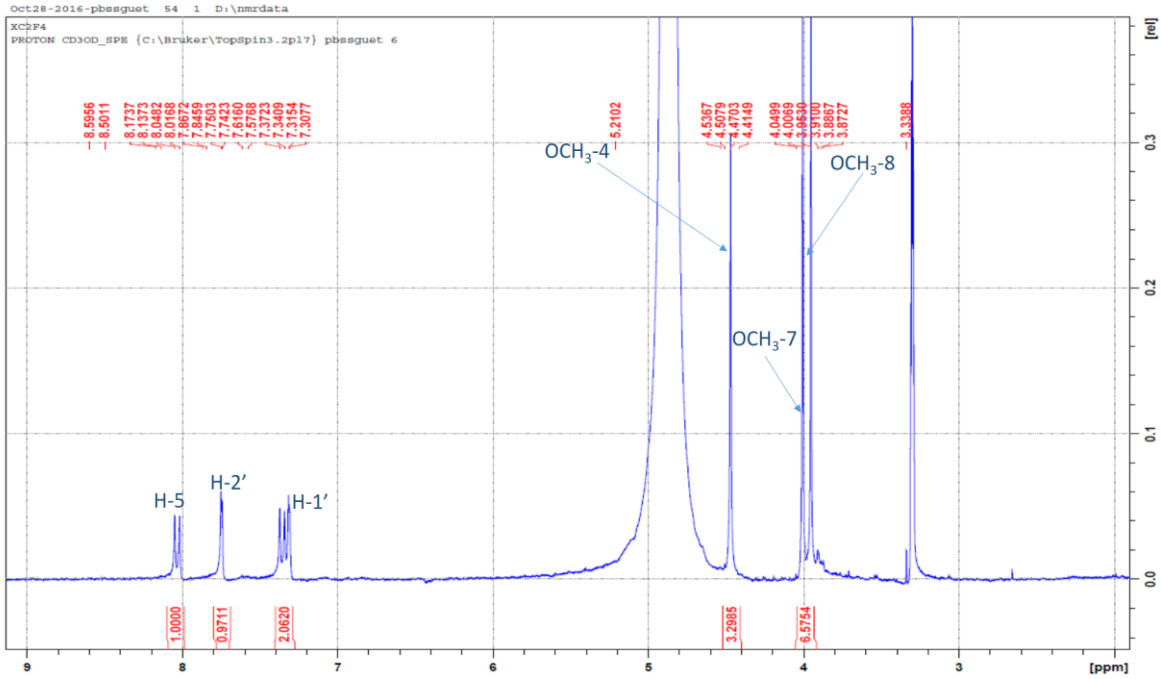

Figure 3.79 ^{1}H NMR (300 MHz, CD_3OD) of **55**

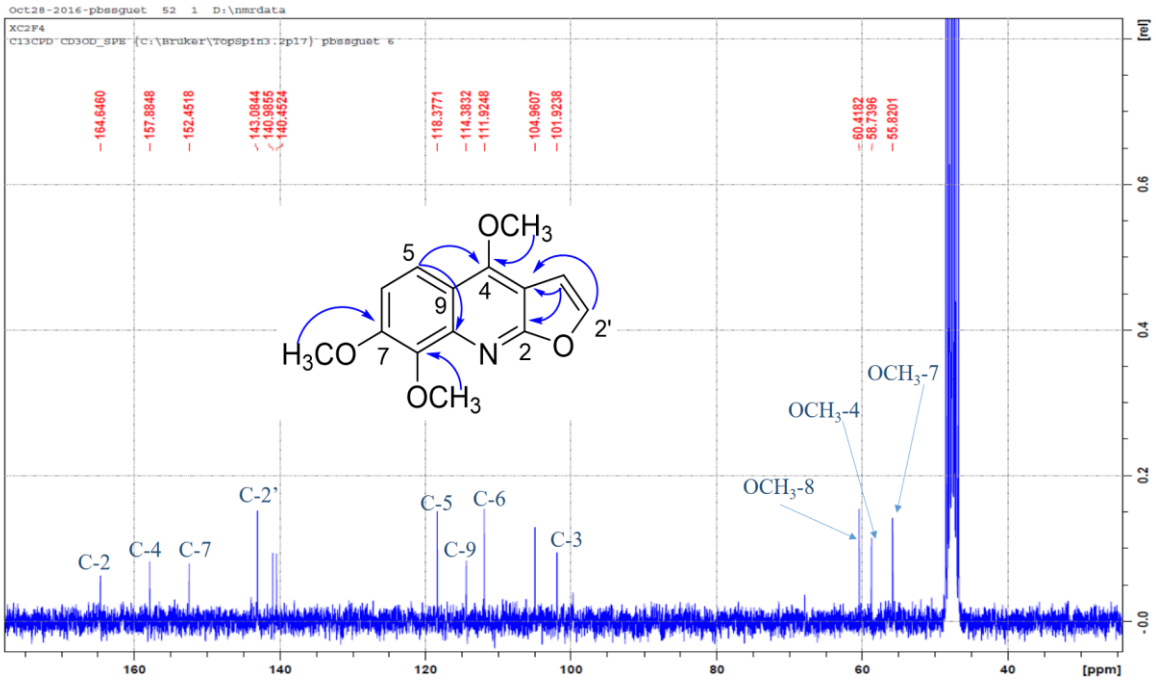

Figure 3.80 ^{13}C NMR (75 MHz, CD_3OD) and key HMBC correlations of **55**

3.3.5.2 Structure elucidation of *N*-methylplatydesminium cation (**183**)

Compound **183** was isolated as a dark yellow amorphous powder. Its molecular formula $C_{16}H_{20}NO_3$ was determined from its HR ESI-MS spectrum by the peak at *m/z* 274.1440 $[M]^+$ calculated for $C_{16}H_{20}NO_3$, 274.1438. Its ^{1}H NMR spectrum (Figure 3.81, Table 3.18) showed characteristic signals of an *ortho*-disubstituted benzene ring at δ_H 8.32 (d, *J* = 9.0 Hz), 8.03 (ov), 7.96 (ov) and 7.71 (td, *J* = 6.0, 9.0 Hz). Four methyl singlets including two deshielded methyls at δ_H 4.11 and 4.53; a methylene at δ_H 3.97 (dd, *J* = 6.0, 15.0 Hz) and an oxymethine at δ_H (dd, *J* = 6.0, 15.0 Hz) were also observed. Analysis of its ^{13}C NMR (Figure 3.82, Table 3.18) led to the identification of 16 signals which could be attributed to four methyls including an *N*-methyl at δ_C 33.0 (δ_H 4.11); a methylene at δ_C 28.6; five methines including an oxymethine at δ_C 94.3 and six quaternary carbons including the deshielded signal at δ_C 166.1 suggesting the presence of an amide in the molecule. In the HMBC spectrum, correlations observed between the methyl signals at δ_H 1.25 (3H-4') and 1.42 (H-5') with the carbons at δ_C 23.4 or 24.6 (C-4' or C-5'), 70.5 (C-3') and 94.3 (C-2') suggested they were in *geminal* position on the carbon C-3' and the entire group fixed on C-2'. Correlations observed between the methyl at δ_H 4.11 (*N*-CH_3) and the carbons at δ_C 136.7 (C-10) and 166.1 (C-2) confirmed its position on the nitrogen atom. The proton H-2'was determined to be *β*-oriented due to the observed coupling constants (*J* = 6.0, 15.0 Hz) with the adjacent methylene 2H-1'. All the ^{1}H and ^{13}C NMR data (Table 3.18) of **183** were in good agreement with those published for *N*-methylplatydesminium cation (Boyd and Grundon, 1967; Boyd *et al.*, 2007). Thus, compound **183** was identified as *N*-methylplatydesminium cation, a quaternary quinoline alkaloid first isolated from *Skimmia Japonica* (Rutaceae) (Boyd and Grundon, 1967).

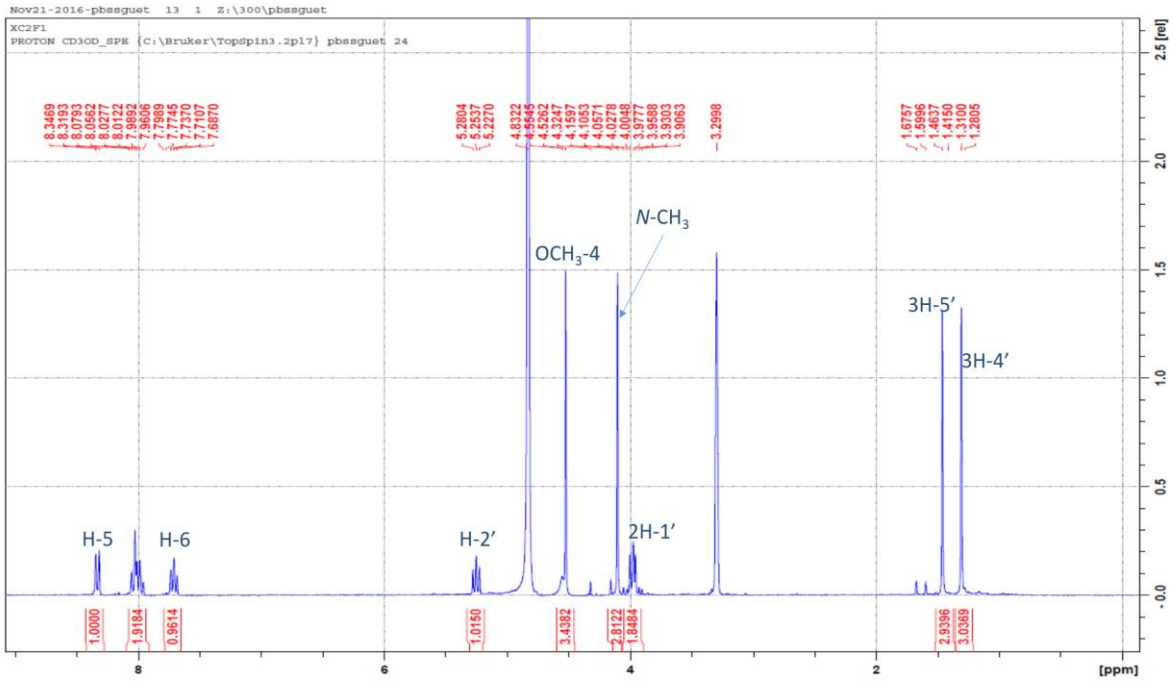

Figure 3.81 ^{1}H NMR (300 MHz, CD_3OD) of **183**

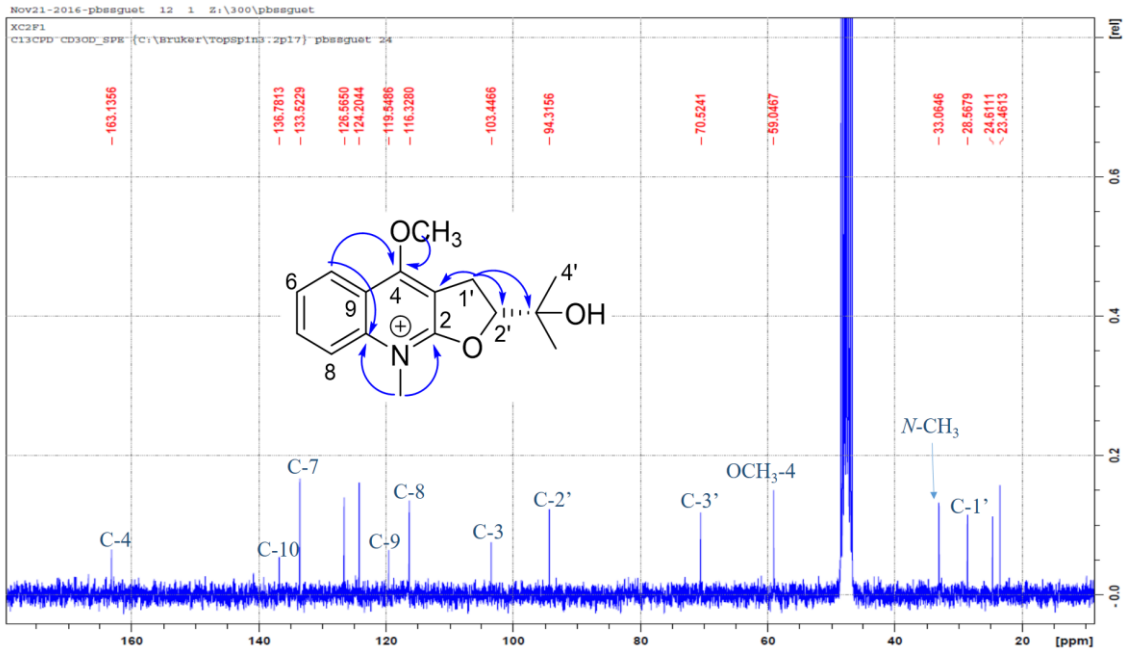

Figure 3.82 ^{13}C NMR (75 MHz, CD_3OD) and key HMBC correlations of **183**

3.3.5.3 Structure elucidation of isoplatydesmine (**184**)

Compound **184** was isolated as yellow amorphous powder. Its molecular formula $C_{15}H_{17}NO_3$ was determined from its HR ESI-MS spectrum obtained in positive ion mode by the peak at *m/z* 260.1284 $[M+H]^+$ calculated for $C_{15}H_{17}NO_3H$, 260.1281. Its 1D and 2D NMR spectra were similar to those of **183**. The only difference was the absence in the ^1H NMR spectrum (Figure 3.83, Table 3.18) of **184** of the methoxy proton signal present in that of **183** suggesting a demethylation on position C-4. This was further confirmed by the different ^{13}C chemical shifts in the ^{13}C NMR (Figure 3.84) especially the carbon C-4 which appeared at δ_C 172.6 as well as the key correlations observed in its HMBC spectra (Figure 3.84). Therefore, compound **184** was identified as isoplatydesmine and all its ^1H and ^{13}C NMR data (Table 3.18) were in good agreement with the published data (Boyd and Grundon, 1967; Boyd *et al.*, 2007).

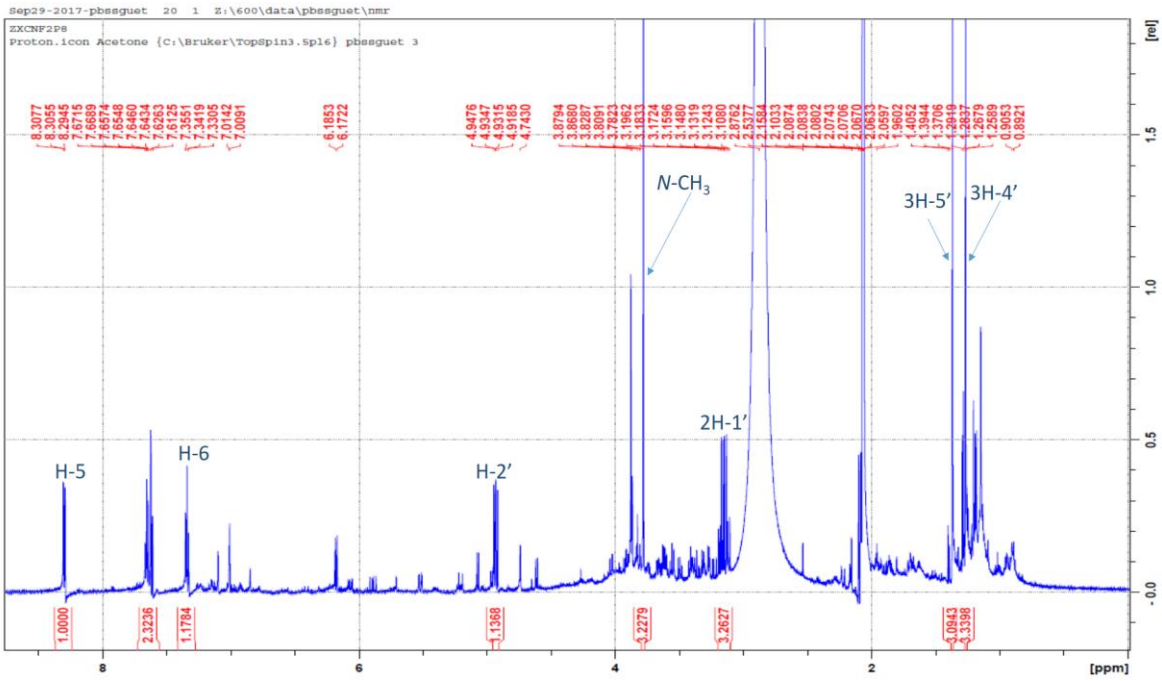

Figure 3.83 ^1H NMR (600 MHz, acetone-d_6) of **184**

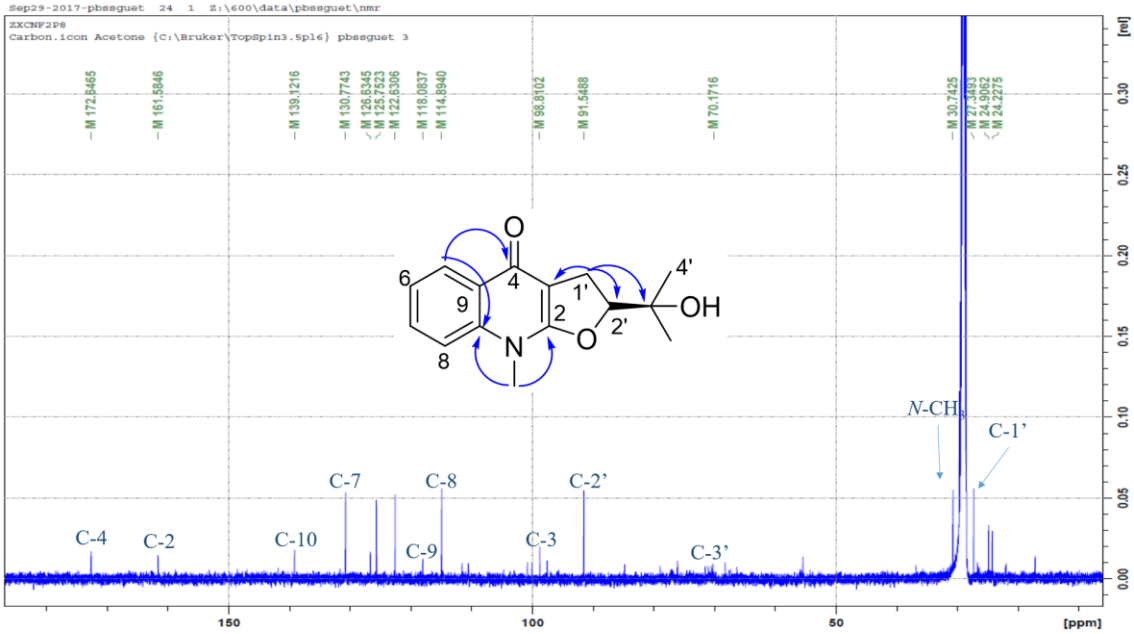

Figure 3.84 ^{13}C NMR (150 MHz, acetone-d_6) and key HMBC correlations of **184**

3.3.5.4 Structure elucidation of ribalinine (**186**)

Compound **186** was isolated as yellow amorphous powder. Its molecular formula $C_{15}H_{17}NO_3$ was determined from its HR ESI-MS spectrum obtained in positive ion mode by the peak at *m/z* 260.1284 $[M+H]^+$ calculated for $C_{15}H_{17}NO_3H$, 260.1281. Its 1D and 2D NMR spectra were very similar to those of **184**. The only difference was the chemical shifts observed for the C-3 side chain. In the ^{1}H NMR spectrum (Figure 3.85, Table 3.18) of **186**, the H-2' proton (δ_H 3.91, dd, J = 5.0, 5.6 Hz) was found to be shielded compared to the corresponding proton in **184**. In the ^{13}C NMR spectrum (Figure 3.86, Table 3.18), the signal of carbon C-3' (δ_C 84.3) bearing the two *gem*-methyls was deshielded while that of C-2' (δ_C 69.0) was shielded compared to the values observed for the same carbons in **184**. This observation suggested a six membered side ring. The 2'-OH was determined to be *β*-oriented due to the small coupling constants (*J* = 5.0, 5.6 Hz) for its coupling with the 2H-1' protons. Therefore, compound **186** was identified as ribalinine (Corral and

Orazi, 1967). Its ^{1}H and ^{13}C NMR data (Tables 3.21-3.22) were in good agreement with the published data (Corral and Orazi, 1967; Boyd *et al.*, 2007).

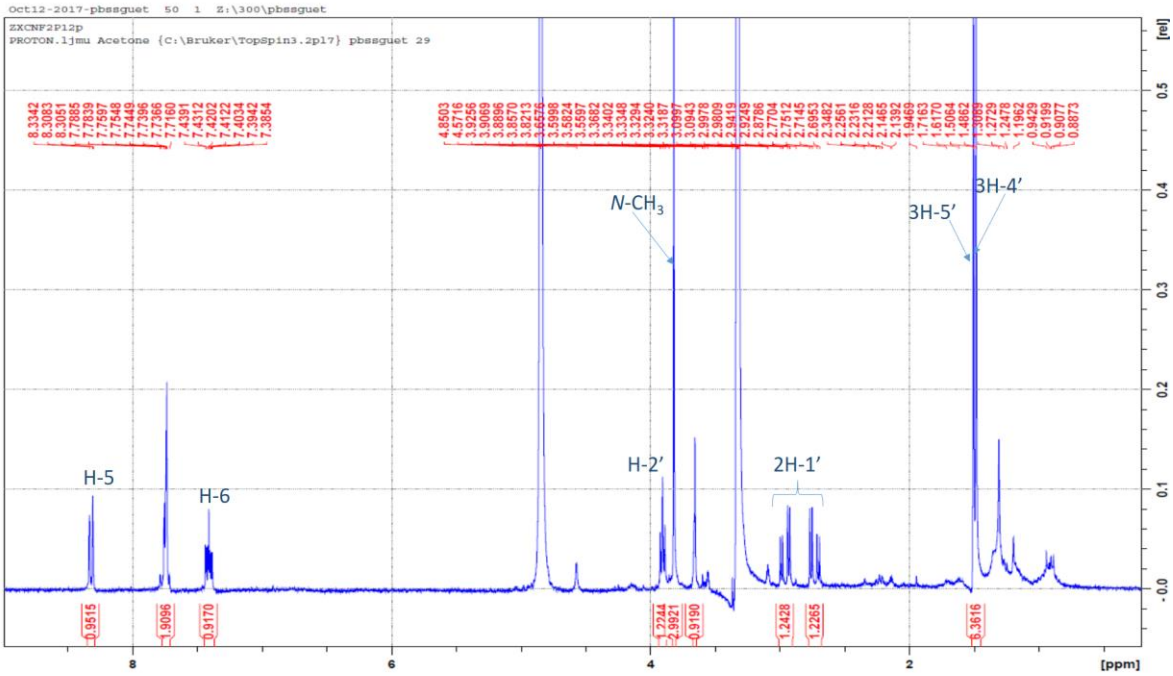

Figure 3.85 ^{1}H NMR (300 MHz, CD_3OD) of **186**

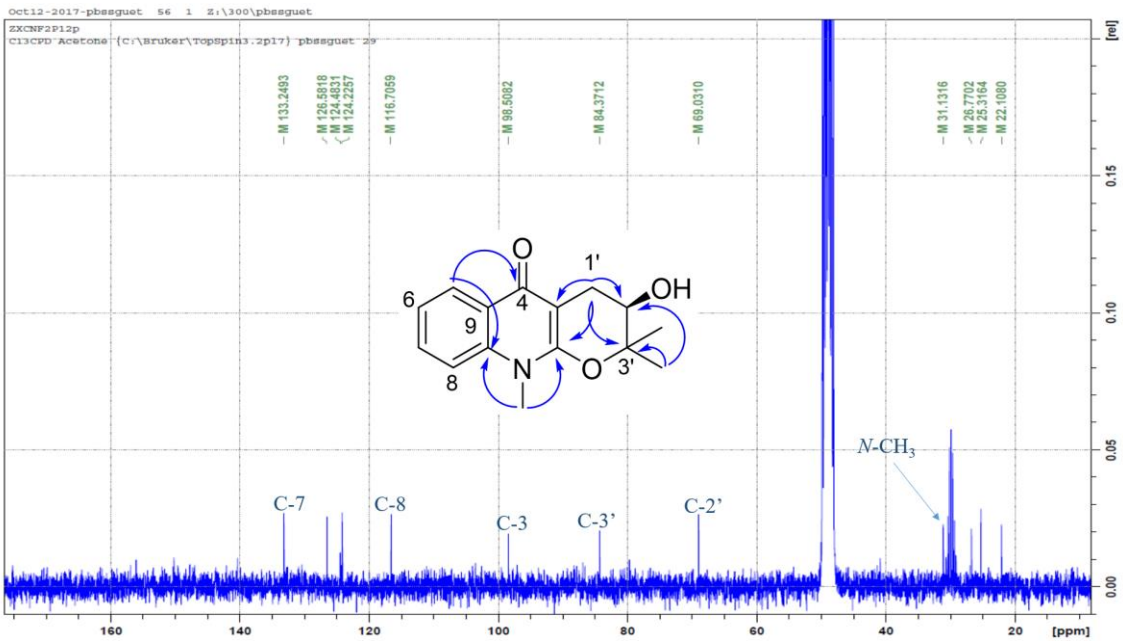

Figure 3.86 ^{13}C NMR (75 MHz, CD_3OD) and key HMBC correlations of **186**

3.3.5.5 Structure elucidation of atanine (**128**)

Compound **128** was isolated as yellow amorphous powder. Its molecular formula $C_{15}H_{17}NO_2$ was determined from its HR ESI-MS spectrum obtained in positive ion mode by the peak at *m/z* 244.1337 $[M+H]^+$ calculated for $C_{15}H_{17}NO_2H$, 244.1338. Its 1D and 2D NMR spectra similar to those of **183** also suggested a quinoline skeleton. The chemical shifts observed for the C-3 side chain in **128** suggested an open cycle compared to the previous isolated quinolones. In addition, the absence of the *N*-methyl signal in the ^{1}H NMR spectrum (Figure 3.87, Table 3.18) of **128** was clearly visible. The methine signal appearing at δ_H 5.25 showing cross peak correlation in the HSQC-DEPT spectrum with the carbon at δ_C 122.7 was attributed to H-2'. In the HMBC spectrum (Figure 3.87), correlations observed between the two *gem*-methyls (δ_C 25.8, C-4'; 18.0, C-5'; δ_H 1.71, H-4'; 1.82, H-5') with the carbons at δ_C 18.0 or 25.8 (C-5' or C-4'), 122.7 (C-2') and 133.3 (C-3') suggested the C-3 side chain to be a dimethylallyl moiety. The ^{1}H and ^{13}C NMR data (Table 3.18) of **128** were in good agreement with those published for atanine (Brown, 1980). Thus, compound **128** was identified as atanine, a quinolone alkaloid first isolated from *Z. zanthoxyloides* by Eshiett and Taylor (1968).

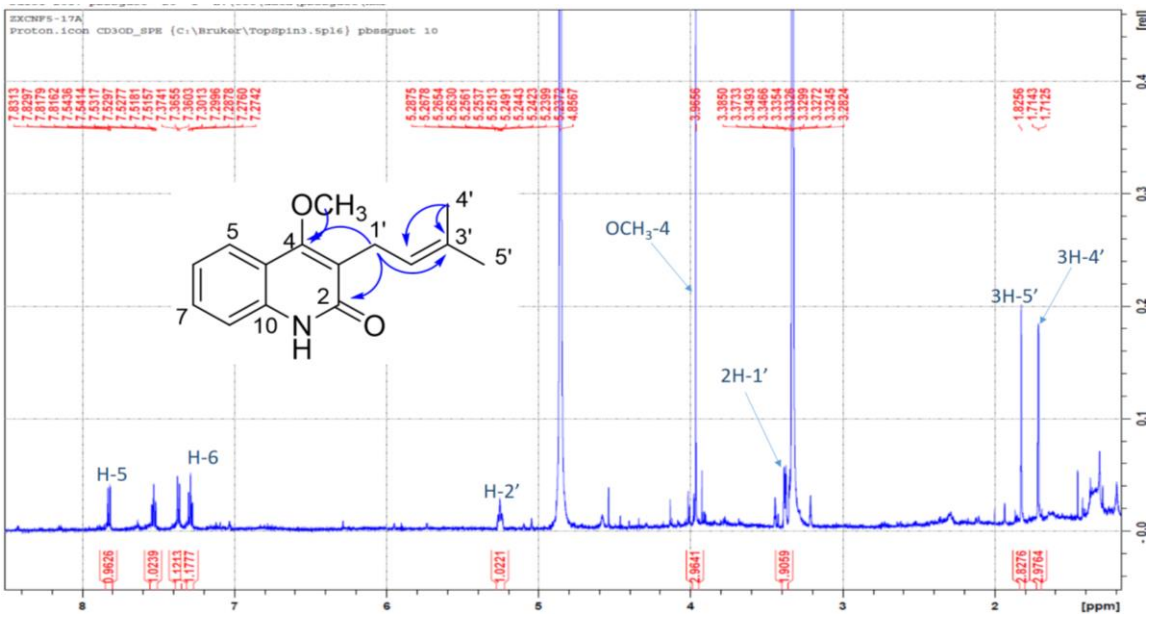

Figure 3.87 ^{1}H NMR (600 MHz, CD_3OD) and key HMBC correlations of **128**

3.3.5.6 Structure elucidation of *N*-methylatanine (**187**)

Compound **187** was isolated as yellow amorphous powder. Its molecular formula $C_{16}H_{19}NO_2$ was determined from its HR ESI-MS spectrum obtained in positive ion mode by the peak at *m/z* 258.1494 $[M+H]^+$ calculated for $C_{16}H_{19}NO_2H$, 258.1494. Its 1D and 2D NMR spectra were very similar to those of **128**. The only difference was the presence in the ^1H NMR spectrum (Figure 3.88, Table 3.18) of **187** of a singlet methyl at δ_H 3.74 attributable to *N*-methyl. This attribution was confirmed in the HMBC spectrum (Figure 3.88) by the correlation between the *N*-methyl protons and the carbons at δ_C 139.0 (C-10) and 164.5 (C-2). Thus, **187** was identified as *N*-methylatanine and all its ^1H and ^{13}C NMR data (Table 3.18) were in good agreement with the published data (Brown, 1980).

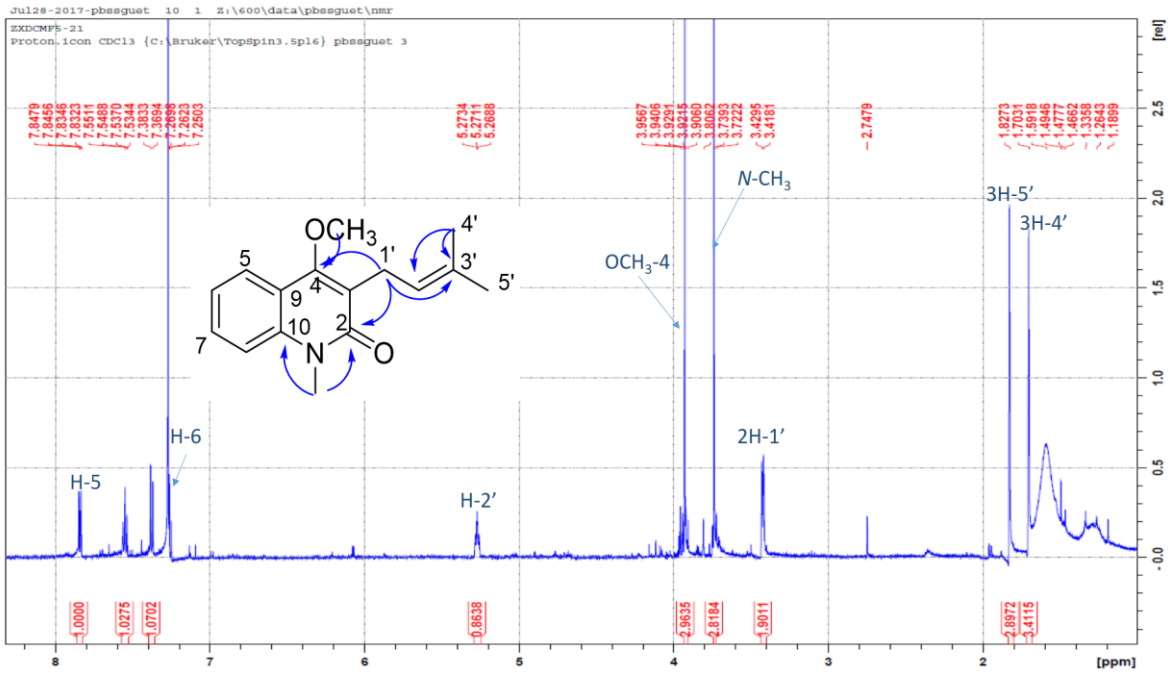

Figure 3.88 ^1H NMR (600 MHz, $CDCl_3$) and key HMBC correlations of **187**

Table 3.18 ^{1}H and ^{13}C NMR data of **55**, **128**, **183-184** and **186-187**

Position	δ_H m (*J* in Hz)						δ_C					
	55	**128**	**183**	**184**	**186**	**187**	**55**	**128**	**183**	**184**	**186**	**187**
1							-	-	-	-	-	-
2							164.6	164.3	166.1*	161.2	156.8	164.5
3							101.9	122.7	103.4	98.0	98.4	122.6
4							157.8	162.1	163.1	172.6	nd	159.8
5	8.05 d (*9.4*)	7.82 dd (*1.0*, *8.1*)	8.32 d (*9.0*)	8.31 dd (*1.4*, *7.9*)	8.32 dd (*1.4*, *7.9*)	7.84 dd (*1.4*, *7.9*)	118.3	124.0	124.2	125.8	124.1	123.4
6	7.36 d (*9.4*)	7.29 ddd (*1.2*, *7.1*, *8.1*)	7.71 td (*6.0*, *9.0*)	7.34 ddd (*1.0*, *7.0*, *7.9*)	7.40 m	7.27 m	111.9	123.5	126.5	122.0	126.5	121.8
7		7.53 ddd (*1.3*, *7.1*, *8.3*)	7.96 ov	7.65 ddd (*1.5*, *6.4*, *8.4*)	7.75 ov	7.56 td (*1.4*, *7.2*, *8.4*)	152.4	131.4	133.5	130.7	133.2	130.0
8		7.36 d (*8.2*)	8.03 ov	7.63 brd (*8.4*)	7.75 ov	7.39 d (*8.4*)	104.9	116.6	116.3	114.8	116.6	114.1
9							114.6	117.0	119.5	118.0	124.4	117.8
10							104.4	142.1	136.7	139.1	140.7	139.0
1’	7.28 d (*2.6*)	3.37 ov	3.97 dd (*6.0*, *15.0*)	3.13 dd (*7.4*, *16.6*)	2.74 dd (*5.6*, *16.5*)	3.43 d (*6.8*)	104.9	24.2	28.6	27.3	26.7	24.3
				3.17 dd (*9.6*, *16.6*)	2.96 dd (*5.0*, *16.5*)							
2’	7.75 d (*2.6*)	5.25 m	5.25 dd (*6.0*, *15.0*)	4.98 dd (*9.6*, *7.4*)	3.91 dd (*5.0*, *5.6*)	5.28 m	143.9	122.7	94.3	91.5	69.0	121.5

Table 3.18 *continued*

Position	δ_H m (*J* in Hz)						δ_C					
	55	**128**	**183**	**184**	**186**	**187**	**55**	**128**	**183**	**184**	**186**	**187**
3’		-	-	-	-	-	-	133.3	70.5	70.1	84.3	132.5
4’		1.71	1.25 s	1.29 s	1.48 s	1.71 s	-	25.8	23.4	24.2	25.3	25.7
5’		1.82 s	1.42 s	1.38 s	1.50 s	1.83 s	-	18.0	24.6	24.9	22.1	18.0
N-CH_3		-	4.11 s	3.78 s	3.82 s	3.74 s	-	-	33.0	30.7	31.1	29.7
4-OCH_3	4.49 s	3.96 s	4.53 s	-			58.7	62.4	59.0	-	-	61.7
7-OCH_3	4.02 s	-	-	-			55.8					
8-OCH_3	3.89 s	-	-	-			60.4					

*Values determined from the HMBC spectrum

3.3.5.7 Structure elucidation of zanthoamides G (**188**)

Compound **188** was obtained as white viscous liquid. Its molecular formula was determined as $C_{18}H_{29}NO_4$ from its HR ESI-MS spectrum (Figure 3.89) by the *pseudo*molecular ion at *m/z* 346.1984 calculated 346,1989 for its sodium adduct $[M + Na]^+$ ($C_{18}H_{29}NO_4Na$). The ^{1}H NMR spectrum of **188** (Figure 3.90, Table 3.19) exhibited 14 signals corresponding to 24 protons including the signals of the proton of a secondary amine at δ_H 8.56 (1H, brs), six olefinic protons at δ_H 7.12 (1H, dd, *J* = 10.4, 15.1 Hz), 6.60 (1H, dd, *J* = 11.1, 15.1 Hz), 6.27 (1H, dd, *J* = 10.8, 15.1 Hz), δ5.99 (1H, d, *J* = 15.0 Hz), 5.70 (1H, dd, *J* = 6.4, 15.0 Hz) and 5.44 (1H, m, *J* = 7.4 Hz), signals at δ_H 1.18 (6H, brs) and 1.11 (3H, d, *J* = 6.3 Hz) for three methyls, two oxygenated methines at δ_H 3.58 (1H, m, *J* = 6.3 Hz) and 3.91 (1H, m, *J* = 6.4 Hz) and three methylene signals including a broad singlet at δ_H 3.27 and two double doublets at δ_H 2.29 (*J* = 7.0, 13.2 Hz) and 2.35 (*J* = 7.3, 14.8 Hz). Overlapping signals occurring between δ_H 6.0-6.15 ppm resulting from two olefinic protons resonances were also observed. The ^{13}C NMR spectrum (Figure 3.91, Table 3.19) revealed signals for 18 carbons attributable to three methyls (δ_C 27.2 x 2, δ_C 18.8), three methylenes with one appearing relatively downfield at δ_C 51.1, ten methines including two oxymethines at δ_C 77.8 and 71.7, eight olefinic methines at δ_C 143.0, 142.3, 134.0, 131.7, 130.2, 129.9, 128.2 and 123.2, and two quaternary carbons including an amide at δ_C 169.4 and an oxygenated quaternary carbon at δ_C 71.6. The assignment of the carbon signals was consistent with the resonances observed in the ^{1}H NMR experiment as well as the ^1J ^{1}H-^{13}C correlations observed in the HSQC-DEPTQ spectrum (Figure 3.92). In the ^{1}H-^{1}H COSY spectrum (Figure 3.93), a chain of vicinal correlations observed from H-2 to H-14, helped to construct one part of the compound structure as CH_3-CH=CH-CH=CH-CH_2-CH_2-CH=CH-CH=CH-. In the HMBC spectrum (Figure 3.94), correlations from δ_C 1.18 (H-3' and H-4') to carbon signals at δ_C 51.1 (C-1'), 71.6 (C-2') and 27.2 (C3' or C-4'), and from δ_C 3.27 (s, H-1') to C-2', C-3' and C-4' identified the

other part of the molecule as 2-hydroxy-isobutyl moiety. Further correlations in the HMBC spectrum from H-1' (δ_H 3.27), H-2 (δ_H 5.99) and H-3 (δ_H 7.12) to C-1 (δ_C 169.4), in addition to the appearance of the methylene of the isobutyl moiety at δ_C 55.1, established that the 2-hydroxy-isobutyl moiety was linked to the nitrogen of the amide group and the aliphatic moiety to the carbonyl of the amide. The geometry of the double bond C_2-C_3 was deduced as *trans* ($J_{H2/H3}$ = 15.0 Hz) like those of C_4-C_5, C_8-C_9 and C_{10}-C_{11}. Compound **188** did not show any optical activity suggesting that it was obtained as a racemic mixture. Thus compound **188** was identified as (12*RS*, 13*RS*)-(2*E*, 4*E*, 8*E*, 10*E*)-*N*-(2-hydroxy-2-methylpropyl)-12,13-dihydroxy-2,4,8,10-tetradecatetraenamide, a new alkamide from natural source and given the trivial name zanthoamide G. The ^{1}H and ^{13}C NMR data (Table 3.19) were similar to those published for zanthoamide C isolated from *Zanthoxylum bungeanum* (Wang *et al.*, 2016) with the only difference being the additional olefinic bond between C3 and C6 present in **188**.

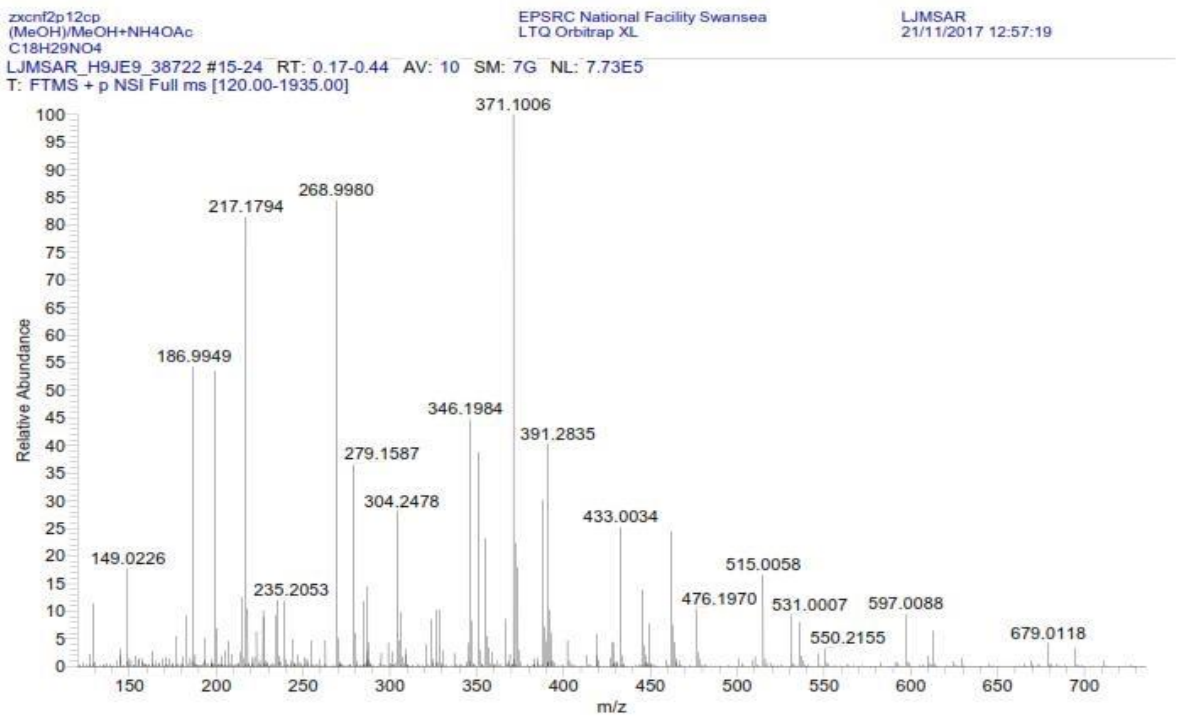

Figure 3.89 ESI-MS spectrum of **188**

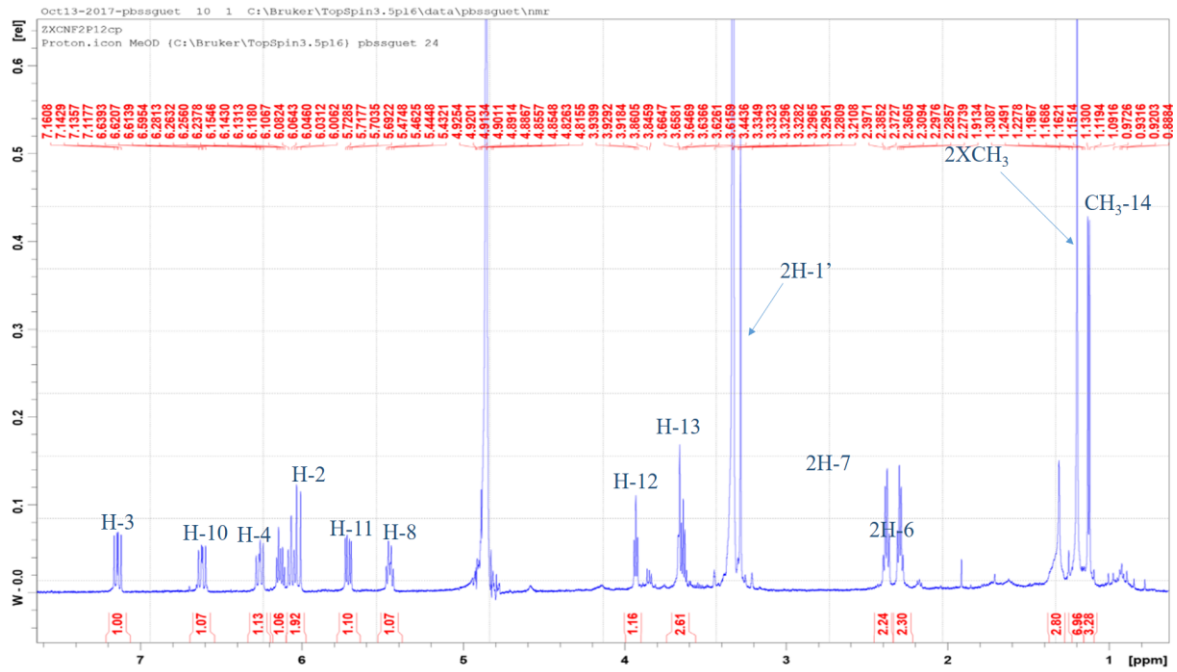

Figure 3.90 ^{1}H NMR (600 MHz, CD_3OD) of **188**

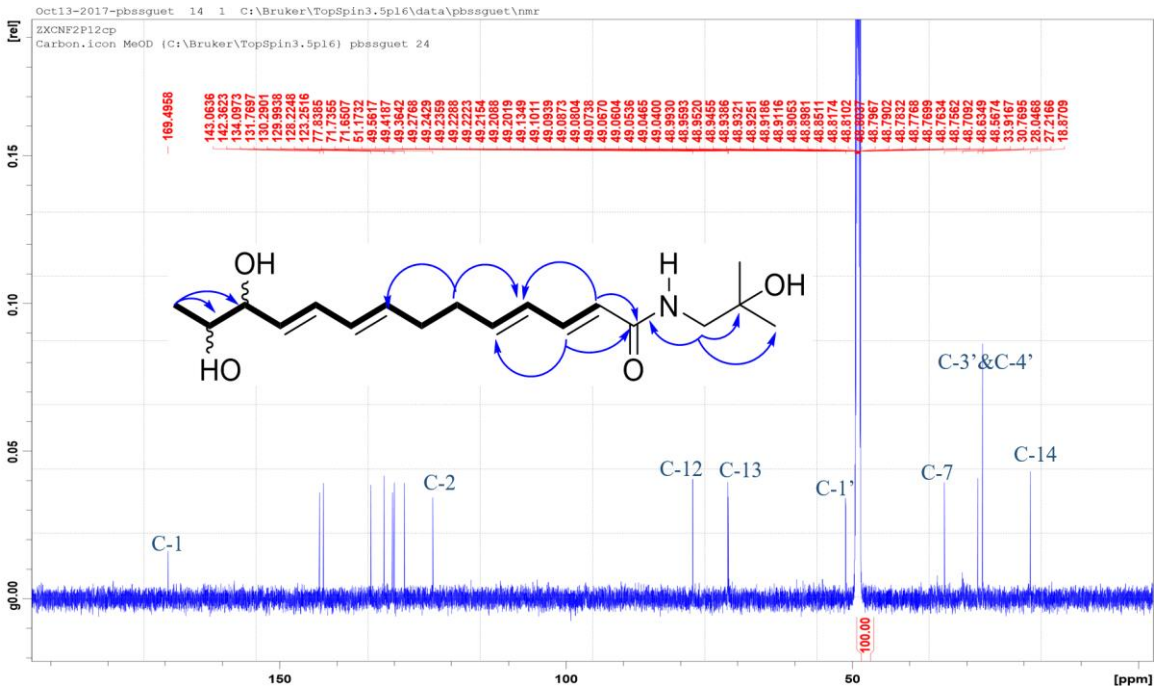

Figure 3.91 ^{13}C NMR (150 MHz, CD_3OD), COSY (−) and Key HMBC (→) correlation of **188**

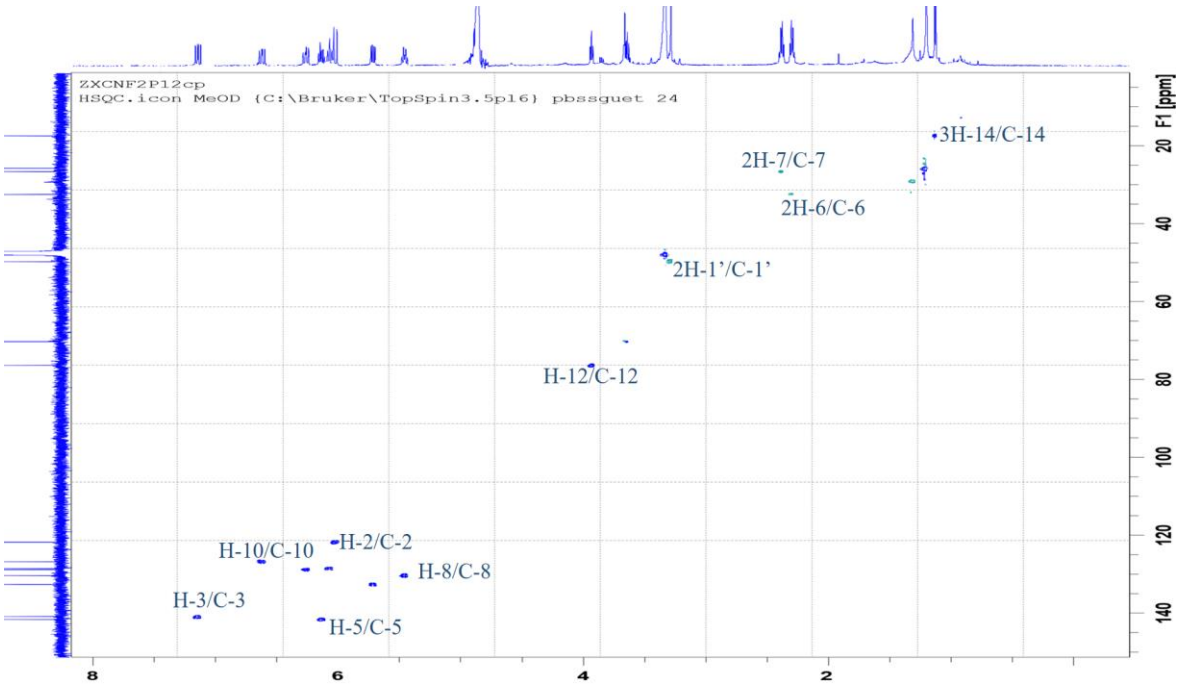

Figure 3.92 HSQC spectrum of **188**

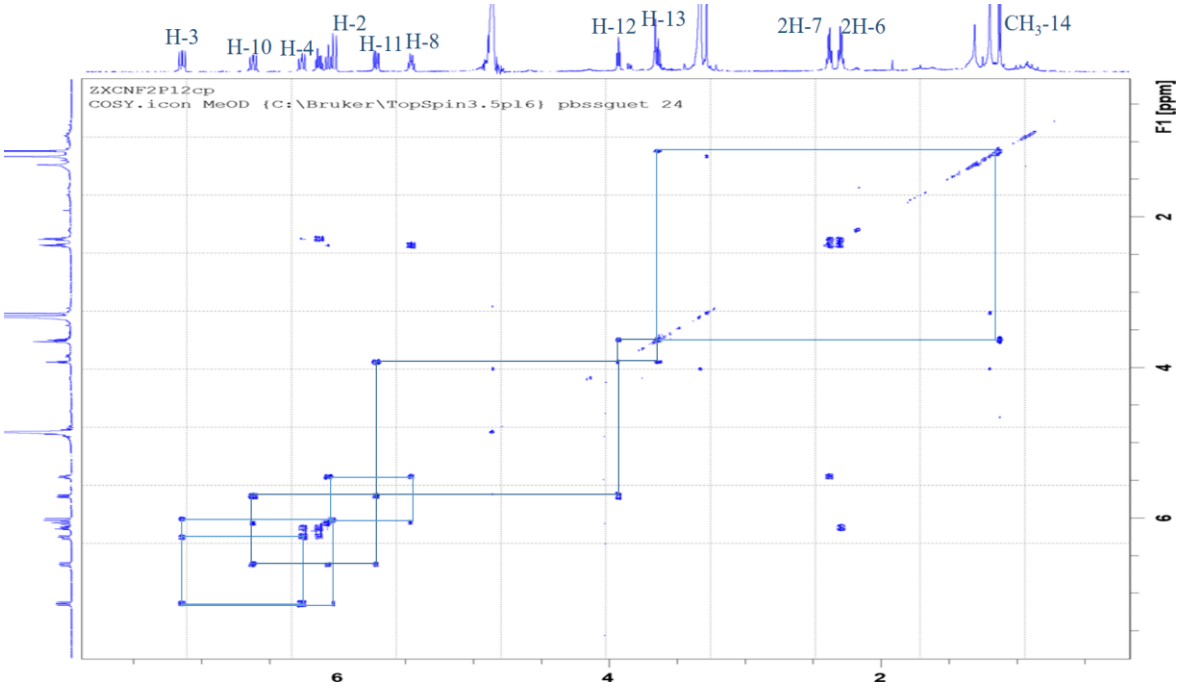

Figure 3.93 ^{1}H-^{1}H COSY spectrum of **188**

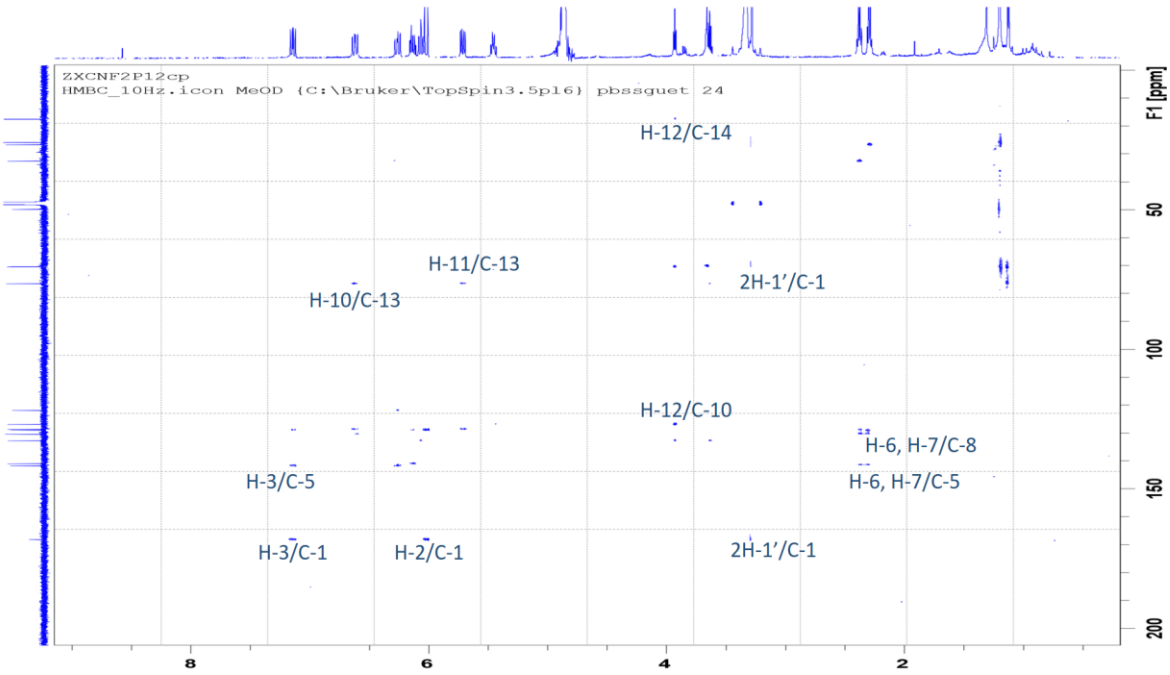

Figure 3.94 HMBC spectrum of **188**

3.3.5.8 Structure elucidation of zanthoamides H (**189**)

Compound **189** was also obtained as white viscous liquid. Its molecular formula was determined as $C_{18}H_{29}NO_4$ from its HR ESI-MS spectrum, where a *pseudo*molecular ion was observed as at *m/z* 346.1992 $[M + Na]^+$ (calculated 346.1989 for $C_{18}H_{29}NO_4Na$). The ^1H and ^{13}C NMR spectra (Figures 3.95-3.96, Table 3.19) of **189** established it as an aliphatic amide, similar to **188**, with the only difference being the placement of the two oxymethines, which were not adjacent to each other like in **188**. The COSY spectrum (Figure 3.96) revealed scaler couplings between oxymethine at δ_H 4.28 (H-13) and the methyl at δ_H 1.20 (H-14) and with the olefinic proton at δ_H 5.73 (H-12), and the correlations from the other oxymethine at δ_H 4.10 (H-8) to the methylene at δ_H 1.60 (H-7) and the olefinic proton at δ_H 5.68 (H-9). These correlations could be further confirmed from the HMBC spectrum (Figure 3.96), where correlations from H-8 to C-6 (δ_C 29.9), C-7 (δ_C 37.4) and C-9 (δ_C 137.0), and from H-13 to C-12 (δ_C 138.6) and C-14 (δ_C 23.5)

were observed. The geometry of the olefinic bonds were confirmed as *trans* from relevant coupling constants ($J_{H2/H3}$ = 15.1, $J_{H4/H5}$ = 15.2, $J_{H9/H10}$ = 14.6 and $J_{H11/H12}$ = 14.5). Compound **189** was optically inactive suggesting that it was a racemic mixture. Therefore, compound **189** was identified as (8*RS*, 13*RS*)-(2*E*, 4*E*, 9*E*, 11*E*)-*N*-(2-hydroxy-2-methylpropyl)-8,13-dihydroxy-2,4,9,11-tetradecatetraenamide, and given the trivial name, zanthoamide H.

3.3.5.9 Structure elucidation of zanthoamides I (**190**)

Compound **190** had a molecular formula $C_{18}H_{27}NO_4$ determined at *m/z* 322.2017 by HR ESI-MS $[M+H]^+$ (calculated for $[C_{18}H_{27}NO_4+H]^+$, 322.2013) corresponding to six double bonds and rings equivalent. The comparison of ^{1}H NMR spectrum (Figure 3.97, Table 3.19) of **190** to those of **189** clearly disclosed that **190** was also an aliphatic amide. The obvious difference between the two compounds was that the hydroxyl group at C-8 on **189** was replaced by a ketone group in **190**, which was confirmed by the signal at δ_C 202.0 in the ^{13}C NMR spectrum (Figure 3.98, Table 3.19) of **190**. The position of the ketone group was confirmed using HMBC spectrum (Figure 3.98) by the correlation observed between this later and the protons at δ_H 2.48 (H-6), 6.21 (H-9), 2.79 (H-7) and 7.29 (H-10). This was also supported by the downfield shifts of C-10 and C-12 from δ_C 129.8 and 138.6 in **189** to δ_C 144.5 and 149.3 respectively in **190** confirming the presence of a ketone group nearby. The geometry of the double bonds C_2-C_3, C_4-C_5, C_9-C_{10} and C_{11}-C_{12} was determined as trans-configured (J = 15.0, 15.0, 15.6 and 15.1 Hz, respectively). Compound **190** was found to be optically active, $[\alpha]_D^{25}$ = -25.6. However, the absolute configuration could not be determined because of paucity of this sample. Thus, compound **190** was identified as (13*)-(2*E*, 4*E*, 9*E*, 11*E*)-*N*-(2-hydroxy-2-methylpropyl)-13-hydroxy-2,4,9,11-tetradecatetraenamide and given the trivial name, zanthoamide I.

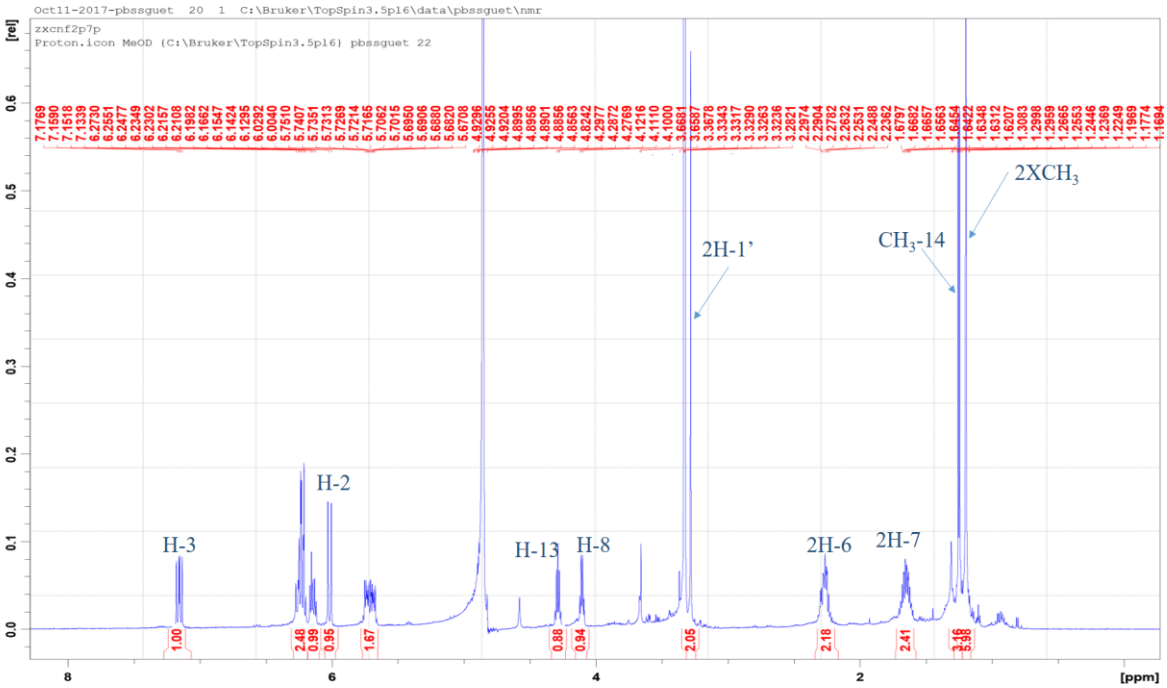

Figure 3.95 ^{1}H NMR (600 MHz, CD_3OD) of **189**

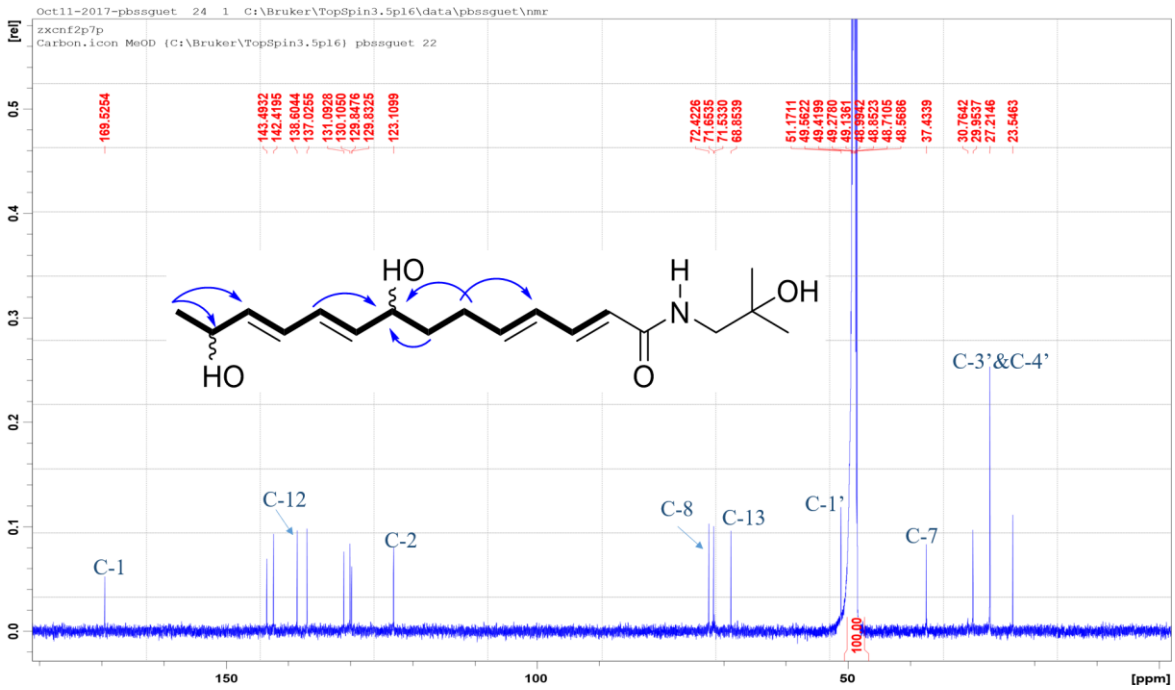

Figure 3.96 ^{13}C NMR (150 MHz, CD_3OD), COSY (−) and Key HMBC (→) correlation of **189**

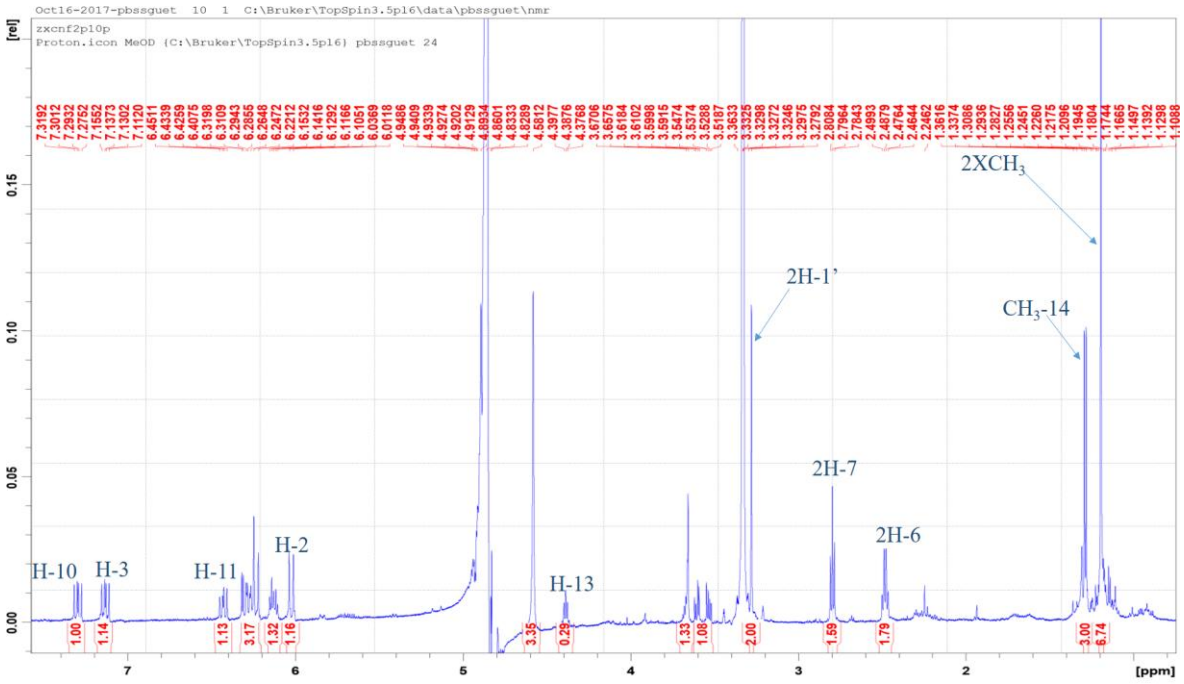

Figure 3.97 ^{1}H NMR (600 MHz, CD_3OD) of **190**

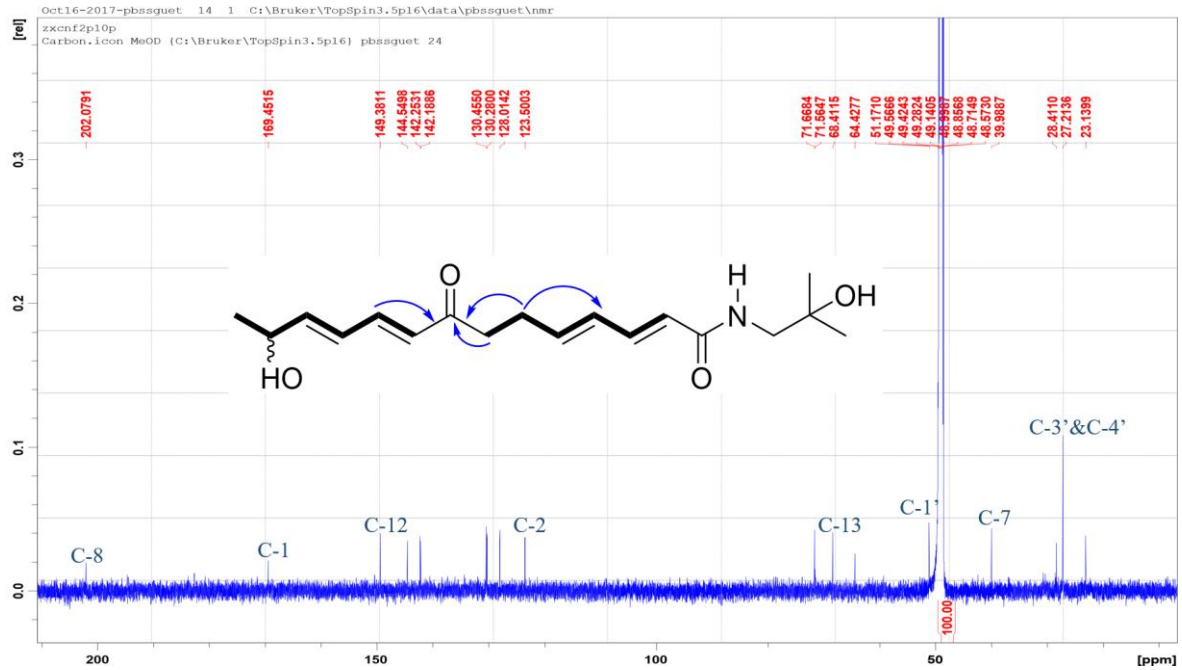

Figure 3.98 ^{13}C NMR (150 MHz, CD_3OD), COSY (−) and Key HMBC (→) correlation of **190**

Table 3.19 ^{1}H (600 MHz) and ^{13}C (150 MHz) NMR Data of zanthoamide G-I (**188-190**)

1	δ_H m (*J* in Hz)			δ_C		
	188	**189**	**190**	**188**	**189**	**190**
1	-	-	-	169.4	169.5	169.4
2	5.99 d (*15.0*)	6.01 d (*15.1*)	6.01 d (*15.0*)	123.2	123.1	123.5
3	7.12 dd (*10.4*, *15.1*)	7.15 dd (*10.7*, *15.0*)	7.13 dd (*10.7*, *15.1*)	142.3	142.4	142.1
4	6.27 dd (*10.8*, *15.1*)	6.25 dd (*10.7*, *15.2*)	6.26 m	130.2	130.1	130.4
5	6.11 m	6.14 m	6.13 dt (*7.0*, *15.0*)	143.0	143.4	142.2
6	2.29 dd (*7.0*, *13.2*)	2.20 m	2.48 dd (*7.2*, *14.1*)	33.9	29.9	28.4
7	2.35 dd (*7.3*, *14.8*)	1.60 m	2.79 dd (*7.2*, *14.5*)	28.0	37.4	39.9
8	5.44 dd (*7.2*, *15.1*)	4.10 q (*6.5*, *13.0*)	-	131.7	72.4	202.0
9	6.07 m	5.68 dd (*6.7*, *14.6*)	6.21 d (*15.6*)	129.9	137.0	130.2
10	6.60 dd (*11.1*, *15.1*)	6.20 m	7.29 dd (*10.8*, *15.6*)	128.2	129.8	144.5
11	5.70 dd (*6.4*, *15.0*)	6.20 m	6.42 dd (*10.3*, *15.1*)	134.0	131.0	128.0
12	3.91 dd (*6.4*, *12.9*)	5.73 m	6.31 m	77.8	138.6	149.3
13	3.58 m	4.28 q (*6.3*, *12.5*)	4.38 m	71.7	68.8	68.4
14	1.11 d (*6.3*)	1.20 d (*6.4*)	1.22 d (*6.5*)	18.8	23.5	23.1
1’	3.27 s	3.28 s	3.27 s	51.1	51.1	51.1
2’	-	-	-	71.6	71.6	71.5
3’	1.18 s	1.19 s	1.18 s	27.2	27.2	27.2
4’	1.18 s	1.19 s	1.18 s	27.2	27.2	27.2
NH	8.56 br s	8.56 br s	8.56 br s	-	-	-

3.3.5.10 Structure elucidation of hesperetin (**191**)

Compound **191** was isolated as yellow amorphous powder. Its molecular formula $C_{20}H_{30}O_2$ was determined from its HR ESI-MS spectrum (Figure 3.99) obtained in negative ion mode by the peak at *m/z* 301.2170 $[M-H]^-$ calculated for $C_{20}H_{29}O_2$, 301.2173. Its ^{1}H NMR spectrum (Figure 3.100, Table 3.20) revealed the presence of a methoxy at δ_H 3.88 (s); a 1,3,4-trisubstituted benzene ring formed by the protons at δ_H 7.06 (d, J = 1.7 Hz), 7.00 and 6.99; two meta coupling protons at δ_H 5.97 (dd, J = 3.0, 16.8 Hz) and an oxymethine at δ_H 5.45 (dd, J = 3.0, 12.6 Hz) which were found to couple in the COSY spectrum with the methylene protons appearing at δ_H 2.76 (dd, J = 3.0, 16.8 Hz) and 3.16 (dd, J = 12.6, 16.8 Hz). The ^{13}C NMR spectrum (Figure 3.101, Table 3.20) of **191** depicted sixteen peaks which could be assigned based on the correlation observed in the HSQC spectrum to one methoxy at δ_C 55.2; one methylene at δ_C 42.9, six methines including an oxymethine at δ_C 79.0 and eight quaternary carbons including the highly deshielded carbon at δ_C 196.2 suggesting a conjugated carbonyl. The ^{1}H and ^{13}C NMR data (Table 3.20) of **191** and its key HMBC correlations (Figure 301) were in good agreement with those described for hesperetin (EI-Shafae *et al.*, 2002). The C-2 proton at δ_H 5.97 (d, J = 3.0, 16.8 Hz) was determined to be β-oriented due to the coupling constant observed from its coupling with the C-3 methylene. Thus, compound **191** was identified as hesperetin, a flavone commonly isolated from *Citrus* species (Rutaceae) (EI-Shafae *et al.*, 2002; Gattuso *et al.*, 2007).

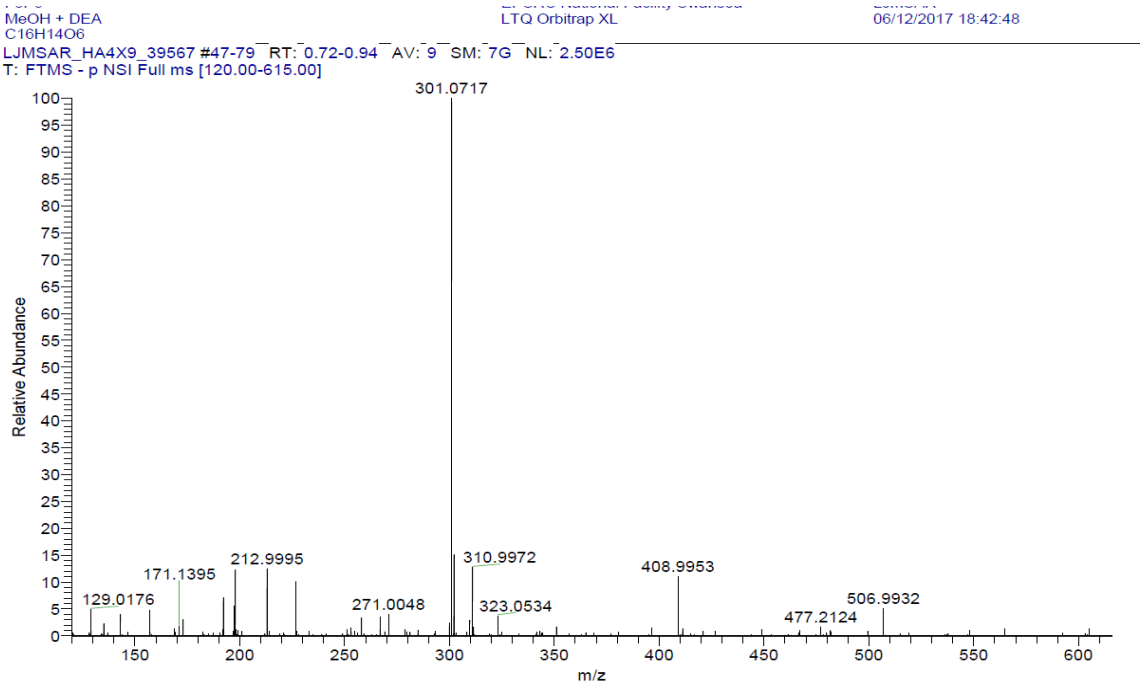

Figure 3.99 ESI-MS spectrum of **191**

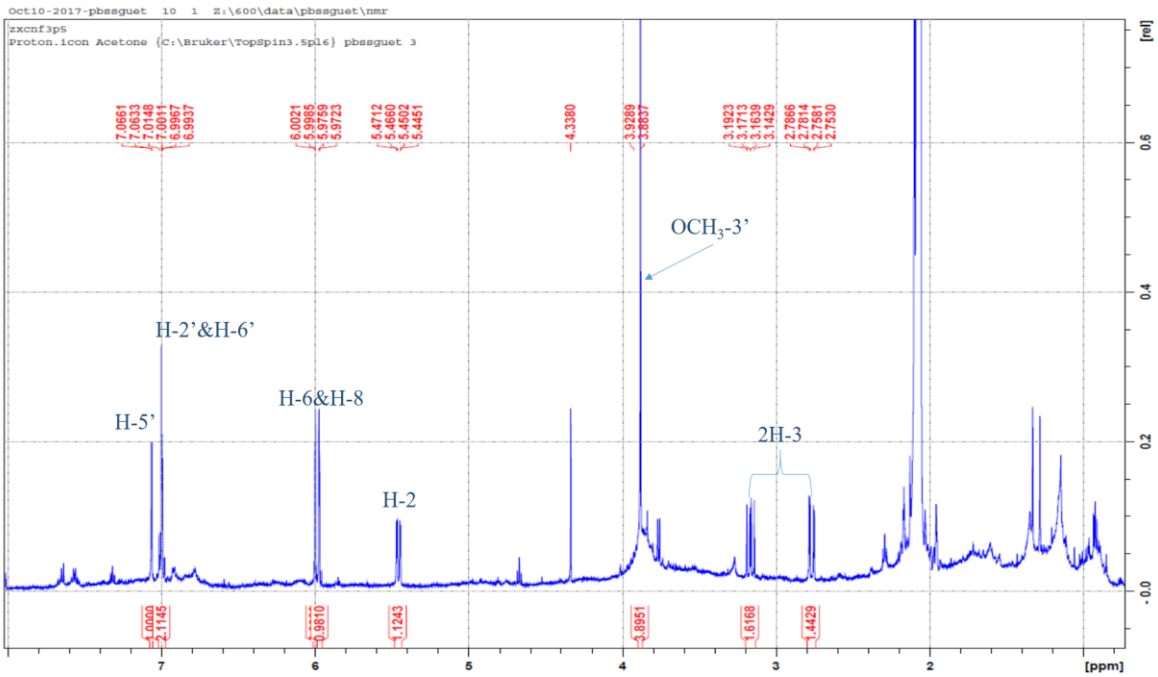

Figure 3.100 ^{1}H NMR (600 MHz, acetone-d_6) of **191**

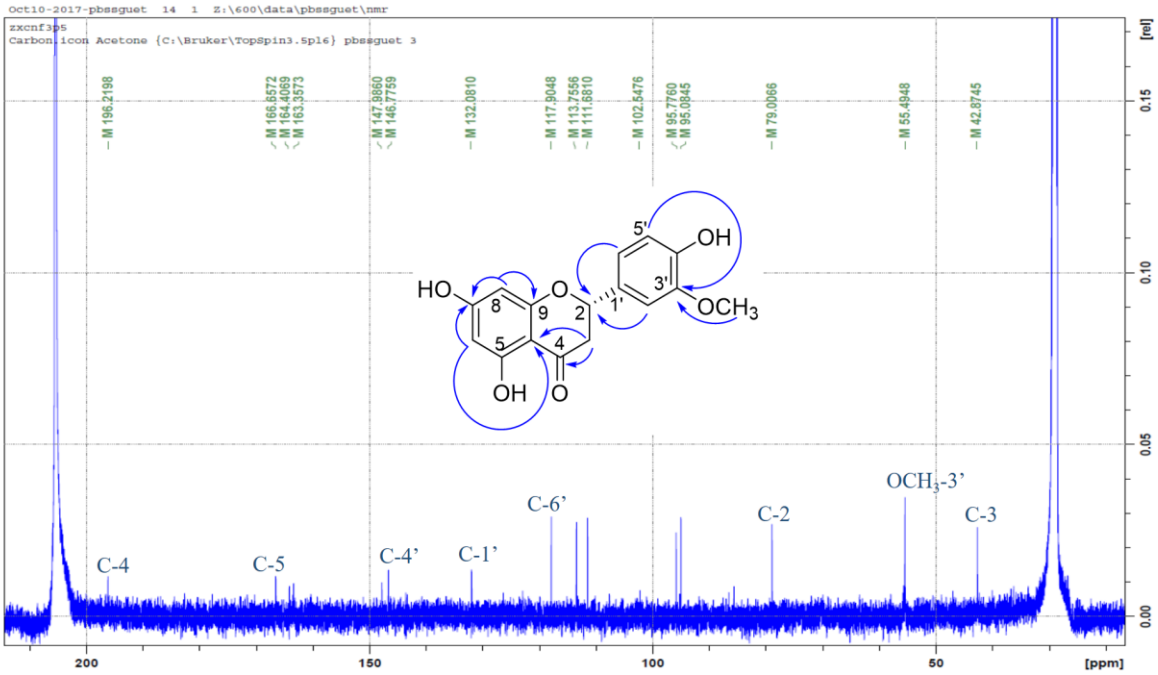

Figure 3.101 ^{13}C NMR (150 MHz, acetone-d$_6$) of compound **191**

Table 3.20 ^{1}H (600 MHz, acetone-d$_6$) and ^{13}C NMR data (150 MHz, acetone-d$_6$) of **191**

Position	δ_H m (*J* in Hz)	δ_c	Position	δ_H m (*J* in Hz)	δ_c
1	-	-	9	-	163.3
2	5.45 dd (*3.0*, *12.6*)	79.0	10	-	102.5
3	2.76 dd (*3.0*, *16.8*)	42.8	1’	-	132.0
	3.16 dd (*12.6*, *16.8*)		2’	7.00 ov	111.6
4	-	196.2	3’	-	147.9
5	-	166.6	4’	-	146.7
6	5.97 d (*2.1*)	95.7	5’	7.06 d (*1.7*)	113.7
7	-	164.4	6’	6.99 ov	117.9
8	6.00 d (*2.1*)	95.0	OCH_3	3.88 s	55.4

3.4 Biogenesis and chemotaxonomic significance of isolated compounds

Three main classes of secondary metabolites including alkaloids, diterpenes and flavonoids were isolated in the course of this study.

3.4.1 Alkaloids

Quinoline alkaloids (**55**, **128**, **183-187**) and alkamides (**188-190**) were isolated from *Z. zanthoxyloides* (Rutaceae). *Zanthoxyllum* is a rich source of alkaloids including acridone, aliphatic and aromatic amides, aporphine and benzophenantridine (Adesina, 2005; Patino *et al.*, 2012).

This is the first report on the occurrence of compounds **183-187**, in addition to three new alkamides (**189-191**), in *Z. zanthoxyloides*. Several alkamides with structures similar to zanthoamides G-I **(189-191)** were previously reported in several *Zanthoxylum* species including *Z. zanthoxyloides, Z. bungeanum, Z. syncarpum, Z. piperitum, Z. ailanthoides, Z. integrifoliolum, Z. schinifolium, Z. armatum, Z. tessmannii, Z. achtoum, and Z. heitzii* (Ross *et al.*, 2005; Wang *et al.*, 2016; Chruma *et al.*, 2018). *N*-methylplatydesminium catium **(183)** was previously isolated from *Z. usambarense* and *Z. chalybeum* (Kato *et al.*, 1996), isoplatydesmine (**184**) from *Z. nididum* (Ishikawa *et al.*, 1995), myrtopsine (**185**) from *Z. integrifoliolum* (Ishii *et al.*, 1982), ribalinine (**186**) from *Z. mayu* (Torres and Cassels, 1978), and *N*-methylatanine (**187**) from *Z. beecheyanum* (Cheng *et al.*, 2004) and *Z. rigidum* (Moccelini *et al.*, 2009).

Quinoline alkaloids are biosynthesized from anthranilic acid, which is formed from chorismate and L-glutamine, while alkamides derived from the condensation of amino acid and/or cinnamic acid unit (Waterman, 1975). For quinoline synthesis, anthranilic acid is acetylated followed by cyclisation to form the basic 2,4-dihydroxyquinoline ring,

which may then undergo a nucleophilic addition of an isoprenyl unit on the highly reactive C-3 carbon to give rise to 3-(3',3'-dimethylallyl)-4-hydroxy-2-quinolone (Waterman, 1975; Grundon, 1988). Subsequent modifications on the obtained quinolone including alkylation, cyclisation (e.g. C-2 and C-2' or C-3') and oxidation may lead to the formation of the known quinoline alkaloids such as those isolated from *Z. zanthoxyloides* in the course of this study (Figure 3.102) (Fish and Waterman, 1973; Waterman, 1978; Boyd *et al.*, 2000).

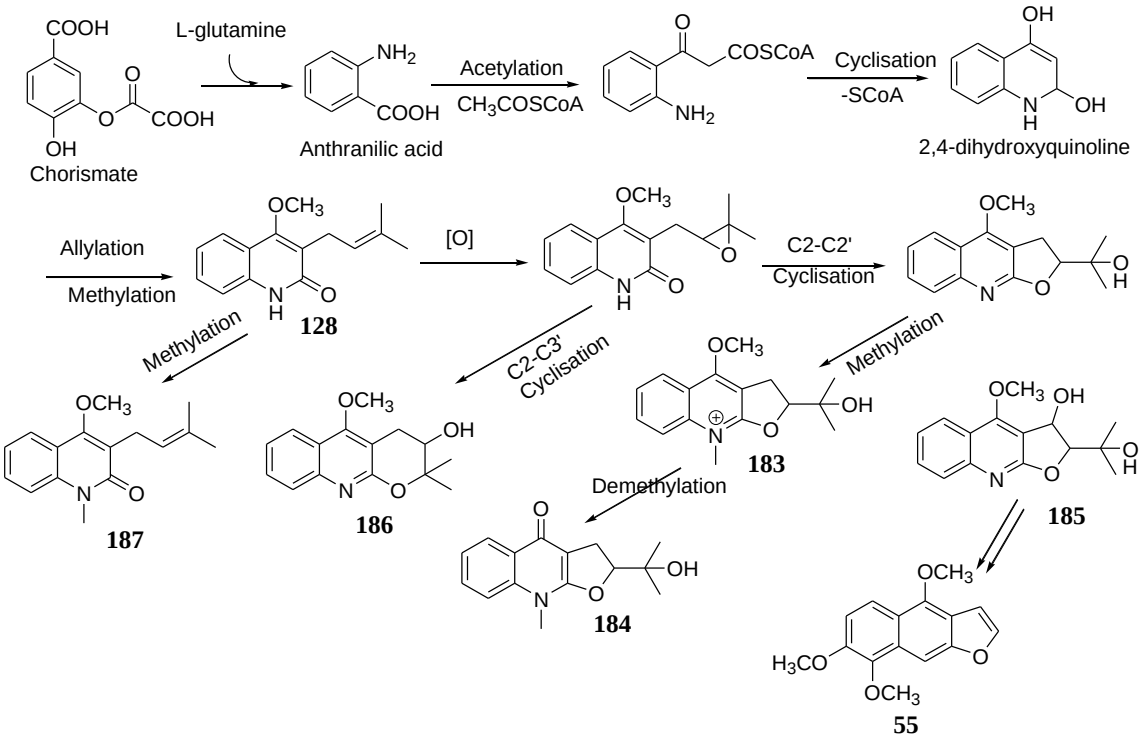

Figure 3.102 Possible biosynthesis pattern of the quinolines isolated from *Z. zanthoxyloides*

3.4.2 Diterpenes

Abietane and clerodane were isolated from *C. oligandrus*, and kaurane from *Z. leprieurii*, respectively.

The genus *Croton* is a great natural source of diterpenes. Its phytochemical studies have led to the isolation of several diterpenes including clerodanes and abietanes, which represent about 27% and 4%, respectively, of all the diterpenes isolated (Xu *et al.*, 2018). A previous study of *C. oligandrus* has led to the isolation and identification of clerodane, trachylobane and labdane type diterpenes (Abega *et al.*, 2014).

Regarding *Z. leprieurii*, this is the first report on the occurrence of kaurane diterpenes in *Z. leprieurii*, and in the genus *Zanthoxylum* in general. Diterpenes are rare in the Rutaceae, and only a few including abietane, clerodane, kaurane and labdane have been reported from the genera *Citrus*, *Evodia*, *Fortunella*, *Glycosmis*, *Pamburus* and *Phebalium* (Cannon *et al.*, 1966; Dreyer and Park, 1975; Billet *et al.*, 1976; Seger *et al.*, 1998; Luis *et al.*, 2000; El-Shafae and Ibrahim, 2003). In addition to alkaloids, *Zanthoxylum* is known to be rich in coumarins and lignans, and contains few flavonoids (Adesina, 2005; Patino *et al.*, 2012; Li *et al.*, 2014). Alkaloids including acridone, alkamide, aporphine and benzophenanthridine, coumarins and lignans have been reported from *Z. leprieurii* (Adesina, 2005; Tchinda *et al.*, 2009). In the present study, in addition to kauranes, two flavonoids and a lignan previously reported from other *Zanthoxylum* species, have also been identified.

The biogenesis of diterpenes have extensively been studied. Diterpenes are now recognized to derive from geranylgeranyl diphosphate (GGPP) (Peters, 2010), though some few have been found to arise from carotene degradation (Seger *et al.*, 1998). Acid catalyzed cyclisation of GGPP can give rise to a fused decalin bicylic intermediate, copalyl diphosphate (CPP), from which subsequent modifications including internal additions, rearrangements and elimination may lead to bicyclic, tricyclic and tetracyclic diterpenes e.g. clerodane, abietane and kaurane, respectively (Figure 3.103) (Wilson *et al.*, 1976; Gershenzon and Croteau, 1993; Brunetton, 1999; Peters, 2010). Secondary modifications including oxidization and addition of different oxygen containing groups

may give rise to the range of diverse structural diterpenes occurring in nature (Gershenzon and Croteau, 1993) such as those isolated in the present study.

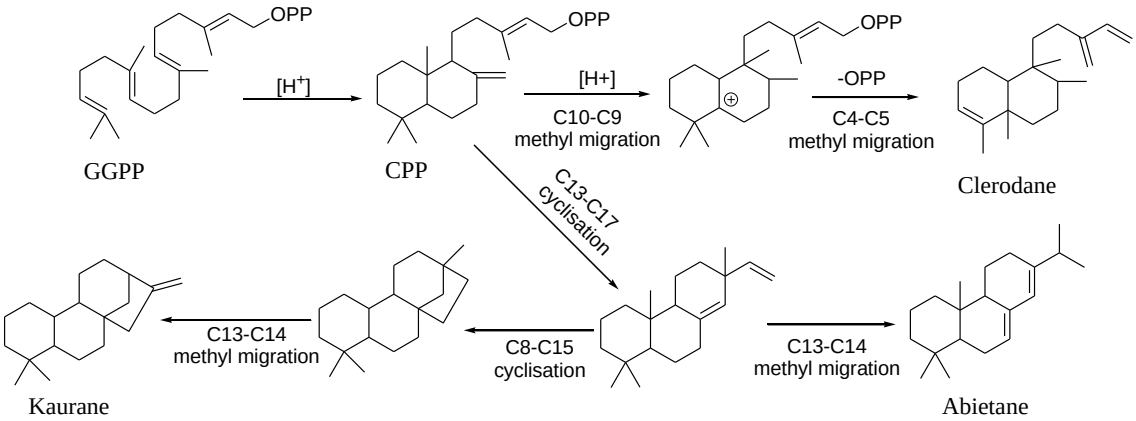

Figure 3.103 Summarised biosynthetic pathway toward abietane, clerodane and kaurane diterpenoids basic skeletons

3.4.3 Flavonoids

Flavonoids were isolated from *J. hypocrateriformis* and *P. microcarpa*. This is the first phytochemical study of *P. microcarpa* and the third of *J. hypocrateriformis*.

Previous phytochemistry of *J. hypocrateriformis* have reavealed the presence of pyrrolidine alkaloids (Roessler *et al.*, 1978; Neukomm *et al.*, 1983). In the current study, in addition to pyrrolidine alkaloids, we have also isolated flavones. A similitude in terms of phytochemical constituents were found between *J. hypocrateriformis* and two other Acanthaceae species, *Justicia secunda* and *Graphtophyllum grandulosum* as all the compounds isolated, excluding the two new reported flavonoids **166** and **167**, have also been reported earlier in those two species.

Regarding *P. microcarpa*, two of the flavonoids isolated, **164** and **166**, have also been identified in *J. hypocrateriformis*. The genus *Pseudospondias* is constituted of two species, *P. microcarpa* and *P. longifolia*, and this study constitutes the first phytochemical

study of the genus. Species known today within *Pseudospondias* genus, were once members of the *Spondias* genus (Burkill, 1985). *Spondias* is a rich source of phenolic compounds including, tannins, flavonoids and phenolic acid derivatives (Sameh *et al.*, 2018). Flavonoids have been reported from *Spondias* as well as other Anarcadiaceae genus e.g. *Rhus* from which isovitexin and several glycosylated flavones and flavonols have been identified and isolated (Shrestha *et al.*, 2012; Abu-Reidah *et al.*, 2015).

Flavonoids are a large group of natural products. They usually occur in plants as glycosides (Ikan, 1991). Flavonoid subclasses are all related by a common biosynthetic pathway, which incorporates precursors from both the shikimate and acetate-malonate pathways. Condensation between *p*-coumarylCoA and three acetylCoA units results in the formation of a chalcone, the biogenetic intermediate to other structural subclasses of flavonoids (Figure 3.104) (Markham, 1982; Ikan, 1991; Schijlen *et al.*, 2004). Further modification of the flavonoids skeleton including addition (or reduction) of hydroxyl groups, arylation, dimerization and glycosylation may occur at various stages resulting in the diverse structural known flavonoids (Markham, 1982).

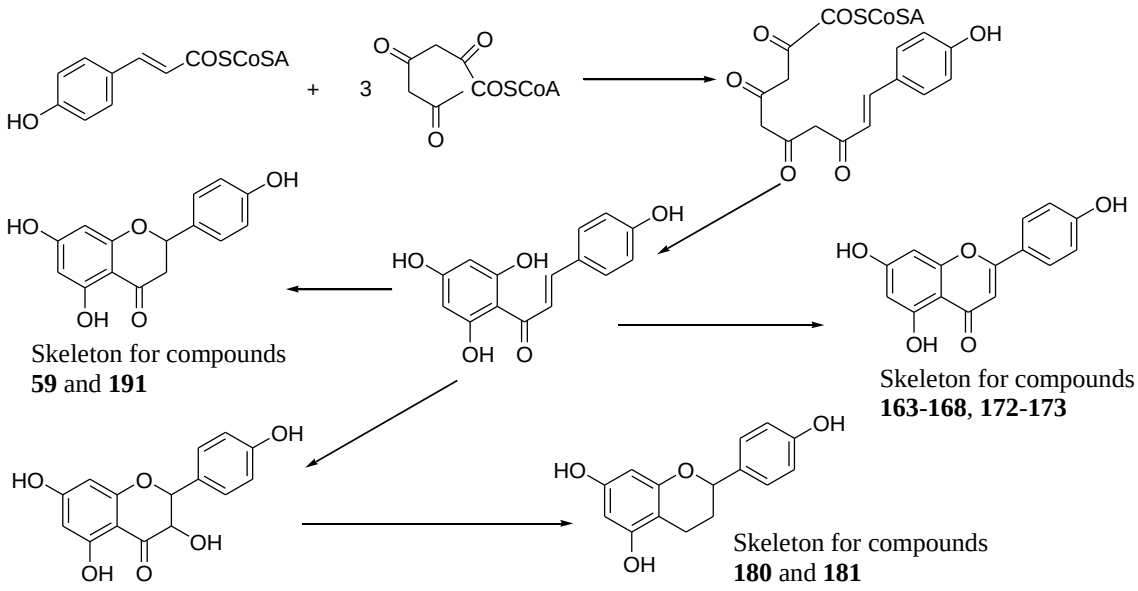

Figure 3.104 Summarised biosynthetic pathway toward basic flavonoid skeletons isolated

3.5 Bio-activity of the isolated compounds

3.5.1 Cytotoxicity of isolated compounds

The cytotoxicity of the isolated compounds (except **114**, **155**, **169**, **181** and sucrose) were evaluated against A549 (adenocarcinomic human alveolar basal epithelial), MCF7 (human breast adenocarcinoma), PC3 (human prostate cancer) and PNT2 (human normal prostate epithelium) cells using the MTT assay. The obtained LC_{50} values are shown in Table 3.21. Doxorubicin was used as positive control.

Table 3.21 Cell viability effect (LC_{50} in µM) of isolated compounds against cancer and non-cancer (PNT2) cells

Plant	Cpds	LC_{50} in µM			
COB		A549	MCF-7	PC-3	PNT2
	7	136.8 ± 18.9	>200	172.3 ± 39.7	167.5 ± 25.3
	8	>200	>200	135.6 ± 21.1	>200
	147	>200	>200	>200	>200
	148	>200	>200	>200	106.6 ± 6.0
	149/150	>200	>200	160.9±36.2	>200
	151	106.6 ± 27.2	>200	>200	>200
	152	>200	>200	131.1 ± 10.8	>200
	153	63.8 ± 13.8	136.2 ± 22.7	>200	>200
	154	138.6 ± 22.1	171.3 ± 51.4	>200	>200
	156/157	128.6 ± 31.0	>200	111.2 ± 2.9	>200
	158/159	>200	>200	>200	>200
	160	>200	>200	153.0 ± 9.1	97.6 ± 8.9
	161	>200	>200	68.9 ± 6.6	>200
	162	>200	>200	>200	197.7 ± 14.9
JHL	**163**	>200	>200	>200	>200
	164	>200	>200	146.6 ± 20.4	>200
	165	>200	>200	128.1 ± 8.5	>200
	166	>200	>200	87.1 ± 10.6	>200

Table 3.21 *continued*

Plant	Cpds	LC_{50} in µM			
JHC		A549	MCF-7	PC-3	PNT2
	167	>200	>200	117.4 ± 12.3	>200
	168	>200	>200	>200	>200
	170/171	>200	>200	>200	>200
PMB and PML	**103**	>200	>200	125.7 ± 11.8	>200
	172	>200	>200	>200	>200
	173	>200	>200	112.5 ± 9.4	>200
	174	>200	>200	180.5 ± 23.4	>200
ZLF	**175**	>200	132.1 ± 14.9	33.3 ± 9.1	>200
	176	>200	>200	138.9 ± 16.0	>200
	177	82.0 ± 7.2	62.0 ± 1.8	94.4 ± 6.9	10.6 ± 3.6
	178	>200	>200	147.9 ± 14.1	>200
	179	116.8 ± 13.7	167.9 ± 10.1	>200	>200
	180	>200	>200	112.7 ± 7.5	>200
	182	>200	>200	149.5±21.9	>200
ZZF	**54**	108.5 ± 22.1	>200	33.4 ± 9.8	>200
	55	113.4±0.15.8	53.7±09.5	164.7±0.21.3	104.4 ± 16.2
	59	29.5 ± 7.5	74.2 ± 17.8	51.7 ± 8.7	129.0 ± 20.3
	79	>200	>200	>200	>200
	128	112.0 ± 17.4	>200	195.3 ± 22.6	>200
	183	>200	152.2 ± 33.6	>200	>200
	184	>200	172.2 ± 31.4	>200	>200
	185	>200	>200	>200	>200
	186	>200	>200	>200	>200
	187	114.7 ± 18.3	142.5 ± 17.0	>200	>200
	188	>200	153.6 ± 32.7	>200	>200
	189	>200	>200	>200	181.6 ± 35.7
	190	>200	>200	>200	>200
	191	151.4 ± 25.4	>200	159.7 ± 28.5	>200
	Doxy	1.3 ± 0.3	0.7 ± 0.1	16.4 ± 2.9	1.5 ± 0.3

Data are represented as mean ± SEM (n = 3); LC_{50} = sample concentration that caused 50% of cells death

The LC_{50} values of the screened compounds ranged from 29.5 to 138.6 μM (A549), 53.7 to 172.2 μM towards MCF-7 cells, 33.3 to 195.3 μM (PC-3), and 10.6 to 197.7 μM (PNT2). The isolated flavonoids from JHL, PMB and PML were found to have selective effect on PC-3 cells. None of the isolated compounds has shown a significant cytotoxic effect. They have showed moderate or low cytotoxic effect at the tested concentrations. A pure compound to be consider as promising candidate for drug development should have its LC_{50} value below 25 μM (Choudhary and Thomsen, 2003). Among the tested compounds, kaurenoic acid (**175**) and sesamin (**54**) were found to exert reasonable cytotoxicity against PC3 with IC_{50} both about 33 μM. Hesperidin (**59**) and *ent*-kauran-16*β*-ol-19-oic acid (**177**) were the only compounds with wide active spectrum, having effect against all the cell lines tested even on the normal prostate cells PNT2 with IC_{50} 129.0 ± 20.3 and 10.6 ± 3.6 μM, respectively. Hesperidin was the most active compound with IC_{50} 29.5 ± 7.5, 74.2 ± 17.8 and 51.7 ± 8.7 μM against A549, MCF-7 and PC3, respectively.

3.5.2 Chemopreventive activity of isolated compounds

3.5.2.1 Cytotoxicity of the compounds against AREc32 cells

Compounds isolated from plants extracts, which have shown potent chemopreventive properties, were screened to assess their chemopreventive property by evaluating their effect on the activation of the level of luciferase in AREc32 cells. This include compounds isolated from *C. oligandrus* and *Z. zanthoxyloides*. The toxicity of the compounds on the viability of AREc32 cells was first determined by the MTT assay to find a suitable concentration at which to conduct the following luciferase assay which would not cause significant cell death (concentrations causing more than 10% cell death, relative to control were not used, Table 3.22).

Table 3.22 Least toxic concentration (no more than 10% cells death) of isolated compounds against AREc32 cells

C. oligandrus				*Z. zanthoxyloides*			
Cpds	LC_{10} (μM)	Cpds	LC_{10} (μM)	Cpds	LC_{10} (μM)	Cpds	LC_{10} (μM)
7	6.0	**153**	12.5	**54**	6.0	**185**	12.5
8	12.5	**154**	12.5	**55**	6.0	**186**	12.5
147	25.0	**156/157**	6.0	**59**	6.0	**187**	6.0
148	25.0	**158/159**	6.0	**79**	25.0	**188**	6.0
149/150	25.0	**160**	25	**128**	25.0	**189**	6.0
151	6.0	**161**	6.0	**183**	12.5	**190**	25.0
152	6.0	**162**	6.0	**184**	12.5	**191**	12.5

3.5.2.2 Luciferase activity

The luciferase activity was measured using the Steady-Glo luciferase kit provided by Promega Corp. After the exposure of AREc32 cells for 24 h to *t*BHQ 6 and 12 μM, the activity of luciferase increased by 2.51 and 7.37-fold compared to the control (Figure 3.105). Among the tested compounds, the mixtures of epimeric clerodanes **156**/**157** and **158**/**159** (crotonolins A-D), skimmianine (**55**), hesperidin (**79**) and myrtopsine (**185**) were found to produce 2.7, 2.4, 2.4, 1.8 and 2.0-fold induction, respectively. Other tested compounds had slight or negligible effects on the luciferase activity at the dosage tested. The results suggested the above active compounds might be potential activators of the NrF2 pathway, meaning potent chemopreventive compounds at non cytotoxic dosages. The diterpenes **156-159** were the most activitors of the Nrf2 activity. Their activities were comparable to that *t*BHQ when tested at the same concentration. Several diterpenes including clerodanes have been reported to possess cytoprotective and cytotoxic

properties (Thoppil and Bishayee, 2011; Islam, 2017). For example, the clerodane columbin has been revealed to have chemoproventive activity against colorectal cancer when administered as a diet to male rats in the early phase of azoxymethane-induced colon carcinogenesis (Kohno *et al.*, 2002). Therefore, clerodanes, represent an interesting group of compounds to explore for the discovery of cancer chemopreventive agents.

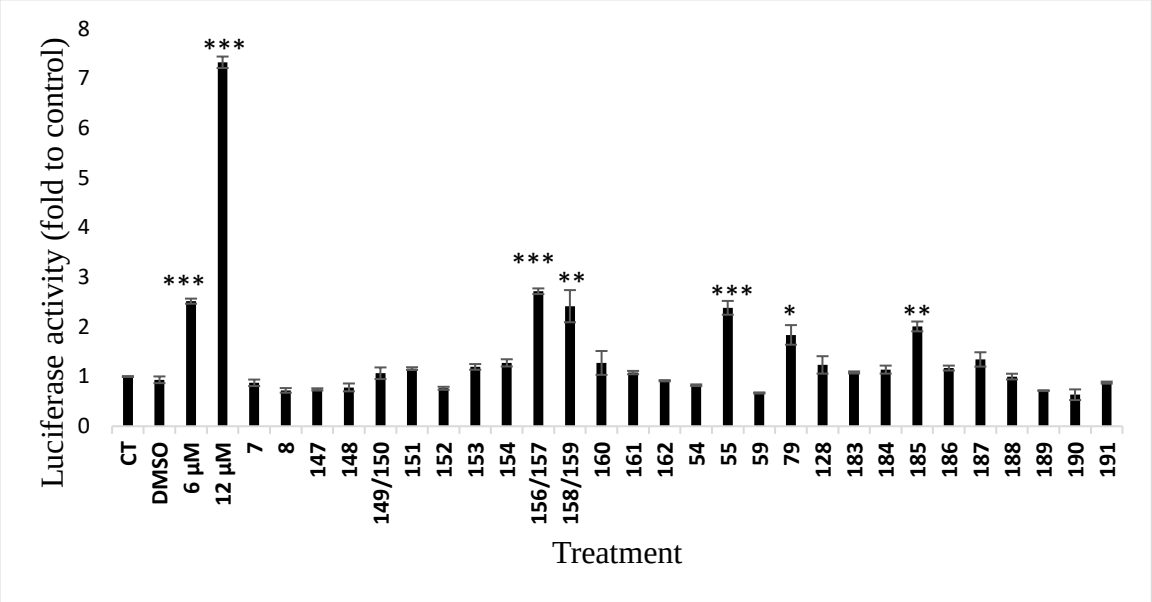

Figure 3.105 Luciferase activity of isolated compounds

AREc32 cells were seeded in 96-well plates at 1.2 x 10^4 cells/well. After 24 h, *t*BHQ (6 and 12 µM) and the compounds were added to the medium. The cells were then incubated for another 24 h and assayed for luciferase activity as detailed in Chapter 2, 2.4.4. The value of luciferase activity of untreated cells (CT) was set at 1. Values shown are mean ± SEM of three experiments. *$p < 0.01$; **$p < 0.001$, ***$p < 0.0001$, significantly increased versus control. DMSO 0.1%: (cells treated with 0.1% DMSO medium).

3.5.3 Haem polymerisation assay of the isolated compounds

The isolated compounds from extracts, which have shown antimalarial activity, were screened to evaluate their antimalarial potential using haem polymerisation assay.

Quinoline antimalarials in use today, such as chloroquine, mefloquine and quinine, have been reported to act in the erythrocytic stage of the parasite life cycle by blocking the polymerisation of free haem generated during haemoglobin digestion to its polymer haemozoin, a step which is essential for the parasite survival (Foley and Tilley, 1998). None of the isolated compounds have demonstrated an effect at the tested concentration (0-250 µM). These compounds included the diterpenes isolated from *C. oligandrus* and *Z. leprieurii*, and flavonoids from *J. hypocrateriformis* and *P. microcarpa*. These results were not consistent with our early finding regarding the activity associated with the extracts from which the compounds have been isolated. However, as previously noted, the activity of an extract is the result of different interactions occurring between the chemical constituents within the extract. In addition, the isolated compounds might not be iron chelators making it difficult to bind with haem via the ion present at its center (Sarker *et al.*, 2016), hence their inactivity.

Chapter 4 Conclusion and Future Prospects

4. Conclusion and future prospects

Bioassay-guided isolation of active compounds was carried out with five Cameroonian medicinal plants, including *Croton oligandrus* Pierre ex Hutch (Euphorbiaceae), *Justicia hypocrateriformis* (Vahl) Milne-Redh (Acanthanceae), *Pseudospondias microcarpa* (A. Rich.) Engl. (Anacardiaceae), *Zanthoxylum lepreurii* Guill. and Perr. and *Zanthoxylum zanthoxyloides* (Lam.) Zepern. and Timler (Rutaceae).

The *n*-hexane and the DCM extracts of *Croton oligandrus* bark, and the DCM and MeOH extracts of *Z. zanthoxyloides* fruits were active in the luciferase assay causing 18, 21, 34 and 36-fold induction of the level of luciferase in AREc32 cells, respectively. The diterpenes crotonolins A-D, isolated from the DCM extract of *C. oligandrus* were identified as the most active principle of the plant with 2-fold or greater. From *Z. zanthoxyloides*, skimmianine isolated from both the DCM and MeOH extracts, and hesperidin and myrtopsine isolated from the MeOH extract, increased the level of luciferase by 2.4, 1.8 and 2.0-fold, respectively.

The antimalarial activity of the selected plants was evaluated using the haem polymerisation assay. *Pseudospondias microcarpa* was the most active plant with IC_{50} 73.9 ± 25.8, 2.5 ± 1.5 and 4.0 ± 1.7 µM for the stem bark *n*-hexane, DCM and MeOH extracts, respectively, and 13.0 ± 9.0 µM for the leaves MeOH extract. No inhibition of haem polymerisation was observed for the isolated compounds at the assayed concentrations.

Three major classes of phytochemicals including alkaloids, diterpenes and flavonoids were isolated from the five plants studied. Some of the compounds, 12-*epi*-megalocarpoloide D (**154**), crotonolins A-F (**155-160**), justicialosides A and B (**166-167**) and zanthoamides G-I (**188-190**) were being reported for the first time from natural sources. Kaurane diterpenes were reported for the first time from the genus *Zanthoxylum*

and the quinoline alkaloids *N*-methylplatydesminium cation (**183**), isoplatydesmine (**184**), myrtopsine (**185**), ribalinine (**186**) and *N*-methylatanine (**187**) from the species *Z. zanthoxyloides* for the first time. Other isolated compounds included two triterpenes, acetyl aleuritolic acid (**7**) and lupeol (**8**); two lignans, sesamine (**54**) and icariside D2 (**183**); ferulic acid derivatives (**114**, **147-150**); a quindoline, 10*H*-quindoline (**169**); a coumarin, scopoletin (**103**); and a chromanone, pithecellobiumol B (**174**). The cytotoxicity of all the isolated compounds were evaluated against three cancer cell lines (A549, MCF7 and PC3) and a non cancer cell line (PNT2). Hesperidin (**59**) was the most cytotoxic compound with LC_{50} 29.5 ± 7.5, 74.2 ± 17.8, 51.7 ± 8.7 and 129.0 ± 20.3 µM against A549, MCF7, PC3 and PNT2, respectively.

This study generated the first, second and third phytochemical report of *P. microcarpa*, *C. oligandrus* and *J. hypocrateriformis*, respectively. The chemotaxonomy of the isolated compounds has also been discussed. *J. hypocrateriformis* and *J. secunda* were observed to have similar compounds and should be investigated further to establish whether the two names refer to the same species, and kaurane diterpenes were identified as new markers of *Z. leprieurii*.

This study also supports the use of *C. oligandrus* and *Z. zanthoxylum* as alternative and complementary medicine for the treatment and prevention of cancer, and *P. microcarpa* for the treatment of malaria. However, further studies need to be carried out to define standardised dosage as those plants were found to contain moderate cytotoxic compounds against the human normal prostate epithelium cells (PNT2).

Future studies may involve:

- chemical modification of active compounds as well as the novel compounds and evaluation of the activity of obtained analogues;

- investigation of the mechanism of action of chemopreventive extracts and compounds identified;
- investigation of the antimalarial activity of isolated compounds using a different assay e.g. *in vitro* against parasites;
- investigation of synergism, antagonism and additive interactions as a contributor to activity of crude plant extracts specially those active in the antimalarial assay.

References

Abdul-Ghani, R., Farag, H.F. and Allam, A.F. (2013). Sulfadoxine-pyrimethamine resistance in *Plasmodium falciparum*: A zoomed image at the molecular level within a geographic context. *Acta Tropica*, 125(2), 163-190.

Abega, D.F., Kapche, D.W.F.G., Ango, P.Y., Mapitse, R., Yeboah, S.O. and Ngadjui, B.T. (2014). Chemical Constituents of *Croton oligandrum* (Euphorbiaceae). *Zeitschrift für Naturforschung C*, 69, 5-6.

Abu-Reidah, I. M., Ali-Shtayeh, M. S., Jamous, R. M., Arraez-Roman, D. and Segura-Carretero, A. (2015). HPLC–DAD–ESI-MS/MS screening of bioactive components from *Rhus coriaria* L. (Sumac) fruits. *Food Chemistry*, 166, 179-191.

Achan, J., Talisuna, A.O., Erhart, A., Yeka, A., Tibenderana, J.K., Baliraine, F.N., Rosenthal, P.J. and D'Alessandro, U. (2011). Quinine, an old anti-malarial drug in a modern world: role in the treatment of malaria. *Malaria Journal*, 10(1), 144.

Adamska-Szewczyk, A., Glowniak, K. and Baj, T. (2016). Furochinoline alkaloids in plants from Rutaceae family - a review. *Current Issues in Pharmacy and Medical Sciences*, 29(1), 33-38.

Adekunle, A. S., Kamdem, J. and Rocha, J. B. (2012). Antioxidant activity and HPLC analysis of *Zanthoxylum zanthoxyloides*. *Report and Opinion*, 4, 6-13.

Adesanya, S. and Sofowora, A. (1983). Biological Standardisation of *Zanthoxylum* Roots for Antisickling Activity. *Planta Medica*, 48(05), 27-33.

Adesina, S. (2006). The Nigerian *Zanthoxylum*; chemical and biological values. *African Journal of Traditional, Complementary and Alternative Medicines (AJTCAM)*, 2 (3), 282-301.

Adjanohoun, J. E., Ahyi, M. R. A., Ake Assi, L., Alia, A. M., Amai, C. A., Gbile, Z. O. and Morakinyo, O. (1993). Contribution to ethnobotanical and floristic studies in Uganda. Organization of African Unity: Scientific Technical and Research Commission.

Adjanohoun, J., Aboubakar, N., Dramane, K., Ebot, M., Ekpere, J., Enow-Orock, E., Focho, D., Gbile, Z., Kamanyi, A. and Kamsu-Kom, J. (1996). Traditional medicine and pharmacopoeia: contribution to ethnobotanical and floristic studies in Cameroon. *OUA/STRC: Lagos*, 301.

Adongo, D.W., Kukuia, K.K.E., Mante, P.K., Ameyaw, E.O. and Woode, E. (2015). Antidepressant-like effect of the leaves of *Pseudospondias microcarpa* in mice: Evidence for the involvement of the serotoninergic system, NMDA receptor complex, and nitric oxide pathway. *BioMed Research International*, 1-15.

Adongo, D.W., Mante, P.K., Edem Kukuia, K.K., Ameyaw, E.O., Woode, E. and Azi, I.H. (2016). Anxiolytic-like effect of the leaves of *Pseudospondias microcarpa* (A. Rich.) Engl. in mice. *Journal of Basic and Clinical Physiology and Pharmacology*, 27(5).

Agbor, G.A., Longo, F., Makong, E.A. and Tarkang, P.A. (2014). Evaluation of the antidiarrheal and antioxidant properties of *Justicia hypocrateriformis*. *Pharmaceutical Biology*, 52(9), 1128-1133.

Aggarwal, B.B., Takada, Y. and Oommen, O.V. (2004). From chemoprevention to chemotherapy: common targets and common goals. *Expert Opinion on Investigational Drugs*, 13(10), 1327-1338.

Agnaniet, H., Akagah, A., Mounzéo, H., Menut, C. and Bessière, J. M. (2005). Aromatic plants of tropical central Africa. XLI. Volatile constituents of *Croton oligandrum* Pierre ex Hutch growing in Gabon. *Journal of Essential Oil Research*, 17(2), 201-203

Agrawal, P. K. (1992). NMR spectroscopy in the structural elucidation of oligosaccharides and glycosides. *Phytochemistry*, 31(10), 3307-3330.

Agyare, C., Asase, A., Lechtenberg, M., Niehues, M., Deters, A. and Hensel, A. (2009). An ethnopharmacological survey and *in vitro* confirmation of ethnopharmacological use of medicinal plants used for wound healing in Bosomtwi-Atwima-Kwanwoma area, Ghana. *Journal of Ethnopharmacology*, 125(3), 393-403.

Akpona, H.A., Akpona, J.D.T., Awokou, S.K., Yemoa, A. and Dossa, L.O.S.N. (2009) Inventory, folk classification and pharmacological properties of plant species used as chewing stick in Benin Republic. *Journal of Medicinal Plants Research*, 3(5), 382-389.

Aloke, C., Ngwu, N., Ugwuja, E., Idenyi, J., Nwachi, O. and Oga, I.O. (2012). Effects of *Zanthoxylum zanthoxyloides* leaves on blood glucose, lipid profile and some liver enzymes in alloxan induced diabetic rats. *International Journal of Science and Nature*, 3, 497-501.

Amin, A.R.M.R., Kucuk, O., Khuri, F.R. and Shin, D.M. (2009). Perspectives for cancer prevention with natural compounds. *Journal of Clinical Oncology*, 27(16), 2712-2725.

Arbonnier, M. (2004). Trees, shrubs and lianas of West African dry zones. Editions Quae.

Aubréville, A. (1950). Flore forestière soudano-guinéenne: AOF, Cameroun, AEF.

Baldé, A. M., Claeys, M., Pieters, L. A., Wray, V. and Vlietinck, A. J. (1991). Ferulic acid esters from stem bark of *Pavetta owariensis*. *Phytochemistry*, 30(3), 1024-1026.

Balunas, M.J. and Kinghorn, A.D. (2005). Drug discovery from medicinal plants. *Life Sciences*, 78(5), 431-441.

Barnabas, B. B., Mann, A., Ogunrinola, T. S. and Anyanwu, P. E. (2010). Screening for Anthelminthic activities from extracts of *Zanthoxylum zanthoxyloides*, N*eocarya macrophylla* and *Celosia laxa* against *ascaris* infection in rabbits. *International Journal of Applied Research in Natural Products*, 3(4), 1-4.

Bautista, E., Maldonado, E. and Ortega, A. (2012). Neo-clerodane diterpenes from *Salvia herbacea*. *Journal of Natural Products*, 75(5), 951-958.

Beaufay, C., Bero, J. and Quetin-Leclercq, J. (2018). *Antimalarial Terpenic Compounds Isolated from Plants Used in Traditional Medicine (2010–July 2016). Sustainable Development and Biodiversity*: Springer International Publishing**:** 247-268.

Beier, R. C., Mundy, B. P. and Strobel, G. A. (1980). Assignment of anomeric configuration and identification of carbohydrate residues by ^{13}C NMR. 1. Galacto-and glucopyranosides and furanosides. *Canadian Journal of Chemistry*, 58(24), 2800-2804.

Bero, J. and Quetin-Leclercq, J. (2010). Natural products published in 2009 from plants traditionally used to treat malaria. *Planta Medica*, 77(06), 631-640.

Berry, P.E., Hipp, A.L., Wurdack, K.J., Van Ee, B. and Riina, R. (2005). Molecular phylogenetics of the giant genus *Croton* and tribe Crotoneae (Euphorbiaceae sensu stricto) using ITS and TRNL-TRNF DNA sequence data. *American Journal of Botany*, 92(9), 1520-1534.

Betti, J. (2013). An ethnobotanical and floristical study of medicinal plants among the Baka Pygmies in the periphery of the Ipassa- Biosphere Reserve, Gabon. *European Journal of Medicinal Plants*, 3(2), 174-205.

Billet, D., Durgeat, M., Heitz, S., Brouard, J. P. and Ahond, A. (1976). Constituants d'*Evodia floribunda* baker. II-1ère Partie. L'acide floridiolique, nouveau diterpene de type clerodane. *Tetrahedron Letters*, 17(32), 2773-2776.

Blas, B., Zapp, J. and Becker, H. (2004). *ent*-Clerodane diterpenes and other constituents from the liverwort *Adelanthus lindenbergianus* (Lehm.) Mitt. *Phytochemistry*, 65(1), 127-137.

Bloland, P.B. and Organization, W.H. (2001). Drug resistance in malaria.

Boiteau, P. (1964). Triterpénoïdes en physiologie végétale et animale.

Boyd, D. R. and Grundon, M. F. (1967). Quinoline alkaloids of *skimmia Japonica* thunb. *Tetrahedron Letters*, 8(28), 2637-2638.

Boyd, D. R., Sharma, N. D., Barr, S. A., Carroll, J. G., Mackerracher, D. and Malone, J. F. (2000). Synthesis and absolute stereochemistry assignment of enantiopure dihydrofuro-and dihydropyrano-quinoline alkaloids. *Journal of the Chemical Society, Perkin Transactions, 1*(20), 3397-3405.

Boyd, D. R., Sharma, N. D., Loke, P. L., Malone, J. F., McRoberts, W. C. and Hamilton, J. T. (2007). Synthesis, structure and stereochemistry of quinoline alkaloids from *Choisya ternata*. *Organic and Biomolecular Chemistry*, 5(18), 2983-2991.

Boyd, M.R., Hallock, Y.F., Cardellina, J.H., Manfredi, K.P., Blunt, J.W., McMahon, J.B., Buckheit, R.W., Bringmann, G., Schäffer, M., Cragg, G.M., Thomas, D.W. and Jato, J.G. (1994). Anti-HIV michellamines from *Ancistrocladus korupensis*. *Journal of Medicinal Chemistry*, 37(12), 1740-1745.

Boye, A., Koffuor, G. A., Boampong, J. N., Amoateng, P., Ameyaw, E. O., Owusu Ansah, E. and Penu, D. K. A. (2012). Gastroprotective effect and safety assessment of *Zanthoxylum Zanthoxyloides* (Lam) Waterm root bark extract. *American Journal of Pharmacology and Toxicology*, 7(2), 73-80.

Breitmaier, E. and Sinnema, A. (1993). Structure elucidation by NMR in organic chemistry: A practical guide. First edition, Wiley and Sons Ltd. West Sussex, England.

Brown, N. M. D., Grundon, M. F., Harrison, D. M. and Surgenor, S. A. (1980). Quinoline alkaloids-XXI1: the 13C NMR spectra of hemiterpenoid quinoline alkaloids and related prenylquinolines. *Tetrahedron*, 36(24), 3579-3584.

Bruce-Chwatt, L. J., Black, R. H., Canfield, C. J., Clyde, D. F., Peters, W., Wernsdorfer, W. H. and World Health Organization. (1986). Chemotherapy of malaria.

Bruno, E. (2013). Research in clinical phytopharmacology to develop health care in developing countries: State of the art and perspectives. *Phytopharmacology*, 4(2), 149-205.

Bruneton, J. (1999). Pharmacognosie, phytochimie–plantes médicinales–3ème Ed Techniques et documentations. Paris.

Bryan, H.K., Olayanju, A., Goldring, C.E. and Park, B.K. (2013). The Nrf2 cell defence pathway: Keap1-dependent and-independent mechanisms of regulation. *Biochemical Pharmacology*, 85(6), 705-717.

Bunalema, L., Fotso, G.W., Waako, P., Tabuti, J. and Yeboah, S.O. (2017). Potential of *Zanthoxylum leprieurii* as a source of active compounds against drug resistant *Mycobacterium tuberculosis*. *BMC Complementary and Alternative Medicine*, *17*(1).

Burch, D. G. and Demmy, E. W. (1986). Acanthaceae in Florida Gardens. *Proceedings of the Florida State Horticultural Society*, 99, 186 - 188.

Burkill, H.M. (1985). The useful plants of west tropical Africa. Edition 2. Vol. 1: families AD. *Kew, Royal Botanic Gardens*.

Cairns, J. (1981). The origin of human cancers. *Nature*, *289*(5796), 353-357.

Cannon, J. R., Chow, P. W., Jefferies, P. R. and Meehan, G. V. (1966). Isolation of (-)-Kaur-16-en-19-oic acid and 15*β*-Hydroxy-(–)-kaur-16-en-l9-oic acid from *Phebalium* rude Bartl. *Australian Journal of Chemistry*, 19(5), 861-867.

Carvalho, B. O., Lopes, S. C., Nogueira, P. A., Orlandi, P. P., Bargieri, D. Y., Blanco, Y. C. and Oliveira, T. R. (2010). On the cytoadhesion of *Plasmodium vivax*-infected erythrocytes. *The Journal of Infectious Diseases*, 202(4), 638-647.

Chaaib, F., Queiroz, E.F., Ndjoko, K., Diallo, D. and Hostettmann, K. (2003). Antifungal and antioxidant compounds from the root bark of *Fagara zanthoxyloides*. *Planta Medica*, 69(4), 316-320.

Chang Huang, K. (1998). *The Pharmacology of Chinese Herbs, Second Edition*. CRC Press.

Chakravarty, A. K., Sarkar, T., Masuda, K. and Shiojima, K. (1999). Carbazole alkaloids from roots of *Glycosmis arborea*. *Phytochemistry*, 50(7), 1263-1266.

Chavatte, J.M., Chiron, F., Chabaud, A. and Landau, I. (2007). Fidélisation du couple hôte-vecteur facteur probable de spéciation: 14 espèces de *Plasmodium* de la Pie. *Parasite*, 14(1), 21-37.

Chen, C. and Kong, A. N. T. (2004). Dietary chemopreventive compounds and ARE/EpRE signaling. *Free Radical Biology and Medicine*, *36*(12), 1505-1516.

Cheng, M. J., Wu, C. C., Tsai, I. L. and Chen, I. S. (2004). Chemical and antiplatelet constituents from the stem of *Zanthoxylum beecheyanum*. *Journal of the Chinese Chemical Society*, 51(5A), 1065-1072.

Cheng, T., Li, Q., Zhou, Z., Wang, Y. and Bryant, S.H. (2012). Structure-based virtual Screening for Drug Discovery: a Problem-Centric Review. *The AAPS Journal*, 14(1), 133-141.

Cheung, H. A., Miyase, T., Lenguyen, M. P. and Smal, M. A. (1993). Further acidic constituents and neutral components of *Pinus massoniana* resin. *Tetrahedron*, 49(36), 7903-7915

Chen, K.L. and Kong, A.N., 2010. Molecular targets of dietary phenethyl isothiocyanate and sulforaphane for cancer chemoprevention. *The AAPS Journal*, 12(1), 87-97.

Cheung-Ong, K., Giaever, G. and Nislow, C. (2013). DNA-damaging agents in cancer chemotherapy: Serendipity and chemical biology. *Chemistry and Biology*, 20(5), 648-659.

Chlebowski, R.T. (2015). IBIS-I tamoxifen update: maturity brings questions. *The Lancet Oncology*, 16(1), 7-9.

Choudhary, M. I. and Thomsen, W. J. (2003). Bioassay techniques for drug development. CRC Press.

Choumessi, A.T., Loureiro, R., Silva, A.M., Moreira, A.C., Pieme, A.C., Tazoacha, A., Oliveira, P.J. and Penlap, V.B. (2012). Toxicity evaluation of some traditional African spices on breast cancer cells and isolated rat hepatic mitochondria. *Food and Chemical Toxicology*, 50(11), 4199-4208.

Chruma, J. J., Cullen, D. J., Bowman, L. and Toy, P. H. (2018). Polyunsaturated fatty acid amides from the *Zanthoxylum* genus–from culinary curiosities to probes for chemical biology. *Natural Product Reports*, 35(1), 54-74.

Clyde, D.F., Hlaing, N. and Tin, F. (1972). Resistance to chloroquine of *Plasmodium falciparum* from Burma. *Transactions of the Royal Society of Tropical Medicine and Hygiene*, 66(2), 369-370.

Cohen, S.M. and Ellwein, L.B. (1995). Relationship of DNA adducts derived from 2-acetylaminofluorene to cell proliferation and the induction of rodent liver and bladder tumors. *Toxicologic Pathology*, 23(2), 136-142.

Cordell, G.A., Farnsworth, N.R., Beecher, C.W.W., Soejarto, D.D., Kinghorn, A.D., Pezzuto, J.M., Wall, M.E., Wani, M.C., Brown, D.M., O'Neill, M.J., Lewis, J.A., Tait, R.M. and Harris, T.J.R. (1993). *Novel Strategies for the Discovery of Plant-Derived Anticancer Agents.ACS Symposium Series*: American Chemical Society**:** 191-204.

Coronado, L. M., Nadovich, C. T. and Spadafora, C. (2014). Malarial hemozoin: from target to tool. *Biochimica and Biophysica Acta (BBA)-General Subjects*, 1840(6), 2032-2041.

Corral, R. A. and Orazi, O. O. (1967). Isolation, structure and synthesis of (±)-ribalinine. *Tetrahedron Letters*, 8(7), 583-585.

Correa, G. M. and Alcantara, A. F. D. C. (2012). Chemical constituents and biological activities of species of Justicia: a review. *Revista Brasileira de Farmacognosia*, 22(1), 220-238.

Counts, J.L. and Goodman, J.I. (1994). Hypomethylation of DNA: An epigenetic mechanism involved in tumor promotion. *Molecular Carcinogenesis*, 11 (4), 185-188.

Cowman, A.F. and Crabb, B.S. (2006). Invasion of red blood cells by malaria parasites. *Cell*, 124(4), 755-766.

Cox, F.E.G. (2010). History of the discovery of the malaria parasites and their vectors. *Parasites and Vectors*, 3(1), 5.

Cragg, G.M. and Newman, D.J. (2005a). Biodiversity: A continuing source of novel drug leads. *Pure and Applied Chemistry*, 77(1), 7-24.

CR-UK (2018). http://www.cancerresearchuk.org/health-professional/cancer-statistics-for-the-uk accessed on 3/04/2018

Cragg, G.M. and Newman, D.J. (2005b). Plants as a source of anticancer agents. *Journal of Ethnopharmacology*, 100(1-2), 72-79.

Cragg, G.M., Schepartz, S.A., Suffness, M. and Grever, M.R. (1993). The Taxol supply crisis. New NCI policies for handling the large-scale production of novel natural product anticancer and anti-HIV agents. *Journal of Natural Products*, 56(10), 1657-1668.

Crews, P., Rodriquez, J., Jaspars, M. and Crews, R. J. (1998). Organic Structure Analysis. Second Edition, Oxford University Press. New York, USA

Daily, J.P. (2006) Antimalarial drug therapy: The role of parasite biology and drug resistance. *The Journal of Clinical Pharmacology*, 46(12), 1487-1497.

Darmawan, A., Kosela, S., Kardono, L. B. and Syah, Y. M. (2012). Scopoletin, a coumarin derivative compound isolated from *Macaranga gigantifolia* Merr. *Journal of Applied Pharmaceutical Science*, 2(12), 175.

Deachathai, S., Mahabusarakam, W., Phongpaichit, S. and Taylor, W. C. (2005). Phenolic compounds from the fruit of *Garcinia dulcis*. *Phytochemistry*, 66(19), 2368-2375.

De Albuquerque, U.P. and Hanazaki, N. (2009). Five problems in current ethnobotanical research and some suggestions for strengthening them. *Human Ecology*, 37(5), 653-661.

Denis, M. B., Tsuyuoka, R., Poravuth, Y., Narann, T. S., Seila, S., Lim, C. and Christophel, E. M. (2006). Surveillance of the efficacy of artesunate and mefloquine combination for the treatment of uncomplicated falciparum malaria in Cambodia. *Tropical Medicine and International Health*, 11(9), 1360-1366.

Devi, P.U. (2004) Basics of carcinogenesis. *Health Administrator*, 17(1), 16-24.

Dhanasekaran, M., Baskar, A. A., Ignacimuthu, S., Agastian, P. and Duraipandiyan, V. (2009). Chemopreventive potential of Epoxy clerodane diterpene from *Tinospora cordifolia* against diethylnitrosamine-induced hepatocellular carcinoma. *Investigational New Drugs*, 27(4), 347-355.

Dias, D.A., Urban, S. and Roessner, U. (2012). A historical overview of natural products in drug discovery. *Metabolites*, 2 (2), 303-336.

DiMasi, J.A., Hansen, R.W., Grabowski, H.G. and Lasagna, L. (1991). Cost of innovation in the pharmaceutical industry. *Journal of Health Economics*, 10(2), 107-142.

Dinan, L. (2006). Dereplication and partial identification of compounds. In: (ed.) *Natural Products Isolation.* Springer. pp. 297-321.

Dinkova-Kostova, A.T. and Kostov, R.V., 2012. Glucosinolates and isothiocyanates in health and disease. *Trends in Molecular Medicine*, 18(6), 337-347.

Dreyer, D. L. and Park, K. H. (1975). Flavones and diterpenes of *Pamburus missionis* (rutaceae). *Phytochemistry*, 14(7), 1617-1620.

Duke, J.A. (1992). *Handbook of Biologically Active Phytochemicals and Their Activities*. CRC Press, Inc.

Edeoga, H.O., Okwu, D.E. and Mbaebie, B.O. (2005). Phytochemical constituents of some Nigerian medicinal plants. *African Journal of Biotechnology*, 4(7), 685-688.

Egan, T.J., Mavuso, W.W. and Ncokazi, K.K. (2001). The mechanism of β-hematin formation in acetate solution, parallels between hemozoin formation and biomineralization processes. *Biochemistry*, 40(1), 204-213.

Egan, T.J., Ross, D.C. and Adams, P.A. (1994). Quinoline anti-malarial drugs inhibit spontaneous formation of β-haematin (malaria pigment). *FEBS Letters*, 352(1), 54-57.

Ekor, M. (2014). The growing use of herbal medicines: issues relating to adverse reactions and challenges in monitoring safety. *Frontiers in Pharmacology*, 4, 177.

El-Shafae, A. M. (2002). Bioactive polymethoxyflavones and flavanone glycosides from the peels of *Citrus deliciosa*. *The Chinese Pharmaceutical Journal*, 54(3), 199-206.

El-Shafae, A. M. and Ibrahim, M. A. (2003). Bioactive kaurane diterpenes and coumarins from *Fortunella margarita*. *Die Pharmazie-An International Journal of Pharmaceutical Sciences*, 58(2), 143-147.

Elujoba, A.A. and Nagels, L. (1985). Chromatographic isolation and estimation of zanthoxylol: An antisickling agent from the roots of *Zanthoxylum* species. *Journal of Pharmaceutical and Biomedical Analysis*, 3(5), 447-451.

Eshiett, I. T. and Taylor, D. A. H. (1968). The isolation and structure elucidation of some derivatives of dimethylallyl-coumarin, chromone, quinoline, and phenol from *Fagara* species, and from *Cedrelopsis grevei*. *Journal of the Chemical Society C: Organic*, 481-484.

Ermert, V., Fink, A.H., Morse, A.P. and Paeth, H. (2011). The impact of regional climate change on malaria risk due to greenhouse forcing and land-use changes in tropical Africa. *Environmental Health Perspectives*, 120(1), 77-84.

Endringer, D. C., Taveira, F. S., Kondratyuk, T. P., Pezzuto, J. M. and Braga, F. C. (2014). Cancer chemoprevention activity of labdane diterpenes from rhizomes of *Hedychium coronarium*. *Revista Brasileira de Farmacognosia*, 24(4), 408-412.

Epifano, F., Curini, M., Carla Marcotullio, M. and Genovese, S. (2011). Searching for novel cancer chemopreventive plants and their products: the genus *Zanthoxylum*. *Current Drug Targets, 12(13), 1895-1902.*

Etkin, N.L. (1993). Anthropological methods in ethnopharmacology. *Journal of Ethnopharmacology*, 38(2-3), 91.

Fabricant, D.S. and Farnsworth, N.R. (2001). The value of plants used in traditional medicine for drug discovery. *Environmental Health Perspectives*, 109 (s1), 69-75.

Fang, Z., Jun, D. Y., Kim, Y. H., Min, B. S., Kim, A. K. and Woo, M. H. (2010). Cytotoxic constituents from the leaves of *Zanthoxylum schinifolium*. *Bulletin of the Korean Chemical Society*, 31(4), 1081-1084.

Fankam, A.G., Das, R., Mallick, A., Kuiate, J.R., Hazra, B., Mandal, C. and Kuete, V. (2017). Cytotoxicity of the extracts and fractions from *Allanblackia gabonensis* (Clusiaceae) towards a panel of cancer cell lines. *South African Journal of Botany*, 111, 29-36.

Farnsworth, N.R., Akerele, O., Bingel, A.S., Soejarto, D.D. and Guo, Z. (1985). Medicinal plants in therapy. *Bulletin of the world health organization*, 63 (6), 965.

Ferlay, J., Soerjomataram, I., Ervik, M., Dikshit, R., Eser, S., Mathers, C., Rebelo, M., Parkin, D., Forman, D. and Bray, F. (2013). *Globocan. 2012. Cancer incidence and mortality worldwide: IARC CancerBase No. 11. Lyon, France: International Agency for Research on Cancer*.

Fink, D.J. (1979). Cancer overview. *Cancer research*, 39 (7 Pt 2), 2819-2821.

Fish, F. and Waterman, P.G. (1972a). Lirioresinol-B-dimethyl ether from the bark of *Fagara leprieurii*. *Phytochemistry*, 11(4), 1527-1528.

Fish, F. and Waterman, P.G. (1972b). Methanol-soluble quaternary alkaloids from African *Fagara* species. *Phytochemistry*, 11(10), 3007-3014.

Fish, F. and Waterman, P. (1973). Chemosystematics in the Rutaceae II. The Chemosystematics of the *Zanthoxylum*/*Fagara* Complex. *Taxon*, 22(2/3), 177-203

Fogang, H.P.D., Tapondjou, L.A., Womeni, H.M., Quassinti, L., Bramucci, M., Vitali, L.A., Petrelli, D., Lupidi, G., Maggi, F., Papa, F., Vittori, S. and Barboni, L. (2012). Characterization and biological activity of essential oils from fruits of *Zanthoxylum xanthoxyloides* Lam. and Z. *leprieurii* Guill. and Perr., two culinary plants from Cameroon. *Flavour and Fragrance Journal*, 27(2), 171-179.

Foley, M. and Tilley, L. (1997). Quinoline antimalarials: Mechanisms of action and resistance. *International Journal for Parasitology*, 27 (2), 231-240.

Foley, M. and Tilley, L. (1998). Quinoline antimalarials: mechanisms of action, resistance, and prospects for new agents. *Pharmacology and Therapeutics*, 79(1), 55-87.

Ganbaatar, C., Gruner, M., Mishig, D., Duger, R., Schmidt, A. W. and Knölker, H. J. (2015). Flavonoid Glycosides from the Aerial Parts of *Polygonatum odoratum* (Mill.) Druce Growing in Mongolia. *Open Natural Products Journal*, 8, 1-7.

Gansane, A., Sanon, S., Ouattara, P. L., Hutter, S., Ollivier, E., Azas, N. and Sirima, B. S. (2010). Antiplasmodial activity and cytotoxicity of semi purified fractions from *Zanthoxylum zanthoxyloïdes* Lam. bark of trunk. *IJP-International Journal of Pharmacology*, 6(6), 921-925.

Garcia, P. A., De Oliveira, A. B. and Batista, R. (2007). Occurrence, biological activities and synthesis of kaurane diterpenes and their glycosides. *Molecules*, 12(3), 455-483.

Gattuso, G., Barreca, D., Gargiulli, C., Leuzzi, U. and Caristi, C. (2007). Flavonoid composition of citrus Juices. *Molecules*, 12(8), 1641-1673.

Gershenzon, J. and Croteau, R. (1993). *Terpenoid biosynthesis: the basic pathway and formation of monoterpenes, sesquiterpenes, and diterpenes* (Vol. 333). CRC Press, Boca Raton, FL.

Ghosh, A., Das, B.K., Roy, A., Mandal, B. and Chandra, G. (2007). Antibacterial activity of some medicinal plant extracts. *Journal of Natural Medicines*, 62(2), 259-262.

Gibbons S. (2012). An Introduction to Planar Chromatography and Its Application to Natural Products Isolation. In: Sarker S., Nahar L. (eds) Natural Products Isolation. Methods in Molecular Biology (Methods and Protocols), vol 864. Humana Press.

Gotsis, E., Anagnostis, P., Mariolis, A., Vlachou, A., Katsiki, N. and Karagiannis, A. (2015). Health benefits of the Mediterranean diet: an update of research over the last 5 years. *Angiology*, 66(4), 304-318.

Gregson, A. (2005). Mechanisms of resistance of malaria parasites to antifolates. *Pharmacological Reviews*, 57(1), 117-145.

Grundon, M. F. (1988). Quinoline alkaloids related to anthranilic acid. In *The Alkaloids: Chemistry and Pharmacology* (Vol. 32, pp. 341-439). Academic Press.

Grundy, A., Poirier, A.E., Khandwala, F., Grevers, X., Friedenreich, C.M. and Brenner, D.R. (2017). Cancer incidence attributable to lifestyle and environmental factors in Alberta in 2012: summary of results. *CMAJ Open*, 5 (3), E540-E545.

Gullo, V.P. (1994). *PREFACE.Discovery of Novel Natural Products with Therapeutic Potential*: Elsevier**:** xv-xvi.

Happi, G.M., Talontsi, F.M., Laatsch, H., Zühlke, S., Ngadjui, B.T., Spiteller, M. and Kouam, S.F. (2018). *seco* -Tiaminic acids B and C: Identification of two novel 3,4-seco-tirucallane triterpenoids isolated from the root of *Entandrophragma congoënse* (Meliaceae). *Fitoterapia*, 124, 17-22.

Hartwell, J.L. (1971). Plants used against cancer. A survey. *Lloydia*, 34 (2), 204-255.

Hien, N. T. T., Nhiem, N. X., Yen, D. T. H., Hang, D. T. T., Tai, B. H., Quang, T. H. and Kim, S. H. (2015). Chemical constituents of the *Annona glabra* fruit and their cytotoxic activity. *Pharmaceutical Biology*, 53(11), 1602-1607.

Hien, T., Thuy-Nhien, N., Phu, N., Boni, M.F., Thanh, N., Nha-Ca, N., Thai, L., Thai, C., Van Toi, P., Thuan, P., Long, L., Dong, L., Merson, L., Dolecek, C., Stepniewska, K., Ringwald, P., White, N.J., Farrar, J. and Wolbers, M. (2012 In vivo susceptibility of *Plasmodium falciparum* to artesunate in Binh Phuoc Province, Vietnam. *Malaria Journal*, 11(1), 355.

Hoffmann, E., Charette, J. and Stroobant, V. (1996). Mass spectrometry: principles and applications. 1996. Chichester: Wiley, 12(340), 43.

Howes, M.-J.R. (2015) Book Review for the Botanical Journal of the Linnean Society: by Schmelzer, GH and Gurib-Fakim, A (2013). Plant Resources of Tropical Africa. 11(2). Medicinal Plants 2. PROTA Foundation, Wageningen, Netherlands. *Botanical Journal of the Linnean Society*, 179(3), 546-547.

Huang, Z., Chen, G. and Shi, P. (2008). Emodin-induced apoptosis in human breast cancer BCap-37 cells through the mitochondrial signaling pathway. *Archives of Pharmacal Research*, 31(6), 742-748.

Hussain, A. I., Anwar, F., Rasheed, S., Nigam, P. S., Janneh, O. and Sarker, S. D. (2011). Composition, antioxidant and chemotherapeutic properties of the essential oils from two *Origanum* species growing in Pakistan. *Revista Brasileira de Farmacognosia*, 21(6), 943-952.

Igweh, J. and Okwa, O. (2012). Malaria Parasites.

Ikan, R. (1991). Natural products - A laboratory guide. Second Edition, Academic Press, Inc. San Diego, p. 1–22.

Iqbal, J., Abbasi, B.A., Mahmood, T., Kanwal, S., Ali, B., Shah, S.A. and Khalil, A.T. (2017). Plant-derived anticancer agents: A green anticancer approach. *Asian Pacific Journal of Tropical Biomedicine*, 7 (12), 1129-1150.

Ishii, H., Chen, I.S. and Akaike, M. (1982). Studies on the chemical constituents of Rutaceous plants. XLIV. The chemical constituents of *Xanthoxylum integrifoliolum* (MERR.) MERR. (*Fagara integrifoliola* MERR.). I. The chemical constituents of the root wood. *Yakugaku Zasshi*, 102(2), 182-195.

Ishikawa, T., Seki, M., Nishigaya, K., Miura, Y., Seki, H., Chen, I. S. and Ishii, H. (1995). Studies on the chemical constituents of *Xanthoxylum nitidum* (Roxb.) DC (*Fagara nitida* Roxb.). III. The chemical constituents of the wood. *Chemical and Pharmaceutical Bulletin*, 43(11), 2014-2018.

Islam, M. T. (2017). Diterpenes and their derivatives as potential anticancer agents. *Phytotherapy Research*, 31(5), 691-712.

Ivers, L. C. and Ryan, E. T. (2012). Pharmacology of Parasitic Infections. Chp 36. In: Principles of Pharmacology: The Pathophysiologic Basis of Drug Therapy. 3rd Edition. Golan DE *et al* (Eds). Lippincott Williams and Wilkins.

Jaramillo, M.C. and Zhang, D.D. (2013). The emerging role of the Nrf2-Keap1 signaling pathway in cancer. *Genes and Development*, 27(20), 2179-2191.

Jeong, W.-S., Jun, M. and Kong, A.-N.T. (2006). Nrf2: A potential molecular target for cancer chemoprevention by natural compounds. *Antioxidants and Redox Signaling*, 8(1-2), 99-106.

Jiofack, T., Fokunang, C., Guedje, N. and Kemeuze, V. (2009). Ethnobotany and phytomedicine of the upper Nyong valley forest in Cameroon. A*frican Journal of Pharmacy and Pharmacology*, 3(4), 144-150.

Kappe, S.H.I., Vaughan, A.M., Boddey, J.A. and Cowman, A.F. (2010). That was then but this is now: Malaria research in the time of an eradication agenda. *Science*, 328(5980), 862-866.

Kassim, O. O., Loyevsky, M., Elliott, B., Geall, A., Amonoo, H. and Gordeuk, V. R. (2005). Effects of root extracts of *Fagara zanthoxyloides* on the in vitro growth and stage distribution of Plasmodium falciparum. *Antimicrobial Agents and Chemotherapy*, 49(1), 264-268.

Kato, A., Moriyasu, M., Ichimaru, M., Nishiyama, Y., Juma, F. D., Nganga, J. N. and Ogeto, J. O. (1996). Isolation of alkaloidal constituents of *Zanthoxylum usambarense* and *Zanthoxylum chalybeum* using ion-pair HPLC. *Journal of Natural Products*, 59(3), 316-318.

Kaur, K., Jain, M., Kaur, T. and Jain, R. (2009). Antimalarials from nature. *Bioorganic and Medicinal Chemistry*, 17(9), 3229-3256.

Kayser, O. and Kolodziej, H. (1995). Highly oxygenated coumarins from *Pelargonium sidoides*. *Phytochemistry*, 39(5), 1181-1185.

Kisangau, D. P., Lyaruu, H. V., Hosea, K. M. and Joseph, C. C. (2007). Use of traditional medicines in the management of HIV/AIDS opportunistic infections in Tanzania: a case in the Bukoba rural district. *Journal of Ethnobiology and Ethnomedicine*, 3(1), 29.

Koffi, E. N., Le Guernevé, C., Lozano, P. R., Meudec, E., Adjé, F. A., Bekro, Y. A. and Lozano, Y. F. (2013). Polyphenol extraction and characterization of *Justicia secunda* Vahl leaves for traditional medicinal uses. *Industrial Crops and Products*, 49, 682-689.

Kohno, H., Maeda, M., Tanino, M., Tsukio, Y., Ueda, N., Wada, K. and Tanaka, T. (2002). A bitter diterpenoid furanolactone columbin from *Calumbae Radix* inhibits azoxymethane-induced rat colon carcinogenesis. *Cancer Letters*, 183(2), 131-139.

Kotecha, R., Takami, A. and Espinoza, J.L., 2016. Dietary phytochemicals and cancer chemoprevention: a review of the clinical evidence. *Oncotarget, 7(32), 52517.*

Krafczyk, N., Kötke, M., Lehnert, N. and Glomb, M. A. (2008). Phenolic composition of rhubarb. *European Food Research and Technology*, 228(2), 187.

Kremsner, P.G., Winkler, S., Brandts, C., Neifer, S., Bienzel, U. and Graninger, W. (1994). Clindamycin in combination with chloroquine or quinine is an effective therapy

for uncomplicated *Plasmodium falciparum* malaria in children from Gabon. *Journal of Infectious Diseases*, 169(2), 467-470.

Kuete, V. and Efferth, T. (2010). Cameroonian medicinal plants: Pharmacology and derived natural products. *Frontiers in Pharmacology*, 1.

Kuete, V., Krusche, B., Youns, M., Voukeng, I., Fankam, A. G., Tankeo, S. and Efferth, T. (2011). Cytotoxicity of some Cameroonian spices and selected medicinal plant extracts. *Journal of Ethnopharmacology*, 134(3), 803-812.

Kuo, C.-C., Chen, H.-H. and Chiang, W. (2012). Adlay (薏苡 yì yǐ; "soft-shelled job's tears"; the seeds of *Coix lachryma-jobi* L. var. ma-yuen Stapf) is a Potential Cancer Chemopreventive Agent toward Multistage Carcinogenesis Processes. *Journal of Traditional and Complementary Medicine*, 2(4), 267-275.

Kusuda, M., Inada, K., Ogawa, T. O., Yoshida, T., Shiota, S., Tsuchiya, T. and Hatano, T. (2006). Polyphenolic constituent structures of *Zanthoxylum piperitum* fruit and the antibacterial effects of its polymeric procyanidin on methicillin-resistant Staphylococcus aureus. *Bioscience, Biotechnology, and Biochemistry*, 70(6), 1423-1431.

Kwak, M.K., Egner, P.A., Dolan, P.M., Ramos-Gomez, M., Groopman, J.D., Itoh, K., Yamamoto, M. and Kensler, T.W. (2001). Role of phase 2 enzyme induction in chemoprotection by dithiolethiones. *Mutation Research/Fundamental and Molecular Mechanisms of Mutagenesis*, 480, 305-315.

Landis-Piwowar, K. R., and Iyer, N. R. (2014). Cancer chemoprevention: current state of the art. Cancer growth and metastasis, 7, CGM-S11288.

Lau, A., Villeneuve, N., Sun, Z., Wong, P. and Zhang, D. (2008). Dual roles of Nrf2 in cancer. *Pharmacological Research*, 58(5-6), 262-270.

Lee, J.H., Khor, T.O., Shu, L., Su, Z.Y., Fuentes, F. and Kong, A.N.T., 2013. Dietary phytochemicals and cancer prevention: Nrf2 signaling, epigenetics, and cell death mechanisms in blocking cancer initiation and progression. *Pharmacology and Therapeutics*, 137(2), 153-171.

Legrand, E., Volney, B., Meynard, J.B., Mercereau-Puijalon, O. and Esterre, P. (2007). In Vitro Monitoring of *Plasmodium falciparum* Drug Resistance in French Guiana: a Synopsis of Continuous Assessment from 1994 to 2005. *Antimicrobial Agents and Chemotherapy*, 52(1), 288-298.

Li, R., Morris-Natschke, S. L. and Lee, K. H. (2016). Clerodane diterpenes: sources, structures, and biological activities. *Natural product reports*, 33(10), 1166-1226.

Li, W., Zhou, W., Shim, S. H. and Kim, Y. H. (2014). Chemical constituents of *Zanthoxylum schinifolium* (Rutaceae). *Biochemical Systematics and Ecology*, (55), 60-65.

Lind, M.J. (2011). Principles of cytotoxic chemotherapy. *Medicine*, 39 (12), 711-716.

Lopes, L. M., Bolzani, V. D. S., Trevisan, L. M. and Grigolli, T. M. (1990). Terpenes from *Aristolochia triangularis*. *Phytochemistry*, 29(2), 660-662.

Loub, W.D., Farnsworth, N.R., Soejarto, D.D. and Quinn, M.L. (1985). NAPRALERT: computer handling of natural product research data. *Journal of chemical information and computer sciences*, 25(2), 99-103.

Luis, J. G., Herrera, J. R. and Bello, A. (2000). The Isolation of Carnosic Acid-11-Methylether from *Citrus* Roots Infected by Nematode *Tylenchulus semipenetrans*. *Natural Product Letters*, 14(5), 379-385.

Macfoy, C. (2013). *Medicinal plants and traditional medicine in Sierra Leone*. iUniverse.

Mahato, S. B. and Kundu, A. P. (1994). 13C NMR spectra of pentacyclic triterpenoids-a compilation and some salient features. *Phytochemistry*, 37(6), 1517-1575.

Makins, J.F., Holt, G. and Macdonald, K.D. (1983). The Genetic Location of Three Mutations Impairing Penicillin Production in Aspergillus nidulans. *Microbiology*, 129(10), 3027-3033.

Maldonado, E., Galicia, L., Chávez, M. I. and Hernández-Ortega, S. (2016). Neo-clerodane diterpenoids and other constituents of *Salvia filipes*. *Journal of Natural Products*, 79(10), 2667-2673.

Malebo, H.M., Tanja, W., Cal, M., Swaleh, S.A.M., Omolo, M.O., Hassanali, A., Sequin, U., Hamburger, M., Brun, R. and Ndiege, I.O. (2010). Antiplasmodial, anti-trypanosomal, anti-leishmanial and cytotoxicity activity of selected Tanzanian medicinal plants. *Tanzania Journal of Health Research*, 11(4).

Manna, S. K., Mukhopadhyay, A. and Aggarwal, B. B. (2000). Resveratrol suppresses TNF-induced activation of nuclear transcription factors NF-κB, activator protein-1, and apoptosis: potential role of reactive oxygen intermediates and lipid peroxidation. T*he Journal of Immunology*, 164(12), 6509-6519.

Markham, K. R. (1982). Techniques of flavonoid identification (Vol. 31). London: Academic press.

Matu, E. (2011) *Zanthoxylum zanthoxyloides* (Lam.) Zepern. and Timler. *PROTA (Plant Resources of Tropical Africa/Ressources végétales de l'Afrique tropicale)*.

Mbatchi, S., Mbatchi, B., Banzouzi, J., Bansimba, T., Ntandou, G.N., Ouamba, J.-M., Berry, A. and Benoit-Vical, F. (2006). In vitro antiplasmodial activity of 18 plants used in Congo Brazzaville traditional medicine. *Journal of Ethnopharmacology*, 104(1-2), 168-174.

McMahon, M., Campbell, K. H., MacLeod, A. K., McLaughlin, L. A., Henderson, C. J. and Wolf, C. R. (2014). HDAC inhibitors increase NRF2-signaling in tumour cells and blunt the efficacy of co-adminstered cytotoxic agents. *PloS one*, 9(11), e114055.

McRae, J., Yang, Q., Crawford, R. and Palombo, E. (2007). Review of the methods used for isolating pharmaceutical lead compounds from traditional medicinal plants. *The Environmentalist*, 27(1), 165-174.

Meshnick, S.R. (2002). Artemisinin: mechanisms of action, resistance and toxicity. *International Journal for Parasitology*, 32 (13), 1655-1660.

Mettlin, C. (1997). Chemoprevention: Will it work? *International Journal of Cancer*, 71(S10), 18-21.

Miller, A.B., Baines, C.J., To, T. and Wall, C. (1992). Canadian National Breast Screening Study: 1. Breast cancer detection and death rates among women aged 40 to 49 years. *CMAJ: Canadian Medical Association Journal*, 147(10), 1459.

Miller, L.H., Baruch, D.I., Marsh, K. and Doumbo, O.K. (2002). The pathogenic basis of malaria. *Nature*, 415(6872), 673-679.

Milne-Redhead, E. (1936). Eranthemum of the "Flora of Tropical Africa". *Bulletin of Miscellaneous Information (Royal Gardens, Kew)*, 1936(4), 255.

Misra, D. R. and Khastgir, H. N. (1970). Terpenoids and related compounds-XI: Chemical investigation of *Aleurites montana* and the structure of aleuritolic acid-a new triterpene acid. *Tetrahedron*, 26(12), 3017-3021.

Misra, L.N., Wouatsa, N.A.V., Kumar, S., Venkatesh Kumar, R. and Tchoumbougnang, F. (2013). Antibacterial, cytotoxic activities and chemical composition of fruits of two Cameroonian *Zanthoxylum* species. *Journal of Ethnopharmacology*, 148(1), 74-80.

Mitchell, J. D. and Daly, D. C. (2015). A revision of *Spondias* L. (Anacardiaceae) in the Neotropics. *PhytoKeys*, 55, 1.

Mitscher, L. A., Rao, G. S. R., Veysoglu, T., Drake, S. and Haas, T. (1983). Isolation and identification of trachyloban-19-oic and (-)-kaur-16-en-19-oic acids as antimicrobial agents from the prairie sunflower, *Helianthus annuus*. *Journal of Natural Products*, 46(5), 745-746.

Miyase, T., Ueno, A., Takizawa, N., Kobayashi, H. and Oguchi, H. (1989). Ionone and lignan glycosides from *Epimedium diphyllum*. *Phytochemistry*, 28(12), 3483-3485.

Moccelini, S. K., Silva, V. C. D., Ndiaye, E. A., Sousa Jr, P. T. D. and Vieira, P. C. (2009). Phytochemical study from root barks of *Zanthoxylum rigidum* Humb. and Bonpl. ex Willd (Rutaceae). *Quimica Nova*, 32(1), 131-133.

Morris, B. D., Foster, S. P., Grugel, S. and Charlet, L. D. (2005). Isolation of the diterpenoids, *ent*-kauran-16α-ol and *ent*-atisan-16α-ol, from sunflowers, as oviposition stimulants for the banded sunflower moth, *Cochylis hospes*. *Journal of Chemical Ecology*, 31(1), 89-102.

Moerman, D.E. (2007) Agreement and meaning: Rethinking consensus analysis. *Journal of Ethnopharmacology*, 112(3), 451-460.

Mosmann, T. (1983). Rapid colorimetric assay for cellular growth and survival: application to proliferation and cytotoxicity assays. *Journal of Immunological Methods*, 65(1-2), 55-63.

Mpondo, E. M., Vandi, D., Ngouondjou, T., Foze, P. B. M. O., Enyegue, E. E. and Dibong, S. D. (2017). Contribution des populations des villages du centre Cameroun aux traitements traditionnels des affections des voies respiratoires. *Journal of Animal and Plant Sciences*, 32(3), 5223-5242.

Murakami, A., Ohigashi, H. and Koshimizu, K. (1996). Anti-tumor Promotion with Food Phytochemicals: A Strategy for Cancer Chemoprevention. *Bioscience, Biotechnology, and Biochemistry*, 60 (1), 1-8.

Napiroon, T., Bacher, M., Balslev, H., Tawaitakham, K., Santimaleeworagun, W. and Vajrodaya, S. (2018). Scopoletin from *Lasianthus lucidus* Blume (Rubiaceae): A potential antimicrobial against multidrug-resistant *Pseudomonas aeruginosa*. *Journal of Applied Pharmaceutical Science*, *8*(09), 001-006.

Ncokazi, K.K. and Egan, T.J. (2005). A colorimetric high-throughput β-hematin inhibition screening assay for use in the search for antimalarial compounds. *Analytical Biochemistry*, 338(2), 306-319.

Ndunda, B., Langat, M., Mulholland, D., Eastman, H., Jacob, M. R., Khan, S. and Midiwo, J. O. (2016). New *ent*-clerodane and abietane diterpenoids from the roots of Kenyan *Croton megalocarpoides. Planta Medica*, 82(11-12), 1079-1086.

Neukomm, G., Roessler, F., Johne, S. and Hesse, M. (1983). Zur Struktur von Hypercratin, einem weiteren Alkaloid aus *Ruspolia hypercrateriformis*. *Planta Medica*, 48(08), 246-252.

Newman, D.J. and Cragg, G.M. (2016). Natural Products as Sources of New Drugs from 1981 to 2014. *Journal of Natural Products*, 79(3), 629-661.

Ngane, A.N., Biyiti, L., Zollo, P.A. and Bouchet, P. (2000). Evaluation of antifungal activity of extracts of two Cameroonian Rutaceae: *Zanthoxylum leprieurii* Guill. et Perr. and *Zanthoxylum xanthoxyloides* Waterm. *Journal of Ethnopharmacology*, 70(3), 335-342.

Ngbolua, K. N., Benamambote, B. M., Mpiana, P. T., Muanda, D. M., Ekutsu, E., Tshibangu, D. S. T. and Baholy, R. (2013). Ethno-botanical survey and Ecological Study of some Medicinal Plants species traditionally used in the District of Bas-Fleuve (Bas-Congo Province, Democratic Republic of Congo). *Research Journal of Chemistry*, 1(2), 1-10.

Ngoumfo, R.M., Jouda, J.-B., Mouafo, F.T., Komguem, J., Mbazoa, C.D., Shiao, T.C., Choudhary, M.I., Laatsch, H., Legault, J. and Pichette, A. (2010). In vitro cytotoxic activity of isolated acridones alkaloids from *Zanthoxylum leprieurii* Guill. et Perr. *Bioorganic and Medicinal Chemistry*, 18(10), 3601-3605.

Nguyen, T., Nioi, P. and Pickett, C.B. (2009). The Nrf2-antioxidant response element signaling pathway and its activation by oxidative stress. *Journal of Biological Chemistry*, 284(20), 13291-13295.

Nioi, P. and Hayes, J.D. (2004). Contribution of NAD (P) H: quinone oxidoreductase 1 to protection against carcinogenesis, and regulation of its gene by the Nrf2 basic-region leucine zipper and the arylhydrocarbon receptor basic helix-loop-helix transcription factors. *Mutation Research/Fundamental and Molecular Mechanisms of Mutagenesis*, 555(1), 149-171

Nkongmeneck, B., Mapongmetsem, P., Pinta, Y., Nkuinkeu, R., Tsabang, N., Fongnzossie, E., Kemeuze, V., Jiofack, T., Johnson, M. and Asaha, S. (2007). Etat des lieux des plantes médicinales importantes à conserver et des jardins de plantes médicinales à promouvoir. *Yaounde: Rapport CEN/OMS/MEM*.

Noedl, H., Se, Y., Schaecher, K., Smith, B. L., Socheat, D. and Fukuda, M. M. (2008). Evidence of artemisinin-resistant malaria in western Cambodia. *New England Journal of Medicine*, 359(24), 2619-2620.

Noté, O.P., Simo, L., Mbing, J.N., Guillaume, D., Aouazou, S.A., Muller, C.D., Pegnyemb, D.E. and Lobstein, A. (2016). Two new triterpenoid saponins from the roots of *Albizia zygia* (DC.) J.F. Macbr. *Phytochemistry Letters*, 18, 128-135.

Noumi, E. and Yomi, A. (2001). Medicinal plants used for intestinal diseases in Mbalmayo Region, Central Province, Cameroon. *Fitoterapia*, 72(3), 246-254.

Ntie-Kang, F., Lifongo, L.L., Mbaze, L.M.A., Ekwelle, N., Owono Owono, L.C., Megnassan, E., Judson, P.N., Sippl, W. and Efange, S.M.N. (2013). Cameroonian medicinal plants: a bioactivity versus ethnobotanical survey and chemotaxonomic classification. *BMC Complementary and Alternative Medicine*, 13(1).

Nzila, A. (2006) The past, present and future of antifolates in the treatment of *Plasmodium falciparum* infection. *Journal of Antimicrobial Chemotherapy*, 57(6), 1043-1054.

Ogunbolude, Y., Ibrahim, M., Elekofehinti, O., Adeniran, A., Abolajif, A., Rochab, J. and Kamdem, J. (2014). Effects of Tapinanthus globiferus and *Zanthoxylum zanthoxyloides* extracts on human leukocytes in vitro. *Journal of Intercultural Ethnopharmacology*, 3(4), 167.

Olotu, A., Urbano, V., Hamad, A., Eka, M., Chemba, M., Nyakarungu, E. and Maas, C. D. (2018). Advancing Global Health through Development and Clinical Trials Partnerships: A Randomized, Placebo-Controlled, Double-Blind Assessment of Safety, Tolerability, and Immunogenicity of PfSPZ Vaccine for Malaria in Healthy Equatoguinean Men. *The American journal of tropical medicine and hygiene*, 98(1), 308-318.

Onana, J.M. (2015). The World Flora Online 2020 project: will Cameroon come up to the expectation? *Rodriguésia*, 66(4), 961-972.

Oriowo, M. (1982). Anti-Inflammatory Activity of Piperonyl-4-Acrylic Isobutyl Amide, an Extractive from *Zanthoxylum zanthoxyloides*. *Planta Medica*, 44 (01), 54-56.

Orji, O. U., Ibiam, U. A., Aja, P. M., Obasi, O. D., Ezeani, N., Aloke, C., Anayo, S. and Inya-Agha, O. R. (2016). Effect of Ethanol Extract of *Ruspolia hypocrateriformis* Leaf on Haematological Parameters in Lead Poisoned Albino Rats. *World Journal of Medical Sciences* 13(4), 225-235

Orji, O.U., Ibiam, U.A., Uraku, A. J., Obasi, O.D., Aloke, C. E. and Awoke J. N. (2017). Investigations of Phytochemical and Nutritional Composition of *Ruspolia Hypocrateriformis* Leaf. *Journal of Applied Sciences*, 2(2), 70-81.

Osterdahl, B. G. (1979). Chemical studies on bryophytes, 22: Flavonoid C-glycosides of *Mnium undulatum* [moss, saponarin, schaftoside, neoschaftoside, isoschaftoside, neoisoschaftoside, vicenin-2, 6-C-arabinosyl-8-C-hexoside]. *Acta Chemica Scandinavica. Series B (Denmark).*

Ouattara, B., Jansen, O., Angenot, L., Guissou, I.P., Frédérich, M., Fondu, P. and Tits, M. (2009). Antisickling properties of divanilloylquinic acids isolated from *Fagara zanthoxyloides* Lam. (Rutaceae). *Phytomedicine*, 16(2-3), 125-129.

Pacheco, A. G., Machado de Oliveira, P., Piló-Veloso, D. and Flávio de Carvalho Alcântara, A. (2009). ^{13}C-NMR data of diterpenes isolated from *Aristolochia* species. *Molecules*, 14(3), 1245-1262.

Patino, L. O. J., Prieto, R. J. A. and Cuca, S. L. E. (2012). *Zanthoxylum* genus as potential source of bioactive compounds. In Bioactive compounds in phytomedicine. I. Rasooli (Ed.), InTech, Rijeka (2012), pp. 185-218

Pelletier, S. W., Chokshi, H. P. and Desai, H. K. (1986). Separation of diterpenoid alkaloid mixtures using vacuum liquid chromatography. *Journal of Natural Products*, 49(5), 892-900.

Pereira, D.A. and Williams, J.A. (2007). Origin and evolution of high throughput screening. *British journal of pharmacology*, 152(1), 53-61.

Perez, J.L., Jayaprakasha, G.K., Cadena, A., Martinez, E., Ahmad, H. and Patil, B.S. (2010). In vivo induction of phase II detoxifying enzymes, glutathione transferase and quinone reductase by citrus triterpenoids. *BMC complementary and alternative medicine*, 10(1), 51.

Peters, R. J. (2010). Two rings in them all: the labdane-related diterpenoids. *Natural Product Reports*, 27(11), 1521-1530.

Pezzuto, J.M. (1997) Plant-derived anticancer agents. *Biochemical Pharmacology*, 53(2), 121-133.

Pezzuto, J.M., Kosmeder, J.W., Park, E.J., Lee, S.K., Cuendet, M., Gills, J., Bhat, K., Grubjesic, S., Park, H.S., Mata-Greenwood, E. and Tan, Y. (2005). Characterization of natural product chemopreventive agents. In Cancer chemoprevention (pp. 3-37). Humana Press.

Picerno, P., Mencherini, T., Loggia, R. D., Meloni, M., Sanogo, R., and Aquino, R. P. (2006). An extract of *Lannea microcarpa*: composition, activity and evaluation of cutaneous irritation in cell cultures and reconstituted human *epidermis*. *Journal of Pharmacy and Pharmacology*, 58(7), 981-988

Plowe, C. V. (2010). The fever: How malaria has ruled humankind for 500,000 years. *The Journal of clinical investigation*, 120(12), 4167-4167.

Prabowo, W. C., Wirasutisna, K. R. and Insanu, M. (2013). Isolation and characterization of 3-acetyl aleuritolic acid and scopoletin from stem bark of *Aleurites Moluccana* (L.) willd. *International Journal of Pharmaceutical Science*, 5(3), 851 - 853.

Prasad, V., Schwerdtfeger, U., El-Awa, F., Bettcher, D. and da Costa e Silva, V. (2015). Closing the door on illicit tobacco trade, opens the way to better tobacco control. *Eastern Mediterranean Health Journal*, 21(6), 379-380.

Prempeh, A.B.A. and Mensah-Attipoe, J. (2009). In vivo inhibition of prostaglandin e2 production by crude aqueous extract of the root bark of *Zanthoxylum xanthoxyloides. Ghana Medical Journal*, 42 (2).

Queiroz, E., Hay, A.-E., Chaaib, F., van Diemen, D., Diallo, D. and Hostettmann, K. (2006). New and Bioactive Aromatic Compounds from *Zanthoxylum zanthoxyloides*. *Planta Medica*, 72(08), 746-750.

Rasool, N., Khan, A. Q. and Malik, A. (1989). A taraxerane type triterpene from *Euphorbia tirucalli*. *Phytochemistry*, 28(4), 1193-1195.

Reggelin, M., Hoffmann, H., Koeck, M. and Mierke, D. F. (1992). Determination of conformation and relative configuration of a small, rapidly tumbling molecule in solution

by combined application of NOESY and restrained MD calculations. *Journal of the American Chemical Society*, 114(9), 3272-3277.

Reid R.G. and Sarker S.D. (2012). Isolation of Natural Products by Low-Pressure Column Chromatography. In: Sarker S., Nahar L. (eds) Natural Products Isolation. Methods in Molecular Biology (Methods and Protocols), vol 864. Humana Press

Reuland, D.J., Khademi, S., Castle, C.J., Irwin, D.C., McCord, J.M., Miller, B.F. and Hamilton, K.L. (2013). Upregulation of phase II enzymes through phytochemical activation of Nrf2 protects cardiomyocytes against oxidant stress. *Free Radical Biology and Medicine*, 56, 102-111.

Reyburn, H. (2010) New WHO guidelines for the treatment of malaria. *BMJ*, 340 (May28 1), c2637-c2637.

Roessler, F., Ganzinger, D., Johne, S., Schöpp, E. and Hesse, M. (1978). *Ruspolia hypercrateriformis* M.R.: Isolierung und Strukturaufklärung von neuen Pyrrolidin-Alkaloiden. 169. Mitt. über organische Naturstoffe. *Helvetica Chimica Acta*, 61 (3), 1200-1206.

Rollinger, J.M., Stuppner, H. and Langer, T. (2008) Virtual screening for the discovery of bioactive natural products. In: (ed.) *Natural Compounds as Drugs Volume I.* Springer. pp. 211-249.

Ross, S. A., Al-Azeib, M. A., Krishnaveni, K. S., Fronczek, F. R. and Burandt, C. L. (2005). Alkamides from the Leaves of *Zanthoxylum syncarpum*. *Journal of Natural Products*, 68(8), 1297-1299.

Rostagno M. A. and Prado J. M. (2013). Natural product extraction: Principles and applications. The Royal Society of Chemistry, Cambridge, UK.

Rowinsky, E.K. and Donehower, R.C. (1991). The clinical pharmacology and use of antimicrotubule agents in cancer chemotherapeutics. *Pharmacology and Therapeutics*, 52(1), 35-84.

Ruffo, C.K., Birnie, A. and Tengnäs, B. (2002). *Edible wild plants of Tanzania*. Regional Land Management Unit/Sida.

Salatino, A., Salatino, M. L. F., & Negri, G. (2007). Traditional uses, chemistry and pharmacology of *Croton* species (Euphorbiaceae). *Journal of the Brazilian Chemical Society*, *18*(1), 11-33.

Sameh, S., Al-Sayed, E., Labib, R. M. and Singab, A. N. (2018). Genus *Spondias*: A Phytochemical and Pharmacological Review. *Evidence-Based Complementary and Alternative Medicine, 2018*. https://doi.org/10.1155/2018/5382904

Sapienza, C. and Issa, J.P. (2016). Diet, nutrition, and cancer epigenetics. Annual review of nutrition, 36, pp.665-681.

Sarkar, S., Siddiqui, A. A., Saha, S. J., De, R., Mazumder, S., Banerjee, C. and Bandyopadhyay, U. (2016). Antimalarial activity of small molecule benzothiazole hydrazones. *Antimicrobial Agents and Chemotherapy*, AAC-01575.

Sarker, S.D. and Nahar, L. (2012). *Hyphenated Techniques and Their Applications in Natural Products Analysis.Methods in Molecular Biology*: Humana Press**:** 301-340.

Sarker, S. D. and Nahar, L. (2018). An Introduction to Computational Phytochemistry. In *Computational Phytochemistry* (pp. 1-41).

Schijlen, E. G., De Vos, C. R., van Tunen, A. J. and Bovy, A. G. (2004). Modification of flavonoid biosynthesis in crop plants. *Phytochemistry*, 65(19), 2631-2648.

Schmelzer, G.H. (2008). *Medicinal plants*. Prota.

Schwikkard, S. and Mulholland, D. (2014). Useful Methods for Targeted Plant Selection in the Discovery of Potential New Drug Candidates. *Planta Medica*, 80(14), 1154-1160.

Scotland, R.W. and Vollesen, K. (2000). Classification of Acanthaceae. *Kew Bulletin*, 55(3), 513.

Seger, C., Hofer, O., VaJrodaya, S. and Greger, H. (1998). Two new nor-diterpenes from *Glycosmis* cf. Cyanocarpa. *Natural Product Letters*, 12(2), 117-124.

Shah, U., Shah, R., Acharya, S. and Acharya, N. (2014). Novel anticancer agents from plant sources. *Chinese Journal of Natural Medicines*, 11(1), 16-23.

Shao, C.-L., Mou, X.-F., Cao, F., Spadafora, C., Glukhov, E., Gerwick, L., Wang, C.-Y. and Gerwick, W.H. (2018). Bastimolide B, an antimalarial 24-membered marine macrolide possessing a *tert*-butyl group. *Journal of Natural Products*, 81(1), 211-215.

Shirota, O., Nagamatsu, K., and Sekita, S. (2006). Neo-clerodane diterpenes from the hallucinogenic sage *Salvia divinorum*. *Journal of Natural Products*, 69(12), 1782-1786.

Shishodia, S., Majumdar, S., Banerjee, S. and Aggarwal, B. B. (2003). Ursolic acid inhibits nuclear factor-κB activation induced by carcinogenic agents through suppression

of IκBα kinase and p65 phosphorylation: correlation with down-regulation of cyclooxygenase 2, matrix metalloproteinase 9, and cyclin D1. *Cancer Research*, 63(15), 4375-4383.

Shrestha, S., Lee, D. Y., Park, J. H., Cho, J. G., Seo, W. D., Kang, H. C. and Baek, N. I. (2012). Flavonoid glycosides from the fruit of *Rhus parviflora* and inhibition of cyclin dependent kinases by hyperin. *Journal of the Korean Society for Applied Biological Chemistry*, 55(5), 689-693.

Sidjui, L.S., Toghueo, R.M.K., Menkem Zeu, E., Mbouna, C.D.J., Leddet, V.M., Herbette, G., Fekam, F.B., Ollivier, E. and Folefoc, G.N. (2016). Antibacterial Activity of the Crude Extracts, Fractions and Compounds from the Stem Barks of *Jacaranda mimosifolia* and *Kigelia africana* (Bignoniaceae). *Pharmacologia*, 7 (1), 22-31.

Silva, L., Reis, R., Moura, E., Amaral, W. and Sousa Jr, P. T. (2015). Plants of the *Xylopia* Genus: Chemical Composition and Pharmacological Potential. *Revista Brasileira de Plantas Medicinais*, 17(4), 814-826.

Singh, B., Sung, L.K., Matusop, A., Radhakrishnan, A., Shamsul, S.S.G., Cox-Singh, J., Thomas, A. and Conway, D.J. (2004). A large focus of naturally acquired *Plasmodium knowlesi* infections in human beings. *The Lancet*, 363 (9414), 1017-1024.

Slater, A.F.G. (1993). Chloroquine: Mechanism of drug action and resistance in *Plasmodium falciparum*. *Pharmacology and Therapeutics*, 57(2-3), 203-235.

Slater, A.F.G. and Cerami, A. (1992). Inhibition by chloroquine of a novel haem polymerase enzyme activity in malaria trophozoites. *Nature*, 355 (6356), 167-169.

Solecki, R.S. (1975). Shanidar IV, a Neanderthal Flower Burial in Northern Iraq. *Science*, 190(4217), 880-881.

Sullivan, D.J. (2002). Theories on malarial pigment formation and quinoline action. *International Journal for Parasitology*, 32(13), 1645-1653.

Surh, Y.-J. (1999). Molecular mechanisms of chemopreventive effects of selected dietary and medicinal phenolic substances. *Mutation Research/Fundamental and Molecular Mechanisms of Mutagenesis*, 428(1), 305-327.

Tabuti, J. (2016). *Zanthoxylum leprieurii* Guill. and Perr. *PROTA (Plant Resources of Tropical Africa/Ressources végétales de l'Afrique tropicale)*, 715-716.

Tagousop, C. N., Ngnokam, D., Harakat, D. and Voutquenne-Nazabadioko, L. (2017). Three new flavonoid glycosides from the aerial parts of *Graptophyllum grandulosum* Turril (Acanthaceae). *Phytochemistry Letters*, 19, 172-175.

Takahashi, J. A., Boaventura, M. A. D. and de Carvalho Bayma, J. (1995). Frutoic acid, a dimeric kaurane diterpene from *Xylopia frutescens*. *Phytochemistry*, 40(2), 607-609.

Takahashi, J. A., Vieira, H. S., Boaventura, M. A. D., Hanson, J. R., Hitchcock, P. B. and Oliveira, A. B. D. (2001). Mono and diterpenes from seeds of *Xylopia sericea*. *Quimica Nova*, 24(5), 616-618.

Tamimi, R.M., Lagiou, P., Adami, H.O. and Trichopoulos, D. (2002) Prospects for chemoprevention of cancer. *Journal of Internal Medicine*, 251(4), 286-300.

Tanaka, R., Ohtsu, H. and Matsunaga, S. (1997). Abietane diterpene acids and other constituents from the leaves of *Larix kaempferi*. *Phytochemistry*, 46(6), 1051-1057.

Tatsadjieu, L.N., Essia Ngang, J.J., Ngassoum, M.B. and Etoa, F.X. (2003). Antibacterial and antifungal activity of *Xylopia aethiopica*, *Monodora myristica*, *Zanthoxylum xanthoxyloïdes* and *Zanthoxylum leprieurii* from Cameroon. *Fitoterapia*, 74(5), 469-472.

Tchabong, T., Jazet, S.R., Sameza, D.P.M., Tchameni, M.L., Mounbain, N.S., Mouelle, F., Menut, S.A. and F, T. (2017). Chemical composition, free radical scavenging and antifungal activity of *Zanthoxylum leprieurii* essential oils against *Epidermophyton floccosum* and *Trichophyton rubrum*. *IOSR Journal of Pharmacy (IOSRPHR)*, 7(3), 1-6.

Tchinda, A., Fuendjiep, V., Sajjad, A., Matchawe, C., Wafo, P., Khan, S., Tane, P. and Choudhary, M. (2009). Bioactive compounds from the fruits of *Zanthoxylum leprieurii*. *Pharmacologyonline*, 1, 406-415.

Tchissambou, L., Chiaroni, A., Riche, C. and Khuong-Huu, F. (1990). Crotocorylifuran and crotohaumanoxide, new diterpenes from *Croton Haumanianus* J. Leonard. *Tetrahedron*, 46(15), 5199-5202.

Te, M. (2013). The Expanding Market for Herbal, Medicinal and Aromatic Plants In Nigeria and the International Scene. *Medicinal and Aromatic Plants*, 2 (6).

Theiler, B. A., Revoltella, S., Zehl, M., Dangl, C., Caisa, L. O. E., König, J. and Glasl, S. (2014). Secundarellone A, B, and C from the leaves of *Justicia secunda* Vahl. *Phytochemistry Letters*, 10, cxxix-cxxxii.

Thoppil, R. J. and Bishayee, A. (2011). Terpenoids as potential chemopreventive and therapeutic agents in liver cancer. *World Journal of Hepatology*, 3(9), 228.

Tine, Y., Renucci, F., Costa, J., Wélé, A. and Paolini, J. (2017). A Method for LC-MS/MS Profiling of Coumarins in *Zanthoxylum zanthoxyloides* (Lam.) B. Zepernich and Timler Extracts and Essential Oils. *Molecules*, 22(1), 174.

Torres, R. and Cassels, B. K. (1978). Leaf alkaloids of *Fagara mayu*. *Phytochemistry*, 17(4), 838-839.

Torto, F.G., Sefcovic, P. and Dadson, B.A. (1966). Medicinal plants of Ghana: Identity of alkaloid from *Fagara xanthoxyloides*. *Tetrahedron Letters*, 7(2), 181-183.

Torto, F. G., Mensah, I. A. and Baxter, I. (1973). Fagaridine: A phenolic benzophenanthridine alkaloid from Fagara xanthoxyloides. *Phytochemistry*, *12*(9), 2315-2317.

Trichopoulos, D., Li, F.P. and Hunter, D.J. (1996). What Causes Cancer? *Scientific American*, 275 (3), 80-87.

Triglia, T. and Cowman, A.F. (1999). The mechanism of resistance to sulfa drugs in *Plasmodium falciparum*. *Drug Resistance Updates*, 2(1), 15-19.

Tripathi, A.K., Gupta, A., Garg, S.K. and Tekwani, B.L. (2001). In vitro β-hematin formation assays with plasma of mice infected with *Plasmodium yoelii* and other parasite preparations. *Life Sciences*, 69(23), 2725-2733.

Tu, Y. (2011). The discovery of artemisinin (qinghaosu) and gifts from Chinese medicine. *Nature Medicine*, 17(10), 1217-1220.

Tuteja, R. (2007). Malaria-an overview. *FEBS Journal*, 274 (18), 4670-4679.

Umadevi, I., Daniel, M. and Sabnis, S. D. (1988). Chemotaxonomic studies on some members of Anacardiaceae. *Proceedings: Plant Sciences*, 98(3), 205-208.

Vieira, H. S., Takahashi, J. A., Oliveira, A. B. D., Chiari, E. and Boaventura, M. A. D. (2002). Novel derivatives of kaurenoic acid. *Journal of the Brazilian Chemical Society*, 13(2), 151-157.

Villa-Ruano, N., Lozoya-Gloria, E. and Pacheco-Hernández, Y. (2016). Kaurenoic acid: a diterpene with a wide range of biological activities. *Studies in Natural Products Chemistry*, 51, 151-174.

Wall, M.E., Wani, M.C. and Taylor, H. (1987). Plant Antitumor Agents, 27. Isolation, structure, and structure activity relationships of alkaloids from *Fagara macrophylla*. *Journal of Natural Products*, 50(6), 1095-1099.

Wandji, J., Nkengfack, A. E., Fomum, Z. T., Ubillas, R., Killday, K. B. and Tempesta, M. S. (1990). A new prenylated isoflavone and long chain esters from two *Erythrina* species. *Journal of Natural Products*, 53(6), 1425-1429.

Wang (2010). Prostate cancer chemopreventive activity of phenethyl isothiocyanate through epigenetic regulation (Review). *International Journal of Oncology*, 37(3).

Wang, X. J., Hayes, J. D. and Wolf, C. R. (2006). Generation of a stable antioxidant response element–driven reporter gene cell line and its use to show redox-dependent activation of Nrf2 by cancer chemotherapeutic agents. *Cancer Research*, 66(22), 10983-10994.

Wang, Y., Li, C. H., Luo, B., Sun, Y. N., Kim, Y. H., Wei, A. Z., and Gao, J. M. (2016). Isobutylhydroxyamides from *Zanthoxylum bungeanum* and their suppression of NO production. *Molecules*, 21(10), 1416.

Wang, Y. X., Ren, Q., Yan, Z. Y., Wang, W., Zhao, L., Bai, M. and Song, S. J. (2017). Flavonoids and their derivatives with β-amyloid aggregation inhibitory activity from the leaves and twigs of *Pithecellobium clypearia* Benth. *Bioorganic and Medicinal Chemistry Letters*, 27(21), 4823-4827.

Wangensteen, H., Ho, G. T. T., Tadesse, M., Miles, C. O., Moussavi, N., Mikolo, B., & Malterud, K. E. (2016). A new benzophenanthridine alkaloid and other bioactive constituents from the stem bark of *Zanthoxylum heitzii*. *Fitoterapia*, *109*, 196-200.

Wani, M.C., Taylor, H.L., Wall, M.E., Coggon, P. and McPhail, A.T. (1971). Plant antitumor agents. VI. Isolation and structure of taxol, a novel antileukemic and antitumor agent from Taxus brevifolia. *Journal of the American Chemical Society*, 93(9), 2325-2327.

Wattenberg, L.W. (1985). Chemoprevention of cancer. *Cancer research*, 45 (1), 1-8.

Waterman, P. G. (1975). Alkaloids of the Rutaceae: their distribution and systematic significance. *Biochemical Systematics and Ecology*, *3*(3), 149-180.

Waterman, P. G., Meshal, I. A., Hall, J. B., & Swaine, M. D. (1978). Biochemical systematics and ecology of the Toddalioideae in the central part of the West African forest zone. *Biochemical Systematics and Ecology*, *6*(3), 239-245.

Webster, G.L. (1993) A provisional synopsis of the sections of the genus *Croton* (Euphorbiaceae). *Taxon*, 42(4), 793.

White, N.J. (2004). Antimalarial drug resistance. *Journal of Clinical Investigation*, 113(8), 1084-1092.

World Cancer Report, (2014). World Health Organization. 2014. pp. Chapter 1.1. ISBN 9283204298.

WHO (2015). Guidelines for the treatment of malaria. World Health Organization.

WHO (2016). World malaria report 2015. World Health Organization. accessed on 15/3/2018

WHO (2017). http://www.who.int/malaria/publications/world-malaria-report-2017/en/ accessed on 8/3/2018

WHO (2018a). www.who.int/cancer/about/facts/en/ accessed on 23/03/2018

WHO (2018b). www.who.int/malaria/areas/treatment/overview/en/ overview on malaria treatment accessed on 15/3/2018

Williamson, E. M. (2001). Synergy and other interactions in phytomedicines. *Phytomedicine*, 8(5), 401-409.

Wirth, D. F. (2002). The parasite genome: Biological revelations. *Nature*, 419(6906), 495.

Wilson, S. R., Neubert, L. A. and Huffman, J. C. (1976). The chemistry of the Euphorbiaceae. A new diterpene from *Croton californicus*. *Journal of the American Chemical Society*, 98(12), 3669-3674.

Wouatsa, V.N.A., Misra, L., Kumar, S., Prakash, O., Khan, F., Tchoumbougnang, F. and Venkatesh, R.K. (2013a). Aromatase and glycosyl transferase inhibiting acridone alkaloids from fruits of Cameroonian *Zanthoxylum* species. *Chemistry Central Journal*, 7(1), 125.

Wouatsa, V. N.A., Misra, L.N., Venkatesh Kumar, R., Darokar, M.P. and Tchoumbougnang, F. (2013b). Zantholic acid, a new monoterpenoid from *Zanthoxylum zanthoxyloides*. *Natural Product Research*, 27(21), 1994-1998.

Xie, D.-Y. (2016) *Artemisia annua*, artemisinin, and the Nobel Prize: beauty of natural products and educational significance. *Science Bulletin*, 61(1), 42-44.

Xu, W. H., Liu, W. Y. and Liang, Q. (2018). Chemical Constituents from *Croton* Species and Their Biological Activities. *Molecules*, 23(9), 2333.

Yokota, J. (2000). Tumor progression and metastasis. *Carcinogenesis*, 21 (3), 497-503.

Yondo, J., Fomekong, G. I. D., Kontangui, M. C., Wabo, J. P., Tankoua, O. F., Kulate, J. R.and Mpoame, B. M. (2009). *In vitro* antioxidant potential and phytochemical constituents of three Cameroonian medicinal plants used to manage parasitic diseases. *Annals of Nutrition and Metabolism*, 55, 205.

Zhang, H., Li, X., Wu, K., Wang, M., Liu, P., Wang, X. and Deng, R. (2016). Antioxidant activities and chemical constituents of flavonoids from the flower of *Paeonia ostii*. *Molecules*, 22(1), 5.

Zhao, P., Dou, Y., Chen, L., Li, L., Wei, Z., Yu, J., Wu, X., Dai, Y. and Xia, Y. (2015). SC-III3, a novel scopoletin derivative, induces autophagy of human hepatoma HepG2 cells through AMPK/mTOR signaling pathway by acting on mitochondria, *Fitoterapia*, 104, 31-41.

Zimniak, P. (2008). Detoxification reactions: Relevance to aging. *Ageing Research Reviews*, 7, 281-300.

Appendix I MS, ^{1}H and ^{13}C NMR spectra of crotonolin E (155)

White amorphous powder, $[\alpha]_D^{25}$ -70.0 (c 0.00005, MeOH).

Molecular formula $C_{22}H_{24}O_8$ determined from the peak at *m/z* 417.1557 calculated for $C_{22}H_{25}O_8$ $[M+H]^+$, 417.1543

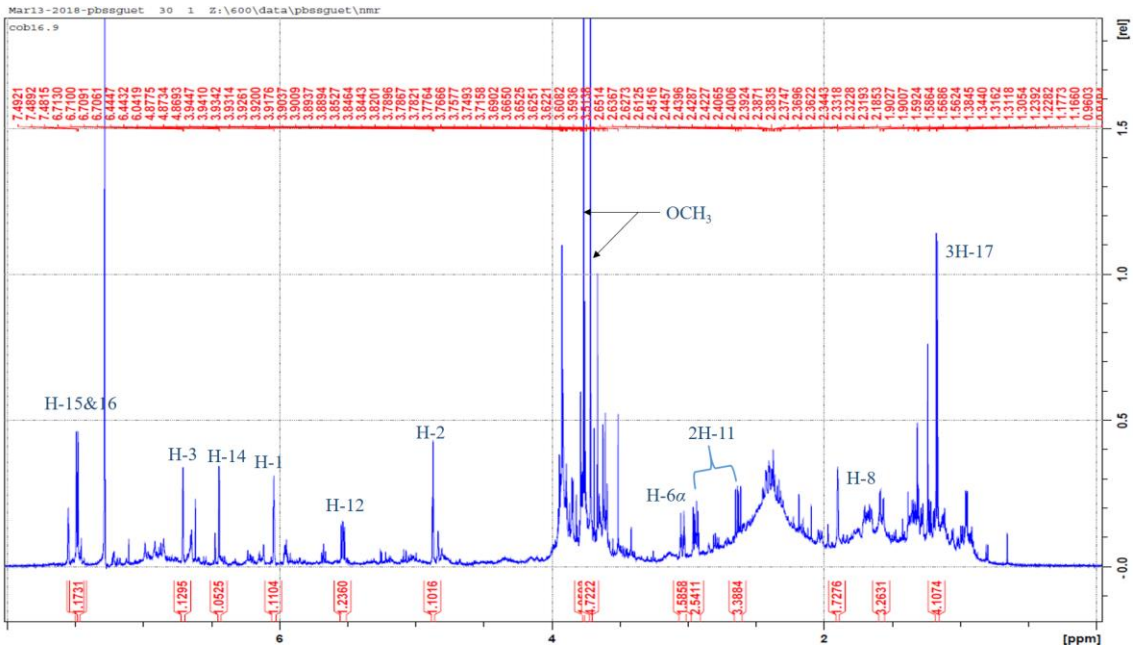

^{1}H NMR spectrum ($CDCl_3$, 600 MHz) of **155**

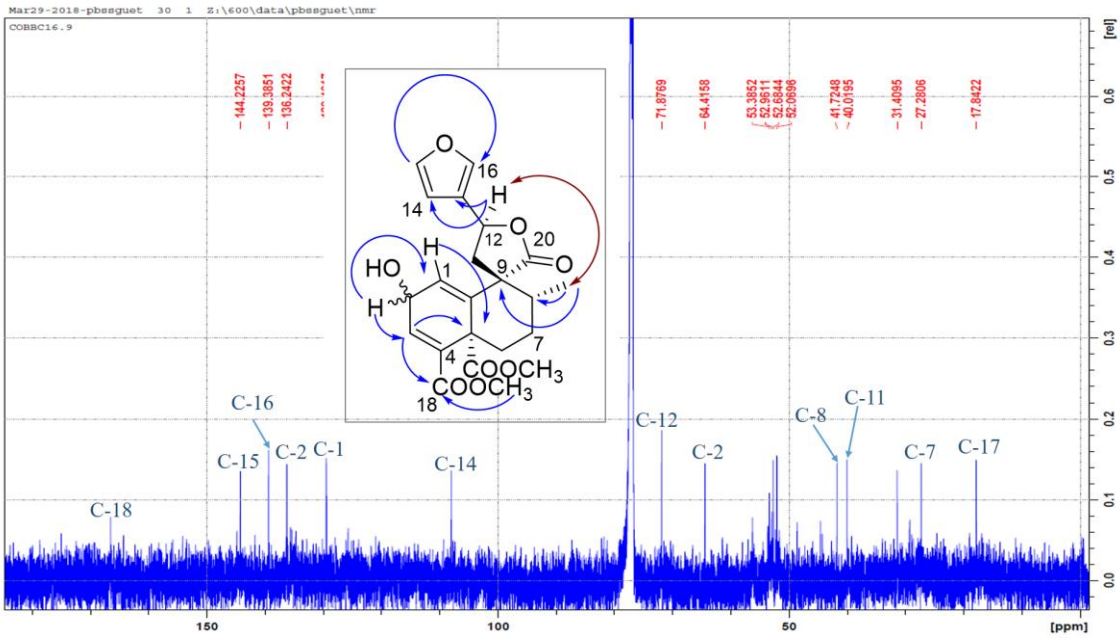

^{13}C NMR spectrum (150 MHz, $CDCl_3$) and Keys ^{1}H-^{1}H NOESY (↔) and HMBC (→) correlations of **155**

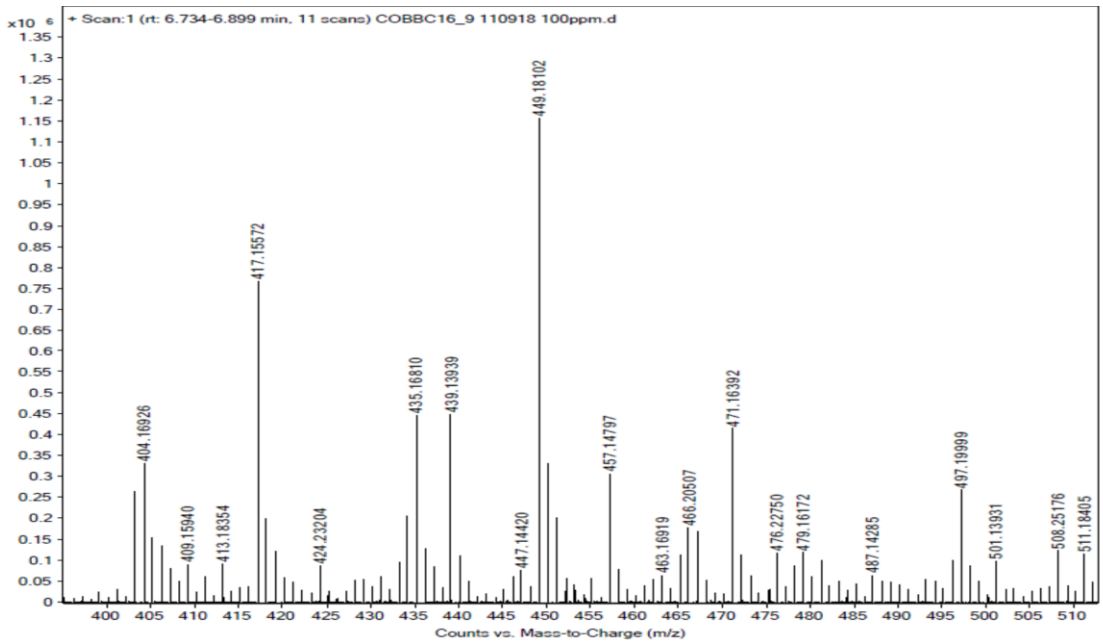

ESI-MS spectrum of **155**

Appendix II ESI-MS spectrum of justivialoside B (167)

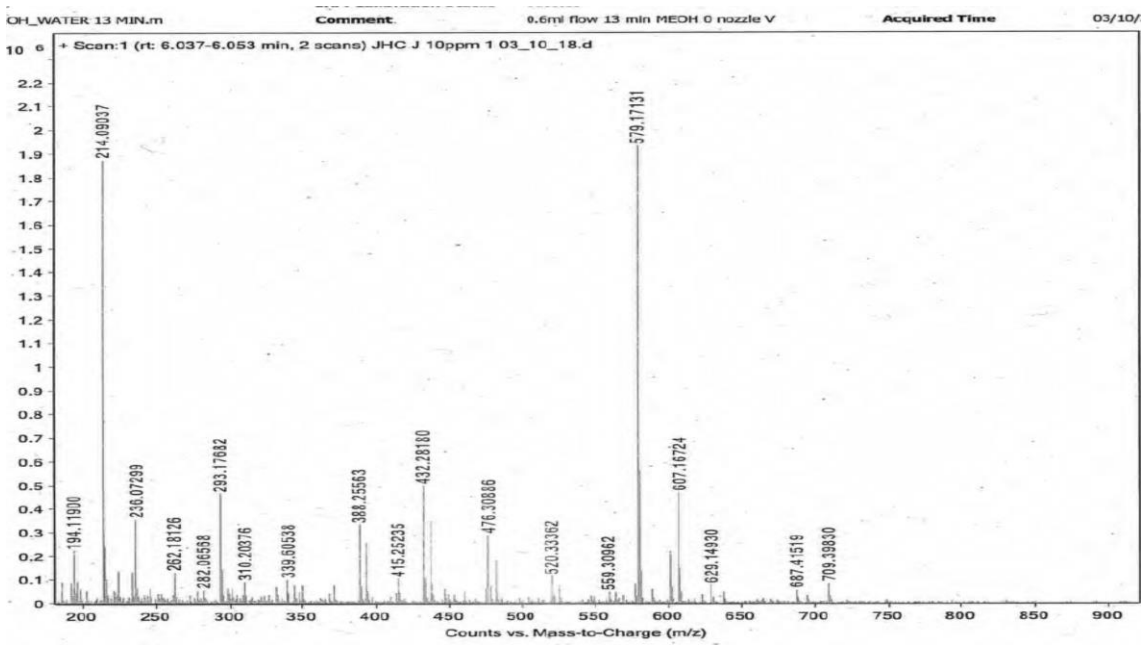

Appendix III ESI-MS spectrum of scopoletin (103)

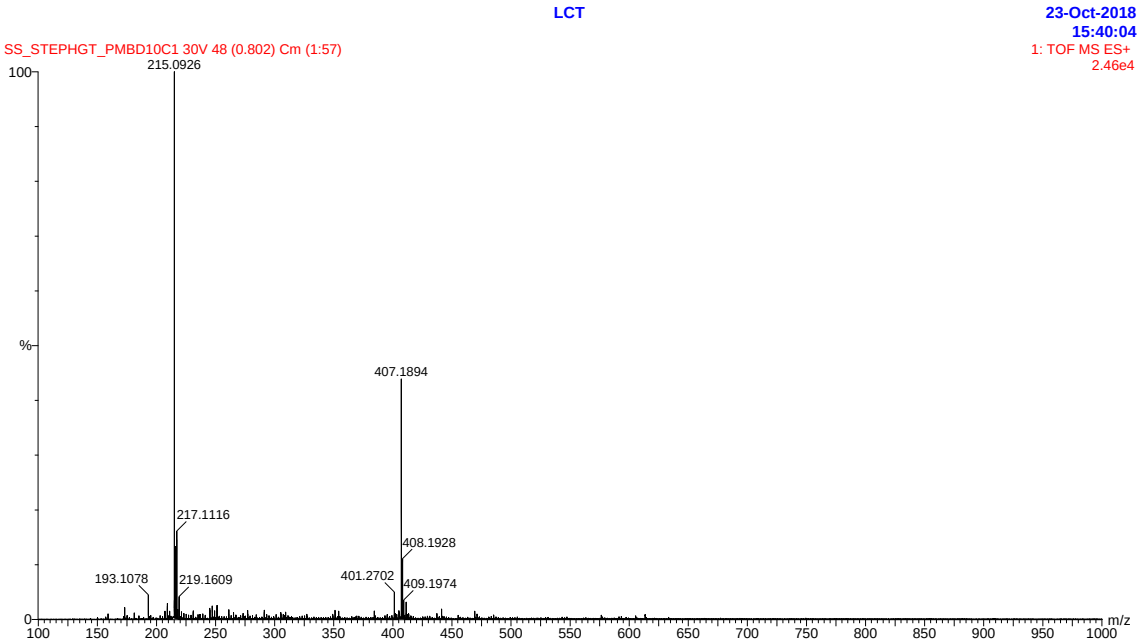

Appendix IV ^{1}H NMR (600 MHz, CD_3OD) spectrum of myrtopsine (185)

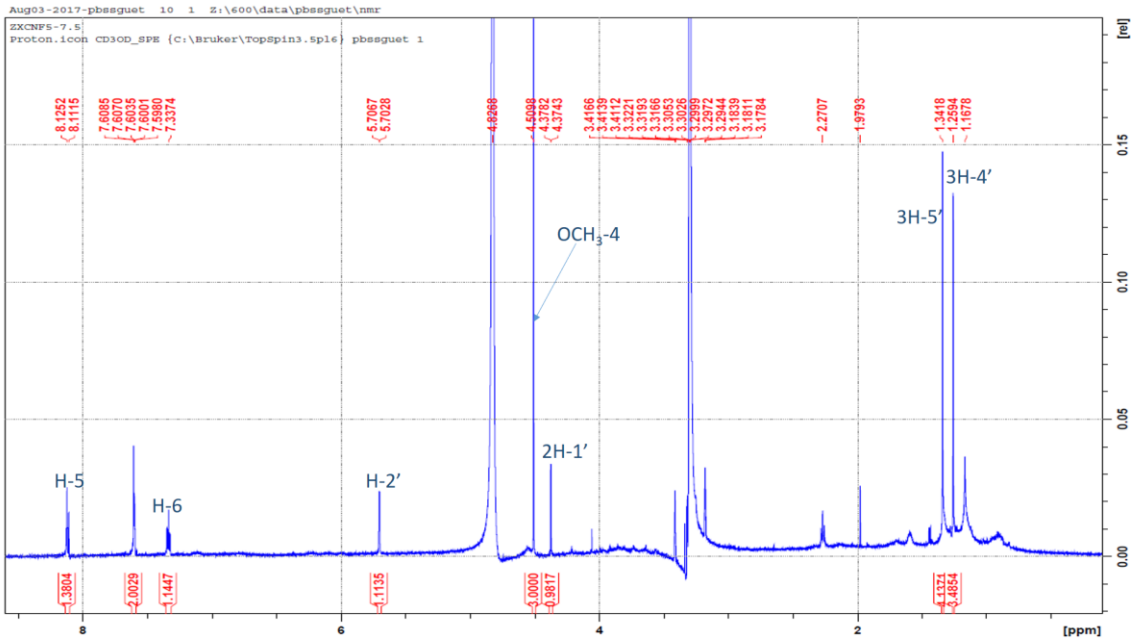

Appendix V List of publications and presentations

Publications

Guetchueng, S.T., Nahar, L., Ritchie, K.J., Ismail, F.M., Wansi, J.D., Evans, A. and Sarker, S.D. (2018). Zanthoamides G-I: Three new alkamides from *Zanthoxylum zanthoxyloides*. *Phytochemistry Letters*, 26, 125-129.

Guetchueng, S.T., Nahar, L., Ritchie, K.J., Ismail, F.M.D., Evans, A.R. and Sarker, S.D. (2018). *Ent*-Clerodane diterpenes from the bark of *Croton oligandrus* Pierre ex Hutch. and assessment of their cytotoxicity against human cancer cell lines. *Molecules*, 23(2), 410-414.

Guetchueng, S.T., Nahar, L., Ritchie, K.J., Ismail, F.M., Wansi, J.D., Evans, A. and Sarker, S.D. (2017). Kaurane diterpenes from the fruits of *Zanthoxylum leprieurii* (Rutaceae). *Records of Natural Products*, *11*(3), 7-11.

Presentations

Guetchueng, S. T., Nahar, L., Ritchie, K. J., Ismail, F. M. D., Dempster, N. M. and Sarker, S. D (2018). *Ent*-clerodanes and other constituents from the bark of *Croton oligandrus* (Euphorbiaceae) and evaluation of their cytotoxicity. Poster presentation- ISCNP30 and ICOB10, Athens, Greece, 25-29 November 2018.

Guetchueng, S. T., Nahar, L., Ritchie, K. J. and Sarker, S. D. (2018). Potential cancer chemopreventive compounds *Croton oligandrus*. Oral presentation- Trends in methods and modelling, Naples, Italy, 04-07 September 2018.

Guetchueng, S. T., Nahar, L., Ritchie, K. J. and Sarker, S. D. (2018). Assessment of potential antimalarial activity of selected Cameroonian medicinal plants. Oral presentation- PSE-YSM 2018, Liverpool, UK, 02-05 July 2018.

Guetchueng, S. T., Nahar, L., Ritchie, K. J. and Sarker, S. D. (2018). Alkamides and other constituents from the fruits of *Zanthoxylum zanthoxyloides*. Poster presentation- PSE-YSM 2018, Liverpool, UK, 02-05 July 2018.

Guetchueng, S. T., Nahar, L., Ritchie, K. J., Ismail, F. M. D., Evans, A. R. and Sarker, S. D. (2018). New alkaloids and other constituents from the fruits of *Zanthoxylum*

zanthoxyloides and evaluation of their cytotoxicity. Oral presentation- PHYTOPHARM 2018, Horgen, Switzerland, 25-27 June 2018.

Guetchueng, S. T., Nahar, L., Ritchie, K. J. and Sarker, S. D. (2017). Screening of extracts of six selected medicinal plants as activators of the keap1-Nrf2 pathway to assess potential cancer chemopreventive activity. Oral presentation- The 9th International Conference of the Kenya Chemical Society (KCS), Kenya, 9-12 May 2017.